Optimal energy management of hybrid systems connected to HVAC and water heating systems in healthcare institutions

By

PERCY ANDREW HOHNE

Thesis submitted in fulfilment of the requirements for the degree:

Doctor of Engineering in Electrical Engineering

In the Department of Electrical, Electronic and Computer Engineering

Faculty of Engineering and Information Technology

Central University of Technology, Free State

Promoter: Prof. K. Kusakana

Co-Promoter: Dr. B.P. Numbi

February 2021

DECLARATION

I, PERCY ANDREW HOHNE, student number , do hereby declare that this research project, which has been submitted to the Central University of Technology Free State, for the degree: Doctor of Engineering in Electrical Engineering, is my own independent work and complies with the Code of Academic Integrity, as well as other relevant policies, procedures, rules and regulations of the Central University of Technology, Free State.

This project has not been submitted before by any person in fulfilment (or partial fulfilment) of the requirements for the attainment of any qualification.

_____

P.A. Hohne Date: **25 February 2021**

DEDICATION

This thesis is dedicated to my beloved late family members; my father, Percy Andrew Hohne Snr, sister, Miranda Hohne, and our precious Chilli. You were taken too soon. To my late grandfather, Philippus Botes and grandmother, Issie Jacobus Botes, your contributions made me what I am today.

To my beautiful fiancée, this would not have been possible without you. I love you.

In loving memory of

My father, sister, grandfather, grandmother, and our precious Chilli.

ACKNOWLEDGMENTS

The realization of this work was possible due to the following people to whom I wish to express my utter gratefulness.

To my supervisors, Professor Kanzumba Kusakana and Doctor Bubele Papy Numbi, I am grateful for the trust in my work and for the motivation demonstrated during this challenging course. Their support was without a doubt crucial for the completion of this research.

I would like to express my profound gratitude to Professor Kanzumba Kusakana, my main promoter, for believing in my capacity to complete this project. I am very grateful for his permanent support, scientific guidance, constant optimism and encouragement, throughout this long walk, with all its "ups and downs". I deeply appreciate his careful revision of all my work. I would further like to thank him for his friendship.

I would like to acknowledge the inspirational instruction, guidance, and the initial driving force to study energy management from Dr. Bubele Papy Numbi, who has given me a deep appreciation and love for the beauty and detail of this subject.

I would also like to acknowledge the support and assistance given to me by the Central University of Technology, Free State (CUT). CUT has been very generous in supporting my academic pursuits and many of my colleagues have contributed with advice and feedback.

I would like to thank my late father and sister, Mr. Percy Hohne Snr and Miranda Hohne, for always believing that I could achieve my dreams and goals, however difficult.

My mother, Mrs. Sonja Hohne, for all the support and reassurance during the study. Dr. Frikkie Kruger, Ms. Erna Vlok and my grandparents for their continuous care and encouragement through the years.

Finally, I would like to thank in a special way, my darling fiancée and her father, Ms. Andrea Walle and Mr. Erich Walter Walle, for their support, prayers, and good wishes. I could not have completed this effort without their assistance, tolerance, and enthusiasm.

Thank you.

LIST OF ABBREVIATIONS

4IR	4th Industrial Revolution
AHU	Air handling unit
BEER	Building energy efficiency retrofit
CIDB	Construction Industry Development Board
COVID	Corona virus disease
CSIR	Council for Scientific and Industrial Research
CSSD	Central sterile services department
CUT	Central University of Technology
DHI	Diffuse horizontal irradiance
DNI	Direct normal irradiance
DSM	Demand side management
ECP	Energy Performance Certificates
EE	Energy Efficiency
EES	Electrical energy storage
EPI	Energy performance index
ESTWH	Electric storage tank water heater
EU	European Union
EUI	Energy Usage Index
FF	Full falling
FI	Feed-in tariff
GHI	Global horizontal irradiance
HVAC	Heating, ventilation and air conditioning
IEEE	Institute of Electrical and Electronic Engineers
IoT	Internet of Things
ISO	International Organization for Standardization
MATLAB	Matrix laboratory
MF	Mixed falling

MFC	Multifunctional chiller
MIL-STD	Military standard
MPC	Model predictive control
NEES	National Energy Efficiency Strategy
OPTI	Optimization
OR	Operating room
PCM	Phase change materials
PDCA	Plan, do, check, act
PI	Proportional integral
PLC	Programmable logic controller
PM	Preventative maintenance
POET	Performance, operation, equipment and technology efficiency
PV	Photovoltaic
RTD	Resistance temperature detector
RTU	Remote telemetry units
SANS	South African national standards
SCADA	Supervisory control and data acquisition
SCIP	Solving Constraint Integer Programs
SOC	State of charge
STD	Standard test conditions
TES	Thermal energy storage
TOU	Time-of-Use
UK	United Kingdom
UPS	Uninterruptable power supply
USA	United States of America
USD	United States Dollar
VRF	Variable refrigerant flow
VSD	Variable Speed Drive

ABSTRACT

Healthcare institutions consume large amounts of energy, ranking the second highest energy intensive building in the commercial sector. This has further been exacerbated by the COVID 19 global pandemic, as healthcare facilities worldwide demand more energy with the substantial increases in patient occupancy. Within developed countries, the energy consumption of healthcare institutions may account for up to 18% of the overall energy usage, in commercial sectors. Within developing countries, such as South Africa, the energy consumption of healthcare institutions is observed to be a close second to the food service sector. Energy consumption of healthcare institutions per bed, typically range from 43 - 92kWh per day. The high energy consumption of these buildings may be attributable to energy intensive systems, that are required to operate at full scale, 24 hours a day. In retrospect, energy intensive equipment, operating continuously or during peak energy periods, result in exceedingly high energy costs, particularly when the consumer is subjected to time-based electricity pricing and maximum demand charges.

The major energy intensive processes that may have their energy efficiency significantly improved, were identified to be heating, ventilation, air conditioning (HVAC) and water heating (WH) processes. The combined energy usage of HVAC and water heating processes may account for approximately 50% of the total energy consumption in the majority of modern healthcare facilities in South Africa. These systems are critical to patient health and may be classified as non-deferrable loads. Accordingly, demand side management techniques are difficult to implement without additional equipment. This renders the scheduling of loads to the lower-cost regions of the Time-of-Use (ToU) tariff, while constantly meeting load requirements, a formidable task. Additionally, the balance between the maximum demand charge and ToU tariff has to be maintained, in order to effectively minimize energy costs.

Generally, to improve the potential for demand side management and energy efficiency of these processes, various methods exist. These include the implementation of energy storage systems, equipment retro fitment/replacement and the application of effective control approaches.

Within the majority of private and a few public hospitals, the energy efficiency of existing equipment leaves little room for improvement. However, the decision to commission additional equipment such, as renewables and energy storage systems, is usually made with caution. The economic feasibility of these systems, at the time of the study, particularly the payback period, appears to be just beyond the acceptable threshold for adequate justification. Consequently, introducing renewable energy systems and energy storage schemes, may reduce energy usage and associated costs, while the application of optimal control techniques may improve the feasibility of such costly implementations. Additional feasibility improvements may include waste thermal energy recovery from processes such as HVAC systems and is transferred to water heating equipment so that energy savings may further be increased.

Effectively applied energy management schemes, using advanced optimization techniques, remain imperative for operational cost minimization. Therefore, in this study, various methods for improving the energy efficiency of HVAC and water heating systems are identified and applied to a large-scale hospital building as a case study. These methods include the implementation of renewable energy technologies with energy storage, equipment retro fitment and the application of optimization strategies. The objective is to minimize energy usage and associated costs, with respect to the ToU tariff and maximum demand charges.

A dual axis PV tracking system and energy storage scheme, with optimal control was proposed, to supply HVAC, water heating systems and other equipment. A model was developed to represent the operation of this hybrid energy scheme.

A second model of a multifarious water heating system, with a total of 57 electric storage tank water heaters (ESTWHs), connected to an HVAC energy recovery system was established. The operation of this multifarious water heating system was simulated to represent the operation of the system. In this case, the simultaneous operation of the various ESTWHs was avoided to lower the risks of incurring unnecessary maximum demand penalties.

Optimal control algorithms were developed, for both models, to minimize energy costs, based on the ToU tariff and maximum demand charges. SCIP (Solving Constraint Integer Problems) in the MATLAB OPTI-Toolbox was used to solve the optimal control problems.

In hindsight, the feasibility of implementing the proposed dual axis PV tracking system with energy storage, supplying mainly HVAC and water heating loads, has been evaluated and discussed. According to the study, if the proposed system were to be installed, the system would break-even within 9.3 years, with lifecycle cost savings of 24.5% over a 20 year period. Applying optimal control to this proposed system, will potentially decrease the break-even point to 7.5 years and increase cost savings by up to 34.5%.

Additionally, the study with a focus on HVAC and water heating processes, with waste heat recovery, revealed that, with the implementation of a multifunctional chiller (MFC), the project should break-even in 7.4 years, with project lifetime energy cost savings of up to 22.02%. The application of the proposed optimal control approach, resulted in a potential break-even point of 5.3 years, with maximum potential savings of 68.23%, achievable over a 20 year life cycle.

These results further indicated that, with the application of optimal operation control algorithms, the feasibility of high investment energy efficiency activities may be improved significantly. This, in turn, serves as a greater incentive for building energy managers to implement these "deep energy retrofit" projects as to better align with international policies to stabilize global greenhouse gas concentrations.

Keywords:

Cost minimization; Hybrid energy systems; HVAC and water heating processes; Optimal scheduling; Energy efficiency; Time based pricing; Maximum demand charges.

TABLE OF CONTENTS

LIST OF FIGURES

LIST OF TABLES

CHAPTER I: INTRODUCTION

1.1 BACKGROUND

The magnitude of the global energy crisis has severely increased over the years, particularly in South Africa, forcing the country to implement energy usage reduction strategies, such as load shedding/curtailment, time-based electricity pricing and maximum demand penalties [1].

Electrical energy consumers, categorized as: residential, commercial, and industrial energy consumers, may be assessed individually, in terms of the amount of energy used [2]. The demands of the industry declined during the COVID 19 pandemic, while an increase in the energy demand for the residential sector has been apparent. This was mainly attributed to travel restrictions and "working from home" arrangements. The commercial sector, as a whole, did not experience this trend, while in contrast and more notably, medical facilities, with higher than normal patient occupancy rates, resulted in a substantial increase in demand. Relevant data collected before the surge of COVID 19 cases, suggested that healthcare institutions within this sector, were the fifth highest consumers of energy [3]. Moreover, the energy use intensity (EUI) of healthcare institutions, is approximately three times that of typical commercial buildings [4]. These buildings require energy intensive processes to maintain patient health and mitigate loss of life [5].

Recent studies suggest that the average hospital energy usage per bed, ranges from 43 – 92 kWh per day [6]. Hospitals are of the few types of buildings that run at full-scale, 24 hours a day. The continuous operational requirements result in high energy costs, particularly during costly regions of Time-of-Use (ToU) tariff. Recent and predicted hikes in electricity tariffs, may result in exceedingly expensive healthcare for South African citizens, many of whom are, at present, incapable of affording this necessity [7]. In retrospect, the situation evolved severely during the current COVID 19 global pandemic, where a large majority of citizens lost the ability to receive the same income prior to the pandemic [8].

Therefore, energy management solutions should be applied as a matter of urgency to reduce costs where possible, while further reducing the energy usage to lessen the greenhouse gas emissions. The first step in any energy management process, is the identification of energy

intensive equipment [9]. The main consumers of energy within hospital buildings were noted to be heating, ventilation and air-conditioning (HVAC) and water heating (WH) processes. These processes consume approximately 50% of the total energy and are considered crucial to human health and comfort [10]. These systems are required to be effectively managed, in terms of energy efficiency, to minimize operational costs, while maintaining sensitive load requirements.

1.2 PROBLEM STATEMENT

The electrical energy usage per bed in healthcare institutions range from 43-92kWh/day. Approximately 50% of this energy may be allocated to inefficiently operated HVAC and WH processes [4]. The main problem arises from the continuous operation requirement of the equipment linked to these processes, which results in substantial energy costs, particularly during the costly regions of the Time-of-Use tariff. Moreover, unpredictable patient occupancies and sparse energy storage capacities limit the potential deferability of the load at healthcare facilities. Consequently, challenges are faced in exercising demand side management (DSM), to avoid the costly regions of the ToU tariff [6]. Furthermore, large scale healthcare facilities are often subjected to a notable additional cost, such as maximum demand penalties. This means that DSM strategies, such as load shifting, as well as peak clipping techniques, are to be applied with precise coordination to minimize energy costs.

Several studies have been conducted on the implementation of energy storage schemes along with renewable energy systems, to minimize energy costs and increase the potential for the application of DSM strategies. However, for the specific load requirements and unique case of hospital buildings, a shortage of research has been noted, particularly where both ToU tariffs and maximum demand charges were involved. Furthermore, the authors of these studies often focused on the load demand as a whole and not the equipment or processes responsible for the demand. In retrospect, this may not represent the dynamic power requirement of each electrical component in the system, leading to inaccurate load behaviour predictions.

In light of the main problem, the following prominent sub-problems were identified:

- Sub-problem 1: A lack of validated models of renewable energy systems, with energy storage schemes were noticed, particularly for dual axis PV tracking systems, operating in the South African climate. This problem is exacerbated for the central regions of South Africa, where solar irradiance is in abundance. The deficit in validated models, provide for poor representations of the real-world operation of these systems. This may lead to unreliable economic feasibility studies.
- Sub-problem 2: Economic analyses on large energy efficiency retrofit projects, often reveal unfavourable payback periods, or break-even points. Optimal control techniques may be applied, to improve the economic feasibility of these systems. However, a significant absence of research on the subsequent economic impact of optimal control techniques, applied to these processes, was observed. This was particularly noticeable for the unique systems and loads that are typically associated with healthcare institutions.
- Sub-problem 3: In order to pre-test the performance of optimal control algorithms on the systems that exist in healthcare institutions, accurate models of these systems are required. The optimal control algorithms may then be applied to these models first, rather than the real-world system, so that unnecessary costs and interruptions of processes are kept to minimum. The problem, in this instance, is the lack of models available for these unique processes or equipment in healthcare institutions.
- Sub-problem 4: Solving the optimization problems, with respect to the ToU tariff and maximum demand charges, while considering several input variable datasets for an entire year, is highly computationally expensive. Therefore, the required models necessitate simplification, as well as validation, against real-world historical data, to achieve the utmost accuracy and, in turn, offer reliable economic feasibility data.

1.3 OBJECTIVES

The aim of this study was the development of optimal control models of the proposed and existing systems connected to HVAC and water heating loads of a healthcare institution as the case study. Therefore, to achieve this aim, the objectives were as follows:

- To critically review energy efficiency initiatives for energy costs minimization in healthcare institutions.
- To develop a model and simulate the operation of a proposed dual axis PV tracking system with energy storage, connected to a healthcare facility, with and without the application of optimal control techniques. Subsequent results are then to be compared to reveal the cost saving potential of the optimal control algorithm.
- To develop a model and simulate the operation of a multifarious water heating system coupled to an HVAC energy recovery scheme, with and without optimal control, the aim here is to evaluate resultant potential cost savings.
- To conduct a techno-economic analysis on the proposed dual axis PV tracking system and the energy recovery system connected to the institutions' HVAC and multifarious water heating system.

1.4 RESEARCH METHODOLOGY

To achieve the objectives of the study, the methodology is as follows:

- Literature review: A comprehensive review of hybrid systems connected to HVAC and water heating schemes, using the Performance, Operation, Equipment and Technology (POET) framework. This includes a thorough survey of literature, related to the operation and control of renewable energy arrangements with energy storage, water heating (multifarious and standalone) systems and HVAC equipment with waste thermal energy recovery systems.

- System variable identification:

  The first system consists of a dual axis PV tracking scheme, with energy storage and a grid connection (Model 1), while the second involves a multifarious water heating systems, connected to an HVAC energy recovery system (Model 2). Optimal control algorithms were applied to these models, to reduce energy costs, subjected to the ToU tariff and maximum demand charges:

  – Independent variables - all input variables (collected variable data)
  – Control variable i.e. decision variable:
    - Model 1: Power flow between hybrid system components
    - Model 2: Switching statuses of each ESTWH
  – Dependent or state variables: all variables affected by any variation or change in the input variables. These are:
    - Model 1 state variable: state of charge of the energy storage system
    - Model 2 state variable: water tank temperatures of each ESTWH

- Data collection (input variables) and case study:
  - Real input variable data collected from SCADA systems at a Hospital (Mediclinic) in the Bloemfontein area, Free State was used, which includes:
  - Solar data (global horizontal, direct normal, diffuse horizontal irradiance)
  - Hot water demand flow rate
  - Energy demand of HVAC, water heating processes and other equipment
  - Inlet temperature of the water supplied to the water heating system
  - Ambient air temperature at the hospital building
  - ToU tariff electricity pricing
  - Other input parameters; sizing and power ratings of equipment, etc.
- System modelling and control, the stepwise process, is shown in Fig. 1.1:
  - The models of the proposed systems, connected to the hospitals' existing HVAC and water heating loads were developed.

- The optimal energy management algorithms to dispatch power economically and reduce operational energy cost requirements of the HVAC and water heating equipment was developed, using MATLAB with OPTI-Toolbox.
- The proposed optimal energy management algorithm was developed to minimize energy costs based on the ToU tariff pricing structure and maximum demand charges.
- The collected data was used to simulate the operation of baseline systems as well as optimal control cases for each respective proposed model.

- Simulation:

  The optimization problem for each model was identified, to be mixed integer and non-linear, while the following capable solvers were chosen for each model problem. These solvers form part of the MATLAB OPTI-Toolbox. The Solving Constraint Integer Programs (SCIP) solver was used for Model 1 and 2, due to its high-speed solving capabilities of the ToU problem.

  - The simulated results include:
    - Model 1: The optimally dispatched power flows between system components, the PV output power of the dual axis PV tracking system, the state of charge of the energy storage system and the cumulative energy costs incurred, based on the ToU tariff and maximum demand charges.
    - Model 2: The optimal switching functions of the ESTWHs, water tank temperatures of the ESTWHs, power consumed by the ESTWHs and the cumulative costs incurred, with respect to the ToU tariff and maximum demand charges.

Fig. 1.1 illustrates the flowchart of the research modelling process for each model. The input variables identification and data collection procedures are the initial steps during the model development process. Initial values are set for the state variables. The optimal control problem is then solved in the final step.

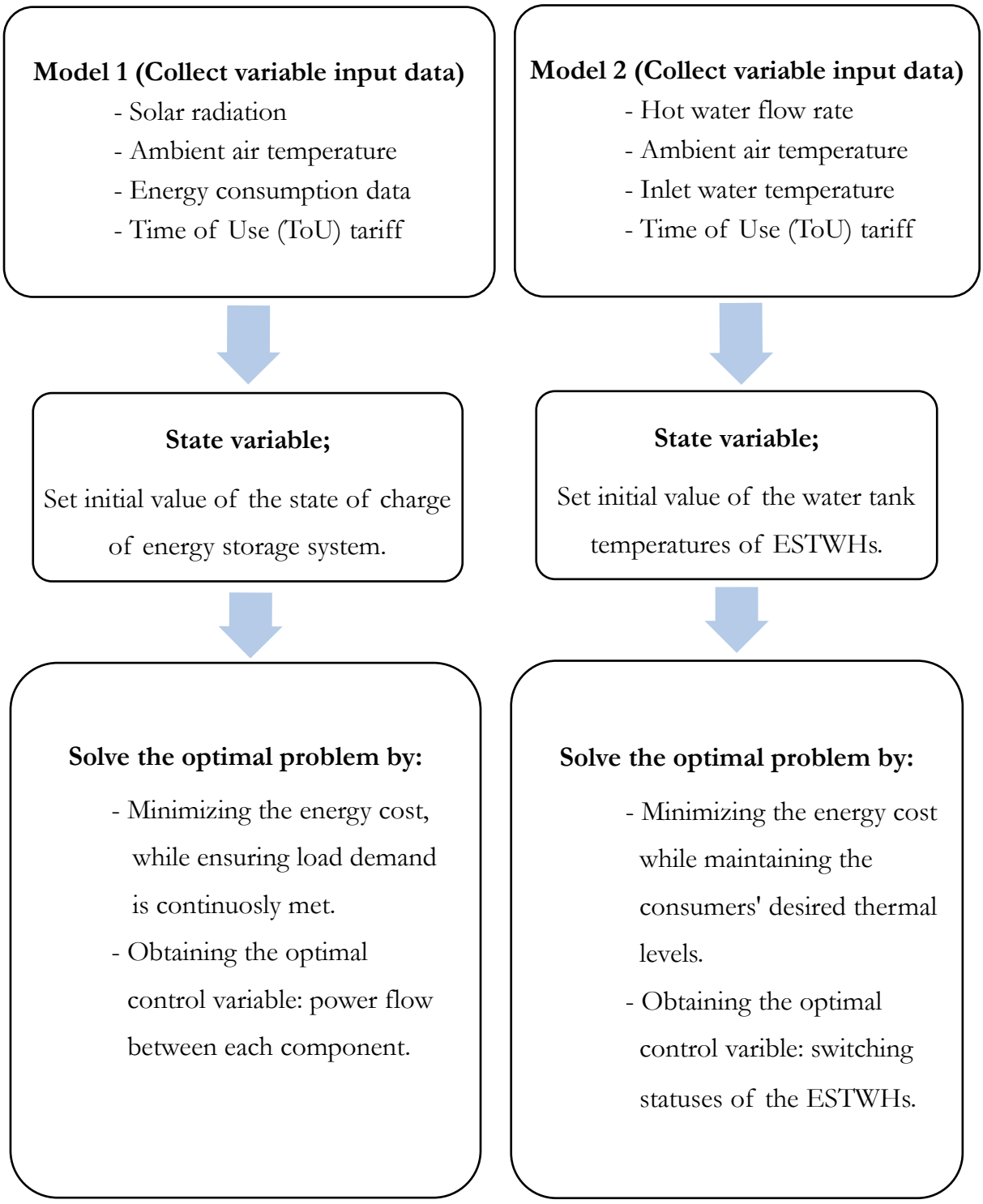

Fig. 1.1: Flowchart of methodology and research design

1.5 CONTRIBUTIONS TO KNOWLEDGE

Model 1 - Optimal power dispatch of a grid-connected dual-axis PV tracking system, with energy storage supplying a healthcare institution (Chapter III):

- A validated mixed integer non-linear model of a dual-axis PV tracking system, with energy storage that considers both the ToU tariff and maximum demand charges, in the minimization of energy costs of a non-deferable variable load demand.

Model 2 - Optimal control of a multifarious water heating system with HVAC waste heat recovery in a healthcare institution (Chapter IV):

- A mathematical non-linear mixed integer model and optimization of a large-scale hybrid multifarious water heating system; taking into consideration individual system parameters, to achieve global coordinated optimal control under the ToU tariff and maximum demand charges.

Social impact:

- The research provides solutions for minimizing the operational energy costs of the HVAC and WH systems in healthcare institutions. This may, in turn, provide lower healthcare charges to patients and the community, while maintaining quality of care.
- A reduction of operating costs may allow for an increase in funding, to upgrade existing medical equipment, or improve the reliability of the electricity supply. This may lead to enhanced patient treatment or mitigate the loss of life.

1.6 HYPOTHESIS

- The implementation of a dual axis PV tracking system, along with energy storage system, will lead to substantial energy and operational cost savings.
- The commissioning of a HVAC heat recovery system, a multifunctional chiller in this study, will lead to significant energy and cost savings and a reduction of peak demand.
- Optimal control strategies applied to the evaluated systems, will improve the economic feasibility of implementing the proposed equipment.

1.7 DELIMITATION

The study was conducted with the following limitations:

- Only a large capacity healthcare institute was considered in this research, due to the worst-case scenario load requirements of this type of building. The energy management initiatives that were proposed in this research, may be applied to any building with similar loads and equipment.
- Open-loop optimal energy management was considered at this stage of the research, to determine the preliminary economic impact and feasibility of implementing the approach to a healthcare institution. Closed-loop simulations are not considered, as the physical implementation is not part of the current study and forms part of future research.
- In this study, only the case of a hospital in Bloemfontein, South Africa, is considered, due to the availability of data in the case study area. However, the same methods in the study may be applied to other healthcare institutions, or commercial buildings in various locations, worldwide.

1.8 PUBLICATIONS DURING THE STUDY

Conference paper(s):

- Hohne, Percy Andrew, Kanzumba Kusakana, and Bubele P. Numbi. "Economic Power Dispatch for Energy Cost Reduction of a Hybrid Energy System Considering Maximum Demand Charges and Time-based Pricing in a Healthcare Institution." In 2020 6th IEEE International Energy Conference (ENERGYCon), pp. 395-400. IEEE.

Journal paper(s):

- Hohne, Percy Andrew, Kanzumba Kusakana, and Bubele Papy Numbi. "Improving Energy Efficiency of Thermal Processes in Healthcare Institutions: A Review on the Latest Sustainable Energy Management Strategies." Energies 13, no. 3 (2020): 569.
- Hohne, P. A., K. Kusakana, and B. P. Numbi. "Model validation and economic dispatch of a dual axis PV tracking system connected to energy storage with grid connection: A case of a healthcare institution in South Africa." Journal of Energy Storage 32 (2020): 101986.
- P.A. Hohne, K. Kusakana, B.P. Numbi "Model development and validation of a Dual-Axis PV Tracking System: A Case of South Africa" International Journal of Electrical and Electronic Engineering & Telecommunications (In press-2021).
- P.A. Hohne, K. Kusakana, B.P. Numbi "Multi-objective optimization for energy cost minimization of multifarious water heating systems with energy recovery in a healthcare institution". (Submitted)

1.9 THESIS LAYOUT

This thesis has been divided into five chapters, with the main research results being presented in Chapters III and IV.

Chapter I presents the background of the work, underlines the problems and provides the objectives and methodology.

Chapter II reports a comprehensive review on the latest sustainable energy management strategies of HVAC and water heating processes in healthcare institutions. Energy efficiency initiatives were identified and categorized to align with the POET framework for energy management.

Chapter III describes the optimal control model formulation of a dual axis PV tracking system, with energy storage connected to HVAC, water heating systems and other equipment. The model, constraints of operation, objective function, variable input data and simulation

results of a proposed dual axis PV tracking system, with energy storage, connected to the grid, are discussed. A thorough economic analysis is presented at the end of the Chapter, with two baseline systems and a case where optimal control techniques were applied, to evaluate the feasibility of the proposed system with and without the application of the control algorithm.

Chapter IV presents an optimal control model of a multifarious water heating system connected to an HVAC waste energy recovery system. Similar to the previous Chapter description, the model development, constraints, objective function, input data and simulation results are discussed. A comprehensive life cycle cost analysis was conducted and evaluated in this Chapter. Similarly, two baseline systems were considered to determine the potential for feasibility improvement of the proposed system, subjected to the optimal control algorithm.

Chapter V concludes the work of this thesis and sets the stage for future studies.

CHAPTER II: A REVIEW ON IMPROVING THE ENERGY EFFICIENCY OF THERMAL ENERGY SYSTEMS IN HEALTHCARE INSTITUTIONS

2.1 INTRODUCTION

In this Chapter, the latest energy management strategies applied to thermal processes in healthcare institutions are reviewed and discussed. These thermal processes involve HVAC and water heating systems.

A systemic review methodology was chosen, based on the POET perspective to assess the possible energy efficiency improvements that may be applied to healthcare institutions. The results include a comparison of energy efficiency initiatives at each level, in terms of energy saved and the associated effort, with respect to the costs involved in implementing the initiatives, at each respective level of the POET framework.

The layout of this Chapter is as follows: Section 2.2 provides justification for the review with Section 2.3 showcasing the sustainability of energy efficiency initiatives, based on the POET framework. Section 2.4 presents the methodology, aim and contribution of this Chapter. In Section 2.5, the literature, pertaining to the energy efficiency of thermal processes in healthcare institutions, are summarized according to the levels of the POET hierarchy. Section 2.6 outlines the key findings on the reviewed literature. Section 2.7 concludes the Chapter, while section 2.8 highlights recommendations for future work.

2.2 REVIEW JUSTIFICATION

According to [11,12], the energy usage of commercial buildings in developed countries (USA, UK, EU, Spain), range from 8-18%, while the world average for these buildings account for up to 7% of the total energy consumed. Healthcare institutions are the fifth highest energy consumer in the commercial sector, in terms of the amount of energy consumed. However, when evaluating the energy use intensity (EUI) of each building type,

healthcare institutions rank the second highest in most developed countries; second only to the food service sector. A similar observation was made for the South African case, where the EUI of healthcare institutions is approximately three times that of typical commercial buildings. Additionally, it was noted that the energy usage of healthcare institutions ranges from approximately 43-92 kWh/bed/day [13]. The high energy demand in these buildings may be attributable to energy intensive systems that are required to operate at full scale, 24 hours a day. Continuous operational requirements result in high energy costs. This is particularly true for systems subjected to time-based pricing structures, otherwise named Time-of-Use (ToU) tariffs. The ToU tariff was implemented by the national electricity supplier, Eskom, in South Africa. However, in the case of health care institutions, loads may be seen as undeferrable, due the unique sensitive load requirements of these buildings. This results in substantial electricity costs, as a consequence of the equipment being operated through peak periods, where electricity costs are at their highest. In hindsight, with the recent hikes in electricity tariffs in South Africa, exceedingly expensive healthcare is expected. This introduces a problem for many of the country's citizens, many of whom are incapable of affording this basic necessity [14].

To reduce the impact of electricity costs on healthcare expenses, energy intensive systems should be managed effectively in terms of energy efficiency. Energy efficiency studies and initiatives may be applied to healthcare buildings, which could result in substantial energy and cost savings, and in turn, reduce the strain on the national grid. A large body of research, with the explicit objective to improve energy efficiency of specific systems in buildings, has been conducted, particularly in the past two decades [15,16]. However, a comprehensive review of scientific articles on energy efficiency initiatives in healthcare institutions is yet to be conducted, substantiating the need for such a review to be conducted. Therefore, the aim of this research is to conduct a review, using a well-established energy management framework. The foremost used method or framework for implementing energy management activities, is the stepwise loop called the PDCA cycle. The PDCA cycle, also known as the Deming cycle, is an iterative approach and forms the basis to which the ISO 50001 standard

procedure is realized. The PDCA cycle consists of four sequential stages, defined as; Plan, Do, Check and Act (PDCA) [17].

The first stage incorporates energy policy and planning, with the aim of obtaining an initial energy baseline, energy performance indicators, strategic and operative energy objectives and action plans. The evaluations and data obtained from this stage, form the basis for the following improvement process, otherwise noted as the "Do" phase. In this second stage, action takes place in the form of implementing the planned energy management practices. The "Check" phase is represented by the monitoring and measurement of energy related performance of the systems, that were implemented in the previous phase. The results obtained at this phase is evaluated and compared to objectives previously established in the planning period. As part of the last stage, the "action" stage, the acquired results are broken down into reports, which form the basis for further improvement studies. These phases are arranged in a circular cycle, which implies that after the last stage has been finalized, all stages will feature again in the same sequential manner to ensure continuous improvement [18].

The PDCA model has the advantage of being a powerful, yet simple methodology, to resolve new and recurring issues, in any industry. This is since the core commitment is continuous improvement. However, three major drawbacks relevant to energy management include oversimplification of the improvement process, its' reactive nature and the inability to encourage radical innovation. The oversimplified and reactive nature of the PDCA model has an overlapping problem. The problem introduces itself with the PDCA's circular paradigm and the first stage of the model. It may be assumed that any energy management program starts with planning. This may not always maximize the potential for energy efficiency improvement in practice and as such, deviation from the rigid circular structure is often necessary [18,19].

Another major drawback, similarly, as a consequence of the circular paradigm and the step-by-step process, are the limitations placed on radical innovation. The core philosophy of PDCA is planning and implementing an activity first and then evaluating the implications or resultant drawbacks of the activity after implementation. Therefore, the PDCA model has its focus on correcting mistakes, rather than preventing them. Consequently, the time

required to implement a program with the best possible outcome, in this case, maximized energy efficiency, is increased substantially [19,20,21].

In retrospect, an alternative approach is deemed necessary, to effectively evaluate the maximum potential energy savings that the various existing energy efficiency initiatives may offer. Energy efficiency may consist of several aspects, such as operational efficiency, performance efficiency, carrier efficiency, maintenance efficiency, conversion efficiency, fuel efficiency, etc. Literature based on these aspects applied to various cases are plentiful and widely available. However, it may be observed that these aspects are not clearly defined or classified and do not follow similar points of departure on the constituents of energy efficiency [22,23].

Therefore, an amalgamating classification of energy efficiency in terms of performance, operation, equipment and technology (POET), was presented in 2010, by the authors Xiaohua Xia and Jiangfeng Zhang in [22,24].

Energy efficiency, in general, is defined as the percentage of the total energy supplied to a process that is consumed as useful work and not wastefully expended as heat or other forms of energy [23]. This is the key principle that is taken into consideration in various energy management, renewable and sustainable energy developments. As stated in [22], multiple aspects exist in the broad category of energy efficiency. These aspects are not clearly defined or categorized and introduce a problem in the energy management field. Addressing this problem entails the design of a framework or guideline, providing clear cut boundaries between various energy efficiency initiatives, for effective and sustainable energy management. Therefore, energy efficiency may be divided into four components: performance (P), operation (O), equipment (E) and technology (T) efficiency, or POET in short, as described in [22]. The POET framework has been successfully applied to various types of systems and buildings; these include commercial buildings [24], heavy haul trains [22], conveyer belt systems [25], wastewater treatment processes [26], pumping systems [27], etc. As noted in [22,24-27], effective energy management is highly dependent on the energy efficiency of electrical equipment used in any building. Maximizing the potential energy cost

savings in these buildings may, in some cases, be a formidable task. To this end, an energy management program may be divided into four levels.

The initial level may incorporate simple energy efficiency activities, while the subsequent levels increase with complexity. Therefore, the first level may be classified as the conceptual level, which entails a basic energy usage analysis, to identify energy efficiency problems within a particular building. The solutions to these problems, within the conceptual level, usually refer to the Pareto principle, also known as the 80/20 rule. This rule implies that if 20% effort is to be applied, an 80% return will be achieved [28].

The second level, the active level, entails a more complex approach. The active level requires more effort, compared to the previous level, resulting in less than an 80% return. Furthermore, the active level requires validation of the problem, addressed at the first level, using additional strategies and equipment, which may result in further potential improvement in efficiency.

The third level, the technical level of the hierarchy, may involve a redesign in terms of retrofitting or introducing new technologies, to replace inefficient existing systems. This level requires further verification of collected data, obtained at the second level for accurate payback period calculations and further relevant feasibility studies.

The last level focuses on optimization, also referred to as the engineering, or further, possible improvement level. This level often overlaps with the technical level, in that validated data is required to apply optimization to existing energy efficient technologies and equipment. Therefore, the last level will provide the maximum possible savings if effectively implemented [25].

2.3 SUSTAINABLE ENERGY EFFICIENCY BASED ON THE POET FRAMEWORK

The sustainability of an energy management program for the improvement of energy efficiency, may be evaluated by considering the following three aspects: organizational structure, compatibility of performance indices and engineering support [24,29].

A well-designed organizational structure supports the sustainability of an energy management program. In order to effectively stimulate the POET efficiency activities and in turn the sustainability of an energy management program, certain external mechanisms, such as energy policies, regulations, incentives and penalties, are necessary. These mechanisms are usually enforced by the governing body of a country and often prove to be highly effective, when appropriately planned and executed. Conversely, internal mechanisms include human sensitization, which involves procedural guidance of workflow, awareness campaigns, skill training, technology roadshows, appointment of energy managers, production exhibitions, etc [30,31].

The compatibility of performance indices is evaluated, in terms of engineering indices and socio-economic indices. Engineering indices may include energy usage, energy security and other technical indicators. Socio-economic indicators, on the other hand, include energy costs, quality of production, environmental impact, etc. In retrospect, it may be observed that the energy efficiency of a certain system is improved when the engineering indices follow an upward trend, while the opposite is noted when evaluating the socio-economic indices. Therefore, both indices are to be taken into consideration to guarantee a positive growth in the performance efficiency of an energy system. This should ultimately provide additional support to the sustainability of an energy management program [32].

Engineering support plays a crucial role in evaluating the technical feasibility of a system. In hindsight, support entails energy analysis, system modelling and the implementation of relevant optimization techniques. Suitable engineering support will improve the reliability of energy solutions, while ensuring sustainability [33].

2.4 METHOD

The POET perspective, originally developed by Xiaohua Xia and Jiangfeng Zhang, serves as a unifying classification of energy efficiency in terms of performance, operation, equipment and technology efficiency (POET in short) [22].

In this Chapter, a comprehensive review on energy efficiency in healthcare institutions is conducted from the POET perspective. The context to substantiate the need for such a

review, has been outlined in the introduction. The remainder of this section will provide an overview on how the review was conducted, as well as the advantages and drawbacks of this approach.

A systemic review methodology was followed, based on the POET perspective, to assess the possible energy efficiency improvements that may be applied to healthcare institutions. Systemic reviews are most often used in clinical practice, to provide the highest level of reliable evidence [34]. The aim of these reviews is to provide a broad, exhaustive summary of current available research evidence. As a result, the researcher is forced to investigate all pertinent studies, as to not be constrained by their own boundaries of experience [35]. In addition, the systemic review and by extension, the POET perspective, aims to answer predefined research questions. Therefore, the aim of this study may further be expanded to answer the following three research questions:

Research Question 1: What is the existing evidence base regarding potential energy and cost savings of current energy efficiency initiatives applied to these buildings available in the literature?

Research Question 2: Could healthcare institutions reach energy targets, in order to align with trajectories developed by CIDB and CSIR through effective implementation of these initiatives?

Research Question 3: Based on the above research questions, what is the economic feasibility of implementing energy efficiency initiatives to reach these energy targets?

With reference to the research questions stated above, the POET framework is used to conduct a comprehensive review, taking into consideration all aspects of energy efficiency.

The search strategy consisted of identifying relevant studies (all aspects of energy efficiency) within research-based sources, represented by scientific papers available in peer-reviewed conference proceedings and journals. Online databases were consulted, in order to retrieve all published articles on the topics related to improving the energy efficiency of thermal processes in healthcare institutions. The decision to evaluate solely thermal processes, is justified in Section 2.5 of this chapter. All efforts have been made to obtain the most recent publications, whereas older studies were only consulted through absolute

necessity. The major sources used to identify relevant scientific literature were Google Scholar, ScienceDirect, IEEE Xplore and PubMed Central.

The selection criteria for this study, besides the general criteria, were the following: solely articles in English were considered, articles available in full-text, date of publication and relevance to the search topics were essential.

In hindsight, evaluating the available literature subjected to the above stated search strategy, in conjunction with the POET perspective, offers a clear advantage over the traditional PDCA method, in that every avenue of the broad category of energy efficiency is consulted [36].

Therefore, the contribution of this study is a comprehensive assessment of the potential energy and associated cost savings, that may be of result if appropriate sustainable energy efficiency measures were to be implemented. Additionally, the presented data, with respect to the ranged average payback periods or economic feasibility of the initiatives at each level, may provide valuable insight to energy managers during the planning phase of energy efficiency projects.

The drawback of the POET perspective presents itself when energy efficiency initiatives are evaluated and categorized within the hierarchy of the framework [37,38]. It may be challenging to determine the exact amount of "effort" required, compared to the potential "profit" of implementing each energy efficiency initiative, as described by the pareto principle in the introduction section. This means that at each level of the hierarchy, it is necessary to express the quantitative data obtained from literature in terms of energy savings and associated payback periods, in averaged ranges, rather than exact values.

2.5 ENERGY EFFICIENCY INITIATIVES BASED ON THE POET ENERGY MANAGEMENT FRAMEWORK

2.5.1 Conceptual level

2.5.1.1 Technology Efficiency

Energy usage data of healthcare institutions may be analyzed, to obtain the typical energy usage spectrum. In Fig. 2.1, the average energy usage of multiple healthcare institutions in South Africa, is shown in the form of a pie chart [39]. From the chart, it is evident that Heating, Ventilation and Air conditioning (HVAC) systems are the single largest energy intensive processes in healthcare institutions, contributing to 45% of the overall energy usage. Lighting consumes approximately 15% of the total energy in healthcare institutions and is the second largest consumer of energy. Medical and office equipment may consume up to 14% of energy, while the processes involved in water heating are responsible for 12% of energy used. The Central Sterile Services Department (CSSD), consumes significantly less energy, when compared to other processes, followed by the kitchen services department, occupying 6% of the total energy usage spectrum.

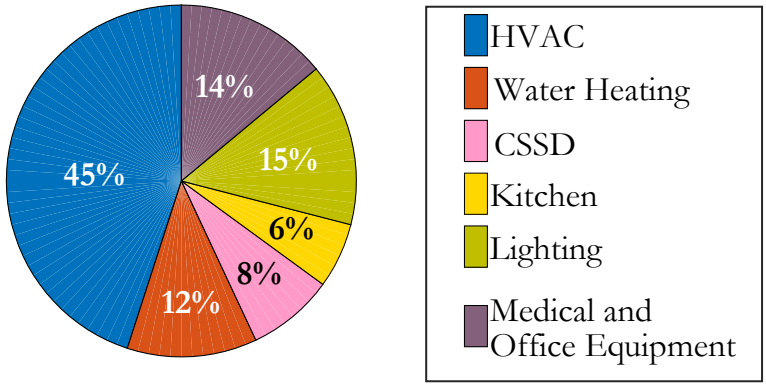

Fig. 2.1: Energy usage spectrum of hospital buildings in South Africa [4,39]

In retrospect, the two major thermal energy intensive processes, accounting for 59% of the overall energy usage, may be identified as HVAC and water heating systems. In this case, the thermal processes are selected, due to the large amounts of energy consumed and the potential for energy efficiency improvement. The remaining categories account for approximately 41% of the total energy consumed, the largest of which are lighting, medical and office equipment, followed by smaller loads, such as the kitchen and CSSD.

2.5.1.2 Equipment Efficiency

After identifying the energy intensive processes, in this case HVAC and water heating systems. Suitable decisions may be made to prioritize and justify equipment replacement. Improving energy efficiency at this level may entail replacement or retro fitment of existing equipment. In general, this improvement may further be referred to as building energy efficiency retrofit (BEER).

2.5.1.2 a) HVAC equipment

Considering HVAC processes, improved equipment components available on the market may be purchased and installed, replacing existing inefficient components. The typical layout of a large-scale HVAC system, is illustrated in Fig. 2.2. According to Ref [39], typical energy usage of HVAC components may be divided into five categories, including fans, cooling, heating, pumps and cooling towers. The energy usage of fans, cooling and heating account for 34%, 27% and 17%, respectively. Pumps and cooling towers are responsible for 16% and 6%, respectively. In hindsight, replacing existing equipment, responsible for these energy intensive processes, with higher efficiency equipment, may offer substantial savings. Furthermore, existing systems are usually outdated and subjected to poor performance, due to degradation over time. The main contributor to the degradation of these systems, may be a result of continuous operation, poor maintenance, and prolonged exposure to environmental conditions.

Moreover, recently developed equipment may offer substantial improvements, in terms of energy efficiency. For instance, the use of variable speed drives to control compressor systems in chillers, as opposed to standalone fixed speed compressors, may offer substantial savings. A demand response component is introduced, as opposed to the constant supply of compressed refrigerant being delivered by the conventional system. In addition, variable speed drives have similarly been introduced to water pumps and fans, to obtain further efficiency gains. Pumps are located in both the evaporator and condenser sections, while

fans, responsible for heat extraction and airflow regulation, are located at the condenser section and the air handling units, respectively.

Other improvements in HVAC design, may incorporate permanent magnet synchronous motors, rather than induction motors, offering average energy efficiency gains of up to 10.4% across the total speed range. To put this into perspective, the overall energy savings in HVAC systems may be as high as 8.58%, as a result of replacing induction motors. Permanent magnet synchronous motors may replace all existing induction motors in the HVAC system, so that overall energy efficiency may be increased. Additionally, permanent magnet synchronous motors generally operate at a near constant efficiency of approximately 96%, at any given speed percentile.

Moreover, when considering the evaporator, significant advancements have been made in recent years to improve evaporator performance. The most commonly used evaporator design in the past, was the flooded type, where refrigerant completely covered water conduits within the evaporator. Two other arrangements were introduced, to decrease the amount of refrigerant required to deliver the same results as the most commonly utilized system i.e. the Flooded type. A reduction in refrigerant may result in less energy spent, in terms of work required to compress and pump refrigerant around the cooling loop. These improved evaporator systems comprise of the mixed falling (MF) film evaporator and the full falling (FF) film evaporator. The MF type evaporator was observed to use approximately 15% less refrigerant than the conventional flooded type, while the FF type may reduce the required refrigerant up to 40%, as compared to the flooded type. Therefore, in choosing the FF type, the energy required through compression and pumping of the refrigerant may be reduced by approximately 40%. This roughly translates into energy savings of approximately 10.8%, considering the total energy usage of HVAC equipment [40].

Additionally, the use of state-of-the-art variable refrigerant flow (VRF) systems may offer savings of 30-40% on overall HVAC energy usage [41].

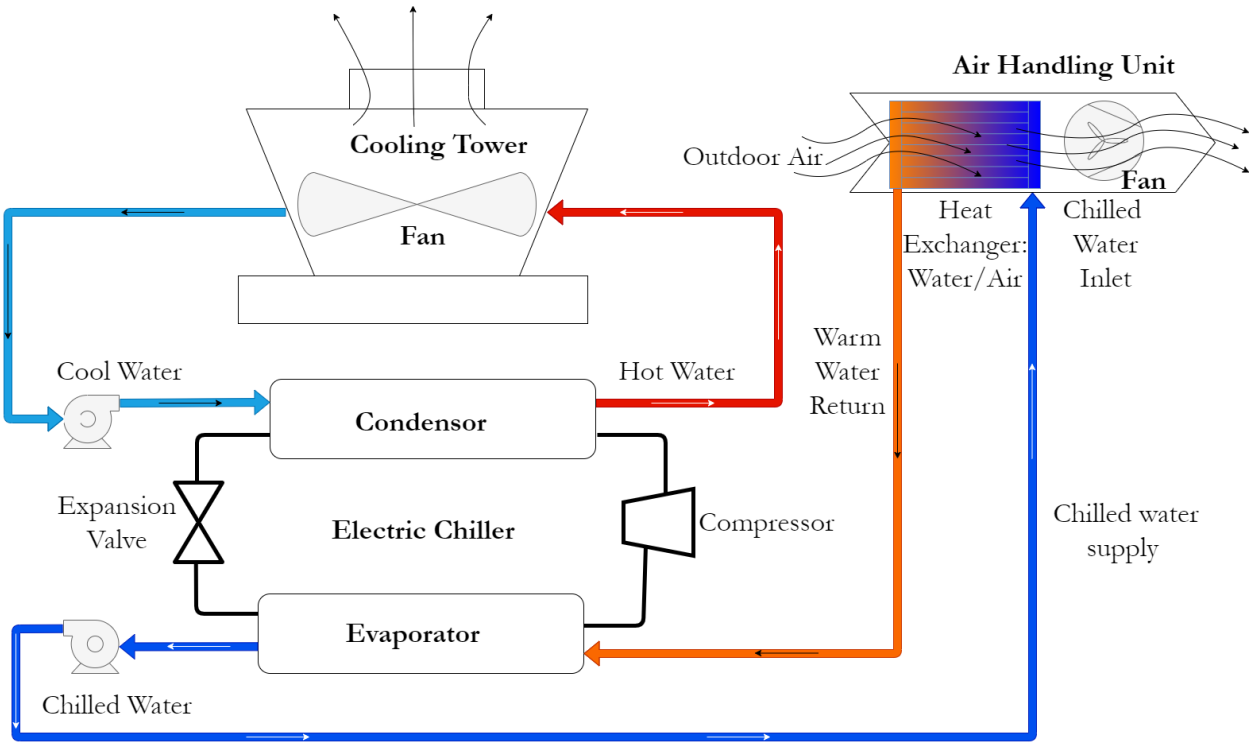

Fig. 2.2: HVAC system layout

2.5.1.2 b) Water Heating systems

Hot water availability in healthcare institutions is of utmost importance to maintain hygiene. While various water heating systems are available on the market, careful consideration is required in selecting the appropriate water heating device. Certain trade-offs exist between the various technologies used for water heating. For instance, the implementation of a heat pump water heater may result in an energy savings of approximately 65%, compared to a traditional electric storage tank water heater (ESTWH) [42]. A major drawback of the heat pump water heater, is the high failure rates and investment costs, as compared to the traditional ESTWH. These factors should be considered in the decision-making process, in terms of replacement.

An instantaneous tankless water heating system, as opposed to the storage tank type water heater, may further be considered. The instantaneous water heater or demand type water heater has the advantage of not being subjected to standby losses, compared to the tank type

water heater. A drawback of this type of system is the enormous amounts of energy required to achieve the temperature levels in a significantly short time [43].

Alternatively, the solar water heater may be considered as a standalone system at this level. However, this introduces the problem of the inadequacy of renewable energy availability, in terms of sufficiently supplying the demand [44]. Hybrid solar water heating systems are discussed at the technical level, as they form part of additional equipment retrofits.

2.5.1.3 Operation Efficiency

Addressing the operation efficiency of a building at this level, might entail basic energy management activities. The major improvement in operation efficiency may be achieved by mitigating standby energy usage of equipment. The four major energy consuming processes discussed in the technology and equipment efficiency section at a conceptual level, may similarly be addressed in this section, in terms of operation efficiency.

2.5.1.3 a) HVAC equipment

The improvement in operation efficiency, in this case, generally entails switching HVAC equipment *off* when consumers are not present and adjusting the set temperature, in order to reduce energy usage.

In Ref. [45], an experimental study was conducted on the impact of shutting down air conditioning systems in operating rooms (OR) on infection control and environmental aspects. In the study, the HVAC system was switched *off* for 10 hours and particles suspended in the air and near the operating table were counted. The OR air temperature was measured and settle plates were exposed and incubated. Conclusions made from results arising from 13 investigations, illustrated that switching HVAC equipment *off* when not in use, resulted in no significant increase in microbial contamination. However, it is recommended to initiate ventilation systems at least 30 minutes before any surgical activity is scheduled to take place. In retrospect, switching air conditioning systems *off* for 10 hours, as

opposed to leaving systems running continuously, may result in daily potential energy savings of up to 41%. Similar observations may be made for patient ward sections, provided that necessary hygienic procedures are followed.

In addition, an effective method of decreasing energy usage of HVAC systems, entails set point temperature adjustment. This involves increasing the cooling set temperature and decreasing the heating set point temperature. Previous research conducted on this matter has proven that by increasing the cooling set point from 22.2°C to 25°C, an approximate average energy saving of 27% may be achieved. Similarly, lowering the heating set point from 21.1°C to 20°C, may result in savings of up to 34 % [46]. Adapted for the South African climate and extrapolation, calculated annual potential savings may be in the order of 28.8%. This effectively translates into savings of 7.8%, in terms of the overall energy usage by HVAC processes.

In addition, considering the implementation of variable speed drives (VSD) at the equipment efficiency stage, basic motor speed matching with thermal loads may be applied, using VSD equipment at the operational level. This allows HVAC fans, pumps and compressors to operate in response to varying thermal load requirements, instead of simply operating in "*on*/*off*" mode.

2.5.1.3 b) Water Heating systems

During hot water demand occurrences, thermostat set temperature levels may be lowered, in order to shorten the *on*-time durations. According to [47], reducing the water heater thermostat temperature by 10°C, may result in savings of up to 5%.

2.5.1.4 Performance Efficiency

The performance efficiency is demarcated by the energy performance index (EPI) of the building or process. The energy security, energy usage, energy cost and carbon emissions per service delivered, may form part of a specific building's EPI.

Energy security of any building, may be enhanced by improving the reliability of supply. One method, entails the implementation of a back-up energy system, to mitigate the interruption of critical system operations. Popular systems include electrical energy storage systems, such as battery backups, in the form of uninterruptable power supplies (UPS) or generator sets. Healthcare institutions may prioritize energy security, due to the sensitive nature of load demands, as compared to other commercial type buildings. UPS systems may be implemented, in conjunction with generator systems, in order to increase the ride through capability of the power supply, in the event of power disruption. UPS systems may sustain the power supplied to the building for short periods, to mitigate the interruption of supply while generator systems are primed. When the generator systems are operational, a supply change-over action will occur, drawing power from the generator, instead of the inactive grid system [48].

The energy usage indicator, also considered at this level albeit basic, offers a tool for improving the performance efficiency. This carried out by evaluating a baseline energy usage profile, taken over a year (monthly intervals) and setting reasonable energy saving targets to be achieved in subsequent years. This would stimulate the implementation of "quick win" energy efficiency initiatives [49].

The energy costs and carbon emissions per service delivered, depends on the energy usage indicator. Assessing the trends of these indices may reveal a directly proportional relationship to the energy usage indicator. In retrospect, if reduced energy costs and carbon emissions are desired, a decrease in energy usage is necessary.

Therefore, improving the energy security and reducing the energy usage of the particular building or system, will result in an improvement of the performance efficiency and in turn, an increase in the overall energy efficiency [50].

2.5.2 Active level

The active level of energy efficiency improvement may require the implementation of additional equipment and software. This level has its emphasis on validation of the energy

usage data and energy efficiency improvement methods, previously established at the conceptual level. Therefore, at this level, further effort is required to improve overall efficiency.

2.5.2.1 Technology Efficiency

At this stage, low-cost rudimentary energy monitoring technologies are implemented and tested. Energy usage may be measured and logged, using web-based energy data acquisition, and monitoring technologies.

Web based energy monitoring systems may be linked to energy metering devices, in order to transmit real time data to technical personnel for condition monitoring. Real time data may be accessed online for increased convenience. These systems may be set to dispatch alerts to personnel, in the event of abnormal energy usages or fault occurrences [51].

2.5.2.2 Equipment Efficiency

At this stage, obsolete equipment has been replaced with higher efficiency equipment available on the market. However, limited energy management activities have been applied, increasing the equipment efficiency at the conceptual level. Therefore, in this section, basic energy management through the implementation of additional equipment is considered.

2.5.2.2 a) HVAC equipment

Recently developed HVAC systems, operating at higher efficiencies, have been purchased and installed. Nevertheless, external HVAC equipment efficiency improvement activities have not been considered. Hence, the following may be considered at the active level, to enhance HVAC equipment efficiency:

- Implementation of VSD motors may be considered, in addition to previously replaced equipment at the conceptual level. This may include the implementation of VSDs to

air handling units, to allow for energy efficient speed control, offering additional savings in energy [52].

- Reduce building air leakage, by replacing existing insulation of building envelopes with dynamic insulating materials, may offer maximum potential heating and cooling energy savings, particularly in mild weather conditions. Additional insulation may be introduced in the form of double-glazed windows, roof and door insulation, compliant with sans 10400-xa building laws, reducing the total heat exchange through building envelopes [53]. Revolving doors may be installed at entrances if a pressure differential is unavoidable, implementation is subjected to practicality and building accessibility considerations. Addressing building air leakage issues could potentially reduce overall HVAC energy usage by approximately 40% [54].

2.5.2.2 b) Water heating systems

Water heating systems may be subjected to standing or standby losses, in that stored hot water may lose thermal energy to the surrounding ambient air, over time. Large standing losses may be predominantly observed in electric storage tank water heaters (ESTWH) and hot water conduits with poor or no insulation. It is evident that standing losses may not be avoided all together, rather, a reduction is possible. This may be accomplished by implementing additional insulation to hot water storage tanks (geyser blankets) and conduits leading to points of hot water usage (pipe lagging). Geyser blankets may be introduced to hot water storage tanks, to promote energy savings of up to 21.74% per day, while pipe lagging may result in energy savings of up to 13.04%. Combined savings, as a result of insulation, may yield savings of up to 26.97% [55].

Standby losses may be prevented to a certain degree, by means of implementing low cost timer systems, to decrease the switching frequency of ESTWH. Timer systems may be set to relay power to the ESTWH system at a predetermined time, prior to when large hot water demands occur. These timer systems may work in conjunction with thermostats within ESTWH systems, to maintain the desired temperature, when required [56].

2.5.2.3 Operation Efficiency

The operation efficiency may be improved, by applying effective control techniques, in conjunction with the newly acquired equipment, as described in section 2.5.2.2. Therefore, in this section, human intervention will be discussed, in terms of implementing effective control techniques to improve the operational efficiency.

2.5.2.3 a) HVAC equipment

Operational efficiency of HVAC equipment is improved by reducing VSD operating speeds. In Ref. [57], a maximum energy saving of 83% was noted when motor speeds were reduced by 60%, while a minimum saving of 22% was obtained at a speed reduction of 10%, in terms of energy consumed by motors (fans) in air handling units (AHUs).

However, these speeds may not satisfy the sensitive load requirements of healthcare institutions. Therefore, intervention by technical personnel may be required to monitor and adjust VSD settings, in order to effectively manage these systems, according to load requirements. In retrospect, the reported maximum savings of 83% may, in fact, not be possible to maintain sufficient air quality. Rather, the only sensible energy saving projection may be located closer to the minimum possible savings of 22%. This translates into a minimum energy saving of 7.48% in terms of overall HVAC energy usage [57].

2.5.2.3 b) Water Heating systems

Operational efficiency may be improved in water heating systems, by evaluating the hot water consumption profiles of users and water temperature requirements throughout the year. The time required to reach the desired temperature and the variation of hot water consumption are major factors that requires consideration.

The lower temperature is dependent on climatic conditions and influences the time required to heat water to the desired temperature. For instance, the time required for water

to reach the desired temperature in winter conditions will be higher than that in summer conditions. Moreover, the high probability of the presence of the bacteria, known as legionella pneumophila in stagnant water ranging from 20°C to 45°C, may constrain the degrees of freedom in terms of operation. It may be recommended to allow water temperatures to reach at least 55°C daily, to guarantee sufficiently low levels of bacteria presence [58].

The amount of time required to heat water from approximately 25°C to 55°C, may be calculated to be 1 hour and 45 minutes, when using the power equation in Ref. [59].

2.5.2.4 Performance Efficiency

The energy security was improved at the conceptual level with the implementation of backup energy systems. Improving the reliability of these systems will, in turn, improve the performance efficiency at the active level. This may be accomplished by establishing a database of all backup systems, while further implementing monitoring devices.

Databases and monitoring systems may contain details of generator systems. These may include: load specifications, diesel storage levels and standby capacity [60,61]. The data pertaining to generator health, in terms of operating hours, temperatures and past maintenance, may be a valuable reliability of supply indicator. Similarly, vital UPS data may include state of charge, remaining charge cycles, voltage levels, temperatures and overall battery health [62].

Evaluation of this data might be useful in determining ads to when the system should be serviced or replaced, maintaining overall energy security.

2.5.3 Technical level

The technical level of energy efficiency improvement, features the implementation of further energy saving initiatives, while verifying the claimed energy efficiency of the conceptual and active levels. At this level, new energy technologies, retro fitment, automation

and control techniques, may be introduced. This level may further introduce cyber-physical systems, as a means to improve overall energy efficiency. Cyber-physical systems generally consist of physical, digital and biological elements operating in unison. Therefore, systems implemented at this level may enter the realm of the fourth industrial revolution, otherwise abbreviated as 4IR [62].

Additionally, at this level, basic energy management techniques may be applied in terms of demand side management. Large scale commercial buildings, such as healthcare buildings, are often subjected to Time-of-Use tariffs. These tariffs were implemented in order to provide an incentive to reduce energy usage during peak demand periods. Effectively implemented demand side management systems may offer substantial energy savings and, in turn, improve the overall energy efficiency respective buildings [63].

2.5.3.1 Technology Efficiency

Advanced web-based energy monitoring dashboards or supervisory control and data acquisition (SCADA) software may be implemented. The software is generally accompanied by measuring devices to provide an in-depth real time energy usage analysis of all major components. Monitoring dashboards form part of SCADA systems and may provide process control functionalities, depending on the software package and application [64]. In order to enable these functionalities, a few additional control devices i.e. programmable logic controllers (PLC) and relevant communication interfaces, such as remote telemetry units (RTUs) are required. This allows technical personnel to control processes, either locally or remotely [65]. Large networks of devices that allow for the control of processes remotely, while real-time data is monitored and logged through web-based systems, may form part of the Internet of Things (IoT). The presence of the IoT devices signals the arrival of the fourth industrial revolution and all the benefits associated with it. These benefits may include energy efficiency improvements to the highest degree [66].

In Fig. 2.3, the various energy monitoring topologies are illustrated. Basic energy monitoring allows web access and limited control functionalities through PLC devices, as

shown in Fig. 2.3(a). Fig. 2.3 (b) illustrates the basic SCADA system layout, while Fig. 2.3(c) introduces a dedicated energy management system to the SCADA network [67].

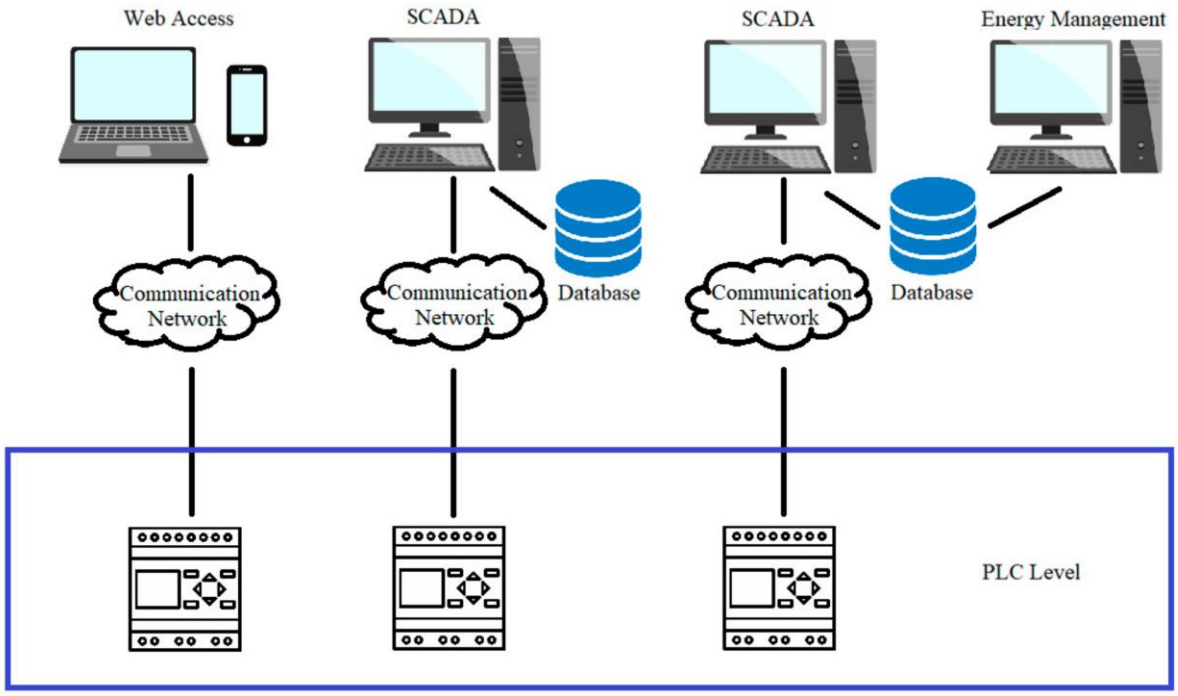

Fig. 2.3: Energy monitoring topologies of web based and SCADA systems

2.5.3.2 Equipment Efficiency

In order to improve the equipment efficiency at the technical level, the implementation of renewable energy source systems is considered. These systems may operate in conjunction with relevant energy storage systems, to increase the demand side management capability of processes. Systems designed to match the load requirements without storage, may offer electrical energy savings of up to 33% [68]. The implementation of hybrid renewable energy systems, depending on the design, may result in electrical energy savings, in the range of 33% to 100% [69]. However, it may not be economically feasible to implement hybrid renewable energy systems for a 100% reduction in electric grid energy usage. Therefore, these systems are optimally designed, in order to attain the lowest possible payback period. In hindsight,

for these systems, the objective is to minimize grid energy usage, based on the ToU electricity tariff.

The aim is to avoid the costly regions of the ToU tariff and use grid energy during the least costly periods. For instance, in the event that all grid energy usage is shifted to the least costly regions of the ToU tariff, an approximate energy cost saving of 52% may be obtained. This is mainly achieved with hybrid energy systems with energy storage capabilities [70].

2.5.3.2 a) HVAC equipment

The equipment efficiency of HVAC systems may be improved by implementing supplementary equipment to these systems; equipment retrofits relevant to healthcare institutions may include the following:

- The use of thermal energy storage (TES) systems or electrical energy storage (EES) in conjunction with HVAC schemes has been popularized in recent years, in that it increases the demand side management capability of these systems. Thermal energy storage systems may consist of either water, ice or phase change materials. These TES systems may shift a proportion of the electrical demand associated with cooling processes from peak to off-peak energy usage periods [71].
- Introducing solid-liquid phase change materials (PCM) to TES systems, may result in energy savings of 6 - 9 % in water chiller systems [72].
- Retrofitting conventional air-conditioning systems with evaporative cooling systems, may offer a saving of 12.05 % in overall building energy usage. Studies suggest that coupling existing systems with regenerative evaporative cooling systems provides potential energy savings of up to 15.69 % [73]
- The implementation of renewable energy systems may be considered, these may include photovoltaic (PV) or wind turbine systems, to reduce the peak energy usage from the electrical grid. These systems coupled to TES or EES may offer further improvements in equipment efficiencies [74].

- Additional PLC systems may be introduced to provide a wider range of control of the various processes that exist in HVAC systems. For instance, PLC devices may be implemented to control AHU units, VSD systems connected to multiple motor driven processes and set point temperatures [75].
- Heat recovery systems may be implemented, additional to existing HVAC systems. However, the efficiency of HVAC systems may not be improved, in that heat is transferred to another process. Other processes, such as water heating systems, may use recovered waste heat to increase the thermal level of water supplied to water heating units. This essentially means that the equipment efficiency of water heating systems is increased, in that water should be preheated prior to being supplied to water heaters, in order to decrease the temperature differential. The decrease in temperature differential should, in turn, reduce the energy required to raise thermal levels to desired levels [76].
- Implementation of multifunctional chiller (MFC) systems, or the replacement of existing chiller systems with MFC systems. Multifunctional chiller systems supply cooling loads, while waste heat is transferred to water heating schemes. Similarly, these systems may increase the equipment efficiencies of other equipment in healthcare institutions, such as water heating units [77].

2.5.3.2 b) Water Heating systems

- Renewable energy source systems, particularly solar water heaters, may be introduced to existing water heating systems. Solar irradiance levels in South Africa are amongst the highest in the world, making the solar water heater a viable option for water heating applications of any regions in the country. According to Ref. [78], a grid energy saving of up to 70% may be achieved, when adequately sized solar water heaters with an electrical backup-element are installed.
- Solar assisted heat pump water heaters, with state-of-the-art phase change materials for thermal energy storage, may be introduced to minimize grid energy usage [79].

- The implementation of hybrid water heating systems, consisting of heat pump water heaters and inline gas boosters warrants consideration. However, the economic feasibility of these systems may be called into question, considering the poor life expectancy and high initial implementation costs associated with heat pump water heaters.
- Implementation of preheated water storage tanks, in conjunction with solar water heater systems or hybrid water heater systems, to improve demand side management capabilities.
- Coupling waste heat recovery systems from multifunctional chillers systems have proven to be an efficient method of increasing thermal levels of preheated water storage systems. Preheated storage systems supply ESTWH, to improve energy efficiencies.
- State-of-the-art phase change materials (PCM) may be incorporated in solar collector storage systems coupled to ESTWH systems overcome thermal losses during night/overcast sky conditions and maximize hot water availability [80].

2.5.3.3 Operation Efficiency

The operational efficiency at the technical level is featured, by effectively managed energy efficiency initiatives at previous levels. This involves control techniques for demand side management, applied by suitably trained personnel, as well as necessary maintenance.

2.5.3.3 a) HVAC equipment

- Basic demand side management, based on Time-of-Use tariff structure, is exercised on systems with TES. HVAC systems charge TES systems during off-peak periods and discharge during peak periods, while load requirements are satisfied. Implementing basic demand side management may not reduce cooling energy usage, in most cases, rather a reduction in energy cost may be observed, if the energy

consumer is subjected to Time-of-Use tariffs. However, if effectively implemented, a maximum energy saving of 5% may be observed, while cost savings may reach up to 55%, in terms of cooling demand, as noted in [81]. In the case of renewable energy systems with energy storage, grid energy savings of up to 52% may be obtained.

- Implementation of Proportional Integral (PI) controllers to regulate temperatures of each zone individually/separately in a multi-zone building, without communicating any information to the neighbouring controllers [82].
- Relevant staff are trained to effectively operate and maintain HVAC, equipment given the new control parameters attained from newly implemented PLC devices, as discussed in the equipment efficiency section.

2.5.3.3 b) Water Heating systems

Water heating systems employed in commercial buildings usually consist of tank type systems, rather than demand type (tankless) systems. These include heat pump water heaters, boiler systems and the electric resistive storage tank water heater. Due to the presence of thermal storage in these systems, the demand side management potential is increased. This means that water may be preheated during less costly regions of time-based pricing structures. In addition, a large proportion of standby losses may be avoided, by scheduling water heating systems to switch on a predetermined time, prior to when hot water is drawn [83]. This reduces the energy usage of these systems, while maintaining load requirements. As a result energy efficiency is increased. In retrospect, this may only be accomplished when most of the hot water is drawn near the least costly regions of time-based pricing regions, or energy requirements may increase [84]. This may be achieved through the following:

- Demand side management is applied to water heating systems by adjusting timer controls to limit power usage during peak and standard periods of the ToU tariff. However, in most cases, energy savings may not be attainable, rather energy cost savings may be substantial [85].
- Energy usage is frequently monitored, in order to identify any potential problems.

- Basic load forecasting is conducted, and timer control settings are adjusted accordingly [86].

2.5.3.4 Performance Efficiency

The energy dashboard in SCADA or web-based systems, is an effective tool to monitor the performance efficiency of systems connected to the network. Energy targets may be set in terms of energy and cost savings.

In Ref. [87], a post-2015 National Energy Efficiency Strategy (NEES), Targets, Measures and Implementation Plan was drafted for the Department of Energy of South Africa. The plan was compiled by the Danish Energy Management division of the Danish Management Group, in April 2016. The plan presents specific goals for accelerating the current rate of improvement in energy efficiency per square meter of lettable/inhabited floor space, in the case of the commercial sector. Additionally, the draft plan provides a review on the status of current energy efficiency improvements, how goals may be achieved and indicators of successful energy efficiency improvement.

Under the current status section, the draft document elaborates on the maximum energy efficiency standards by building type, according to SANS 204:2011. Furthermore, the technical specifications to reduce the usage of energy in new buildings, was defined in the SANS 10400-XA in 2014 [88]. While it was noted that the construction industry has already met these targets in most cases, a further reduction in energy usage is required, in order to align with trajectories developed by CIDB and CSIR.

A major barrier in improving energy efficiency, is the practical and financial challenges faced when considering the retro fitment of the existing building stock. Healthcare institutions may face considerable challenges, in terms of practical implementation, due to the unique load requirements, as opposed to other commercial buildings.

In order to achieve the goal of improving energy efficiency according to the NEES document, the following measures were proposed:

- Introduction of mandatory Energy Performance Certificates (ECPs) under the SANS 1544. ECPs will be produced by an accredited body and enforced by legislation.
- Revision of the existing 12L tax incentive. The tax incentive, according to the Income Tax Act, 1962 (Act No. 58 of 1962), allows incentive for businesses to implement energy efficiency activities. The current 12L incentive offers a tax deduction of 95c per verified kWh saved, as compared to a baseline profile taken throughout one year. A review of the 12L incentive structure is required to accommodate the specific case of healthcare institutions, among other commercial energy consumers. As a result, the feasibility of improving energy efficiency may be increased substantially.
- Develop further tax incentives for deep energy efficiency retrofits. These energy efficiency retrofits entail the implementation of systems with high initial investment costs, resulting in higher payback periods, as compared to systems with relatively low investment costs which, in most cases, subsequently leads to lower payback periods. Tax rebates may be provided to encourage deep retrofits, which would, in turn, reduce payback periods of these systems to within acceptable timeframes.

In addition to improving energy efficiency, all the proposed measures promote job creation. Several other measures were proposed in the NEES document, the remaining measures not discussed in this section have either been addressed in previous sections in this Chapter, or do not hold definite relevance to healthcare institutions in South Africa and may not provide desired/anticipated impact.

The NEES document further states that a potential reduction of 37% in the specific energy usage may be achieved by 2030, compared to the 2015 baseline, if current energy efficiency improvement trends continue, while all proposed measures are implemented. Estimations, based on current trends, amount to an 11% reduction in specific energy usage by 2030. This prediction, however, does consider the effect of the current SANS 10400XA standards and not the proposed measures. Setting a precise target may prove challenging for the case of healthcare institutions. The target may depend on decisions to implement all or some of the proposed measures. If all proposed energy efficiency measures were to be implemented up to the technical level, energy targets of 37 % may easily be attainable.

Therefore, in the case of healthcare institutions, a target range may be provided, which would be subjected to changes according to government decisions to provide suitable incentives. Therefore, proposed energy targets for healthcare institutions, aligned with commercial building sector targets, is a 37% reduction in specific energy usage, relative to the 2015 baseline by 2030 [89].

2.5.4 Further improvement

The further improvement level, otherwise known as the engineering level, involves the implementation of specialized energy efficiency initiatives. This level may be featured by various optimization techniques applied to each POET component. This may entail a comprehensive energy monitoring dashboard, optimal maintenance plans and optimal operational control, to maximize the energy efficiency of the building, in order to ensure that energy saving targets are reached timeously [90].

2.5.4.1 Technology Efficiency

Improve the energy dashboard to include additional information, which may comprise of a simple maintenance schedule, based on training, data analysis and historic efficiency indicators. Additionally, an economic analysis functionality may be incorporated to provide information, which includes cumulative costs, predicted costs and time remaining on the payback period.

The implementation of advanced building automation systems, which provides optimal control functionalities applied to energy intensive processes, in this case, HVAC and water heating systems. Therefore, at this level, dynamic optimization strategies are applied, to achieve the maximum possible energy savings.

2.5.4.2 Equipment Efficiency

At this stage, equipment retro fitment or replacement, is no longer possible, as these activities were considered at previous levels. Therefore, at this level, improved or optimal equipment maintenance is considered, to maximize equipment efficiency. In order to establish a well-planned maintenance schedule, relevant staff will be trained to compile appropriate maintenance timetables, based on equipment specifications and requirements.

In terms of designing ideal equipment maintenance plans, the selection of an optimal maintenance policy is required. The appropriate policy should cover detailed maintenance actions and schedules. As defined in MIL-STD-721C [91], maintenance actions refer to restoring or retaining equipment to a specified condition. Furthermore, the actions may be categorized as corrective maintenance (CM) and preventive maintenance (PM). CM signifies actions performed as a result of failure (restoration), while PM refers to actions required to retain equipment conditions (prevention of failure).

Furthermore, energy dashboards may also be used to plan and compile schedules based on historic equipment performance. The frequency at which maintenance should occur would increase over time, as the equipment ages. This should further be considered, along with the environmental conditions that these systems might be subjected to. In the case of healthcare institutions, where uninterrupted operation is required, schedules should be carefully planned, as to not disrupt processes.

2.5.4.2 a) HVAC equipment

Regular maintenance of HVAC systems may increase energy efficiency; a number of studies quantified the potential energy savings as a result of effective maintenance. These studies are categorized in terms of: HVAC component failures and prospective energy savings for correcting failures in question and interviews with HVAC maintenance specialists. According to these studies, the following energy savings are possible, in terms of HVAC component maintenance [92]:

- Repairing or adjusting economizer actuators or dampers may offer savings of 14 to 40%.
- Repairing failed sensors may provide savings of up to 40% if these sensors are required for optimal economizer operation.
- Maintaining adequate refrigerant charges/levels may introduce savings of 5-11%.

In retrospect, the best practices in HVAC equipment maintenance may reduce energy usage in the range of 10 to 20%, while poor or inadequate maintenance may be responsible for increased energy usage on the order of up to 60% [93].

2.5.4.2 b) Water heating systems

In terms of water heating systems maintenance, the following may be considered [94,95]:

- Hot water conduits inspection (pipe lagging and leaks), leading to points of usage.
- Self-sacrificing anodes inspection and replacement on ESTWH.
- Drip tray outlet inspection (blockage removal).

2.5.4.3 Operation Efficiency

The operational efficiency may be improved, by implementing various dynamic optimization techniques. These techniques may be applied to individual processes and to hybrid renewable energy systems with storage capability. Hybrid renewable energy systems may be optimized, in terms of dispatched power, to achieve additional savings. This may be realized by optimally dispatching energy from renewable sources and storage systems to loads during costly regions of the ToU tariff. The storage systems are recharged during the low-cost regions of the ToU tariff. Excess energy may also be sold back to the grid subjected to a Feed-In-Tariff (FIT). However, grid energy savings may be small, compared to the associated energy cost savings. Energy savings in the order of 5-10%, may be expected, in terms of optimal power dispatch control [96].

Decreased costs of data processing, storage and communication over recent years, have encouraged the design and implementation of more complex optimization control techniques to commercial building processes. In particular, the implementation of model predictive control (MPC) techniques have gained popularity in recent years, due to the several advantages they offer, as opposed to other control techniques, which may include [97]:

- Implementation or use of a system model for anticipatory control, instead of corrective control.
- Incorporation of disturbance rejection through the use of disturbance models.
- Ability to operate closer to constraints and adjust for uncertainties.
- Ability to incorporate a wide range of operating conditions and time-varying system dynamics.
- Ability to effectively control slow moving processes, while subjected to time delays.
- Allow for multiple objectives through the use of a cost function.
- Superior control for processes with multiple control variables.
- Capable of controlling systems at the supervisory, as well as local loop levels.

The MPC method uses a system model to predict future states of the dynamic system process. The MPC controller generates a control vector, in order to minimize a predefined cost function subjected to disturbances and constraints over a certain prediction horizon. Control vector elements are computed for all sampling intervals in the prediction horizon. However, solely the first control vector element is applied at the initial sampling interval, while the remaining vectors are discarded. This process repeats itself for every subsequent sampling interval in the prediction horizon, so that an optimized control vector is generated for each sampling interval in the prediction horizon [98]. The cost function is formulated to achieve an objective.

In the case of improving energy efficiency, the objective will be to minimize the energy usage, or the costs associated with energy usage, while maintaining load requirements. A reduction in the overall energy usage may result in reduced energy costs. Therefore, an optimization algorithm using MPC methods are usually required, to improve the operation

of a certain process. The algorithm is developed to minimize energy usage, while considering time-based pricing, so that unnecessary energy usage may be mitigated. The ability of the MPC method to achieve multiple objectives may prove highly useful in this regard [99,100].

2.5.4.3 a) HVAC equipment

A large body of research has been conducted on controlling HVAC processes, particularly in terms of energy and cost savings. In Ref. [100], the authors have identified a total of 161 papers linked to MPC methods applied to HVAC processes in buildings. From reviewed papers, it was observed that the MPC approach is an effective method to improve HVAC efficiency. Reviewed papers included thermal storage systems, ventilation systems, window control and ground-coupled heat pumps, amongst others. The identified papers were published between 2008 and 2017. Additionally, in the same paper, it was noted that these algorithms result in typical energy savings of approximately 15-20%, as compared to conventional control methods. While a review of the most recently published literature (January 2018 to January 2020), revealed similar findings in terms of energy savings in commercial buildings, a limited number of papers was noted, concerning healthcare institutions in South Africa. It should be noted that past research on the subject may align with the specific case of South Africa, due to some similarities in the variation of system disturbances. However, the unique variability in the combination of disturbances, generally identified as weather, occupancy, cost of energy and loads, particularly in the case of healthcare institutions in South Africa, has not been considered. Therefore, further research in this regard is required, so that accurate approximation ranges could be presented, as opposed to the 15-20% average potential energy savings that MPC could offer in commercial buildings. In retrospect, a preliminary approximation of potential savings achievable may be noted to be approximately 15%.

The accuracy of data pertaining to potential cost savings may further be improved, by simulating processes and control in real-time. This may be achieved through real-time

simulation hardware and software. Moreover, valuable information, in terms of model validation, with regards to real-time dynamic process representation, may be obtained.

2.5.4.3 b) Water Heating systems

Improving the operational efficiency of water heating systems, particularly systems with thermal storage capability, merits attentive consideration. As discussed in previous sections, the set temperature levels, regulated by the thermostat, may be decreased, in order to save substantial amounts of energy. However, thermostat temperature levels may not be set below 55°C, so as to avoid infection from legionella bacteria. Furthermore, when effectively applied, the implementation of demand side management (DSM) activities has shown promising results in reducing the energy usage of water heating systems with thermal storage. In hindsight, the cost saving benefits of DSM activities may far exceed that of specific energy reduction. Several studies concerning the control of water heating systems for DSM have been conducted. In Ref. [101], it was established that when an autonomous optimal control approach was applied to resistive domestic hot water heaters for a particular case study, energy savings of 4% were noted, while energy cost savings of 12% was observed. Moreover, in Ref. [102], it was found that when applying optimal control to a resistive water heating system coupled, to a solar water heater, annual energy savings of 8.32% were noted, while cost savings of 32.86% were obtained, compared to timer-based demand side management applied to the same setup.

Furthermore, in Ref. [103], it was found that DSM activities applied to commercial buildings, using an inline heat pump water heating system, reduced the peak demand of water heating energy usage by 86%. As a result, a reduction of 36% was observed in the peak demand of the entire building. In hindsight, buildings subjected to maximum demand charges may benefit financially from peak demand reduction, otherwise known as peak clipping.

Other studies focused on the optimal control of water heating systems with hybrid renewable energy sources, to reduce grid energy usage and associated costs, as in Refs. [104-

112]. These studies applied open loop optimal control approaches, to control various hybrid renewable systems connected to heat pump water heaters, energy savings ranged from 23.4-51.23%, while cost savings ranged from 33.8-70.74%.

Additional opportunities for energy and cost savings exist in water pressure management. At this level, optimal water pressure management may be applied to further reduce energy usage and associated costs. Energy savings may be attained by implementing optimal control techniques to water pressure systems, which could reduce the energy consumed by pressure pumps and the amount of water lost in cases where leaks are prevalent. Reducing the water lost through leaks, particularly on hot water conduits, may lead to a reduction in hot water usage, which in turn, reduces the energy usage of water heating systems. In Refs. [108,109], an optimal control model has been implemented on water pressure management systems to reduce water leakage.

An MPC (closed loop) approach was applied to a hybrid resistive/heat pump water heater system, coupled to hybrid renewable energy systems subjected to ToU and FI tariffs in [110], energy and associated cost savings of 33.80% and 66.10% were achieved, respectively. From these studies, it may be evident that, to attain maximum energy and cost savings, the implementation of hybrid renewable energy systems and hybrid water heating systems should be considered. Furthermore, in terms of controlling these large multivariable systems, the closed-loop MPC strategy seemed to be the most fitting. Although the MPC approach may in general be computationally expensive, it delivers the only real platform for addressing control problems involving the state, in the presence of constraints and the ability to account for constraint violations [113].

2.5.4.4 Performance Efficiency

As discussed at the technical level, the proposed target for the commercial sector is a 37% reduction in the overall specific energy usage by 2030, relative to a 2015 baseline. Sub-targets may be established in accordance with the various energy efficiency initiatives, applied to energy intensive equipment. These sub-targets may align with potential energy savings, as a

result of implementing these initiatives. Further, the assigned sub-targets may be enhanced, by including financial budget constraints, payback periods and the time allocated to equipment retrofits. In order to improve the accuracy of the aforementioned feasibility measures, savings from tax incentives and rebates should be taken into account. Additional expansions to energy dashboards may be considered, these may include major performance efficiency indicators, as described in Section 2.3. These indicators, comprising of energy cost, carbon emissions, energy losses, skill and knowledge levels of staff, equipment life cycle costs, cost to benefit ratios, among others, may provide valuable insight to energy managers for further efficiency improvements.

In addition, energy dashboards may be linked to other healthcare institutions or branch facilities, in order to compare and evaluate the impact of energy efficiency initiatives in various scenarios. In hindsight, increasing the data measurement and model verification ability of institutions may improve evidence-based policy making [115].

Moreover, when considering the specific case of health care institutions, the security and reliability of the energy supply is of utmost importance. This introduces a problem when implementing unproven optimization techniques, where a risk of disrupting crucial processes may exist. Therefore, system models and optimization techniques should be validated before implementation. This may be possible using real-time simulation hardware and software. In recent years, the cost of real time simulation technologies decreased significantly and, as result, validating models and control techniques have been less costly and time consuming [113]. Any given process may be modelled and simulated using real time technologies, while a physical controller may be tested offline before implementation [116,117]. In this case, a real-time simulator, with analog and digital I/Os, may represent the operation of an existing process and emulate the behaviour of the process, so that a pre-programmed controller may respond accordingly [118]. This will allow the programmer/engineer to detect any errors before implementation. In addition, control loops and tuning factors of various control devices may be adjusted, in order to satisfy system constraints without compromising the actual system.

Major systems may require the use of fast, scalable and flexible real-time simulators to improve model validation and data verification and, in turn, play a key role in improving the performance efficiency of a system and ultimately the overall energy efficiency [119].

2.6 KEY FINDINGS ON REVIEWED LITERATURE

2.6.1 POET-perspective analysis

The POET energy management framework is an effective tool for evaluating and improving a building or large-scale systems' energy efficiency. Potential energy efficiency improvements may be proposed, based on the four POET energy management levels. As discussed throughout this Chapter, these are: the conceptual, active, technical and further improvement level.

A systematic review was conducted, from a POET perspective to which three research questions were raised. The research questions and the motivation behind the questions are presented in the method section of this Chapter. The first research question was introduced, to evaluate the existing evidence base regarding potential energy and cost savings of energy efficiency initiatives applied to healthcare institutions. This prompted the need for an extensive search of available literature. A large body of scholarly articles were available on energy efficiency initiatives with regard to HVAC and water heating systems. However, studies were limited for the specific cases of healthcare institutions. It was further necessary to obtain regional data to assess the environmental influence on particular case studies. For these instances, research was similarly limited. Therefore, with the available data from scholarly articles, approximations were made to attain average energy savings for each energy efficiency initiative. These energy savings are presented throughout the previous sections of this Chapter, while averaged savings at each level is depicted by Fig. 2.4.

The second research question was: "Can healthcare institutions reach energy targets in order to align with trajectories developed by CIDB and CSIR through effective implementation of these initiatives?". In section 2.5.3.4, it was determined that healthcare

institutions may reach energy targets, if proposed measures at the technical level were to be implemented. This, however, depends on the economic feasibility of implementing these measures and external stimulus from government. Therefore, the third research question considers the feasibility of each initiative at each corresponding level of the POET framework.

As previously described, the conceptual level may be analogized by the pareto principle, which denotes a profit (energy saving in this case) of 80% will be attained for an effort of 20%. In retrospect, the subsequent levels may require increasing amounts of effort, in order to achieve significant savings. Comparatively, this means that the rule may roughly change to "60/40" for the active level, "40/60" for the technical level and "20/80" for the further improvement level. This rule may be partially substantiated by comparing the energy savings and payback periods for each of the POET levels in Fig. 2.4 and Fig. 2.5, respectively.

Fig. 2.4 illustrates the maximum potential energy savings attainable at each level. These savings do not account for renewable energy savings, the savings illustrated, were based on electrical energy supplied from the national electricity supplier. It should further be noted that these energy savings were extrapolated, based on findings from available research, as discussed in the previous sections. Therefore, the savings illustrated in this Chapter may only serve as the best-case scenario. Furthermore, the corresponding payback periods have been calculated and extrapolated, based on previous research conducted at each energy management level of POET and is illustrated in Fig. 2.5. In Fig. 2.4 and 2.5, it may be observed that the required effort at the active level is higher, compared to the conceptual level, while it was observed that the resulting energy savings decreased. Only at the technical level, a substantial improvement of energy savings may be observed, as compared to the active level. However, this may be accredited to the implementation of external energy sources, such as renewable energy supplies.

In Fig. 2.5, it may be noted that at the conceptual level, relatively low payback periods for energy efficiency initiatives are to be expected for comparatively high returns. The energy savings drop in Fig. 2.4 during the active level, while a similar trend is observed for the payback period in Fig. 2.5. Further investigation shows that the amount of effort required

to attain significant energy savings at the technical level, in terms of cost, is exceedingly high compared to previous levels.

In most commercial buildings, a system may be deemed economically feasible if the payback period does not exceed 2-4 years [120]. In the case of implementing renewable energy systems, payback periods generally range from 6-12 years. This introduces a predicament, with regards to the justification required for implementing these systems. As a result, additional energy efficiency initiatives may be employed, in order to reduce payback levels and, in turn, the feasibility of these systems. These initiatives were discussed in the further improvements section. This section is mainly featured by optimal operation and maintenance of systems. It may be noted that the energy efficiency improvement potential dropped significantly, as compared to the technical level. However, an average saving of approximately 10% may be attained for relatively low effort, as noted by the comparatively shorter payback periods.

In retrospect, the further improvement section may provide further incentive for the implementation of efficiency measures at the technical level. This implies that the implementation of proposed initiatives up to the further improvement level, may offer the maximum return on investment.

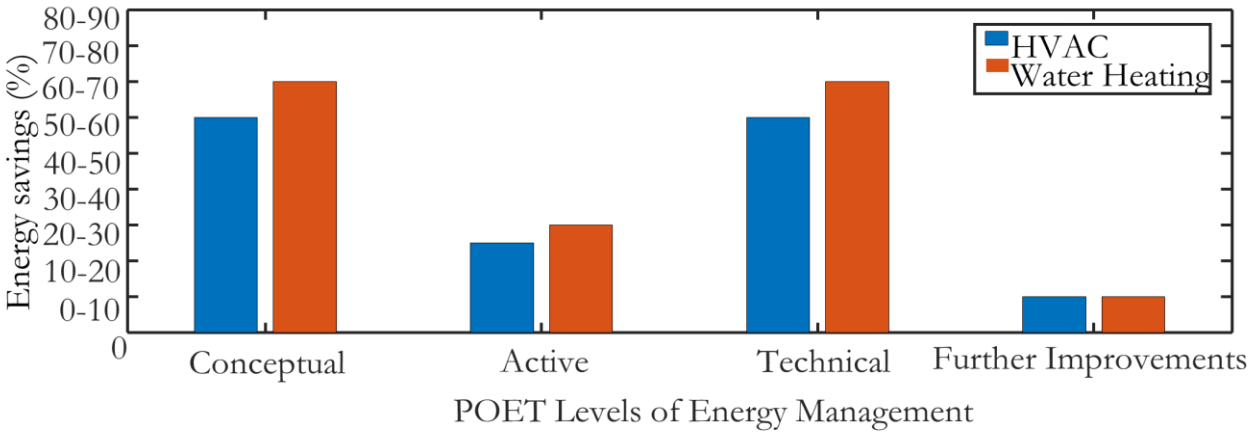

Fig. 2.4: Maximum potential energy savings attainable for each POET energy management level

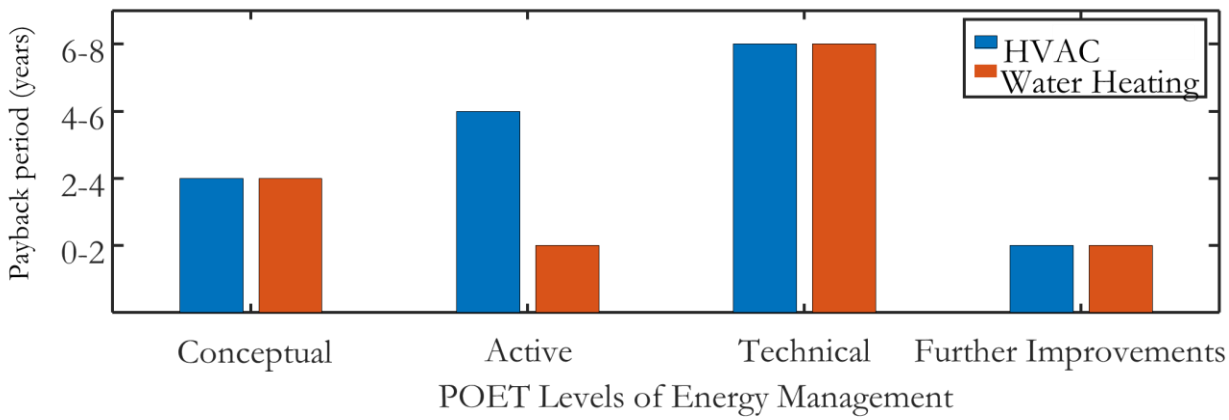

Fig. 2.5: Expected payback period for each POET energy management level

2.6.2 Addressing deficiencies in current available research

It may be challenging to accurately quantify energy savings attainable through optimization prior to implementation, particularly for the case of South African healthcare institutions. A large body of research exists for controlling standalone HVAC and water heating systems, to reduce energy usage and associated costs in commercial buildings. This is particularly true for cases where buildings are subjected to time-based pricing. However, a major deficiency has been observed in research, for the coordinated optimal control of large-scale systems, such as high-capacity HVAC units and multifarious water heating systems. Coordinated optimal control techniques may potentially minimize energy costs, with respect to time-based electricity prices, as well as maximum demand penalty charges.

In hindsight, the potential energy and cost benefits of implementing renewable energy systems, particularly solar systems for the South African climate, for these energy intensive processes have been studied thoroughly. Nevertheless, these studies often only consider stationary PV configurations. A further absence of research was observed on solar tracking PV systems, the potential energy and associated cost (ToU and maximum demand) savings during high demand periods.

Therefore, addressing some of the identified deficiencies in current research may involve studies where renewable energy technologies, particularly solar tracking systems, with energy storage and optimal control, is applied to HVAC and water heating systems. The optimal

control approach may be implemented as an additional energy efficiency initiative, to minimize energy costs based on the ToU tariff and maximum demand charges. This is addressed in Chapter III, where a hospital building in Bloemfontein region, South Africa, was chosen as the case study. Moreover, a deeper investigation into the equipment involved in HVAC and water heating processes may offer opportunities for further potential savings. Therefore, a study, with a focus on the optimal control of a multifarious water heating system with HVAC waste heat energy recovery, is discussed in Chapter IV.

The results attained from these studies may assist in providing the additional quantifiable data that is necessary for effective decision making, regarding the implementation of energy efficiency initiatives.

2.7 CONCLUSION

The energy usage intensity of healthcare institutions, particularly in South Africa, are nearly three times that of typical commercial buildings. Electrical energy usage per bed may range from 43 to 92 kWh per day. Identifying energy intensive processes and areas for improving energy efficiency is essential for reducing the energy usage of any building or large-scale system. The two main thermal energy consumers in South African hospitals were identified as HVAC and water heating systems. These processes account for approximately 59% of the total energy consumed in the evaluated buildings. Therefore, in this Chapter, the POET framework was consulted to improve the energy efficiency of these energy consumers. The POET framework served as an energy management guideline, to assess energy and cost saving potentials. Energy efficiency initiatives and associated potential energy savings were identified at each level, which included: the conceptual level, active level, technical level and further improvement.

The sustainability of the energy management program was introduced and discussed. Additionally, the maximum estimated energy savings, as a result of implementing the proposed systems, were provided. Average possible energy savings ranged from 60-70% at the conceptual level, while energy savings of 20-30% may be expected for energy efficiency initiatives, at the active level. EE activities at the technical level and the further improvement

level, may result in savings of 50-70% and 5-10%, respectively. These savings may not be attainable in some instances, due to economic barriers. These barriers are particularly prominent at the technical level and arise from high implementation costs and, in turn, long pay back periods as a result of deep energy retrofit projects or renewable energy system implementation. However, external stimulus from government remains imperative, in order to reach the set energy reduction target of 37%. Findings from previous research indicate that optimization techniques, discussed at the further improvement level, may offer substantial savings for relatively low implementation costs.

In retrospect, the observed deficiencies in research that were discussed in the previous section, may be addressed, through economic feasibility studies on the implementation of renewables, energy recovery and storage systems, as well as coordinated control techniques applied to these systems. Therefore, in an attempt to decrease the identified deficiencies, the following chapters include coordinated optimal control strategies applied to proposed or existing systems in order to ascertain the maximum potential energy savings. The proposed systems are economically assessed, to determine the feasibility, with and without the application of optimal control techniques. This may increase the availability of data for increased accuracy of potential energy savings and subsequent payback periods at the higher levels of the POET hierarchy. Subsequently, informed decisions may be made regarding the implementation of these energy initiatives, particularly for high investment deep energy retro-fitment projects.

CHAPTER III: OPTIMAL POWER DISPATCH OF A GRID-CONNECTED PV TRACKING SYSTEM WITH ENERGY STORAGE IN A HEALTH CARE INSTITUTION

3.1 INTRODUCTION

In the case of healthcare institutions, where the demand is non-deferrable, renewable and energy storage systems may contribute to a reduction in both, the operating costs and the reliance on the electricity grid [6]. The energy production from these systems should be subjected to effective control techniques, to ensure the load demand is continuously met, while energy costs from the electricity grid is minimized [121].

In this Chapter, multiple dual axis PV tracking systems with energy storage is proposed to be implemented in conjunction with the existing grid connection in the chosen case study. A large-scale medical facility in Bloemfontein, South Africa, was selected as the case study. The proposed dual axis PV tracking system with energy storage will supply HVAC, water heating and other critical equipment in the case study building. The dual axis tracking system was proposed, in order to meet the available space requirements on the roof of the building. The medical facility is located in a metropolitan area, this means that if these systems were to be mounted on the ground level, the PV tracking systems may be rendered ineffective in terms of power production, particularly during early mornings and late afternoons. Appropriate cost-effective support structures may be implemented on the roof top of the building to distribute the weight of the dual axis tracking systems. This may reduce the strain on the roof of the medical facility. Further preference was given to the dual axis PV system over the widely used stationary mounted PV systems due to the tracking systems' ability to produce power during a large portion of the costly ToU tariff regions. Therefore, in terms of the effective PV array, the dual axis system provides a higher energy yield over time as compared to the stationary system. Additionally, during these regions, the risk for incurring unnecessarily high maximum

demand charges is particularly high. The implementation of this system may reduce the risk of being liable for excessive maximum demand charges and ToU tariff costs [122,123].

Therefore, a mathematical model for the optimal dispatch of the proposed systems' power flow is discussed. The model was developed with the aim to minimize energy costs with respect to the ToU tariff and maximum demand charges.

The collected case study load profile data and model development are discussed in Section 3.2, while the validation of the model is presented in Section 3.3. In Section 3.4, the case study, as well as the variable input data and simulation parameters are presented. Section 3.5 provides the simulation results with section 3.6 concluding the Chapter.

3.2 MODEL DEVELOPMENT

3.2.1 Healthcare institution load profile description

Load from one of the transformers, that supplies HVAC, water heating and other critical equipment, in the selected healthcare facility, Mediclinic in Bloemfontein, South Africa, was measured at 30 minute intervals. The HVAC equipment consists of several chillers, one of which is a multifunctional chiller (MFC). All chillers are connected to air-handlers, while the MFC has an additional supply to a waste heat energy storage system. These chiller systems are located on the rooftop of the healthcare facility. In Fig. 3.1, three cooling-only chillers are shown, while Fig. 3.2 depicts two chiller units, the chiller on the left is a cooling-only chiller, and on the right, the MFC is shown.

In Fig. 3.3, a single ESTWH is depicted and represents the many water heating units, distributed across the building. The MFC, through the recovered waste heat storage system, supplies a total of 57 multifarious ESTWHs.

Fig. 3.1: Cooling-only Chillers for HVAC services

Fig. 3.2: Cooling-only chiller (left) and multifunctional Chiller for cooling and waste heat recovery (right)

Fig. 3.3: One of the ESTWHs located inside the medical facility

Relatively small changes in the load profile were observed for the last three years (2018-2020). The monthly energy usage of the medical facility remained fairly similar. Therefore, a well founded assumption will be that the load profile will remain similar for the following years in the near future. The load profile for 2018 was considered in this study, due to availability of input variable data. The most reliable dataset with respect to all input data, including the data used in the following sections, was observed for the selected year. The renewable energy resource and temperature may further be expected to change somewhat from one year to the next. However, this data deviates marginally from average data over a 10-year period. Conclusively, the proposed optimal control approach is capable of minimizing the energy costs for any given dynamic input data set. Nevertheless, the resultant potential energy savings may change for each year under evaluation, depending on the data used for a specific case study.

The measuring device used to acquire the load data, was a Circutor three-phase power analyzer (CVM NRG 96), shown in Fig. 3.4. This device conveys readings from current and voltage transformers, connected at the electricity grid supply point of the healthcare institution. The device translates the measured values from the transformers to voltage, current, active power, reactive power, apparent power and power factor within accuracy ranges

of 0.5-1%. The readings in real time from the Circutor are relayed and then logged at 30-minute averaged intervals using a third generation (networked) supervisory control and data acquisition (SCADA) system.

Fig. 3.4: Circutor three-phase power analyzer

Evaluating the load data, revealed that the maximum demand on the transformer corresponded to the total maximum demand of the entire supply system for that year. The annual load profile of the transformer is shown in Fig. 3.5, the highest load demand occurs during the summer months, particularly in January, November, and December. This is in part due to HVAC systems operation to maintain desired air temperatures within the facility.

During the winter months, also referred to as the high demand season by Eskom, the load remains relatively consistent, rarely exceeding the 475-kW mark. In retrospect, assessing the peak energy usage patterns for the year, reveals that the maximum demand takes place in November. These peaks often exceed the 600-kW mark. This may equate to an additional $5 500 USD per month, when considering only the maximum demand charges on this specific load. Upon further evaluation of the electricity bill of the healthcare institution, approximately 23.8 % of the total bill may be allocated to maximum demand charges. Additional charges or penalties may apply when exceeding the maximum notified demand threshold. The necessity for investigating the energy efficiency or energy management strategies is therefore

substantiated, if significant cost reductions may be achieved, based on maximum demand charges and the ToU tariff.

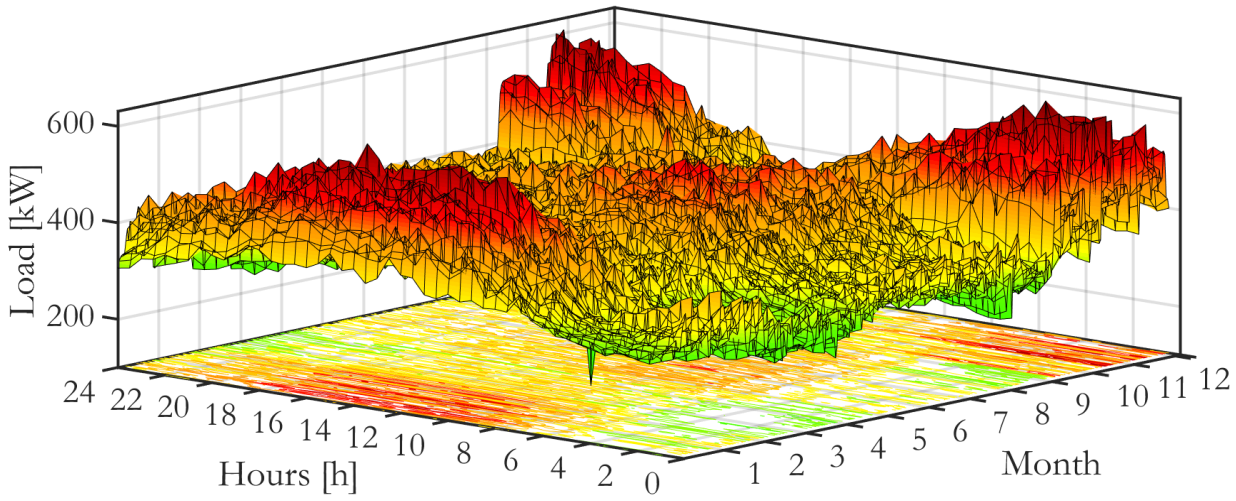

Fig. 3.5: Healthcare entity's annual critical load profile (2018)

3.2.2 Proposed system description

Solar resources in the Bloemfontein area are in abundance, wind on the other hand is highly intermittent [124]. Therefore, to achieve maximum energy savings, a solar PV system is recommended. However, as stated in the introduction of this Chapter, the available space at the healthcare entity is limited. A viable solution to this, is the implementation of dual axis PV tracking systems, which would effectively reduce the PV mounting space required, as compared to a stationary PV system. In addition, an electrical energy storage (EES) system may improve the demand side management capability of the healthcare institution and offer recompense for solar unavailability after sunset. Therefore, a hybrid energy system consisting of a dual axis tracking Photovoltaic (PV) system and EES scheme, with grid connection, is proposed. The PV tracking array supplies energy to the essential load and the EES scheme. The EES scheme may, thereafter, supply the load when it is most economical. This configuration has been proven to reduce energy costs in any building structure and may be

applied to healthcare institutions in locations where solar irradiance is in abundance. The power flow arrangement between the four components is shown in Fig.3.6.

Power from the PV system is to be transferred to the load and in the event that excess is power generated, the EES will be charged. Electrical energy is supplied from the grid to the load as a last resort and when necessary to recharge the EES.

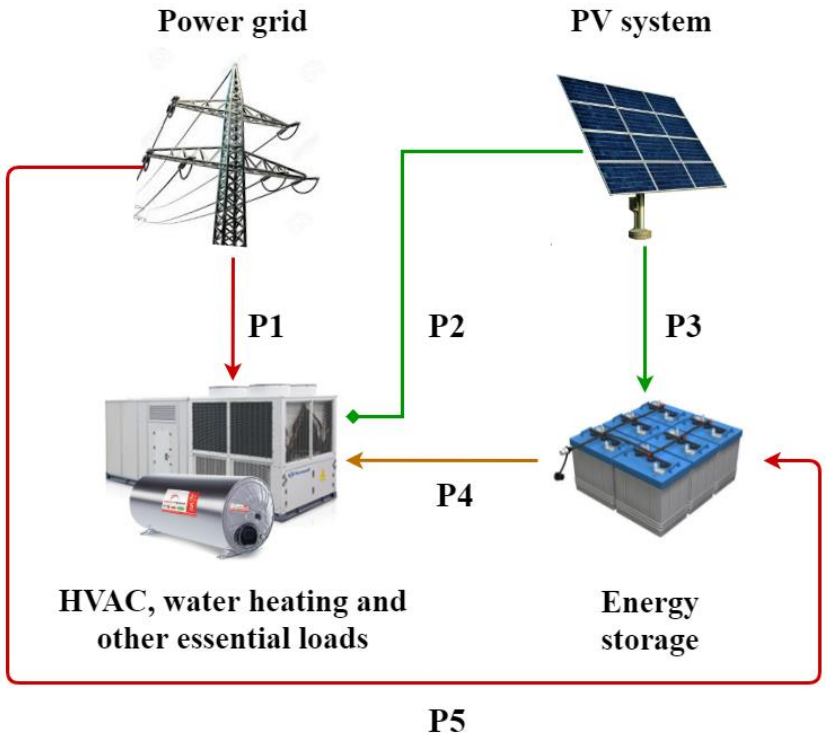

Fig. 3.6: Power flow diagram for the proposed system

Thereafter, the EES may discharge to the load during the high-cost regions of ToU tariff, while solar irradiance and subsequent energy from the PV is insufficient to meet the demand. Therefore, the load requirements are met by the following sequence of priorities; PV, EES and thereafter the grid. The different power flows from Fig. 3.6 may be defined as follows (power flow and all other power figures noted in this Chapter refers to kW, due to the size of the system components):

- P_1: Power from the electricity grid to supply the load.
- P_2: Power from the PV tracking system to the load.

- P_3: Power from the PV tracking system to the EES.
- P_4: Power from the EES to the load.
- P_5: Power from the electricity grid to the EES.

3.2.3 Objective function

The main objective of the developed optimal energy management model is to minimize the daily operation cost function, while optimizing the dispatch of energy for a 24 hour simulation horizon. The ToU tariff is a constituent of the objective function, due to its variation over the 24-hour horizon. A separate method is developed to obtain the optimal threshold for maximum energy savings, in terms of maximum demand. This method is discussed in Section 3.4.1. Consequently, the objective function may be expressed mathematically, as follows:

$$f_1 = min\sum_{j=1}^{N}[\rho_j(P_{1(j)} + P_{5(j)})]\Delta t, \tag{3.1}$$

where: f_1 is the cost function to be minimised, resulting from the different power flows from the grid (P_1+P_5); ϱ_j is the cost of electrical energy from the grid which is demarcated by the ToU tariff further described in Eq. (3.16) and Eq. (3.17); j is the evaluated j^{th} optimization sampling interval; N is the total number of sampling intervals; Δt the evaluated sampling time in the simulation.

In addition, a secondary cost function may be employed to maximize the PV output power transferred to the load, as it is the most efficient use of energy obtained from the renewable resource.

$$f_2 = \max\sum_{j=1}^{N}[P_{2(j)}]\Delta t. \tag{3.2}$$

Where: f_2 is the cost function to be maximized; resulting from the power flow (P_2) from the PV tracking system, as shown in Fig. 3.6.

3.2.4 Variable constraints

3.2.4.1 Load power balance

The load power balance that may be observed in the proposed system, are expressed as follows:

$$P_{Load(j)} = P_{1(j)} + P_{2(j)} + P_{4(j)}. \tag{3.3}$$

Equation (3.3) denotes that the load demand should be met by a combination of the different variables P_1, P_2 and P_4 for each sampling time "j".

3.2.4.2 Inequality constraints

At any sampling time (j), the sum of instantaneous grid power for supplying the load demand or for charging the EES, should be less or equal to the maximum power supplied by the grid. This constraint is given as follows:

$$P_{1(j)} + P_{5(j)} \leq P_{PG(j)}^{\max}. \tag{3.4}$$

Similarly, for each sampling interval (j), the sum of the power flows from the PV system to the EES and the critical load should not exceed the power produced by the PV system.

$$P_{2(j)} + P_{3(j)} \leq P_{PV(j)}^{\max}. \tag{3.5}$$

Furthermore, the sum of the power delivered from the PV system and the grid, should not exceed the rated capacity of the EES scheme.

$$P_{3(j)} + P_{5(j)} \leq P_{EES}^{Rated}. \tag{3.6}$$

3.2.4.3 EES state of charge

At any given sampling interval (j), the battery state of charge (SoC), may be expressed as:

$$SoC_{(j)} = SoC_{(j-1)} + \frac{\Delta t}{C_n} \times \left(\eta_{Ch} \times \sum_{j=1}^{N} (P_{3(j)} + P_{5(j)}) - \frac{\sum_{j=1}^{N} P_{4(j)}}{\eta_{Disc}} \right), \quad (3.7)$$

where: $SoC_{(0)}$ is the initial state of charge at the beginning of every sampling time; C_n is the nominal capacity of the battery storage system in kWh; η_{Ch} and η_{Disc} are the battery charging and discharging efficiencies, respectively.

3.2.4.4 PV power output

The output power of the PV array, may be modelled using Eq. (3.8), as follows [123-125];

$$P_{PV} = P_{PV,STC} N_{PV_P} N_{PV_S} \frac{I_{total}}{1000} [1 - \alpha (T_{cell} - 25)], \quad (3.8)$$

where: P_{PV} is the output power generated by the PV at maximum power point, while subjected to standard test conditions (STC). N_{PV_P} and N_{PV_S} are the number of PV panels connected in parallel and series, respectively. I_{total} denotes the total solar irradiance on a tilted surface, measured in Wh. α represents the temperature coefficient of power. T_{cell} is the temperature of the PV cell in °C. The cell temperature may further be calculated using equation (9) as follows [125];

$$T_{cell} = T_{amb} + \frac{I_{total}}{800} (T_{NOC} - 20), \quad (3.9)$$

where: T_{amb} is the ambient air temperature [°C] and T_{NOC} is the nominal operating cell temperature [°C]. The total irradiance (I_{total}), received by the PV cell, may be calculated with respect to the three components of solar irradiance. These components are direct normal

irradiance (DNI), diffuse horizontal irradiance (DHI) and global horizontal irradiance (GHI) noted as I_{DNI}, I_{DHI} and I_{GHI}, respectively. Eq. (3.10) denotes how these components of solar irradiance may be incorporated to determine the total irradiance on a tilted surface [126];

$$I_{total} = I_{DNI}\cos\theta_{\beta} + I_{DHI}\left(\frac{1-\cos\beta}{2}\right) + \rho I_{GHI}\left(\frac{1-\cos\beta}{2}\right), \tag{3.10}$$

where: θ_{β} is the angle of incidence of the solar irradiance on a tilted surface in degrees (°); β is the tilted angle in degrees (°); ρ is the reflectance factor of the surrounding area.

The model was used to simulate the operation of the dual axis system. The azimuth angle of the sun and tilt angle data retrieved from a SOLYS 2 sensor installed at the Central University of Technology, discussed in Section 3.4.2, was used in the model, to represent a dual axis PV tracking system. The SOLYS 2 sensor tracks the sun, in order to record the solar irradiance intensity. At every recording interval, the SOLYS 2 logs the tilt angle of the sensor, which is perpendicular to the sun's rays. This allows for accurate measurement (sensor), as well as maximum solar irradiance absorption, in the case of PV cells. The single fixed tilted angle in Eq. 3.10 of a stationary PV array, was replaced with the variable tilt angle data (recorded every minute), from the SOLYS 2 sensor, to account for the sun's altitude. Similarly, the variable azimuth angles of the sun were used to calculate the incidence angle of the solar irradiance on the PV surface, at every time interval.

3.2.4.5 Variable boundaries

In order to abide by the safety requirements, the power flow from the various power suppliers in the system should be operated within their minimum and maximum boundaries, according to the specifications of design from the manufacturer [127]. For all the control variables linked to the power flows, these constraints may be expressed as:

$$0 \le P_{i(j)} \le P_{i(j)}^{\max}, \tag{3.11}$$

where: i represents the different control variables; $P_{i(j)}^{\max}$ is the maximum power limit on each respective system, depending on the resource. However, the maximum power may be written as $P_{i(j)}^{Rated}$,in the case where control variables are linked to the battery.

As the state of charge of the battery scheme is the only state variable in the system, the boundaries subjected to this variable may be denoted as [125]:

$$SoC_0 \leq SoC_j \leq SoC^{\max}. \tag{3.12}$$

3.2.4.6 Exclusive power flows

Since the flow of power is limited to one direction at each interval (power flow for charging and discharging may not take place simultaneously) of the EES scheme; the product between the EES system input and output power should be zero, as expressed in the Eq. (3.13), below:

$$(P_{4(j)}) \times (P_{3(j)} + P_{5(j)}) = 0. \tag{3.13}$$

3.2.4.7 Fixed-final state condition

In order to showcase repeated implementation, the optimal control of the hybrid energy model between the components in the system, the SoC of the EES at the end of the control Horizon, should be equal to the SoC at the inception of the control horizon. This may be expressed mathematically, as follows [127]:

$$\sum_{j=1}^{N} \left(P_{3(j)} + P_{5(j)} - P_{4(j)} \right) = 0. \tag{3.14}$$

3.2.4.8 Solver selection

With reference to Eq. (3.13), a non-linearity of the optimal control problem may be observed. This means that the developed model, as a whole, may be addressed as a nonlinear problem when selecting the appropriate solver. Therefore, the problem with the proposed

objective function, as well as constraints of operation, may be solved using any solver able to contend with a non-linear problem. In this case, the SCIP solver in the MATLAB optimization toolbox is selected [128]. The algorithm formulation is described in Appendix A.

3.3 MODEL VALIDATION

3.3.1 Dual axis PV tracking system

Multiple variables are taken into consideration in the developed model, to represent the accurate operation of a dual axis PV tracking system. To this end, model validation is a necessity, to ensure that this representation is verified against the operation of a real-world system. Therefore, historical data was obtained from dual axis tracking systems, previously installed on the Central University of Technology's (CUT) premises located at 29.1217° S, 26.2128° E [128].

A total of 12 PV Tracking units were installed on the premises, each rated at 12.6 kWp. Each tracking unit consists of 42 panels, rated at 300 W each. The output of all the tracking units combined, delivers a total power of 151.2 kWp. On average, the trackers at the CUT yield approximately the same amount of energy throughout the day with slight variances, due to shading from trees, high mast flood lights and buildings close to the PV tracking arrays. This occurs during the early mornings and late afternoons.

Therefore, for model validation purposes, two tracking systems were identified that were not influenced by shading issues throughout the day.

The power yield readings from the energy monitoring dashboard of these existing (real world) systems, logged at 5-minute intervals, were used as historical data, to validate the PV tracking model. The energy dashboard receives data from an ennexOS Data Manager connected to a SMA COM Gateway, which is in turn is connected to the various tracking array inverters and energy metering systems.

Another similar solar tracking system, rated at 12.6 kWp, was installed approximately 4 km away from the University, at a microbrewery yielding near, identical results. In retrospect, the

healthcare entity considered in this case study, is within the same distance from the University. It is therefore, a well-founded assumption that the results obtained from the validated model, should match the real-world operation for the proposed system to be implemented at the healthcare entity. Only slight variances, due to estimation errors, may be noted.

Solar and temperature data obtained from a weather station, located approximately 250 m from the solar tracking arrays at the CUT, were fed into the developed PV tracking model to determine the PV output power for comparison with the existing system.

The variable data acquired from the weather station is substituted at each interval in Eqs. (8-10). The variable data includes: solar irradiance (global horizontal, direct normal, diffuse horizontal irradiance), ambient air temperature, azimuth angle and tilt angle of the irradiance sensor.

In order to simulate the operation of the dual axis tracking PV array, the tilt angle noted by (β) in Eq. (3.10), was equated to the calculated tilt angle of the solar irradiance measurement system of the weather station.

In Fig. 3.7, a graphical comparison between the simulated operation (model) and the actual (real-world) data of the system, is illustrated. This method follows historical data validation procedures, to ensure accurate real-world representation of simulated results.

In Fig. 3.7, a day with relatively low overcast conditions were simulated in terms of PV output power and compared to the two actual existing PV tracking units, installed at the CUT. A slight difference is observed where the solar output power starts to decline near sunset, which could be attributed to the tilt angle of the solar irradiance sensor at the weather station. In hindsight, the calculated average percentage error, was approximately 1.7%.

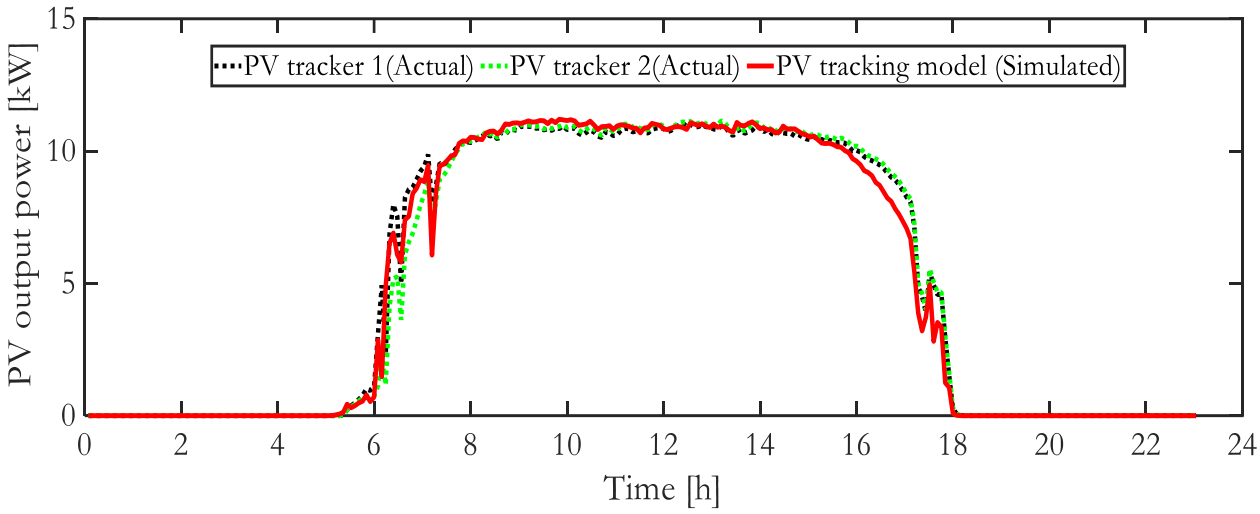

Fig. 3.7: Dual axis PV tracking model vs. actual system (day without overcast conditions)

In Fig. 3.8, the simulated PV output power data vs. the two actual systems, with high overcast (cloudy) conditions for the day in the low demand season, is illustrated.

The results indicate that the model, with overcast conditions, adequately represents real world operation. However, in this case, an average error of 3.2% were noted. This means that the model accuracy is slightly decreased for overcast/cloudy days. However, the accuracy remains within an acceptable range.

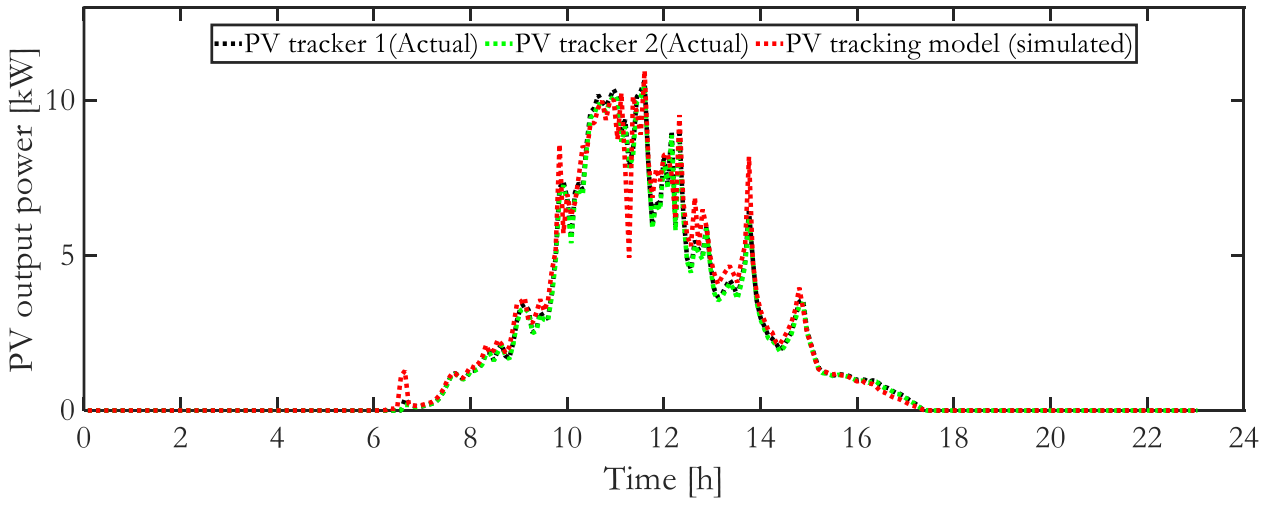

Fig. 3.8: Dual axis PV tracking model vs. actual system (day with overcast conditions)

The validated model of the dual axis PV tracking system is to be upscaled to any size required, in order to simulate the performance of larger systems. This will allow for precise PV output power predictions, based on the solar data measured from the weather station, located near the healthcare entity.

3.3.2 Electrical energy storage system

The mathematical model of the battery energy storage system is not as complex as the PV tracking system. Three constants (charging, discharging efficiencies and the battery nominal capacity), may be taken into consideration, with the only variables being the power flows in and out of the battery system, as shown in Eq. (3.7). This equation was derived from Eq. (3.15), which denotes the common coulomb counting method, to keep track of the SOC of a battery, depicted in Bester et. Al [129]:

$$SoC_{(j)} = SoC_{(j-1)} + \frac{\eta}{C_n \cdot 3600} \cdot \int_0^t P_{batt}\, dt, \tag{3.15}$$

where: η denotes the coulomb efficiency during charging or discharging (separate events, as power cannot flow in opposite directions); C_n is the battery capacity in Wh; P_{batt} presents the power in watt (W) traversing the battery [131].

In hindsight, the validation of the common coulomb method was conducted by Ng et. al [132], where the average estimated error was calculated to be 4.71 %, over several cycles.

3.4 CASE STUDY DESCRIPTION

3.4.1 Load profile for the worst-case scenario day

The worst-case scenario day, in which the maximum demand was observed for the year 2018, was selected to illustrate the performance of the developed model, under peak load

conditions. The worst case scenario day falls within the month of November 2018. The next section features the performance of the system on a daily basis throughout the year.

In Fig. 3.9, the load profile of the "maximum demand" scenario day in November, is illustrated over a 24-hour period. From the figure, the off-peak, standard and peak periods, are shown in green, yellow and red, respectively. Furthermore, it may be observed that the maximum demand occurs during the standard pricing region of Eskom's ToU tariff structure, exceeding the 600-kW mark three times within a timeframe of 4 hours, during the standard pricing region of the ToU tariff.

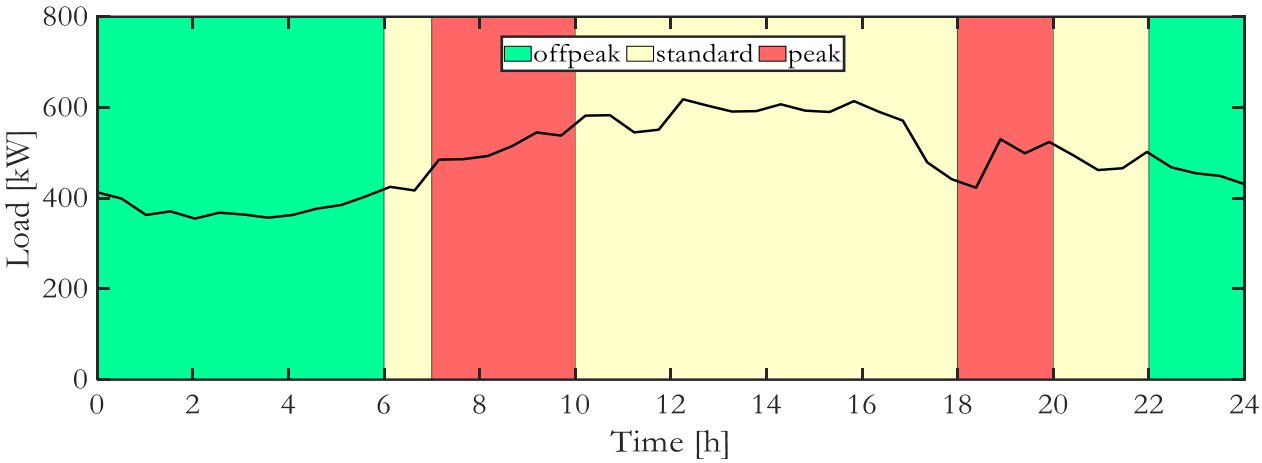

Fig. 3.9: Load profile of healthcare entity's critical load

3.4.2 Solar resource and air temperature data

In Fig. 3.10, the solar irradiance, in terms of global horizontal, direct normal and diffuse horizontal irradiance for the selected day is illustrated. The data was retrieved from the South African Universities Radiometric Network's website, which consists of a database of historic weather data in the nine provinces of the country. The data from the weather station, located at the Central University of Technology, Bloemfontein (latitude: -29:87098, longitude: 26.215909 and elevation: 1397 m), was used for this study [133]. The output power, obtained from the model, simulated throughout the year, is shown in Section 6.

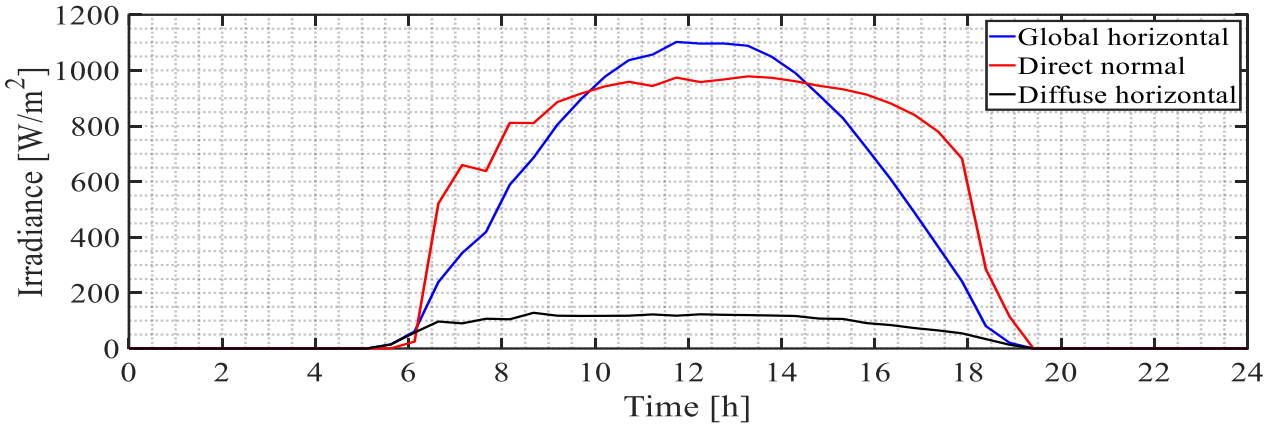

Fig. 3.10: Solar irradiance for the selected summer day

Fig. 3.11 presents the ambient temperature variation during the selected day. The ambient temperature should be considered, in order to effectively model the PV efficiency of the solar tracking system [132]. The temperature variation throughout the year, is illustrated in Section 3.5.2.

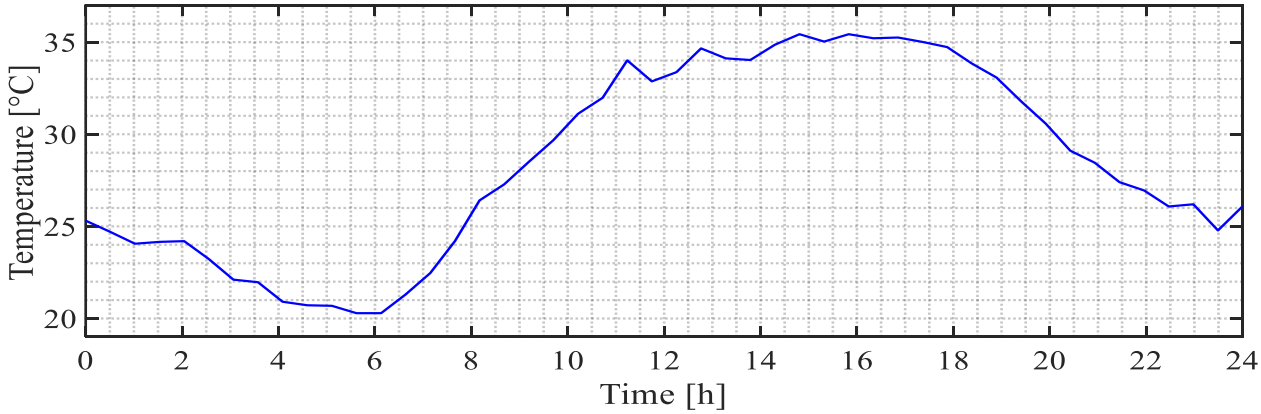

Fig. 3.11: Ambient air temperature for the selected day

In Fig. 3.12., the average global horizontal, diffuse horizontal and direct normal irradiance, are illustrated. These irradiance figures were obtained from the weather station located at the CUT. Typical to a South African case, the total irradiance received from the sun drops significantly, when compared to the summer season, as shown in the figure [133]. This results in a decrease of the average power output of the PV system, that may have otherwise been received during the summer months. Fortunately, when assessing the annual load profile of

the healthcare entity in Fig. 3.5, it may be observed that during the winter months, the power required from the PV system is less, as compared to the summer months.

Similarly, the ambient temperature variation should be considered, in order to accurately replicate the operation of the PV system. The PV cell efficiency is dependent on the ambient temperature, as shown in Eq. (3.9). From the equation, it may be noted that, for temperatures exceeding 25 °C, the efficiency will decline, which results in an output power loss. This should be considered, in order to represent the real-world system, with the highest accuracy possible.

In Fig. 3.13, the minimum, average and maximum temperature variations were used to simulate the output power of the PV system.

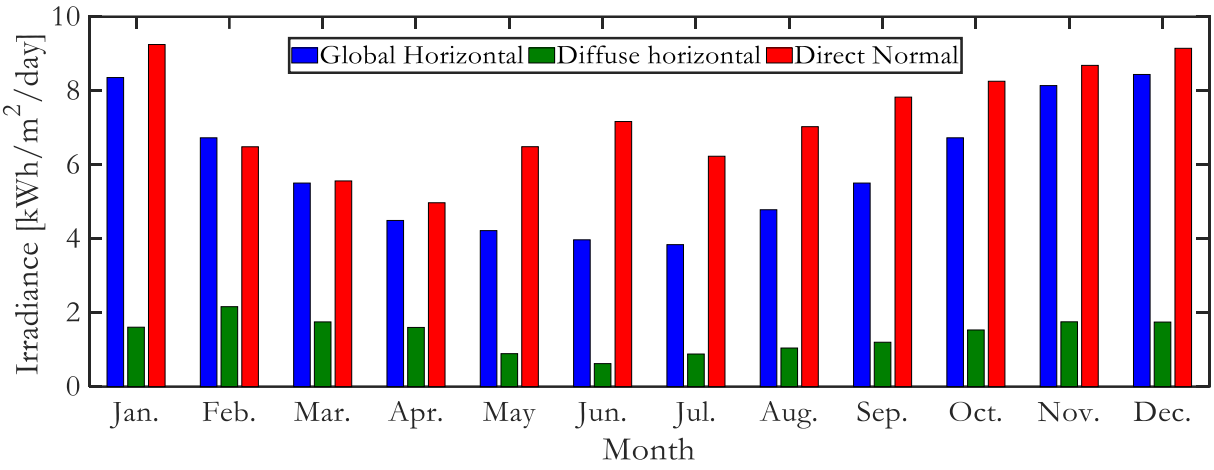

Fig. 3.12: Average daily solar irradiance for each month during 2018.

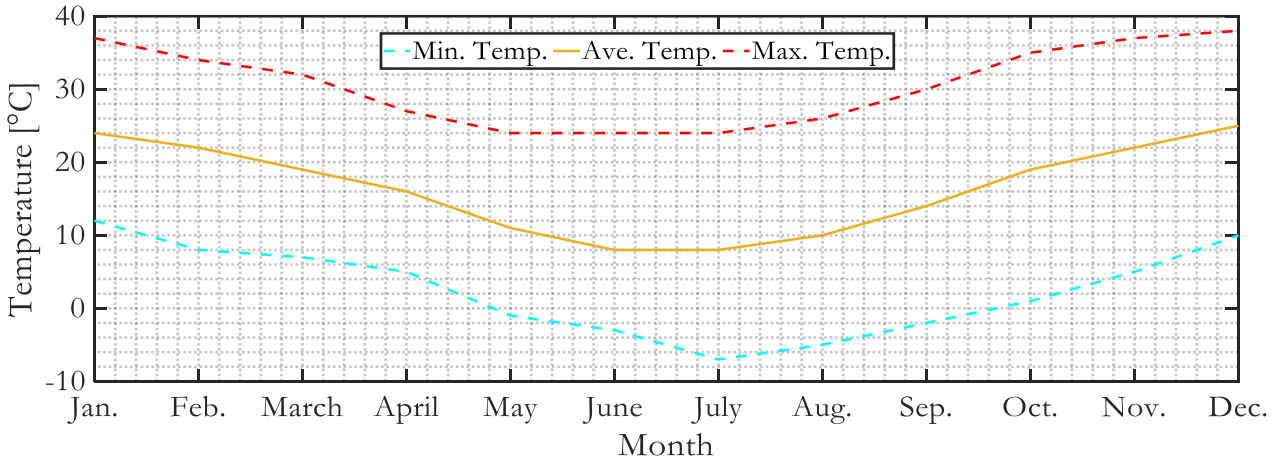

Fig. 3.13: Average ambient temperature for each month during 2018.

3.4.3 System sizing

The sizing of the hybrid system components is shown in Table 3.1. The size of the photovoltaic tracking system is determined by considering the available space on the premises and the essential annual load demand of the healthcare entity. The energy storage system was sized, in order to maximize energy savings, based on the energy demand of the institution. Furthermore, the latest advances in metaheuristic optimization techniques for the optimal sizing of hybrid energy systems have been used in past studies and may not offer a significant contribution to this study. [134].

Table 3.1: Simulation parameters

Item	**Figure**
Sampling time (Δt)	30 min
PV Tracking rated power	504 kWp
Battery nominal capacity (LiFePO4)	2240 kWh
ϱ_k (summer peak rate)	0.092 USD/kWh
ϱ_0 (summer off-peak rate)	0.054 USD/kWh
ϱ_s (summer standard rate)	0.063 USD/kWh
ϱ_k (winter peak rate)	0.189 USD/kWh
ϱ_0 (winter off-peak rate)	0.088 USD/kWh
ϱ_s (winter standard rate)	0.096 USD/kWh
Maximum demand rate	9.039 USD/kVA
SoC_0	46%
SoC^{max}	100%
SoC^{min}	30%
η_{Ch}	85%
η_{Disc}	90%

Several authors have analysed and demonstrated their results in providing accurate solutions for this problem [134,135]. Therefore, the present Chapter does not consider the optimal sizing techniques; the main aim of this work is to minimize the energy cost through the optimal economic power dispatch of the different components in the system, submitted to the dynamic resources, pricing structure and maximum demand. Additional data for the economic analysis is presented in section 3.6.

In hindsight, the system sizing of the different components, ToU costs and other simulation parameters, are shown in Table 3.1. The last four parameters listed in the table represent the battery's initial state of charge (SoC_0), constraints (SoC^{min} and SoC^{max}) and efficiencies (η_{Ch} and η_{Disc}). The initial state of charge was set to 46 %, in order to maintain fixed final state conditions and represent continuous operation beyond the considered 24-hour simulation horizon. The remaining battery constraints and efficiencies are typical for a LiFePO4 battery system.

3.4.4 Power from the utility grid

As stated previously, the cost of energy purchased from the grid, is defined by the ToU tariff. The ToU tariff structure consists of three pricing regions, which are: peak, standard, and off-peak pricing [136]. The times at which these tariffs are charged, are depicted in Eq. (3.16) for the low demand season and Eq. (3.17) for the high demand season:

$$\rho(t) = \begin{cases} \rho_k; t \in P_g, P_g = [7,10)[18,20); \\ \rho_o; t \in P_g, P_g = [0,6)[22,24); \\ \rho_s; P_g, P_g = [6,7)[10,18)[20,22); \end{cases} \tag{3.16}$$

$$\rho(t) = \begin{cases} \rho_k; t \in P_g, P_g = [6,9)[17,19); \\ \rho_o; t \in P_g, P_g = [0,6)[22,24); \\ \rho_s; P_g, P_g = [9,17)[19,22); \end{cases} \tag{3.17}$$

where: ϱ_k , ϱ_0 , ϱ_s are the energy cost during peak; off-peak and standard pricing period; respectively.

3.5 SIMULATION RESULTS AND DISCUSSION

3.5.1 Determination of optimal maximum demand threshold

The optimal operation of the proposed system was simulated based on the parameters in Table 3.1, the load profile in Fig. 3.9, solar irradiance in Fig. 3.10 and ambient air temperature in Fig. 3.11.

An artificial constraint was imposed on the amount of energy that may be transferred to the load from the electricity grid. This was achieved by optimizing the constraint limit $P_{PG(j)}^{\max}$ in Eq. (3.4), through a sensitivity analysis. Introducing this limit to the system may, in turn, result in additional energy savings, by reducing maximum demand charges.

A sensitivity analysis was conducted, by varying the limit in steps of 5 kW to arrive at a point where energy savings were at a maximum. Although the maximum demand is typically measured in kVA (apparent power), for this instance, the active power may be used, as the apparent power depends solely on the power factor. The load considered in the case study had an average power factor of 0.94, varying within the range of 0.91 to 0.99. In Fig. 3.14, this point was noted to be at 335 kW. This translates into an apparent power of 356.38 kVA, considering the average power factor of 0.94. This means that the imposed upper limit/boundary for the grid energy usage of 356.38 kVA, maximum savings will be observed for the specific case.

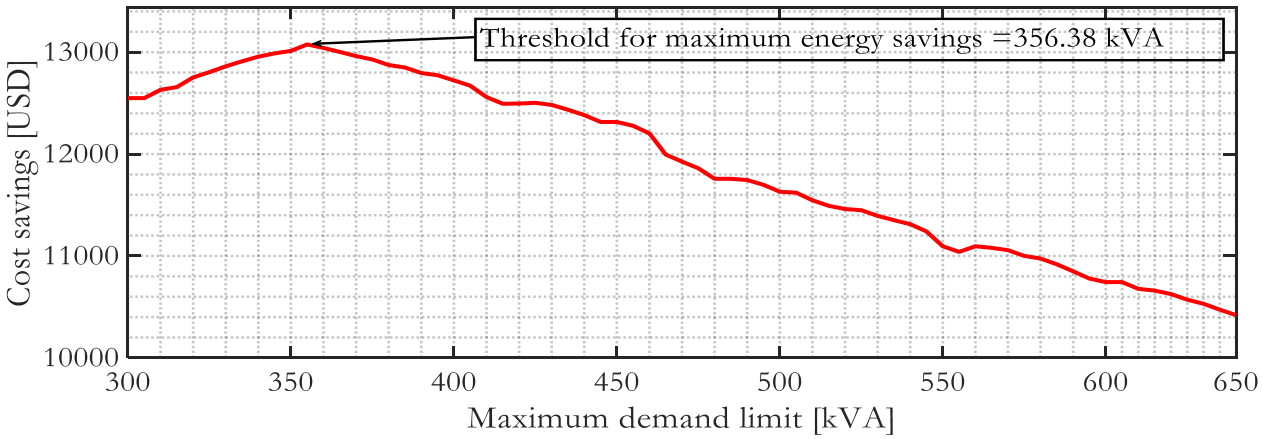

Fig. 3.14: Average monthly cost savings through grid threshold manipulation

3.4.2 Optimal power flow simulation

According to the objective function, the energy costs are minimized based on the time of use tariff. This ensures that grid energy usage is avoided during the costly regions of the ToU tariff. This is achieved through the economical dispatch of power from the PV and battery system, depending on the demand. On the other hand, the costs associated with the maximum demand were minimized through a sensitivity analysis on the optimal cost saving point in Fig. 3.14, where a grid threshold of 356.38 kVA was imposed. For simulation purposes, this was translated to 335 kW (based on the average power factor of 0.94), in order to illustrate all results, in terms of active power. This was carried out in order to reduce the computational load and the resulting time for simulating the operation of the system for the entire year.

The following sections presents the results (Figs. 3.15 to 3.18.), from the optimal control simulation, based on the worst-case scenario day and associated load profile, in Fig. 3.9. The output power for a similar sized stationary tracking system is shown, along with the results for the dual axis tracking system, for PV output comparison in Fig. 3.15.

3.4.2.1 Power flow during the off-peak ToU period [0h00 to 06h00)

From Fig. 3.9, the load remains relatively constant at around 400 kW, during the off-peak period. Referring to Fig. 3.16, due to the low cost of electricity during this period, grid energy (P_1-labeled in red) is used to supply the load up to the 335-kW imposed grid threshold, as shown in Fig. 3.17. This leaves the load short of energy from the grid, with a varying power of up to 65 kW throughout the six hours of the first off-peak period. The required varying 65kW of power to meet demand, is therefore discharged from the battery, as illustrated in Fig. 3.16 (P_4-labeled in yellow), with the associated SoC dynamic, given in Fig 3.18. The power received from the PV system (P_2-labeled in green) remains zero, until the end of the off-peak period, mainly as a result of the unavailability of the solar resource. Therefore, the power supplied by the PV to the battery (P_3-labelled in blue) similarly remains zero throughout the off-peak period and for the rest of the 24 hours, due to the maximization of the solar resource in the second cost function. The battery is only discharging within this period, therefore,

charging (P_5-labelled in purple) does not occur in accordance with the constraint given, as per Eq. (3.15).

3.4.2.2 Power flow during the standard ToU period [06h00 to 07h00)

During the standard period, the cost of electricity is slightly higher, compared to the off-peak period, hence, the power drawn from the grid (P_1) drops, as shown in Fig. 3.16. However, the power output from the PV and, therefore, the power supplied to the load (P_2) by the PV, starts to increase rapidly during the standard period, due to the increase in availability of solar irradiance. From the SoC of the battery, in Fig. 3.18, it may be observed that the battery has reached its lower limit and needs to be recharged. This means that no power may be supplied by the battery to the load (P_4) at this point. Therefore, all the PV power is supplied to the load (P_2), with some assistance from the grid (P_1). Towards the end of this period, energy from the grid is transferred to the battery (P_5), to prepare for the coming peak pricing period.

3.4.2.3 Power flow during the peak ToU period [07h00 to 10h00)

During the first peak period of the day, the PV system begins to reach peak production and is used as the main source of power, in order to maintain the load (P_2). Fig. 3.16 and Fig. 3.17 show that the total power supplied by the grid to the load (P_1), drops significantly, due to the higher electricity price and is solely used to balance the deficit of power from the PV to the load. It may further be seen that the grid is not used to recharge the battery during this period. Similarly, the power transferred from the battery to the load (P_4) remains zero for this period, as the SoC of the battery has not yet recovered, shown in Fig. 3.18.

3.4.2.4 Power flow during the standard ToU period [10h00 to 18h00)

The standard period, with its lowered energy cost, allows the grid (P_1) and the PV (P_2) to supply the growing load. This is also necessary, due to the load peaks, observed in Fig. 3.9. At this point, the PV output has reached its maximum and maintains a relatively constant output until 16h00, where the solar availability starts to decline. Looking at Fig. 3.17, the power

used from the grid does not exceed the 335-kW imposed maximum demand threshold. This power is further used to supply the battery (P_5), at a rate of approximately 200 kW throughout the standard period, in order to replenish the cells for the upcoming peak pricing event. Therefore, the power supplied from the battery to the load (P_4) is also zero, due to the exclusive power flow constraint in Eq. (3.13).

3.4.2.5 Power flow during the peak ToU period [18h00 to 20h00)

At this point, Fig. 3.15 shows that the output power of the PV has dropped rapidly until 19:00, where zero power is delivered to the load by the PV system (P_2). Due to the fully charged battery (SoC=100%) at 18:00, no grid energy is required and transferred to the load (P_1) during this peak period. Rather, the battery supplies most of the load (P_4), with the remaining PV output power available. Consequently, after the PV output power has dropped to zero at 19:00, the battery output to the load (P_4) peaks at approximately 523.6 kW, with a corresponding decrease in SoC, shown on Fig. 3.16. Similar to the previous pricing period, the battery may not be charged and discharged simultaneously.

3.4.2.6 Power flow during the standard ToU period [20h00 to 22h00)

During the third standard period of the day, grid energy supplied to the load (P_1), returns to the upper maximum demand threshold of 335 kW, due to the less costly electricity price, as shown in Figs. 3.16 and 3.17. The battery supplies the rest of the power required by the load (P_4), as was the case for the first off-peak period. At this point and into the next pricing period, the PV output power to the load (P_2) and to the battery (P_3), remains zero. The battery discharges for this whole pricing period, with the corresponding dynamic of the SoC, shown in Fig. 3.18.

3.4.2.7 Power flow during the off-peak ToU period [22h00 to 24h00)

The second off-peak period features the same behaviour as the first off-peak period, in that the upper threshold of the maximum demand limit of 335 kW is maintained by the grid power supplied (P_1), while the battery (P_4), assists with the remaining required power to the

load. The battery is then discharged, to maintain a fixed final state condition, as given by Eq. (3.14). Therefore, while the battery is discharging, no power may flow from the grid to the battery.

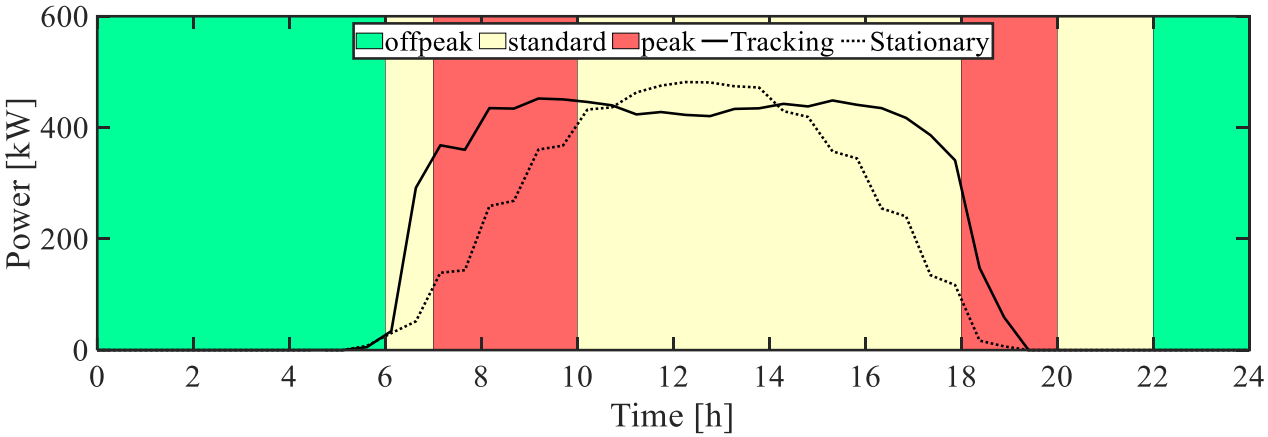

Fig. 3.15: Dual axis PV tracking output power

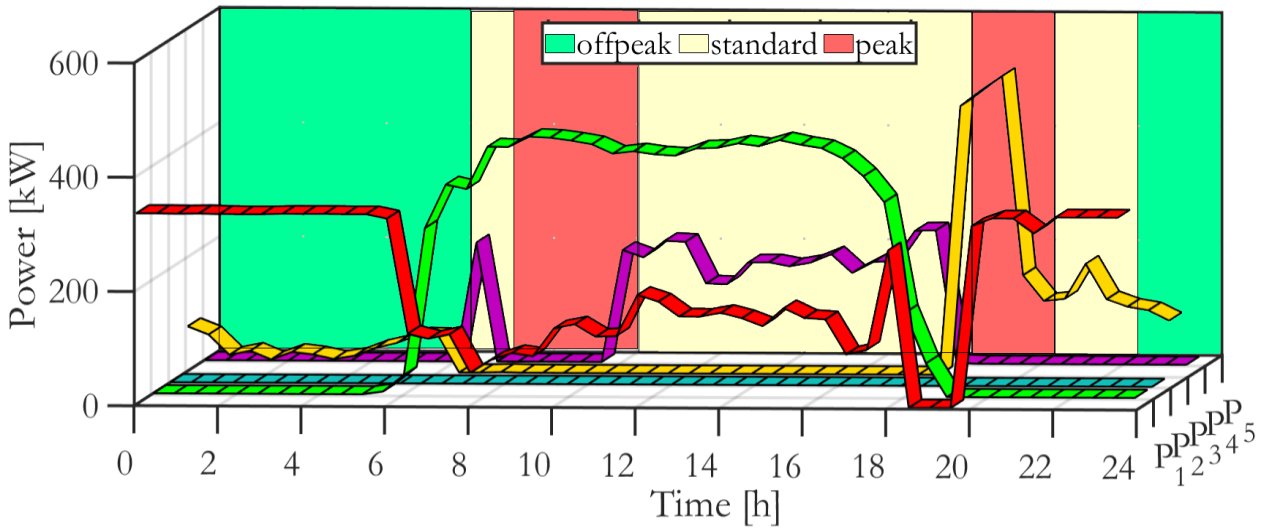

Fig. 3.16: Optimal power flow of P1 to P5

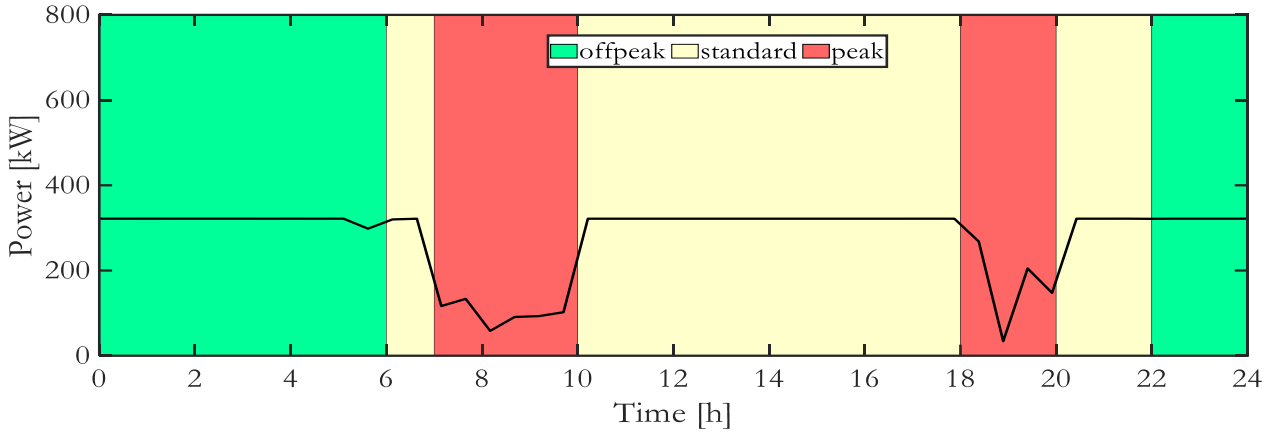

Fig. 3.17: Total power drawn from the grid

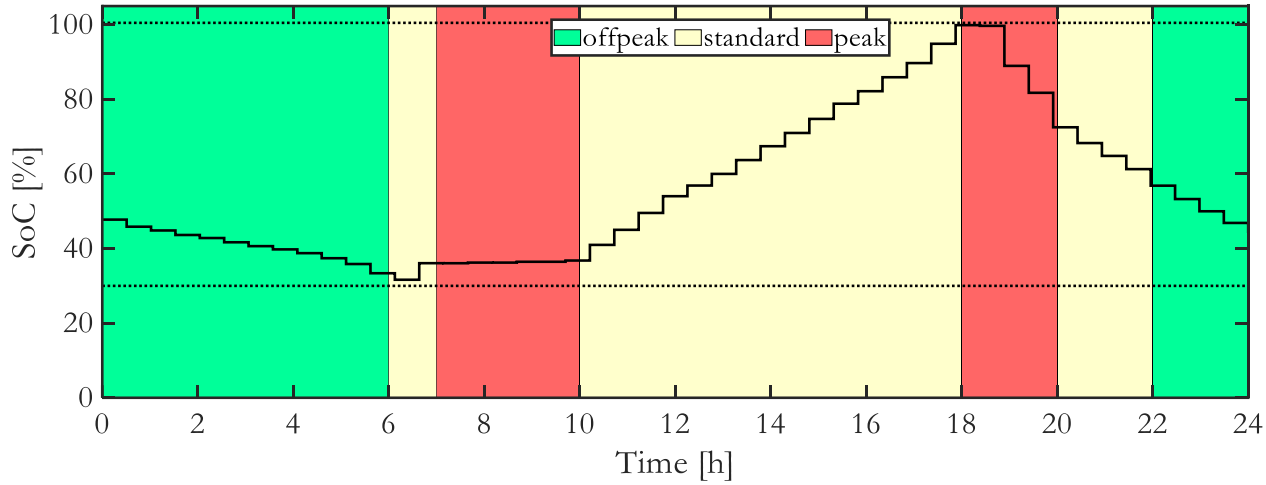

Fig. 3.18: Battery bank state of charge

3.6 ECONOMIC ANALYSIS

3.6.1 Daily economic analysis

An economic analysis was conducted for this worst-case scenario day, to establish the possible energy savings of the proposed system where the maximum demand for the year occurred. In Fig. 3.19, the daily energy cost comparison between the optimally controlled system and the baseline, is shown.

From the graph, it may be observed that at 07:00 in the morning, the cumulative costs of the compared systems, start to diverge significantly. This sudden divergence may be attributed to the output power of the PV system being dispatched to the load, during the first peak pricing period. The second peak period shows a similar trend, equally attributable to the minimization of grid energy usage and the supplementation of energy from the EES scheme. The daily energy cost savings were revealed to be $403.73 USD, which translates into a cost saving of 47.36% for the evaluated period. It should further be noted that this cost saving was solely based on the ToU tariff and not the additional savings, that may be of result from the maximum demand charges.

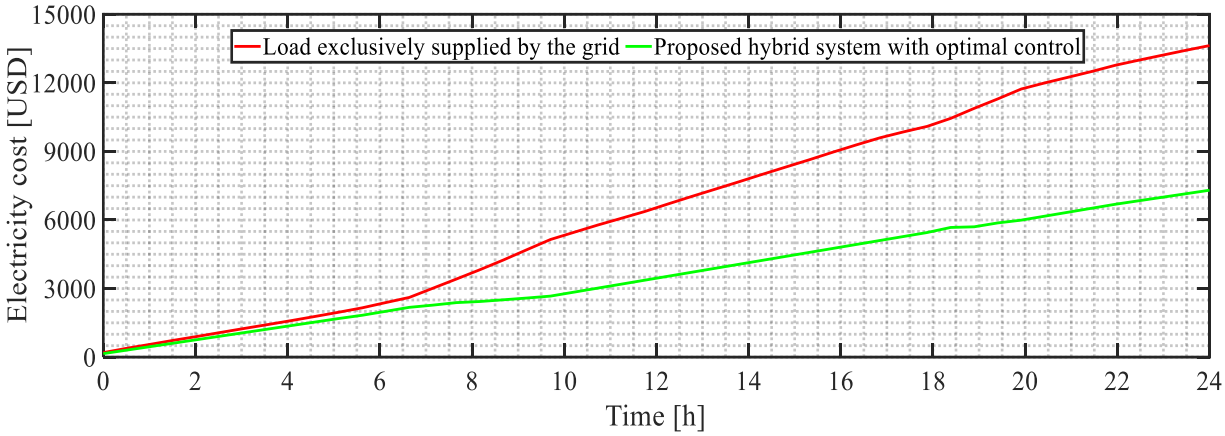

Fig. 3.19: Energy cost comparison for the selected day

3.6.2 Monthly economic analysis

In order to evaluate the cost effectiveness of the system throughout the year, the variation of the solar resource and ambient air temperature during each month of the year should be taken into consideration.

The operation of the proposed system with optimal control was simulated on a daily basis for the year 2018. The annual load data, monthly average irradiance, and ambient air temperatures, shown in Figs. 3.5, 3.12 and 3.13, respectively, were used in the simulation. From Eqs. (3.16) and (3.17), it is observed that the ToU periods and costs differ for the high and low demand seasons. Therefore, the simulated results of the resultant grid energy usage,

after implementation of the proposed system with optimal control, may be split into separate graphical representations. Consequently, the resultant energy supplied by the grid for the low demand season (Jan-May and Sep-Dec), is shown in Fig. 3.20. From the figure, it is observed that the optimal control model, with the imposed grid limit at 335kW, effectively achieved the intended peak clipping and energy management objectives.

Simulation results for the high demand season (June-August), are shown in Fig. 3.21. The high demand season shows less variability in energy usage from the grid, as compared to the low demand season. This may be attributed to the substantial cost difference of electricity during the peak, off-peak and standard time. The cost of energy for the peak region of the ToU tariff structure for the high demand season, is approximately twice the amount of the standard region. However, the off-peak price is almost equal to the standard period price. In hindsight, for the low demand season, the peak ToU price is approximately 1.5 times that of the standard time, with similar trends observed for the off-peak price. Therefore, in the high demand season case, the optimal control algorithm aggressively avoids grid energy usage during peak periods.

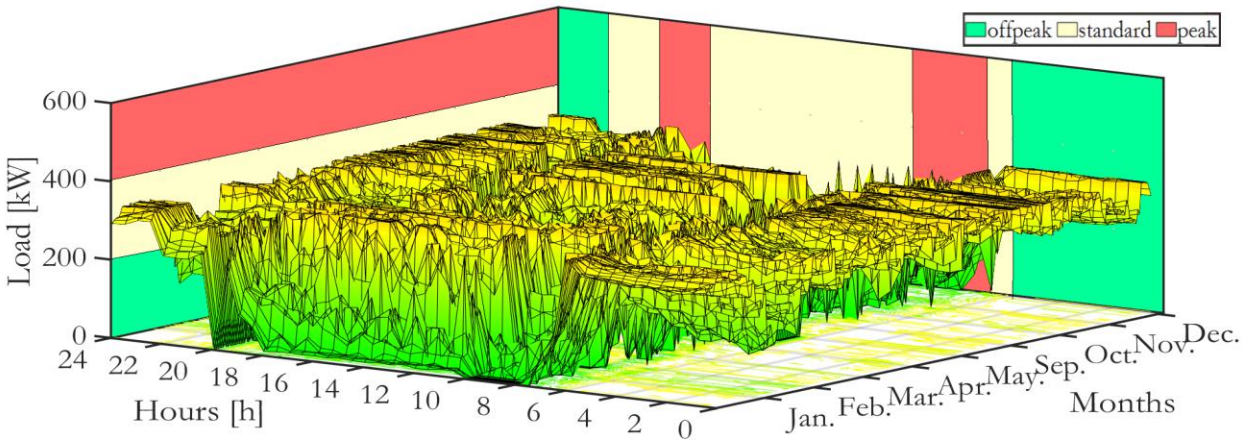

Fig. 3.20: Low demand season (Jan-May and Sep-Dec) grid energy usage after implementation of proposed hybrid energy system with optimal control.

Simulation results for the high demand season (June-August), are shown in Fig. 3.21. The high demand season shows less variability in energy usage from the grid, as compared to the

low demand season. This may be attributed to the substantial cost difference of electricity during the peak, off-peak and standard time. The cost of energy for the peak region of the ToU tariff structure for the high demand season, is approximately twice the amount of the standard region. However, the off-peak price is almost equal to the standard period price. In hindsight, for the low demand season, the peak ToU price is approximately 1.5 times that of the standard time, with similar trends observed for the off-peak price. Therefore, in the high demand season case, the optimal control algorithm aggressively avoids grid energy usage during peak periods.

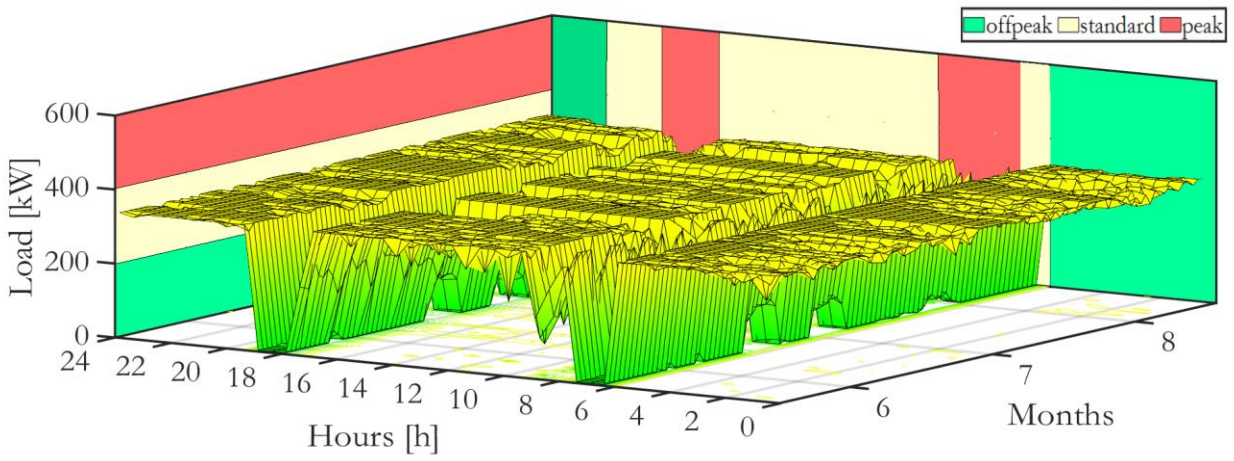

Fig. 3.21: High demand season (June-August) grid energy usage after implementation of proposed hybrid energy system with optimal control.

The energy costs of operating each system on a monthly basis, has been calculated from the simulated results and is shown in Fig. 3.22. In this figure, the operation costs, based solely on the ToU tariff, is shown for the baseline, the proposed system, and the optimal control case. The baseline system represents the load that is exclusively supplied by the grid. The energy costs for the proposed system with and without optimal control, is similarly illustrated, for the sake of comparison.

From the figure, a comparatively small difference is observed between the proposed system with and without optimal control, during the months of January to May and from September to December. Throughout the summer months, the output power from the PV

tracking system meets the majority of the demand, during the costly regions of the ToU tariff. This is a direct result of the extended summer solar hours. Furthermore, this partly substantiates the need for a dual axis tracking system, as compared to a stationary PV tracking system. Fig. 3.15, demonstrates an overlap of PV output power to the costly regions of the ToU tariff. This overlap does not occur so prominently for the winter season. During the winter months a different trend is observed, as the optimal control approach presents improved performance, as opposed to the summer months. The three main factors of this improvement, are the earlier peak pricing region occurrences of the ToU tariff, higher energy costs for the peak and standard periods and the lower winter solar hours. The decreased availability of the solar resource, coupled with the earlier peak period of the winter season, reduces the cost saving ability of the hybrid system, without optimal control. With adequate control applied, the control algorithm effectively manages the power flow to charge and discharge the battery, so that grid energy is solely used during the off-peak period. The optimal control approach, therefore, succeeds in minimizing the energy costs across all months of the year.

Further observations dictate that, during the months of January, November and December, the energy costs are effectively halved for both the hybrid system, with and without optimal control.

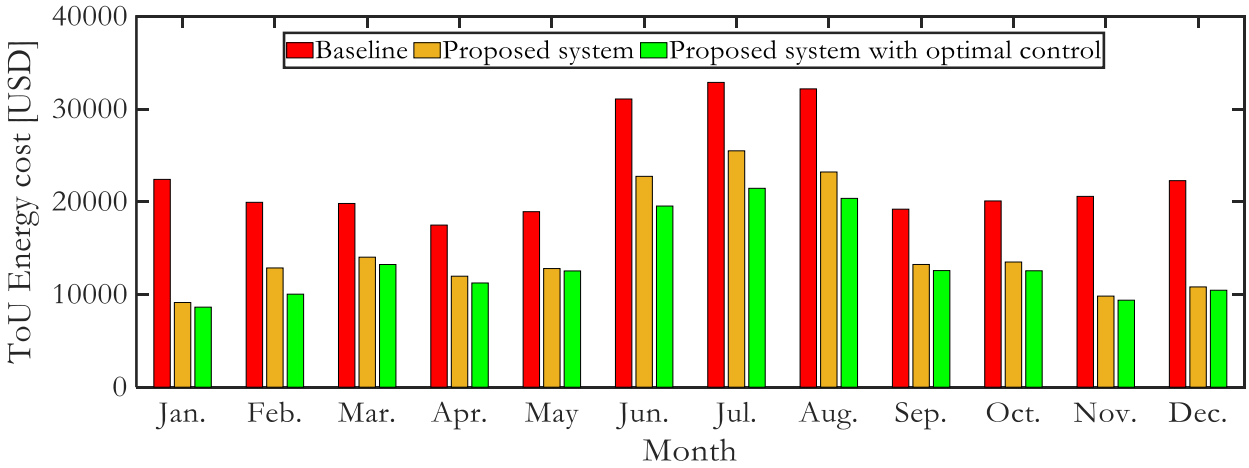

Fig. 3. 22: Monthly energy costs based on the ToU electricity tariff for the year 2018.

The average savings on ToU charges for the year, were noted to be 35,1% for the proposed system, compared to the baseline and 41.5% for the proposed system, with optimal control, as compared to the baseline. The application of the optimal control method was, therefore, simulated to increase savings by approximately 6.4%, when considering the ToU charges.

Fig. 3.23. illustrates the costs incurred as a consequence of reaching certain peak demands during each month. These costs, as previously stated, are additional to that incurred as a result of the ToU tariff. A larger difference between the proposed system with and without optimal control, may be observed, when assessing the results.

The proposed system showed a promising performance trend in the reducing the maximum demand for most months, except October. However, considering the case of the artificially imposed grid limit, the proposed system with optimal control ensured that the 335kW limit was not exceeded and therefore further reduced the maximum demand charges, as opposed to the system without the limit. In hindsight, the proposed system alone, reduced the maximum demand charges by 10.5%, while limiting the grid (optimal control), yielded savings of 38%, as compared to the baseline system. This means that the optimal control technique effectively reduced the maximum demand costs by 27.5%, as compared to the proposed system without optimal control.

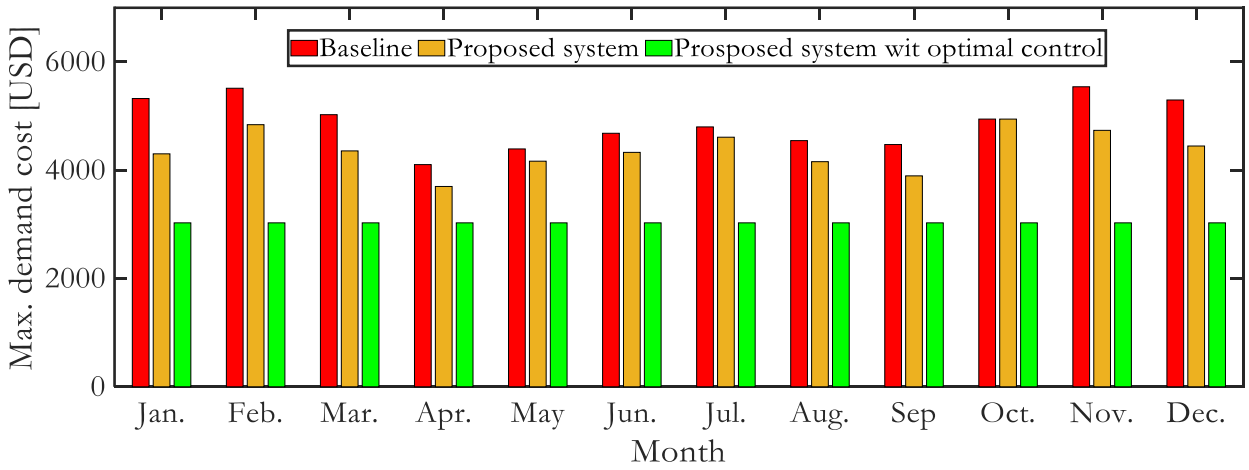

Fig. 3. 23: Maximum demand costs for the year 2018.

In Fig. 3.24., the total energy cost, the sum of the ToU costs and maximum demand charges, for each month is illustrated. These costs, therefore, represent the total billed energy for the healthcare entity's chosen essential load. The total savings achieved by the proposed system, without optimal control amounted to 30.82 %.

The proposed system with optimal control applied, resulted in additional savings of 10.06%. Therefore, based on simulated results, the healthcare entity's total annual energy costs may be reduced by 40.88%, given that the proposed system with optimal control were to be implemented.

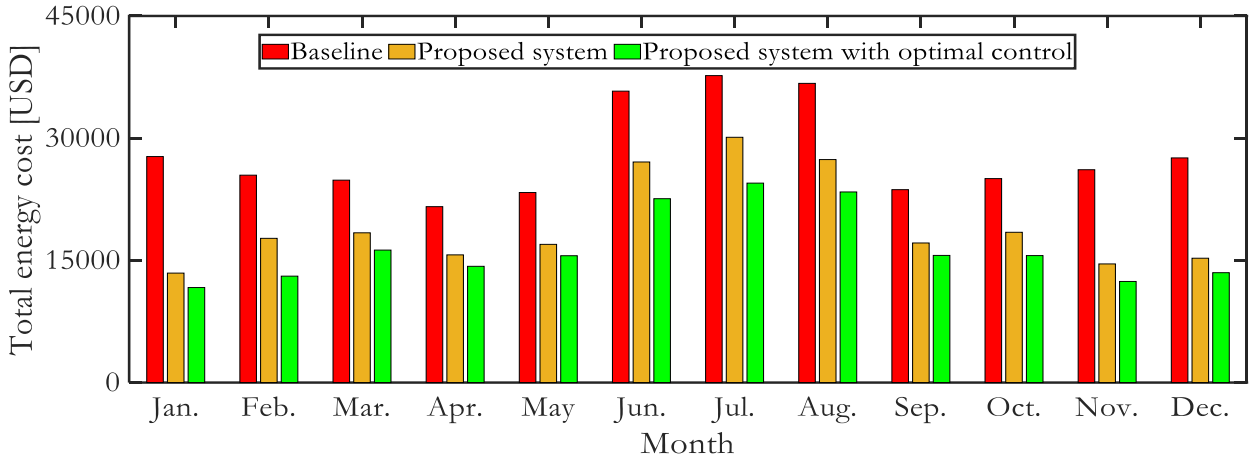

Fig. 3. 24: Total electricity costs for the year 2018.

3.6.3 Life cycle cost analysis

A life cycle cost analysis was conducted on the proposed system, with and without optimal control, compared to the baseline (load exclusively supplied by the grid). The life cycle cost analysis may be used to determine the feasibility of implementing the proposed system over a project lifetime. In this case, a project lifetime of 20 years, from the year 2018, was chosen for the analysis. The total life cycle cost may be calculated using Eq. (3.18):

$$LCC = C_{initial} + C_{OM} + C_{EC}. \tag{3.18}$$

$C_{initial}$ is the initial implementation cost of the proposed system; C_{OM} is the operation and maintenance costs; C_{EC} is the operational costs or in this case the total annual energy costs.

The analysis may reveal the break-even point of the proposed system, as opposed to the load being supplied solely from the grid [137]. The feasibility of the system may be determined, by evaluating the time required to break- even on the implementation costs of the proposed system. These costs are shown in Table 3.2.

In Table 3.2, the initial implementation cost of the PV system, consisting of 40 x 12.6 kWp standalone dual axis tracking systems, are shown. The implementation cost of the dual axis tracking system includes the cost of the PV arrays, inverters with smart charge capability, tracking actuators, sensors, mounting rails, brackets, stands and concrete foundations. The EES system consists of multiple LiFePO4 battery banks, to reach a capacity of 2240 kWh. The cost associated with the battery bank includes cabling, data monitoring (logging) hardware and software.

Table 3.2: Initial implementation costs

Item	**Figure**
Dual axis PV tracking system	950 000 USD
LiFePO4 Battery bank system	690 000 USD
Total	**1 640 000 USD**

In Table 3.3, the energy costs incurred for each system for 2018 is shown. These costs were discussed in Section 3.6.2. The energy costs are required, to evaluate the operational costs throughout the 20-year project lifetime. An increase of 10% in the annual electricity price is considered in the analysis. Further costs include the operation and maintenance costs (1% of the initial investment cost per year), which increase with an average inflation rate of 5.3% each year [138].

Table 3.3: Total annual energy cost (2018)

Cost	Figure
Baseline	335556.50 USD
Proposed system	232124.20 USD
Proposed system - optimal control	198369.90 USD
Savings (Proposed system)	**103432.30 USD**
Savings (Proposed - optimal control)	**137186.60 USD**

Fig. 3.25. illustrates the resultant break-even point of the proposed system, without optimal control techniques applied. The life cycle cost analysis revealed that the proposed system will potentially break-even 9.32 years after $5.99 Million USD was spent. After this point, significant savings in energy costs will be observed. The savings at the end of the evaluated project lifetime of 20 years, were shown to be $8.41 Million, translating into a total cost reduction of 24.48%.

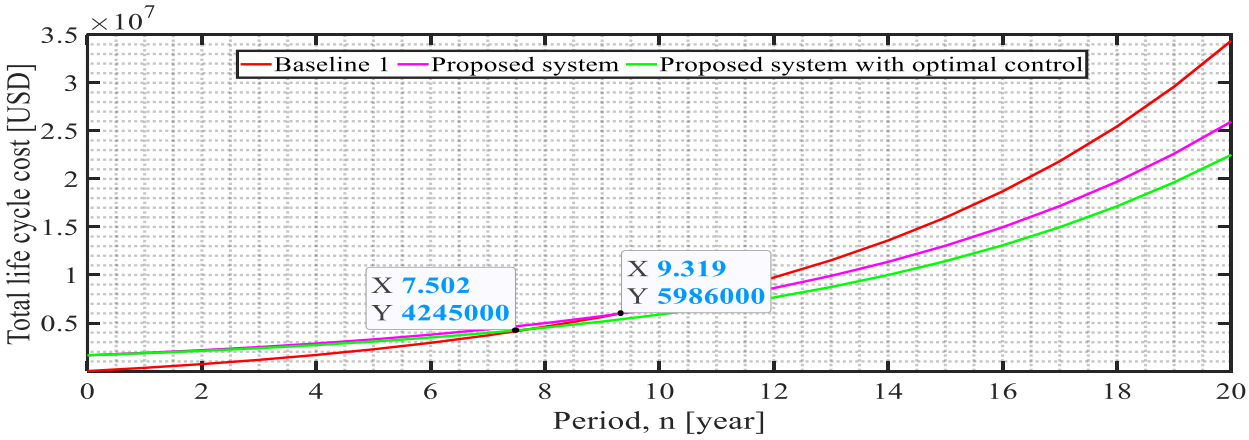

Fig. 3.25: Break-even point analysis between baseline system and proposed system.

The break-even point for the proposed system with optimal control, is presented in the same figure. From the figure, the system is predicted to break-even in 7.5 years, at $ 4.25 Million USD.

Comparatively, this means that, when applying the optimal control technique to the proposed system, the break-even point will occur 1.82 years earlier, with a cost saving of $1.74 Million USD. The savings at the end of the evaluated project lifetime was noted to be $11,87 Million USD. This translates into savings of 34.53 %, 20 years after implementation. The detailed financial life cycle costs for each year is shown in Appendix C.

3.7 CONCLUSION

A model was developed and validated, to accurately represent the economic dispatch of power for a proposed hybrid energy system, connected to a healthcare entity in the Bloemfontein area, in South Africa. The operation of the hybrid energy system was simulated for each day of the year, to evaluate the performance of the system under daily varying weather and load conditions. This ensured an accurate representation of a real-world system, to minimize PV and load uncertainty.

The model of the system, optimal control algorithm and the maximum demand threshold were used, to simulate the performance of the proposed hybrid energy system, in order to conduct a monthly economic analysis.

The simulation results revealed that the proposed system with optimal control, was able to significantly reduce energy costs, compared to the proposed system without optimal control.

Simulation results revealed that a potential annual energy cost saving of 35.1%, would be of result, when solely considering the ToU tariff, if the proposed system were to be implemented. An additional energy saving of 6.4 % was observed, with the application of the optimal control algorithm.

The savings attained from reducing the maximum demand, by limiting the power supplied by the grid, was observed to be 10.5 % for the proposed system, without optimal control and 38 %, with optimal control. The resultant total annual potential energy cost savings amounted to 30.8% for the proposed hybrid energy system and 40.9 % with the application of the optimal control algorithm.

A life cycle cost analysis revealed that a break-even point would be achieved in 8.8 years, with the implementation of the proposed system, while, with the application of control techniques, the break-even point may be reduced by as much as 1.82 years. Additionally, the life cycle cost analysis projected savings of up to $11.87 Million USD, over the project lifetime of 20 years, translating into savings of 34.53%.

In this model, 137 168,60 USD were saved over a period of one year, as a result of reducing the maximum demand and introducing a renewable energy system, with energy storage.

In retrospect, the results illustrate the potential reduction of energy usage and the economic feasibility of implementing renewable energy systems and, in turn, a reduction of the overall carbon footprint of the healthcare entity under evaluation. This will in turn, reduce the total operating costs of the building and ensure sustainable energy management, if implemented.

CHAPTER IV: OPTIMAL ENERGY DISPATCH OF A MULTIFARIOUS WATER HEATING SYSTEM WITH HVAC WASTE HEAT RECOVERY IN A HEALTHCARE INSTITUTION

4.1 INTRODUCTION

Water heating systems often include a form of energy storage device, due to the lengthy process involved in heating water to the desired thermal level [140]. This increases the potential for demand side management strategies to be applied, in the form of load shifting. Shifting loads to the least costly regions of the ToU tariff, may result in substantial cost savings, as well as lowering the risk of incurring dissolute maximum demand penalties.

Therefore, in this Chapter, a mathematical model is developed for a multifarious water heating system, located at the hospital in the case study. The water heating system, at this healthcare entity, consists of a hybrid system, linked to the HVAC scheme of the building. An existing multifunctional chiller system that extracts and recovers heat from water, is connected to multifarious water heating setup. The recovered heat is then transferred to a preheated water storage system. The preheated water is pumped and circulated to 57 electric storage tank water heaters (ESTWHs), distributed across the building. This results in higher than ambient inlet water temperatures, which in turn reduces the temperature differential that should be minimized to reach the desired temperature levels.

The model of this system was developed with the aim to minimize energy costs, with respect to the time-of-use tariff and maximum demand charges, while maintaining the desired temperature of water inside each ESTWH.

The model development is discussed in Section 4.2, while the validation of the model is presented in Section 4.3. In Section 4.4, the case study, as well as the variable input data and simulation parameters, are discussed. Section 4.5 presents the simulation results, with section 4.6 concluding the Chapter.

4.2 MODEL DEVELOPMENT

4.2.1 Water heating model

A model of a single ESTWH was developed and duplicated, to form a comprehensive representation of the entire system. The preheated water flow rate and temperature from the MFC was solely taken as an input to the multifarious ESTWH system. This means that the MFC has not been modelled, rather, the heated water from the chiller and by extension, the temperature of the water in the preheated storage was used as the inlet water to the distributed water heating system. This allows for a simple model and reduces computational requirements.

Therefore, initially, the development of a single ESTWH model is discussed, followed by the methodology for incorporating the duplicates, with different parameters for the representation of the entire system.

In order to develop an accurate model of the ESTWH, the factors influencing the temperature of the water inside the storage tank should be taken into consideration [139].

An energy balance equation is required to represent the temperature dynamic within the storage tank. This will entail the thermal gain and losses in each ESTWH. The electric resistive element of the ESTWH will constitute the thermal gain in the system, while losses include the demand and standby losses through the storage tank surface conduction.

Starting with thermal gain, denoted by $Q_{ERE}(t)$, may be calculated, as shown in Eq. (4.1). A constant power is supplied to the electric resistive element [140]. This means that the full rated power is supplied to the resistive element, while the ESTWH is switched *on*. The energy gain and losses in the system is expressed in Joule, while the power is multiplied with time, to indicate energy in the same SI unit..

$$Q_{ERE}(t) = P_{ERE} t_h, \tag{4.1}$$

where: $Q_{ERE}(t)$ is the variable thermal gain from the resistive element (J); P_{ERE} is the rated power of the element (W); t_h is the time ($3600\,s$).

The energy losses, as a result of the flow of hot water to the user, i.e. demand ($Q_D(t)$) and convectional (standby) loss ($Q_{SL}(t)$) may be calculated, using Eq. 4.2 and 4.3, respectively.

The standby losses, Q_{SL}, represent energy losses across the storage tank casing material, through surface conduction [141]:

$$Q_{SL}(t) = U_s t_h A_s (T_s(t) - T_a(t)), \tag{4.2}$$

where:

U_s is the coefficient of heat loss of the storage tank ($W/m^2.°C$);

A_s is the storage tank area (m^2);

t_h is the time (3600s);

$T_s(t)$ is the variable temperature of the water inside the storage tank ($°C$);

$T_a(t)$ is the variable ambient temperature of the surrounding air ($°C$).

The hot water demand ($Q_D(t)$) occurs when hot water is drawn by the consumer. Therefore, when hot water is required, the hot water demand flow rate is initiated and $T_s(t)$ drops, as cold-water flows into the tank, to maintain a constant volume [142]. Losses, as a result of the hot water demand, are given in Eq. (4.3):

$$Q_D(t) = cD_{HW}(t)(T_s(t) - T_m(t)), \tag{4.3}$$

where:

c is the heat capacity of water ($4184 J/kg/°C$);

$D_{HW}(t)$ is the variable demand flow rate (kg/h);

$T_m(t)$ is the variable cold water temperature of the inlet water ($°C$).

The energy balance equation is noted, in terms of all the heat gains and losses in the system and equated to the energy stored in the tank [143], this is shown in Eq. (4.4):

$$M_s c \dot{T}_s = Q_{ERE} - Q_L - Q_D \tag{4.4}$$

where:

M_s is the mass of water inside the storage tank (kg);

c is the heat capacity of water ($4184 J/kg/°C$),

$\dot{T}_s$ is the derivative of the temperature dynamic of the storage tank water ($°C$).

Substituting Eq. (4.1) -(4.3) into Eq. (4.4), $M_s c_s \dot{T}_s$, can be presented in Eq. (4.5):

$$M_s c \dot{T}_s = S_e(t) Q_{ERE} - cD_{HW}(t_h)(T_s(t) - T_m(t)) - A_s U_s t_h (T_s(t) - T_a(t)), \tag{4.5}$$

where:

$S_e(t)$ is the switching variable status of the electric resistive element.

$\dot{T}_s$ is then made the subject of the formula in Eq. (4.6):

$$\dot{T}_s = \frac{S_e Q_{ERE}}{M_s c} + \frac{cD_{HW}(t_h) + A_s U_s t_h}{M_s c}(T_s(t)) + \frac{cD_{HW}(t) T_m(t)}{M_s c} + \frac{A_s U_s t_{(h)} T_a(t)}{M_s c}. \tag{4.6}$$

Eq. (6) is isolated into the separate components, shown in Eq. 4.7 – 4.9, so that the state space equation, representing the system, is formulated [144,145]. The state space equation is rearranged, so that the water temperature in the storage tank, shown as the state variable, is the subject of the formula, which denotes:

$$A(t) = \frac{cD_{HW}(t) + A_s U_s t_h}{M_s c}, \tag{4.7}$$

$$B = \frac{Q_{ERE}}{M_s c}, \tag{4.8}$$

$$C(t) = \frac{cD_{HW}(t)T_m(t)}{M_s c} + \frac{A_s U_s t_h T_a(t)}{M_s c}, \tag{4.9}$$

$$\dot{T}_s = -A(t)T_s(t) + BS_e(t) + C(t). \tag{4.10}$$

In the state space given by equations (4.7) – (4.9), the control or decision variable is $S_e(t)$, while the state variable is $\dot{T}_s$ and the disturbance variable in the system is $C(t)$.

4.2.2 Discretizing the hot water temperature

Eq. (4.10) is a continuous formulation and should be converted into a general discrete function, with respect to the k^{th} hot water temperature function. This will enable a visualization of the temperature dynamic of the water inside the storage tank, at any given time interval:

$$T_{k+1} = T_k(1 - t_s A_k) + t_s B S_{e_k} + t_s C_k, \tag{4.11}$$

where: T_k in Eq. (4.11) is the temperature inside the storage tank.

Since the state variable, T_{k+1} is to be expressed in terms of its initial value, T_0 and the control variable, S_{e_k}, T_{k+1} at each interval is initially derived as:

Substituting $k = 0$, then T_1 in Eq. (4.11) becomes Eq. (4.12):

$$T_1 = T_0(1 - t_s A_0) + t_s B S_{e_0} + t_s C_0. \tag{4.12}$$

Furthermore, when $k=1$, then T_2 is denoted in Eq. (4.13):

$$T_2 = T_1(1-t_sA_1) + t_sBS_{e_1} + t_sC_1. \tag{4.13}$$

Replacing T_1 from Eq. (4.12) into Eq. (4.13) so that Eq. (4.14) for T_2 will be:

$$T_2 = [T_0(1-t_sA_1) + t_sBS_{e_0} + t_sC_0](1-t_sA_1) + t_sBS_{e_1} + t_sC_1. \tag{4.14}$$

After expansion and factorization, T_2 will be as shown in Eq. (4.15):

$$T_2 = T_0[(1-t_sA_0)(1-t_sA_1)] + t_sB[(1-t_sA_1)S_{e_0} + S_{e_1}] + t_s[(1-t_sA_1)C_0 + C_1]. \tag{4.15}$$

Following the same procedure for Eq. (4.12)-(4.15) with $k=2$, T_3 will then become Eq. (4.16):

$$\begin{aligned} T_3 = {} & [(1-t_sA_0)(1-t_sA_1)(1-t_sA_2)] + t_sB[(1-t_sA_1)(1-t_sA_2)S_{e_0} + (1-t_sA_2)S_{e_1} + S_{e_2}] + \\ & t_s[(1+t_sA_1)(1+t_sA_2)C_1 + C_2], \\ & \vdots \\ T_{(k+1)} = {} & T_0\prod_{j=0}^{k}(1-t_sA_j) + t_sB\sum_{j=0}^{k}S_{e_j}\prod_{i=j+1}^{k}(1-t_sA_i) + t_s\sum_{j=0}^{k}C_j\prod_{j=i+1}^{k}(1-t_sA_i), \end{aligned} \tag{4.16}$$

where:

T_k and T_0 are the k^{th} and initial temperatures of the water inside the tank respectively ($^{\circ}C$);

t_s is the sampling time (s);

S_{e_k} is the switching status with a single binary value (0 or 1).

4.2.3 Objective function

The main objective is to minimize the cost of the energy supplied to all the ESTWHs in the building. The main objective may further be divided into two parts, a primary and secondary objective. The primary objective may be achieved, by minimizing the cost of energy subjected to the ToU tariff. Fundamentally, the control algorithm should find the optimal switching solution that would result in energy usage during the low-cost regions, while avoiding the peak periods. Therefore, the primary objective function is given by Eq. (4.18):

$$J_p = t_s\left(\sum_{k=1}^{N} P_{EL(1)}\psi_k S_{e_{k(1)}} + \sum_{k=1}^{N} P_{EL(2)}\ \psi_k S_{e_{k(2)}} + \ldots\ldots\ldots \sum_{k=1}^{N} P_{EL(N)}\ \psi_k S_{e_{k(N)}}\right), \qquad (4.18)$$

where:

t_s is the sampling time (hours);

$P_{EL(N)}$ is the rated power of each of the electric resistive element (kW);

S_{e_k} is the switching status function for each element of the associated ESTWH.

ψ_k is the ToU tariff function ($\$/kWh$), described in Eq. (4.19) and (4.20);

$$\psi(t) = \begin{cases} \psi_p; t \in T_k, T_k = [7,10)[18,20); \\ \psi_o; t \in T_k, T_k = [0,6)[22,24); \\ \psi_s; T_k, T_k = [6,7)[10,18)[20,22). \end{cases} \qquad (4.19)$$

$$\psi(t) = \begin{cases} \psi_p; t \in T_k, T_k = [6,9)[17,19); \\ \psi_o; t \in T_k, T_k = [0,6)[22,24); \\ \psi_s; T_k, T_k = [9,17)[19,22); \end{cases} \qquad (4.20)$$

where:

ψ_p is the cost of energy during the peak pricing period (\$/kWh);

ψ_o is the cost of energy during the off-peak pricing period (\$/kWh);

ψ_s is the cost of energy during the standard pricing period (\$/kWh).

The power rating is included in the objective function, so that the objective function value, after optimization, will be equal to the total energy cost incurred.

The secondary objective, is to mitigate simultaneous switching of the ESTWHs, in order to reduce the maximum demand to within acceptable limits:

$$J_s = t_s.\varphi.\max\sum_{k=1}^{N}(P_{EL(1)}S_{e_{k(1)}} + P_{EL(2)}S_{e_{k(2)}} + ...P_{EL(N)}S_{e_{k(N)}}), \qquad (4.21)$$

where:

φ is the maximum demand cost (\$/kVA);

S_{e_k} is the switching status function for each element of the associated ESTWH.

Analogous to the primary objective function, the cost of the maximum demand will be added to the total objective function, denoting the total costs incurred. Although, the maximum demand is measured in kVA and the ESTWH rated power is in kW. The assumption may be made that the ESTWHs operate at unity power factor (purely resistive load), so that 1 kW = 1 kVA. This means that the per kVA cost may be allocated to the kW rating of power drawn by each ESTWH. Therefore, the aggregate objective function becomes Eq. (4.22):

$$J_p = t_s(\sum_{k=1}^{N}P_{EL(1)}\psi_k S_{e_{k(1)}}.....+\sum_{k=1}^{N}P_{EL(N)}\ \psi_k S_{e_{k(N)}}) + t_s.\varphi.\max\sum_{k=1}^{N}(P_{EL(1)}S_{e_{k(1)}}.....+P_{EL(N)}S_{e_{k(N)}}). \qquad (4.22)$$

4.2.4 Constraints

The objective function is subjected to the following constraints:

$$T_{s_{\min}} \leq T_0 \prod_{j=0}^{k}(1-t_s A_j) + t_s B \sum_{j=0}^{k} S_{e_j} \prod_{i=j+1}^{k}(1-t_s A_i) + t_s \sum_{j=0}^{k} C_j \prod_{j=i+1}^{k}(1-t_s A_i), \tag{4.23}$$

$$T_0 \prod_{j=0}^{k}(1-t_s A_j) + t_s B \sum_{j=0}^{k} S_{e_j} \prod_{i=j+1}^{k}(1-t_s A_i) + t_s \sum_{j=0}^{k} C_j \prod_{j=i+1}^{k}(1-t_s A_i) \leq T_{s_{\max}}, \tag{4.24}$$

$$S_{e_k} \in \{0,1\}. \tag{4.25}$$

The constraints noted in Eq. (4.23) – (4.25), are required to maintain the desired temperature levels [146].

The $T_{s_{\min}}$ denotes the minimum permissible temperature that the water in the storage tank may reach. $T_{s_{\max}}$ is the maximum threshold that the temperature may not exceed, for any given interval. The general expression attained in Eq. (4.17), represents the actual temperature of the water in the storage tank.

4.2.5 Solver selection

The solver should be able to solve for x, where x is a single binary value for each switching function. The fastest and most appropriate solver for such a large-scale nonlinear problem, is the SCIP (Solving Constraint Integer Problems) solver in the OPTI-toolbox in MATLAB [147].

4.3 CASE STUDY DESCRIPTION

4.3.1 Hybrid water heating system layout

The water heating network of the hospital, Mediclinic in Bloemfontein, consists of 57 electric storage tank water heaters, supplied with pre-heated water from a waste heat recovery system. The waste heat recovery system is a multifunctional chiller, shown in Fig. 4.1, that recovers heat from HVAC processes. The recovered heat is then transferred to a pre-heated storage tank, presented in Fig. 4.2. The pre-heated storage system consists of two 5 kilolitre insulated water tanks, located on the roof of the hospital building. These tanks supply water through pressure pumps to all the electric storage tank water heaters in the building. As soon as water is drawn from any of the ESTWHs, cold (near ambient temperature) make-up water flows into the preheated storage tank, to maintain a constant volume. The preheated water is continuously circulated throughout the entire building, to maintain high thermal levels. Provided the pumps are not active, the water in the conduits will start to lose thermal energy through surface conduction, resulting in low water temperatures for the ESTWH inlets.

Fig. 4.1: Multifunctional chiller

Fig. 4.2: Preheated water storage tanks

Most of the ESTWHs, distributed across the hospital building, have parallel configurations, while six are connected in series, to increase the capacity for higher load demands. This ensures that the desired temperature for these demands is maintained continuously. The basement of the hospital houses the laundry section, with two dedicated ESTWHs supplying an industrial laundry system. Levels 2 to 7 contain the remainder of the ESTWHs that supply the individual rooms and wards. The water heating system configuration is shown in Fig. 4.3. In the figure, the conduits in red indicate the supply, while the orange-coloured pipes denote the return, to be recirculated through the heat exchanger section of the multifunctional chiller. The cold make-up water, entering the system from the municipal supply line, is indicated in blue.

One pressure pump is located between the Multifunctional chiller system and the pre-heated water storage tanks. An additional two pressure pumps are connected in parallel, to circulate the pre-heated water throughout the building. The pressure on each level is continuously measured and logged, to ensure all ESTWHs have a continuous supply of pre-heated water.

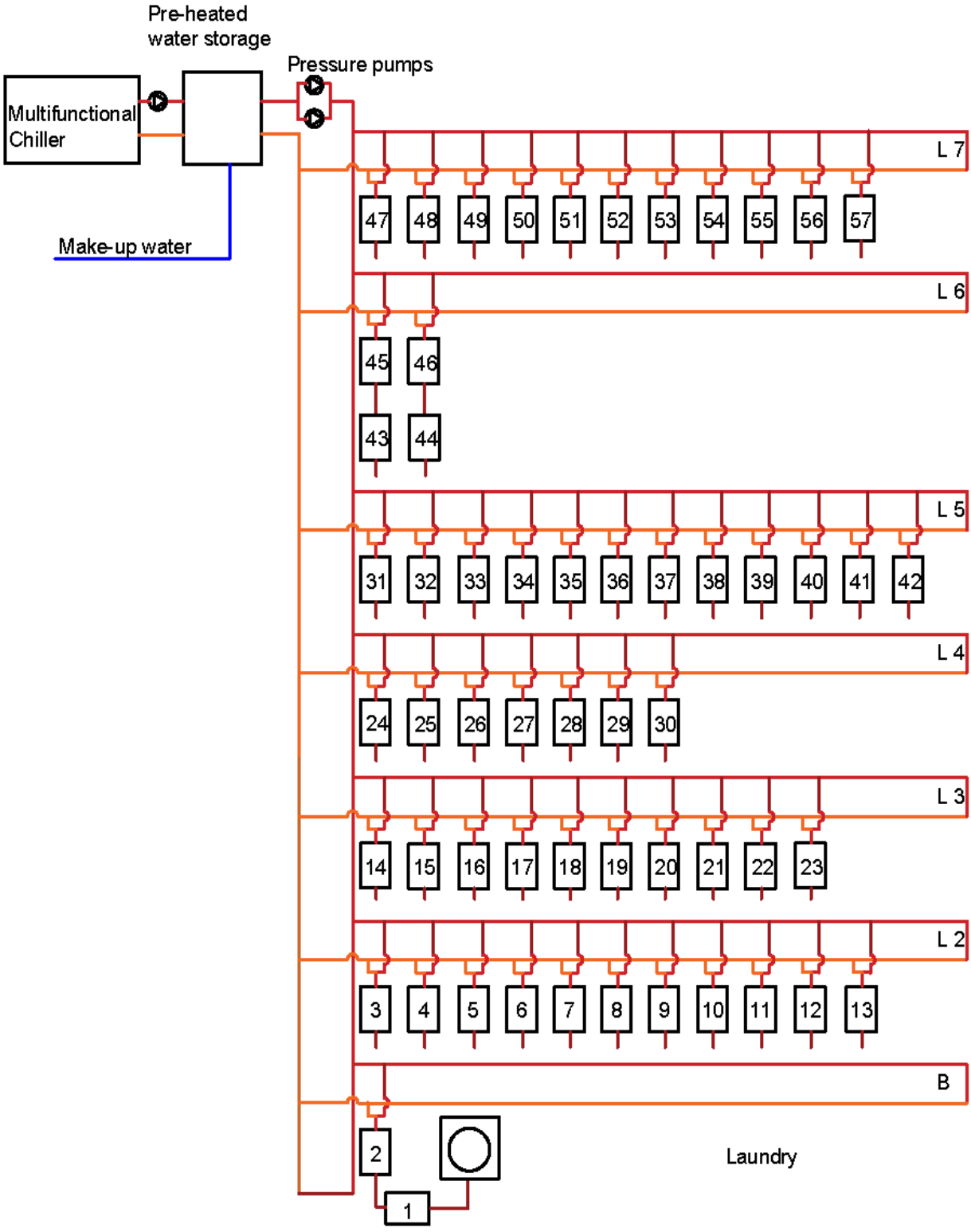

Fig. 4.3: Water heating system configuration.

In Fig 4.4, the connection of a power quality analyzer (PEL 103) to the distribution box, that supplies ESTWHs in the building, is shown. The black clamps are connected to measure the voltage of each busbar, while the red current transformer loops are used to determine the current through each phase. The PEL 103 logs the voltage, current, power and energy usage of the ESTWHs.

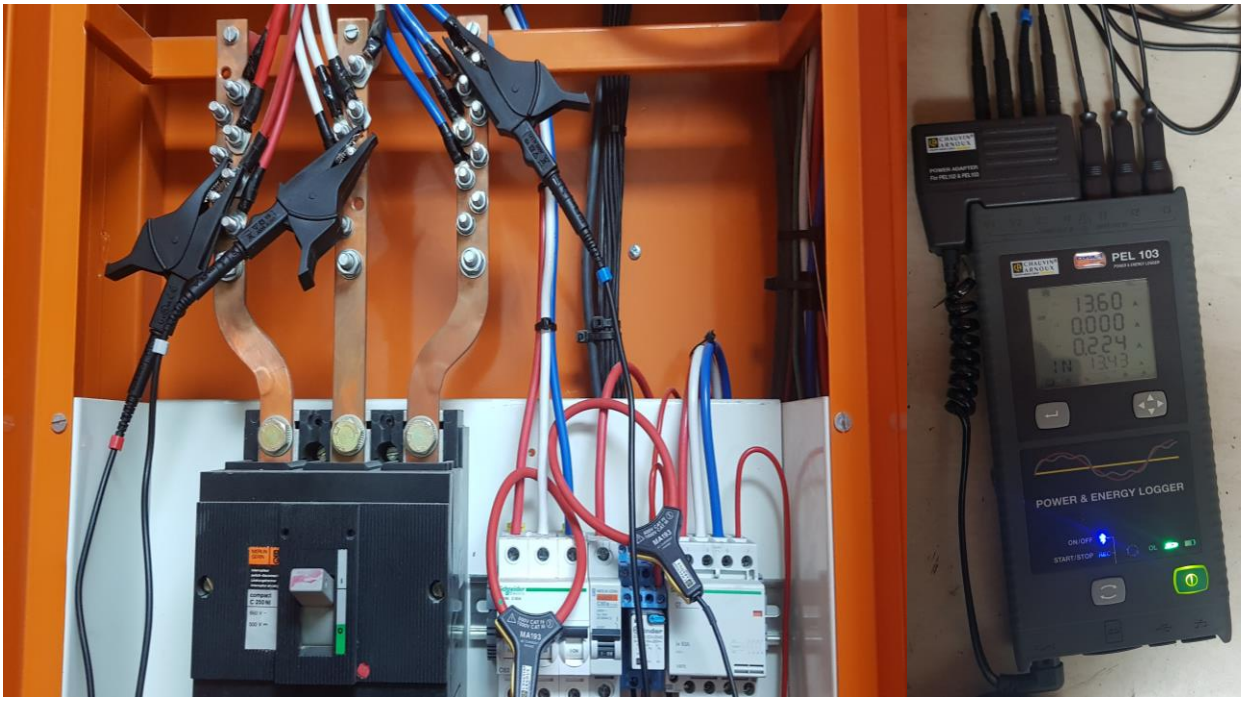

Fig. 4.4: Power and energy logger setup (PEL 103) on water heating distribution board

The ESTWHs' parameters of each level are shown in Table 4.1. The water heaters inside the building have power ratings, ranging from 2 kW, for 100 litre tanks, to 4kW, for 200/250 litre tanks. The ESTWH numbers, in terms of power ratings, are relatively balanced. 18 x 2- and 3-kW units are distributed across the building, near the points of hot water consumption. The remaining 21 units are rated at 4 kW each. This amounts to a cumulative power rating of 174 kW.

Table 4.1: ESTWH power ratings and location

Ward	Level	Location	Qty	Litres	Power
A	7	Cleaners room	1	100	2kW
A	7	Sterile supply room	1	250	4kW
A	7	Dirty linen room	1	150	3kW
A	7	Bathroom in passage	1	150	3kW
A	7	Room 24	1	100	2kW
A	7	Room 23	1	100	2kW
A	7	Equipment room	1	150	3kW
A	7	Staff toilet	1	150	3kW
A	7	Kitchen	1	150	3kW
A	7	Equipment store	1	150	3kW
	7	Public toilet - female	1	100	2kW
B	6	4 Tube system circulation	4	200	4kW
	5	Public toilet - female	1	100	2kW
	5	Public toilet - male	1	100	2kW
C	5	Cleaners room	1	100	2kW
C	5	Room 39-40 bathroom	1	200	4kW
C	5	Staff toilet	1	200	4kW
C	5	Room 22-26 bathroom	1	200	4kW
C	5	Room 20	1	100	2kW
C	5	Room 21	1	100	2kW
C	5	Sterile room	1	200	4kW
C	5	Staff toilet	1	100	2kW
C	5	Store	1	200	4kW
C	5	Room 3 bathroom	1	200	4kW
D	4	Room 39-40 bathroom	1	200	4kW
D	4	Drug store	1	200	4kW
D	4	Medical store	1	200	4kW
D	4	Room 20	1	100	2kW
D	4	Room 21	1	100	2kW
D	4	Staff toilet	1	100	2kW
D	4	Room 3 bathroom	1	200	4kW
E	3	Store at lifts	1	100	2kW
E	3	Room 3-4 bathroom	1	100	2kW
E	3	Equipment store	1	150	3kW
E	3	Room 16	1	100	2kW

E	3	File store	1	100	2kW
E	3	Room 17	1	100	2kW
E	3	Room 18-22	1	150	3kW
E	3	Public toilet	1	150	3kW
E	3	Cleaners store	1	200	4kW
E	3	Cleaners room	1	150	3kW
	2	Male toilet	1	250	4kW
H	2	Female toilet	1	150	3kW
H	2	Room 1-2 bathroom	1	150	3kW
F	2	Room 8-10 bathroom	1	150	3kW
F	2	Room 11	1	150	3kW
F	2	Room 12	1	150	3kW
F	2	Room 17-18 bathroom	1	200	4kW
F	2	Linen room	2	150	3kW
F	2	Baby room	1	150	3kW
F	2	Storeroom	1	150	3kW
	Base	Laundry	1	200	4KW
	Base	Laundry	1	200	4KW

The probability of these units reaching this peak power level is exceptionally low. However, simultaneous switching *on* events occur frequently and may, in part, be responsible for the high maximum demand costs incurred by the facility.

In Table 4.2, the simulation parameters are presented. The sampling time was taken to be 5 minutes, to improve the accuracy of the presented temperature variations in the storage tanks of the ESTWHs. Furthermore, the time interval at which data is available, was at 5 minute intervals. The ToU tariff costs, for the high and low demand seasons, are given in the table. In addition, the maximum demand costs per kVA and other relevant parameters, are further given in the table.

Table 4.2: Simulation parameters

Item	Figure
Sampling time (Δt)	5 min
ϱ_k (summer peak rate)	0.092 USD/kWh
ϱ_0 (summer off-peak rate)	0.054 USD/kWh
ϱ_s (summer standard rate)	0.063 USD/kWh
ϱ_k (winter peak rate)	0.189 USD/kWh
ϱ_0 (winter off-peak rate)	0.088 USD/kWh
ϱ_s (winter standard rate)	0.096 USD/kWh
Maximum demand rate	9.039 USD/kVA
$T_{s_{min}}$	52.8 °C
$T_{s_{max}}$	57 °C
A_s	$0.5\,m^2$ (100L), $0.72\,m^2$ (150L), $0.8\,m^2$ (200L)
U_s	0.3

4.3.2 Hot water demand profile

Hot water demand flow rates were taken over 3 years, using 20 mm pulse output flow meters, with accuracies of approximately 5%. The flow rates over the 3 years were averaged, to represent a typical winter and summer day usage. Due to computational constraints, simulating for longer periods of time, may not be possible.

The measured demand flow rates are shown in Fig. 4.5 and Fig. 4.6, representing the average winter and summer case, respectively. The water heater number in the graphs, correspond to the water heater numbers in Fig. 4.3.

As may be expected, the winter case has shown to have a higher hot water demand, as with the summer case. The amount of hot water drawn, shown at 5 minute intervals, seem to be

similar in magnitude. However, the frequency at which hot water is drawn, is much higher for the winter case, as compared to the summer case.

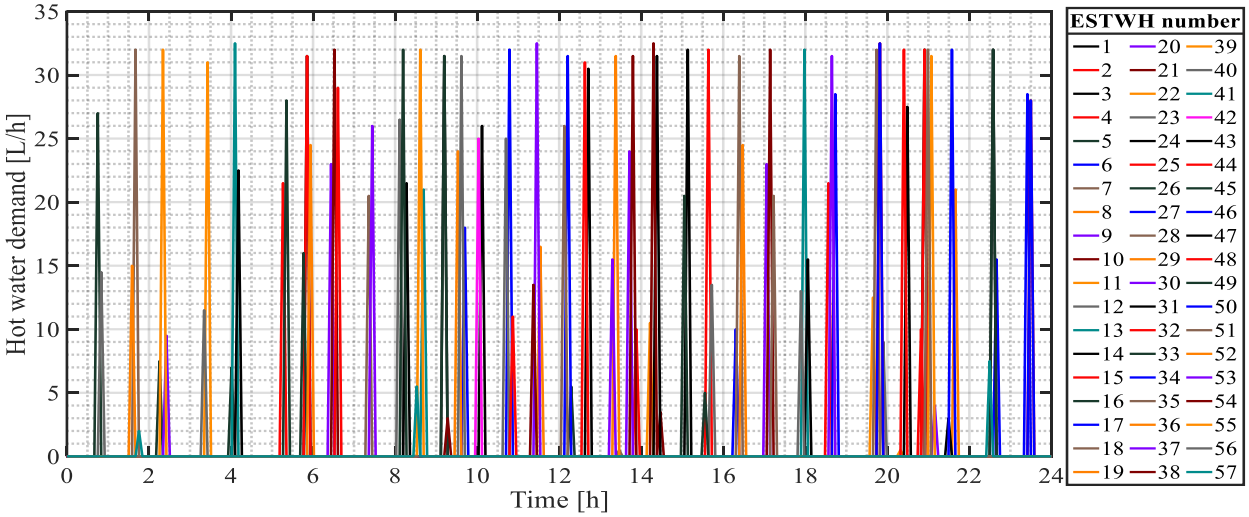

Fig. 4.5: Winter hot water demand flow rates

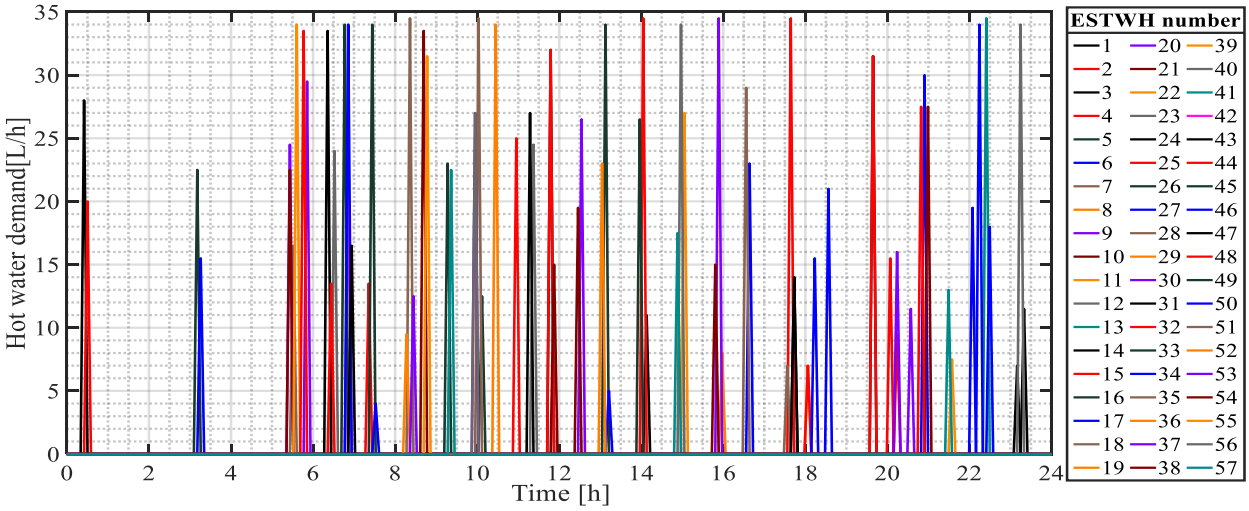

Fig. 4.6: Summer hot water demand flow rates

4.3.3 Inlet (energy recovery system outlet) and ambient air temperature data

In Figs. 4.7 and 4.8, the water inlet temperature of the water supplied from preheated storage system, is shown. To determine the feasibility of the energy recovery system, the water

temperatures of the preheated storage, and by extension, the inlet temperatures of the ESTWHs, were used, when the multifunctional chiller system was offline for maintenance/repair. The days that closely resemble the average ambient temperatures of the average winter and summer days, used in this case study, were chosen to represent the multifarious water heating system, without a multifunctional chiller.

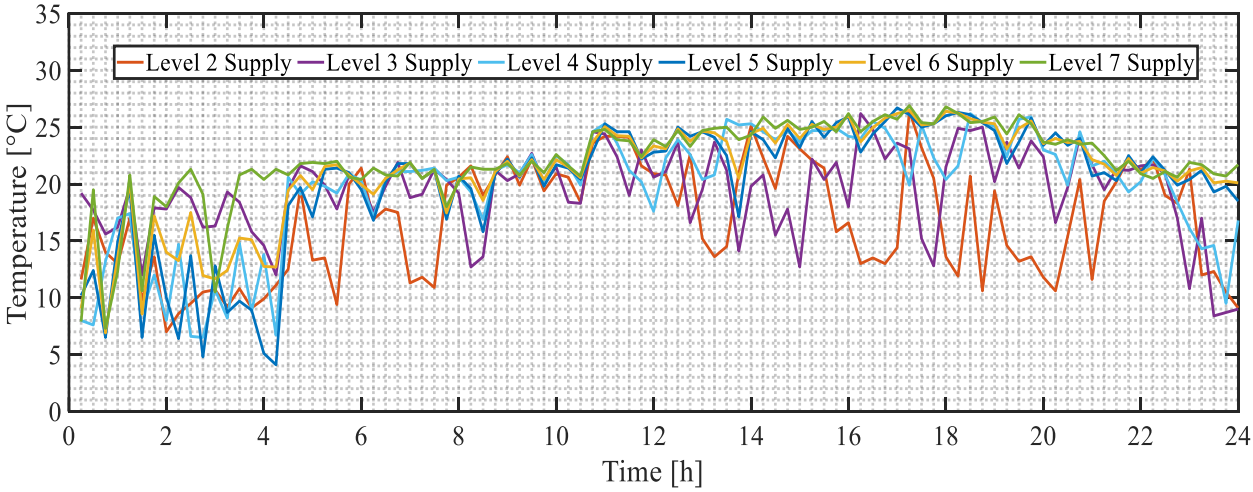

Fig. 4.7: Winter inlet water temperature (without multifunctional chiller)

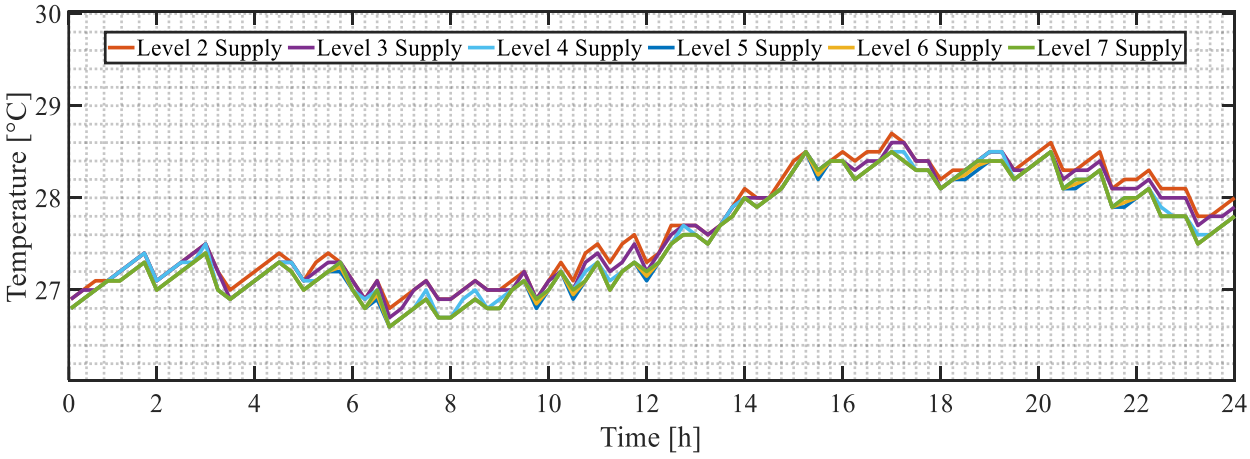

Fig. 4.8: Summer inlet water temperature (without multifunctional chiller)

In Figs. 4.9 and 4.10, the average inlet temperatures over a three-year period, for the winter and summer cases, are shown. The comparatively higher temperature is due to the waste heat received from the heat exchanger, coupled to the multifunctional chiller system (HVAC system).

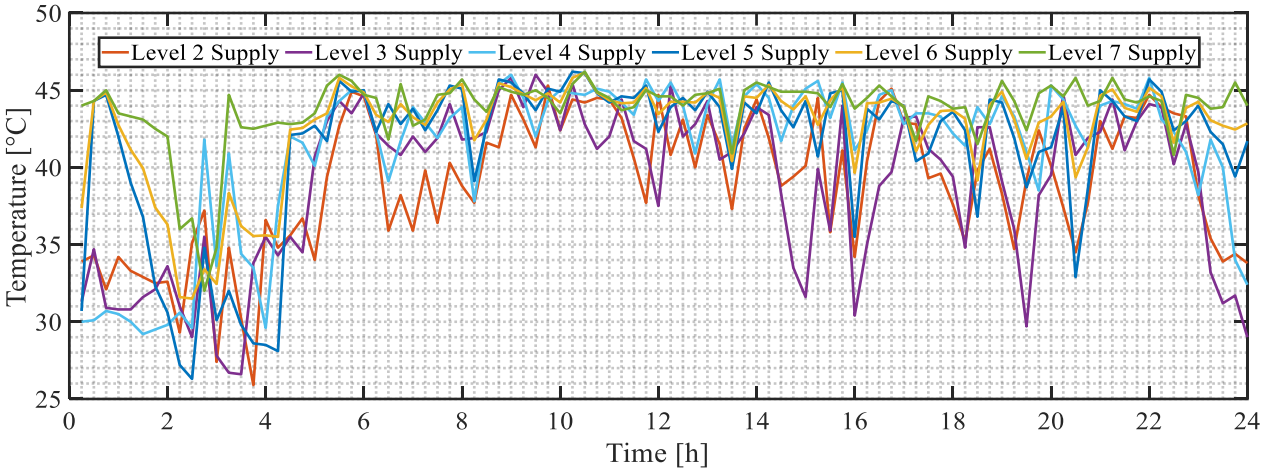

Fig. 4.9: Winter inlet water temperature (with multifunctional chiller)

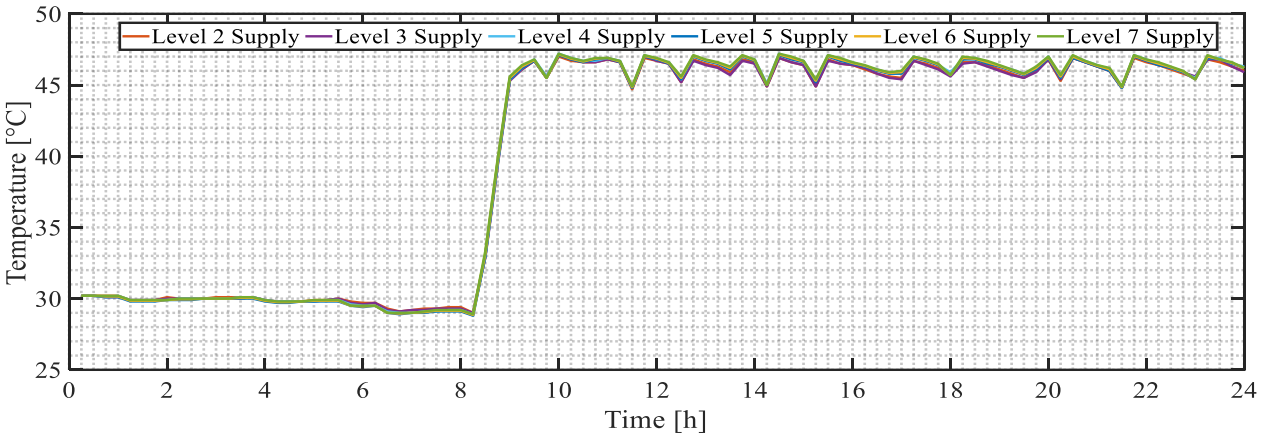

Fig. 4.10: Summer inlet water temperature (with multifunctional chiller)

In Figs. 4.11 and 4.12, the ambient air temperature is measured on the premises of the hospital and relayed to a supervisory control and data acquisition (SCADA) system. The hot water flow rate (demand), water inlet and ambient air temperature was logged at five-minute intervals.

The water inlet and ambient temperatures were collected, using RTD sensors, particularly PT100 sensors, with accuracies of approximately 1%.

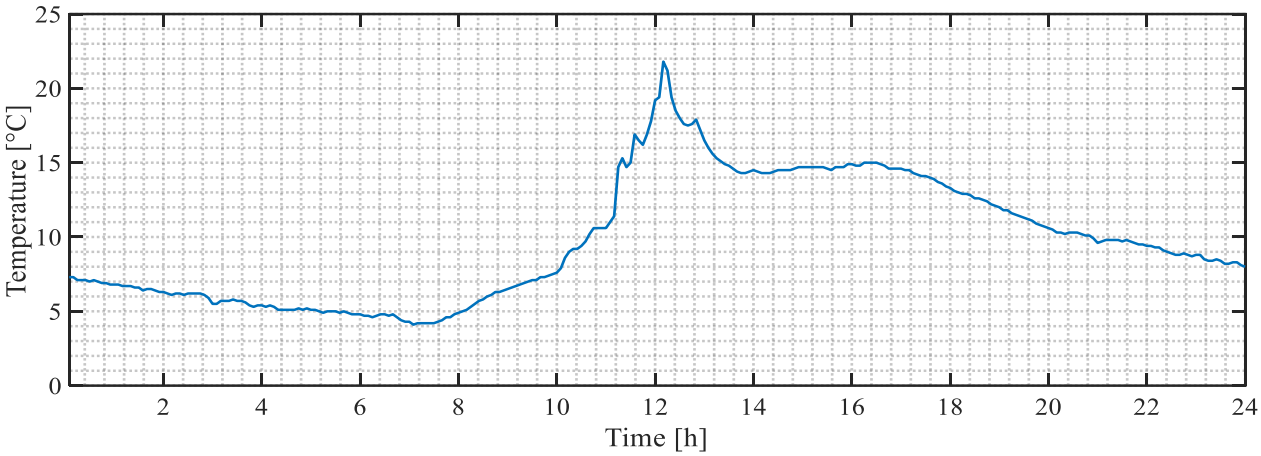

Fig. 4.11: Winter ambient air temperature

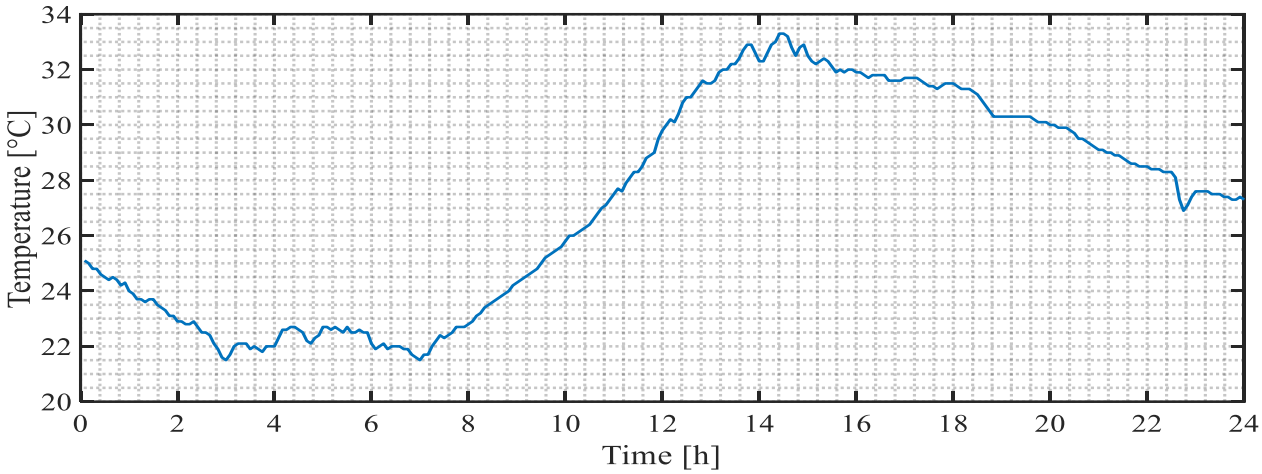

Fig. 4.12: Summer ambient air temperature

The Eskom 2019/2020 ToU tariff periods are represented by Fig. 4.13. The low demand season represents the summer months (September to April) and the high demand season represents the winter months (May to August). From the figure, 5 hours each day, in each season, are considered as peak periods, while 11 hours are allocated to the standard period,

with the remaining 8 hours being charged at the lowest rates. The unit price of electricity for each pricing region, is given in Table 4.2.

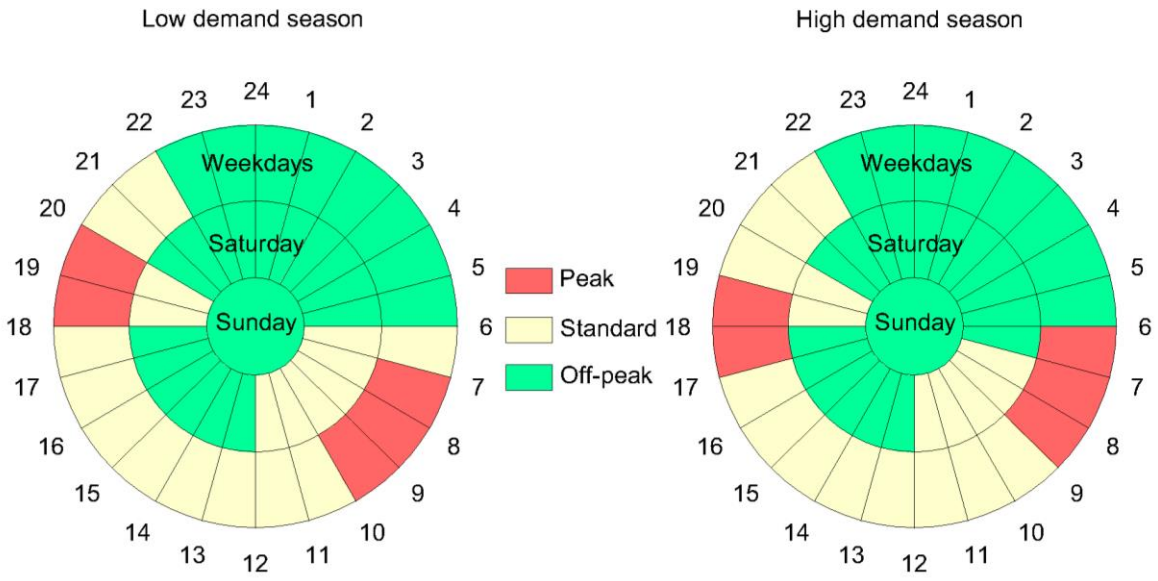

Fig. 4.13: Time-of-Use Periods

4.4 SIMULATION RESULTS AND DISCUSSION

4.4.1 Baseline

Baseline systems were established, in order to evaluate the economic performance of the multifunctional chiller and the proposed optimal control approach. The baselines consist of the entire existing system, with and without a multifunctional chiller. The multifunctional chiller serves as the exergy recovery device. Neither of the two baseline systems have optimal control techniques applied. These baselines are simulated, using the same model, with the same input parameters.

For the sake of reducing the length of the chapter, one level of the hospital was selected, to represent the dynamic changes of the storage tank temperatures and switching functions. This was done to make sense of the simulation results of all the ESTWHs in the system. The entire system dynamic is shown after the level 5 data for each baseline case, as well as the optimal control case. The results for each level in the hospital is shown in Appendix B.

4.4.1.1 Winter case without multifunctional chiller (winter baseline 1)

In this Section, the results for the baseline system 1 during the high demand season (average winter day), is shown. Figs. 4.14 and 4.15, depict the ESTWH tank temperatures and associated switching functions on the fifth level of the hospital building. The level 5 ESTWHs' control and state variable dynamics were introduced prior to the aggregate (entire buildings' ESTWHs) tank temperatures and switching functions, to better elucidate the results. The aggregate tank temperatures are shown in Figs. 4.16 and 4.17.

A challenge in discerning simultaneous switching events is encountered in Fig. 4.17. The solution may be to isolate the simultaneous events on a supplementary plot, or to depict these occurrences as a cumulative plot (on the same graph). A third solution, which serves two purposes, is to use the power draw graph, to both highlight simultaneous switching events and indicate the total power drawn by the entire system, at any given instant. Therefore, for the sake of reducing the number of graphs, the third solution was taken, as shown in Fig. 4.18.

The two baseline systems, in this and the following section, are discussed, with respect to operation of the multifarious system during each ToU tariff region, in Section 4.4.1.3.

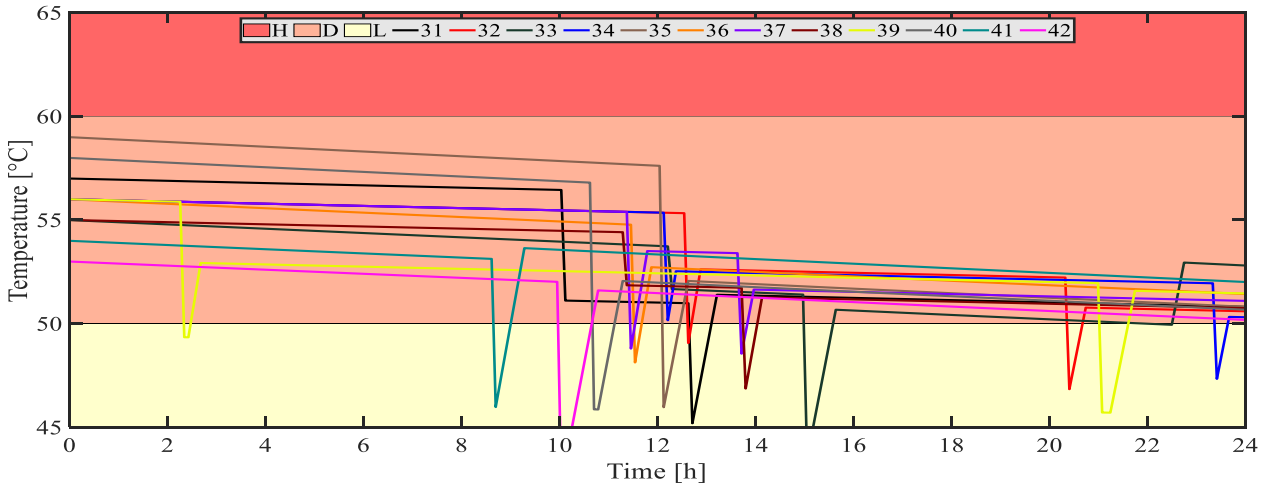

Fig. 4.14: Winter baseline 1 - Level 5 ESTWH temperatures

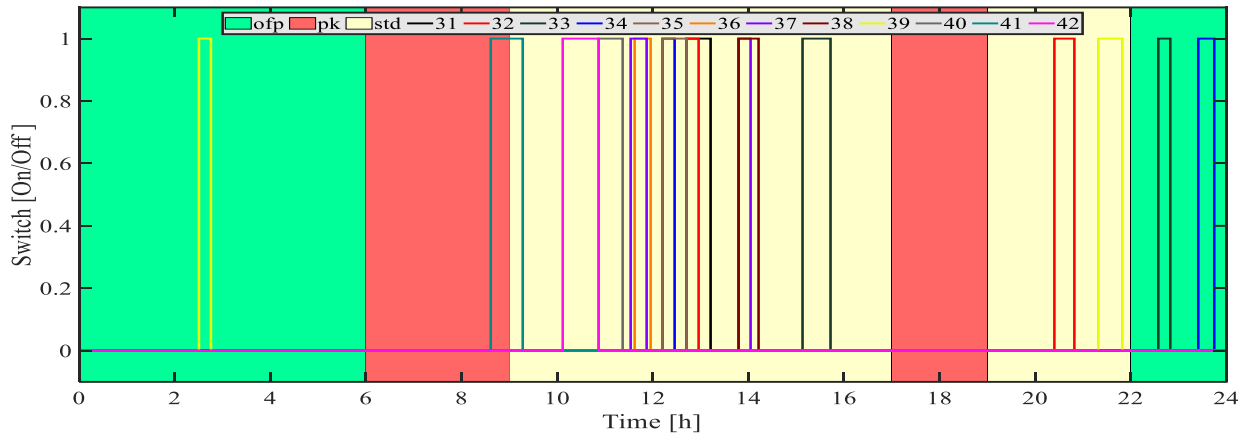

Fig. 4.15: Winter baseline 1 - Level 5 ESTWH switching functions

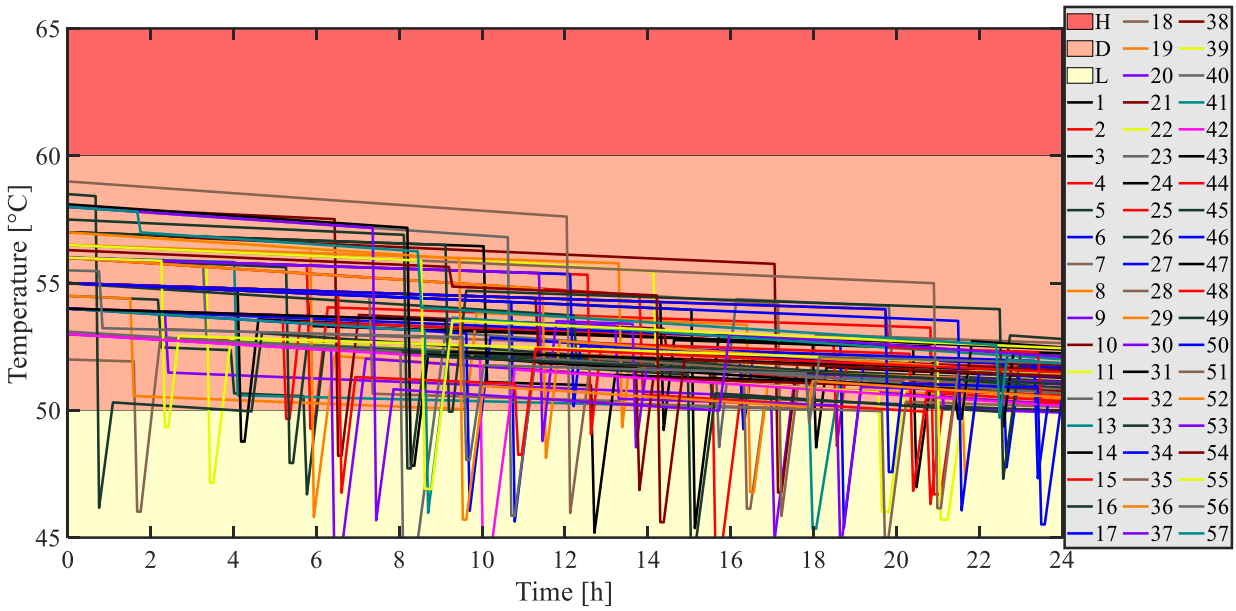

Fig. 4.16: Winter baseline 1 - Aggregate ESTWH storage tank temperatures

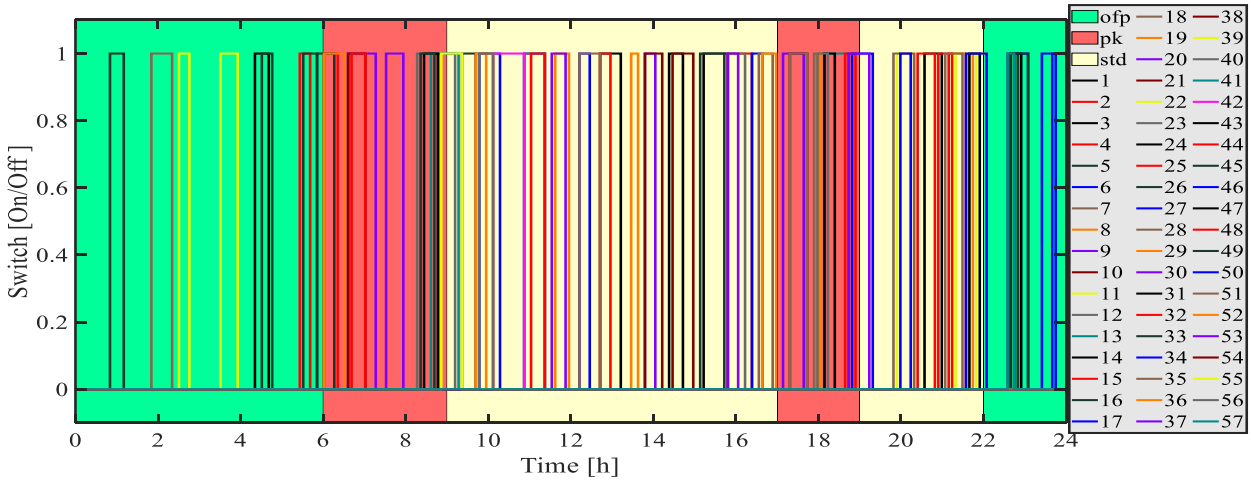

Fig. 4.17: Winter baseline 1 - Aggregate ESTWH switching functions

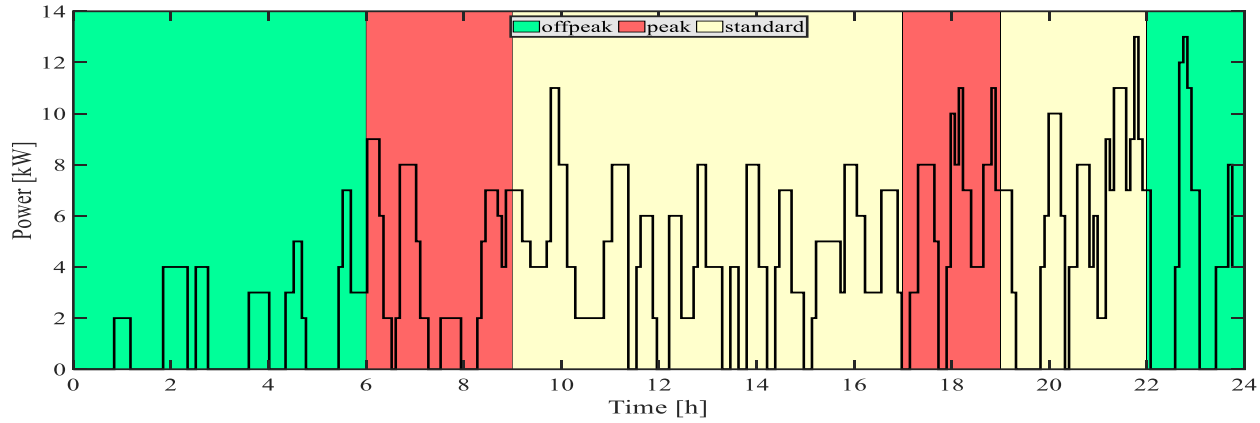

Fig. 4.18: Winter baseline 1 - Total ESTWH power draw

4.4.1.2 Winter case with multifunctional chiller (winter baseline 2)

In this Section, the results of the baseline system 2, representing winter, is shown. The baseline system 2, considers the addition of the multifunctional chiller to the existing multifarious water heating setup as an energy recovery device. As with the previous section, the state variables, control variable dynamics and load profile are shown in Figs. 4.19 to 4.23, respectively. The behaviour of the system, under each ToU region, is discussed in the section that follows.

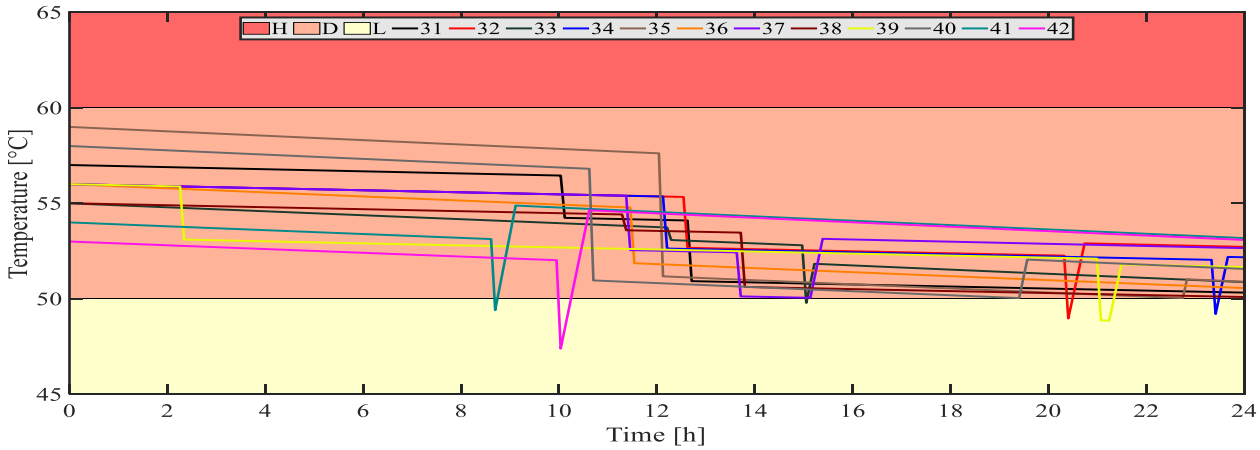

Fig. 4.19: Winter baseline 2 - Level 5 ESTWH temperature

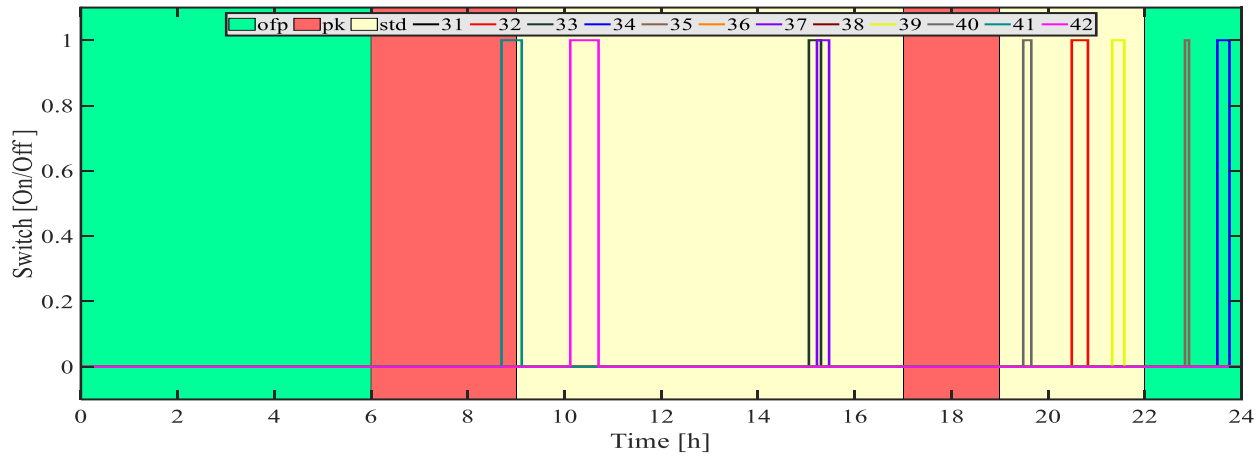

Fig. 4.20: Winter baseline 2 - Level 5 ESTWH switching function

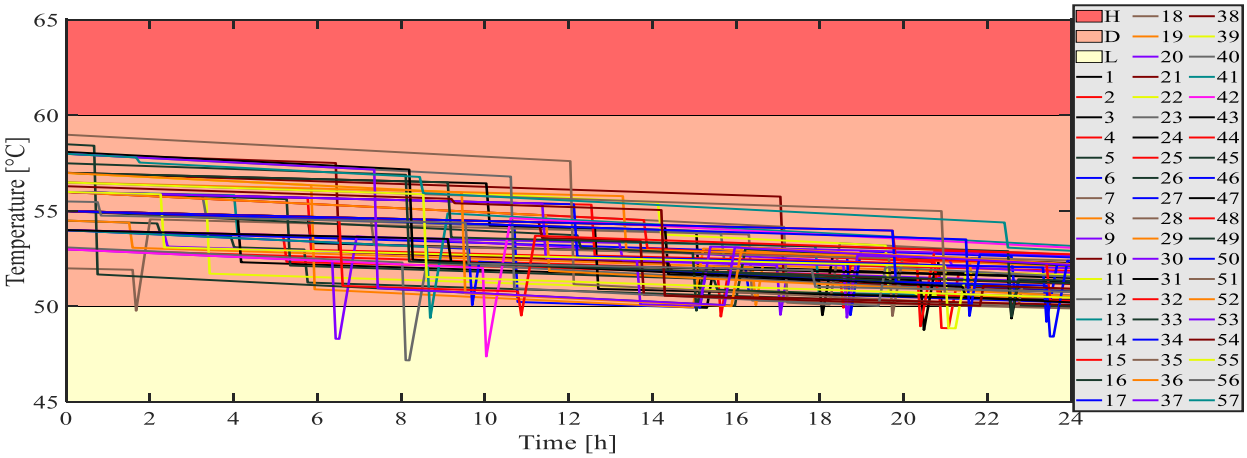

Fig. 4.21: Winter baseline 2 - Aggregate ESTWH storage tank temperature

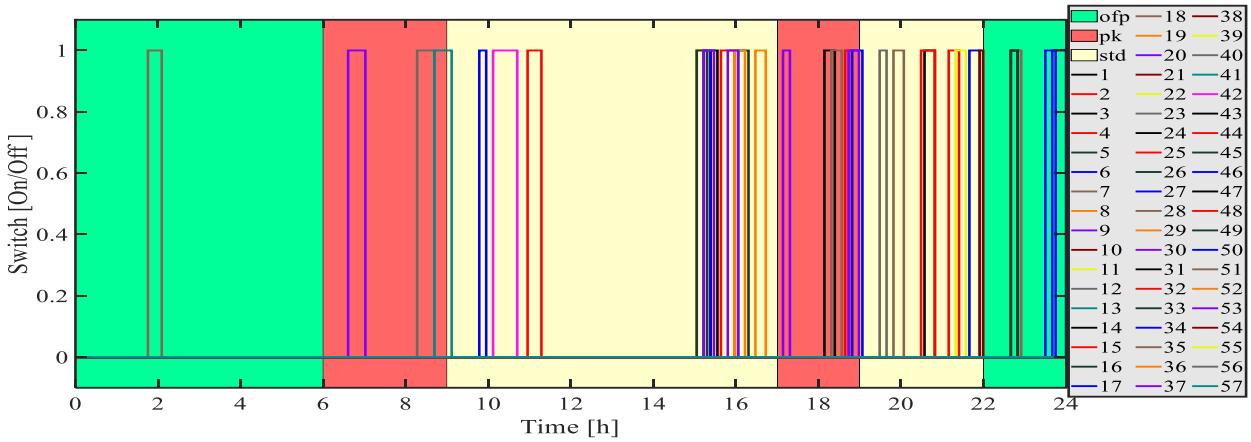

Fig. 4.22: Winter baseline 2 - Aggregate ESTWH switch function

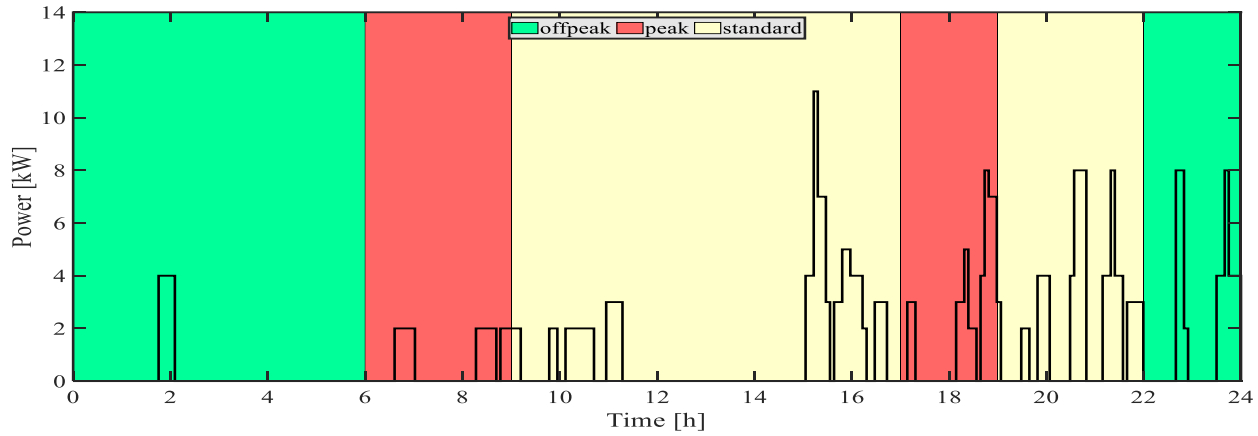

Fig. 4.23: Winter baseline 2 - Total ESTWH power draw

4.4.1.3 Winter case baseline discussion

4.4.1.3 a) Off-peak ToU period [00h00 to 06h00)

With reference to Figs. 4.14 and 4.15, the level 5 ESTWHs have one switching event that occur for the baseline 1 system during the off-peak period. The baseline 2 system, where the multifunctional chiller is present in Figs. 4.19 and 4.20, follows a similar trend. The switching function and the associated storage tank temperatures for the baseline 1 system of the entire system is shown in Figs. 4.16 and 4.17. Figs. 4.21 and 4.22 depict the same for baseline 2.

Comparing these two cases, reveals that ten switching events occur during the off-peak period, when the energy recovery system is not involved. This may be attributed to the lower inlet temperature of the system, where, as a result, the temperature of the water in the storage tank is lowered when colder water enters. In hindsight, with reference to baseline 2, a higher inlet water temperature is maintained, so that the storage tank water temperature remains within acceptable levels. Therefore, the system with the multifunctional chiller does not require as much additional energy to maintain the temperature within the desired limits.

In Figs. 4.18 and 4.23, the associated energy usage is shown for each system. The baseline 1 system, without energy recovery, has multiple occurrences of simultaneous switching events, potentially risking maximum demand penalties. The system with energy recovered, provides sufficient preheated water, so that power is not drawn during this off-peak period.

4.4.1.3 b) Peak ToU period [06h00 to 9h00)

Referring to the same figures as in the off-peak period, the level 5 ESTWHs for both baseline systems, switches *on* once for this entire period. However, assessing the entire system's switching function and temperature profiles, reveals that multiple ESTWHs from other levels, switches *on* during this peak period. In both cases, simultaneous switching events occur with a higher frequency, compared to the first of-peak period. In this instance, the baseline 1 system has a notable spike in power demand, that is 7 kW higher than the highest power draw from baseline 2. The potential risk for maximum demand penalties during this period, is considerably higher in this region, due to higher demands from other equipment in the building.

As may be expected from the baseline 1 system, the overall energy required to maintain the temperature levels within acceptable limits is higher than that of the baseline system 2. Similar to the off-peak behaviour of both systems, a comparatively higher inlet temperature results in a lower energy demand.

4.4.1.3 c) Standard ToU period [09h00 to 17h00)

In this first and longest standard period of the day, the majority of the switching events take place in the level 5 ESTWHs, for both baseline 1 and 2. In this period, as midday approaches, neither of the two baseline systems are able to maintain the temperature of the water inside the storage tanks, and are required to switch *on*.

Referring to the entire system's switching function and storage tank temperatures, a significant difference in the power draw trend is observed. With the baseline system 1, more switching events occur and with higher frequency, as compared to baseline system 2. Additionally, as with the peak period previously discussed, the simultaneous switching *on* events, demands a higher peak power for both baseline systems, with a maximum of 11 kW. Baseline system 1 and 2, reaches the maximum once only, with the first baseline requiring more energy when considering the period as a whole. Therefore, the multifunctional chiller system successfully reduced the energy requirement for maintaining the water thermal levels, which further resulted in minimal simultaneous switching *on* events. This, in turn, reduces the risk for severe maximum demand penalties.

4.4.1.3 d) Peak ToU period [17h00 to 19h00)

The second peak period shows no switching occurrences for the Level 5 ESTWHs, for both baseline systems. This is the first peak period where the level 5 ESTWHs are not required to switch on.

Similar to the first peak region, this period carries a high risk for maximum demand penalties, due to other equipment simultaneously operating during this time of day. In retrospect, the peak power draw for each system in the entire facility was observed to be twice for the baseline system 1 and once for the second baseline.

4.4.1.3 e) Standard ToU period [19h00 to 22h00)

Both baseline systems of the level 5 ESTWH switches *on* during this region. In contrast to the previous ToU tariff periods, the baseline system 2 switches *on* three times, while baseline system 1 switches twice. This is due to the thermal level of one of the ESTWH, in the baseline 2 simulation, dropping below the acceptable threshold, and requires energy to maintain the desired temperature.

Comparing the entire systems' switching function and associated ESTWH temperatures, reveals that simultaneous switching occurrences are significantly more prevalent for baseline system 1, than for the second baseline. In addition, the peak power draw and switching frequency is higher for baseline 1 compared to system 2. However, in this case, the risk for maximum demand penalties is lower than that of the peak period; the peak demand of baseline system 1 may unnecessarily increase the risk for such a penalty to be enforced.

4.4.1.3 f) Off-peak ToU period [22h00 to 24h00)

The last pricing region is a 2-hour long, off-peak period. Referring to the level 5 ESTWHs, switching during this period is minimal to recover the thermal energy that was lost as a result of a single load demand. The other ESTWHs on level 5, however, require additional energy from the electric resistive elements to maintain the desired temperature inside each respective storage tank, which could be attributed to standby losses.

Considering the entire scheme, the baseline system 1 shows six instances of simultaneous switching *on* occurrences, with substantial peak demands, compared to the two instances observed for the second baseline system. During this region, the risk for a high maximum demand cost is low. However, due to the hospitals' high load factor, a significant risk remains.

4.4.1.3 Summer case without multifunctional chiller (summer baseline 1)

In this Section, the results of the baseline system 1, for the summer case, is shown. The baseline system 1 considers the multifarious water heating system, without the energy recovery system. In line with the previous sections, the state variables, control variables dynamics and load profile, are shown in Figs. 4.24 to 4.28, respectively. The switching states and temperature variation of the water in the ESTWHs, as well as the associated power draw, are discussed, based on the ToU tariff regions in Section 4.4.1.5.

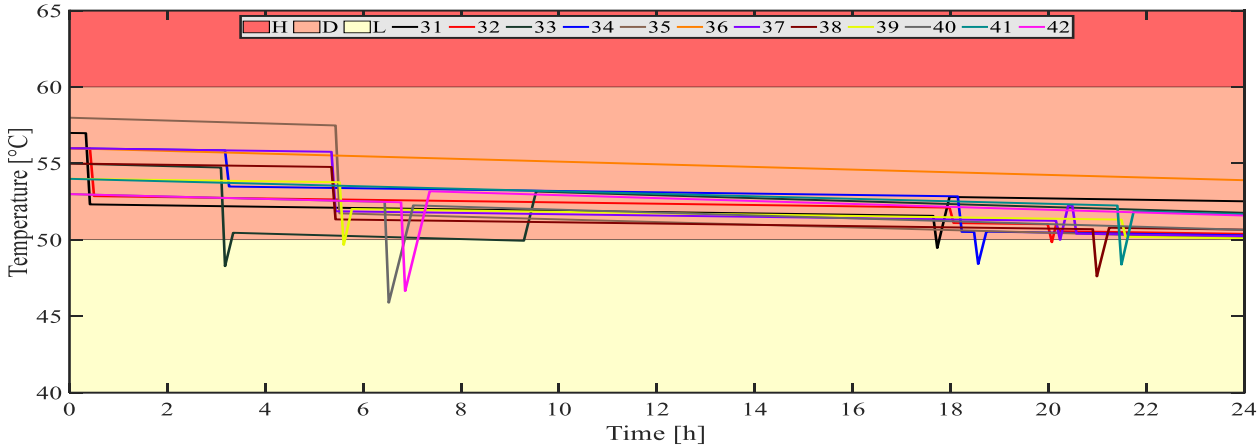

Fig. 4.24: Summer baseline 1 - Level 5 ESTWH temperature

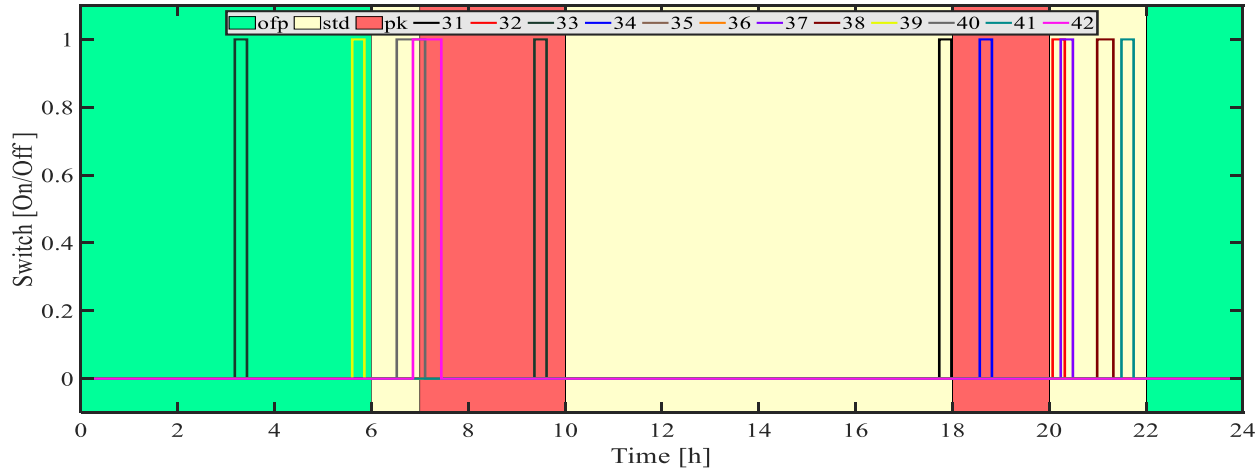

Fig. 4.25: Summer baseline 1 - Level 5 ESTWH switching function

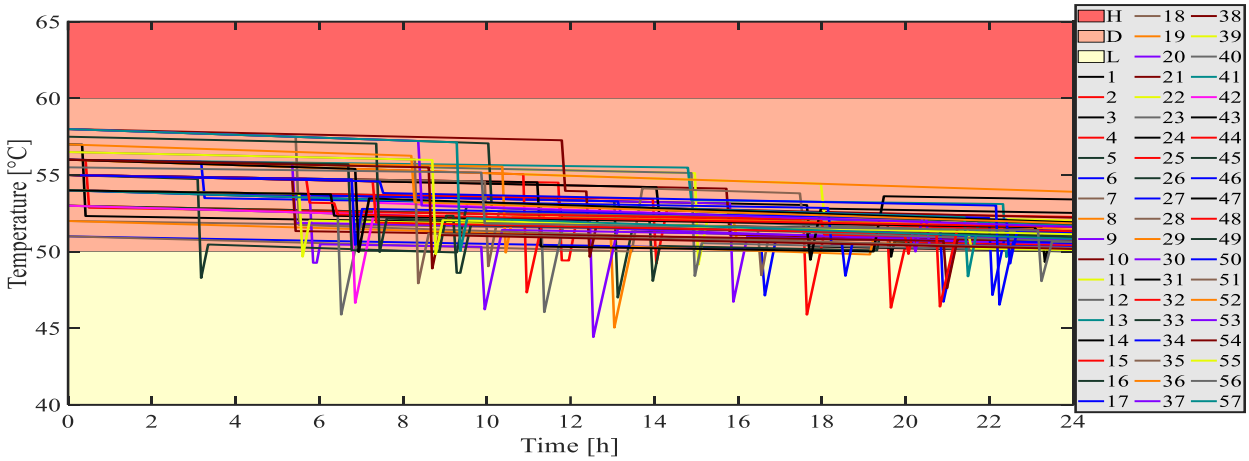

Fig. 4.26: Summer baseline 1 - Aggregate ESTWH storage tank temperatures

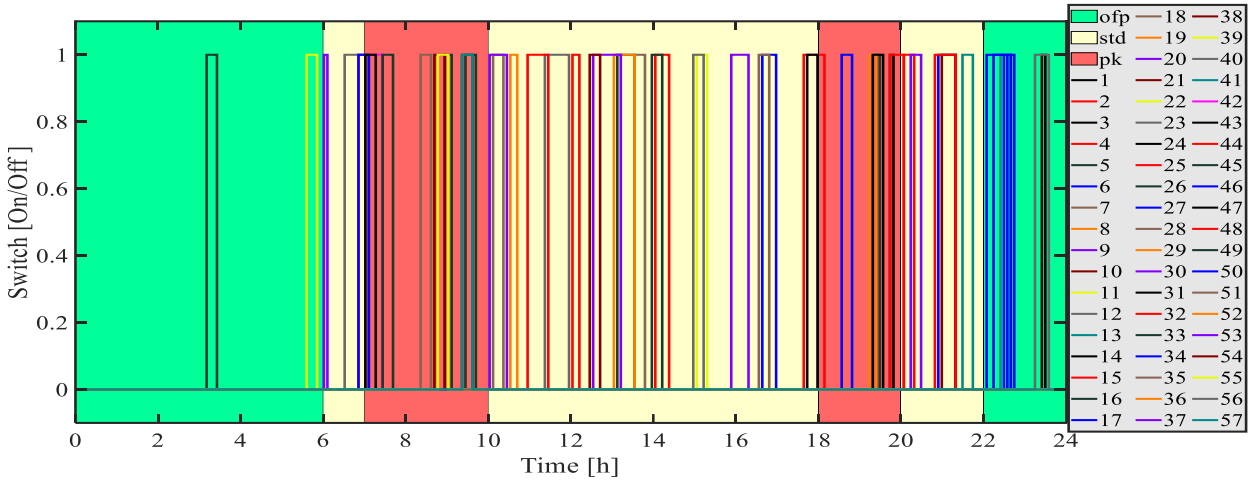

Fig. 4.27: Summer baseline 1 - Aggregate ESTWH switching functions

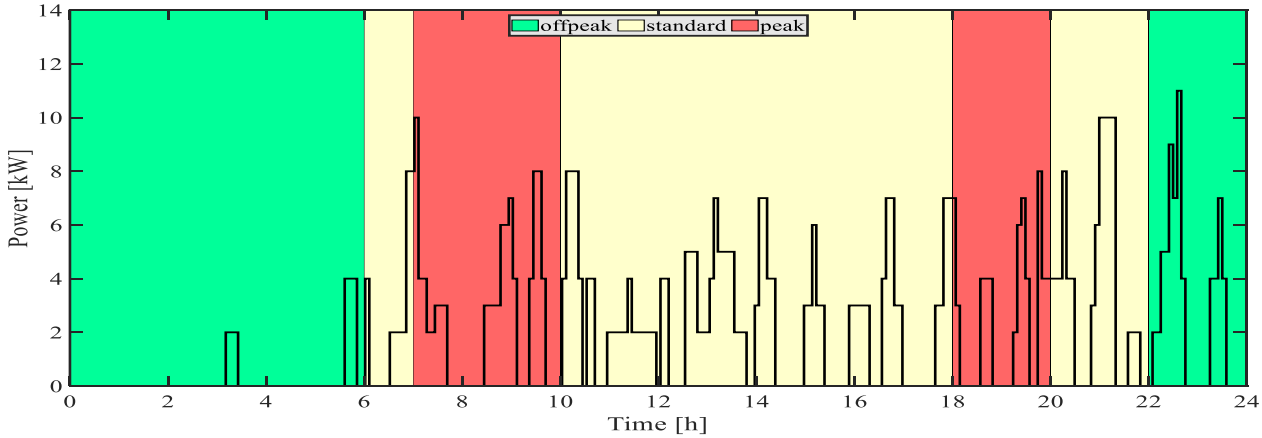

Fig. 4.28: Summer baseline 1 - Total ESTWH power draw

4.4.1.4 Summer case with multifunctional chiller (summer baseline 2)

This section presents the results of the baseline system 2 for the summer case. All variable data, as with the previous section, is depicted in Figs. 4.29 to 4.33, respectively. The variation of the state, control variables and associated power draw, is discussed according to each ToU tariff region in the section that follows.

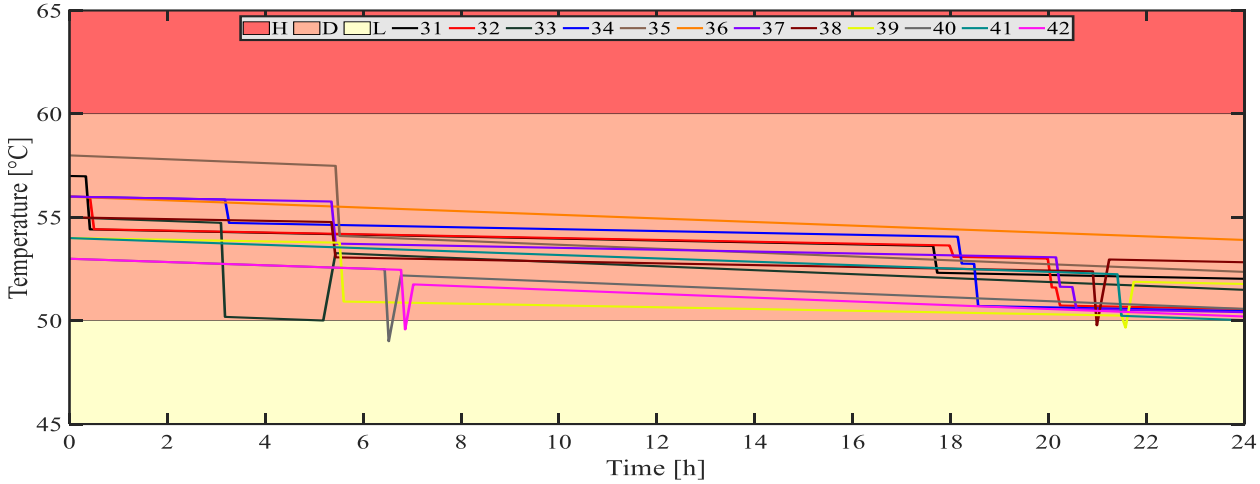

Fig. 4.29: Summer baseline 2 - Level 5 ESTWH temperatures

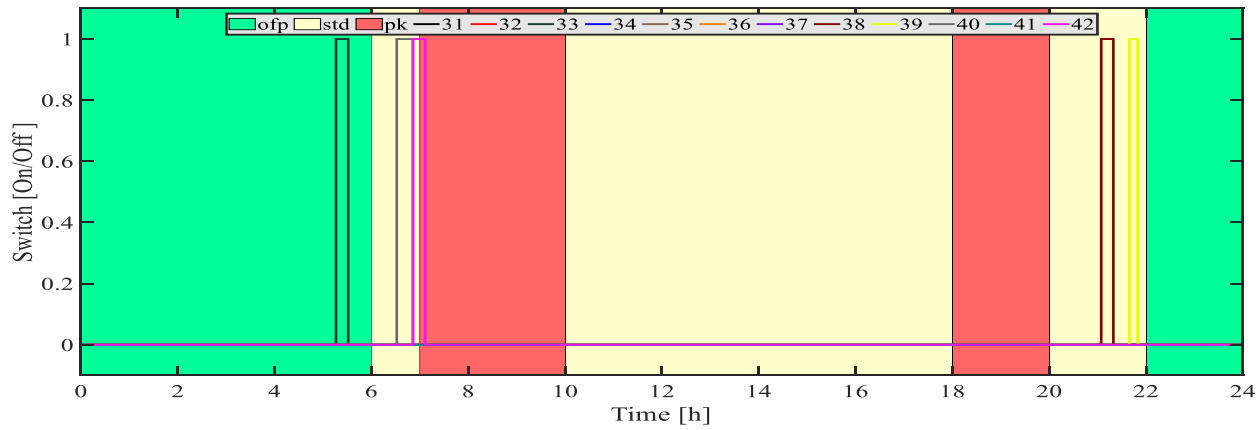

Fig. 4.30: Summer baseline 2 - Level 5 ESTWH switching functions

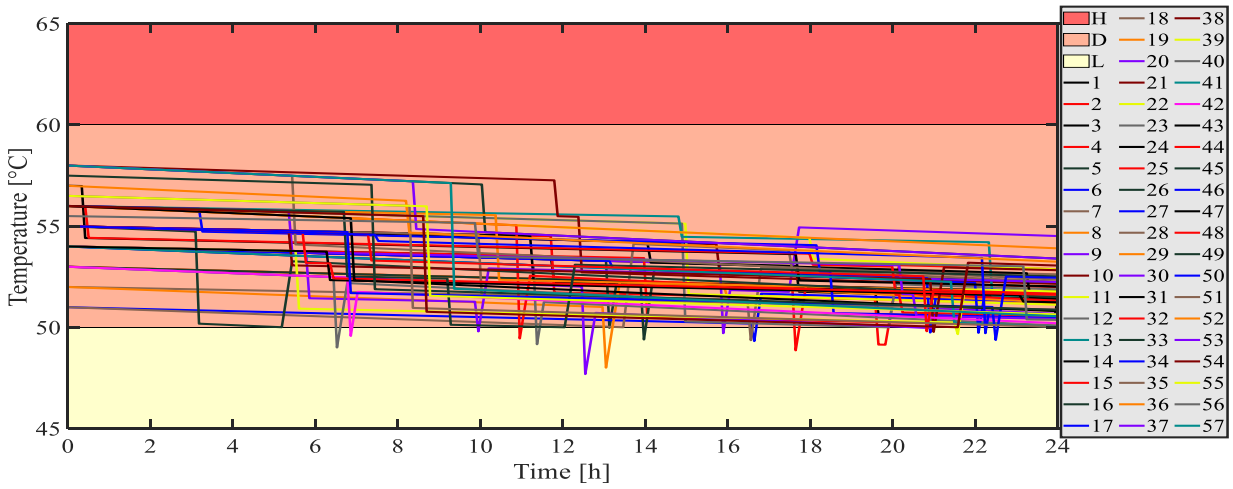

Fig. 4.31: Summer baseline 2 - Aggregate ESTWH storage tank temperatures

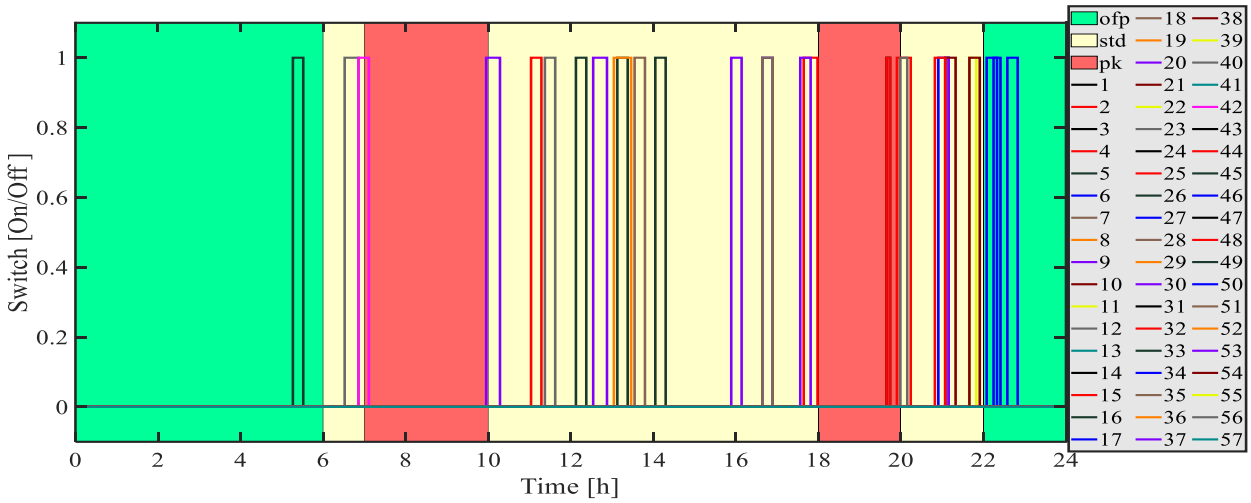

Fig. 4.32: Summer baseline 2 - Aggregate ESTWH switching functions

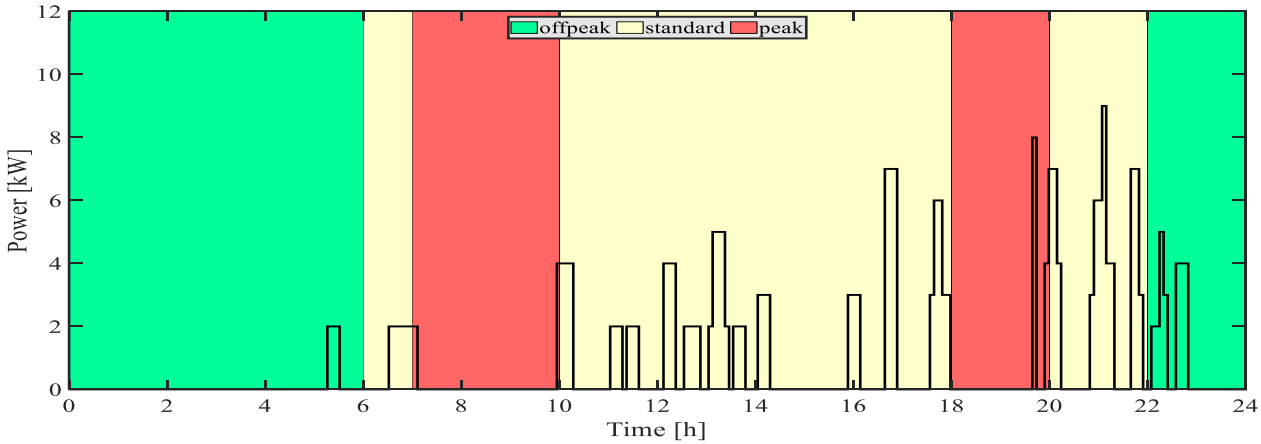

Fig. 4.33: Summer baseline 2 - Total ESTWH power draw

4.4.1.5 Summer case baseline discussion

4.4.1.6 a) Off-peak ToU period [00h00 to 6h00)

With reference to Figs. 4.24 and 4.25, for the baseline 1 system, the level 5 ESTWHs have two switching *on* events that occur during the off-peak period. The baseline 2 system, where the multifunctional chiller is present in Figs. 4.29 and 4.30, requires only one switching *on* event to maintain the desired temperature. The switching function and the associated storage tank temperatures of the entire system, for baseline 1, are shown in Figs. 4.26 and 4.27, while Figs. 4.31 and 4.32 depict the same for baseline 2. Comparing these two cases, reveals that one additional switching *on* event occurs during the off-peak period, when the energy recovery system is not involved. Similar to the winter case, this may be attributed to the lower inlet temperature, due to the absence of recovered energy. Retrospectively, in baseline 2, a higher inlet water temperature is maintained with assistance from the multifunctional chiller, so that the storage tank water temperature of each ESTWH remains within desired levels.

In Figs. 4.28 and 4.33, the associated energy usage is shown for each system. The two baseline systems have no occurrences of simultaneous switching events, reducing the risk for maximum demand penalties in both cases. Compared to baseline system 1, the system with recovered energy provides pre-heated water to the ESTWHs, so that less energy is required from the grid.

4.4.1.5 b) Standard ToU period [06h00 to 07h00)

Referring to the same figures discussed in the previous off-peak section, the level 5 ESTWHs, for both baseline systems, has two switching *on* events during this first standard pricing region. In this instance, the energy recovered from the multifunctional chiller does not seem to have any observable effect on the switching statuses of the ESTWHs.

On the other hand, considering the entire system, simultaneous switching events occur for baseline 1 and not for baseline 2, which indicates that the energy recovery device reduced the

risk for incurring high maximum demand penalties. A comparison between the baseline systems reveals that the overall energy required to maintain the temperature levels, within acceptable limits.

4.4.1.5 c) Peak ToU period [07h00 to 10h00)

The level 5 ESTWHs uses energy during this peak period for both baseline systems. Assessing the entire systems' switching function and temperature profiles, reveals that multiple ESTWHs from other levels further switch *on* during this peak period. In the case of baseline 1, multiple simultaneous switching events occur, with a higher frequency, compared to the baseline system 2. The potential risk for maximum demand penalties during this period, is the highest in this region, due to other equipment demands.

4.4.1.5 d) Standard ToU period [10h00 to 18h00)

In this second and longest standard period of the day, less switching events take place, for both baselines, compared to the winter case.

Referring to the entire systems' switching function and storage tank temperatures and comparing the previous regions, a significant difference in the energy usage is observed. In terms of the baseline system 1, more switching events occur and with higher frequency in contrast to baseline system 2. Moreover, the simultaneous switching events taking place in this region, results in a higher peak power for baseline 1 than for baseline 2. There is no peak power difference between these two baseline systems, as with the winter case.

4.4.1.5 e) Peak ToU period [18h00 to 20h00)

The second peak period shows fewer switching occurrences for the Level 5 ESTWHs, for both baseline systems, this is in contrast to the first peak period.

In terms of the switching function and the associated temperatures of the water inside each respective ESTWH, in the entire system, for baseline 1, it may be observed that the switching

frequency is much higher, as compared to baseline 2. However, simultaneous switching in baseline 1, results in a peak significantly larger than the peak power draw of the second baseline, during this peak period. Similar to the first peak region, this period carries a high risk for maximum demand penalties, due to other equipment demands.

4.4.1.5 f) Standard ToU period [19h00 to 22h00)

During this third standard period of the day, the baseline system 1 of the level 5 ESTWHs, switches *on* twice, with longer *on* durations, during this region. Three switching occurrences were observed for the baseline 2 system, with shorter *on* durations, compared to baseline 1.

A comparison of the entire systems' switching function and associated ESTWH temperatures, reveals that simultaneous switching occurrences are, once again, more frequent for the baseline system 1, when compared to baseline system 2. Additionally, the peak power draw is higher for baseline system 1. In this case, the risk for maximum demand penalties is slightly lower than that of the peak period; the peak demand of baseline system 1 may again be an unnecessary risk for such a penalty to be enforced, particularly with such a comparatively high peak.

4.4.1.5 g) Off-peak ToU period [22h00 to 24h00)

Similar to the winter case, this last pricing region is a 2-hour long off-peak period. Referring to the level 5 ESTWHs, both baseline systems require no switching events to maintain the desired temperature level.

Evaluating all systems, reveals that multiple switching events are required to maintain the temperature. The energy cost for the resultant power required will be low.

In this region, the risk for maximum demand penalties remains, due to the hospital's high load factor, however, the baseline system 2 provides enough pre-heated water to minimize these risks.

4.4.2 Optimal control case with multifunctional chiller

This section presents the results of the optimal control algorithm applied to the multifarious water heating setup, with the energy recovery system. As with the baseline cases discussed in the previous sections, the same average winter and summer day data was used to simulate the optimal operation of the system. In Section 4.4.2.1, the winter case results are depicted, while Section 4.4.2.2 illustrates the results for the summer case. Section 4.4.2.3 provides a discussion of the results in the preceding sections.

4.4.2.1 Winter case

In this Section, the results of the optimal operation of the multifarious water heating system with energy recovery, is shown. This Section follows the same organizational structure of variable data illustration, as with the baseline cases. The control and state variable data is shown in Figs. 4.34 to 4.37. In Fig. 4.38, the resultant total power draw is indicated. The load profile serves two purposes, as discussed with the baseline case; to identify simultaneous switching events and indicates the power draw at any given moment of the entire multifarious water heating system. The subsequent section includes the discussion based on each ToU tariff region.

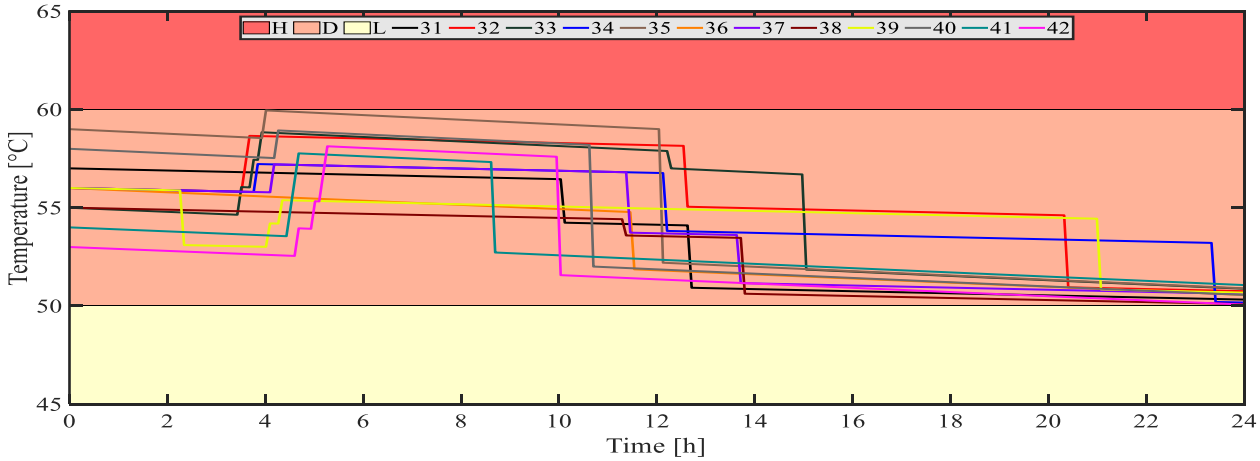

Fig. 4.34: Winter optimal control case - Level 5 ESTWH temperatures

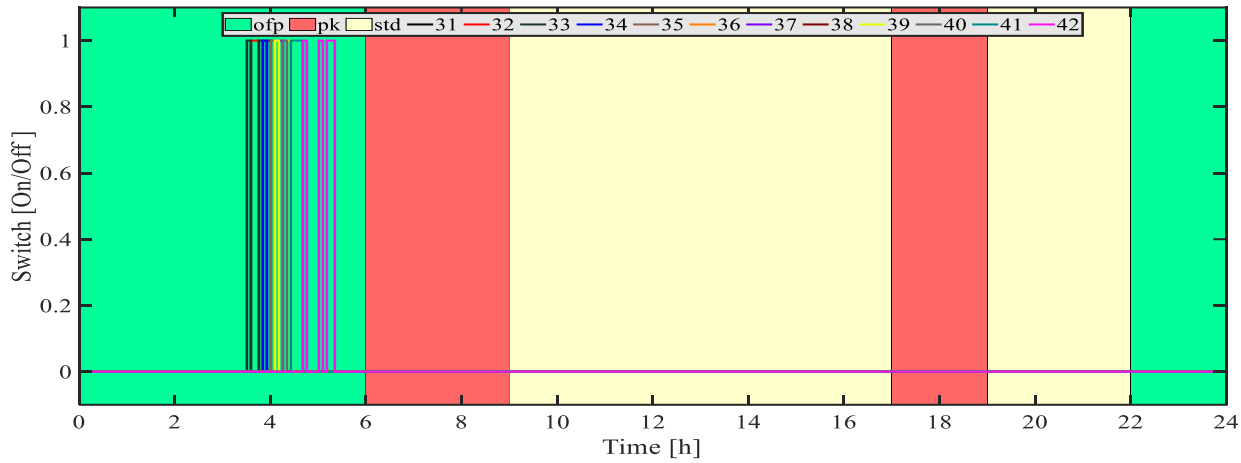

Fig. 4.35: Winter optimal control case - Level 5 ESTWH switching functions

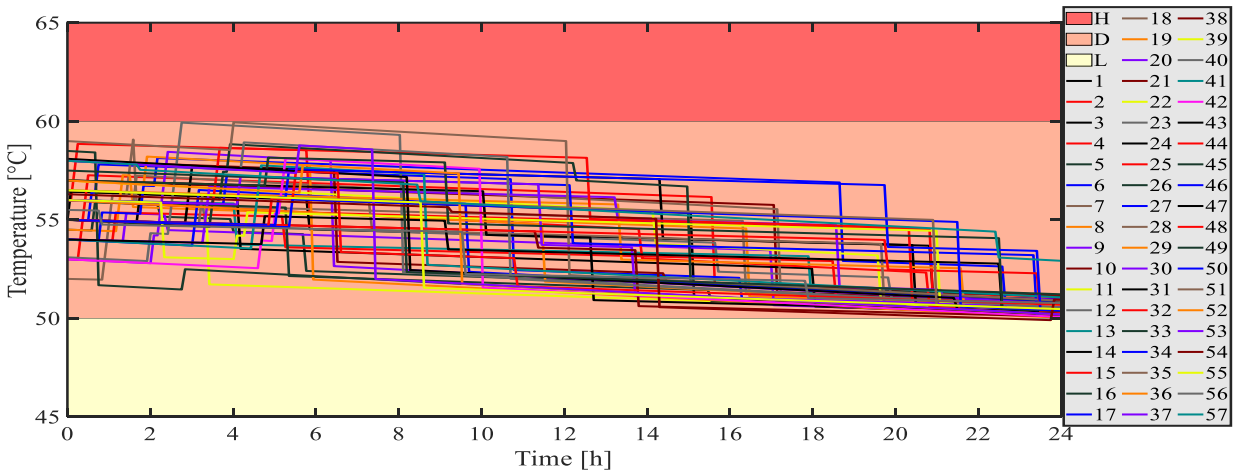

Fig. 4.36: Winter optimal control case - Aggregate ESTWH storage tank temperatures

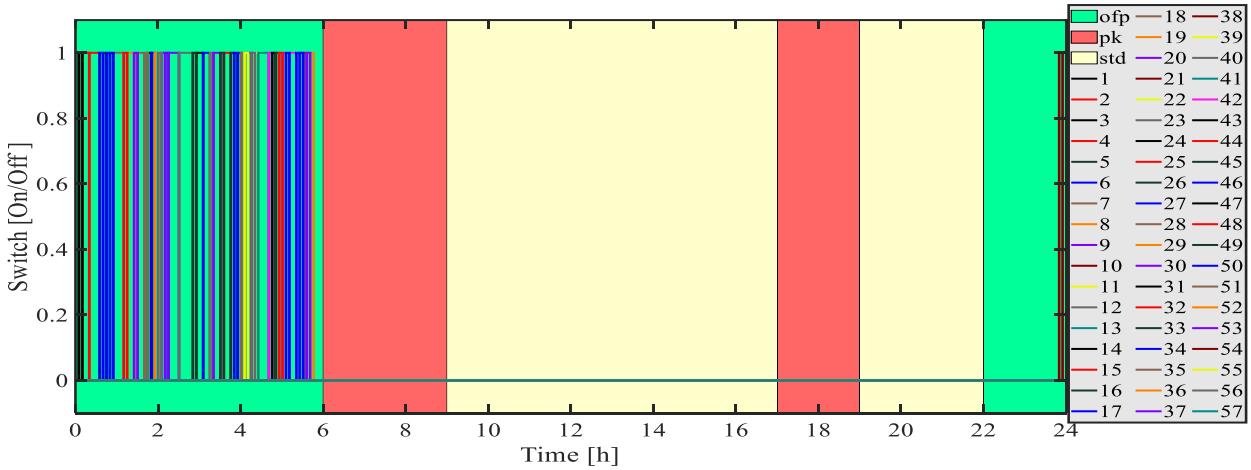

Fig. 4.37: Winter optimal control case - Aggregate ESTWH switching functions

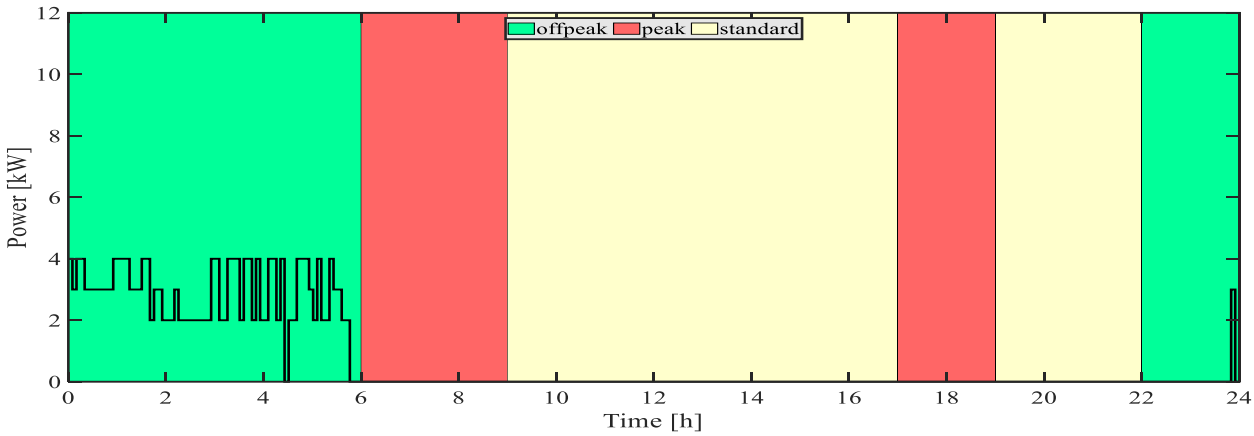

Fig. 4.38: Winter optimal control case - Total ESTWH power draw

4.4.2.2 Winter optimal control case discussion

4.4.2.2 a) Off-peak ToU period [00h00 to 06h00)

With reference to Figs. 4.34 and 4.35, the level 5 ESTWHs have the majority of the switching events occurring during this off-peak period. This occurs so that water is heated in preparation for the upcoming hot water demands, shown in Fig. 4.5.

The switching function and the associated storage tank temperatures for the entire system are shown in Figs. 4.36 and 4.37. Similar to the level 5 ESTWHs, most of the switching events take place during this period. In addition, it may be noted that power is consumed for the entire off-peak period, due to the low electricity price. Furthermore, in Fig. 4.38, it may be noted that no simultaneous switching events occur to reduce the risk for maximum demand charges. The peak energy usage for this period was 4 kW, which represents the power rating of the 200 L ESTWHs.

4.4.2.2 b) Peak ToU period [06h00 to 09h00)

Referring to the same figures as in the off-peak period, the level 5 ESTWHs, through the algorithm, avoid switching *on* for the entire peak period. This is substantiated when assessing

the entire systems' switching function and temperature profiles, where no switching for any of the ESTWHs occurs.

In hindsight, the lack of switching means that there is no risk of maximum demand charges for this period, where peak energy usage is often penalized. Additionally, the power draw in Fig.4.38, for this period is zero, also due to the lack of switching events.

4.4.2.2 c) Standard ToU period [09h00 to 17h00)

In the first standard period, no switching events are recorded for the level 5 ESTWHs. This is mainly due to the temperature of the water in each associated storage tank of the ESTWHs.

Referring to the entire systems' switching function and storage tank temperatures, no difference in the power draw trend is noted, as no switching takes place during this region. This means that the algorithm successfully prioritized which systems require energy before load demands take place to minimize energy costs.

4.4.2.2 d) Peak ToU period [17h00 to 19h00)

Similar to the first peak, the second peak period shows no switching occurrences for the Level 5 ESTWHs. As this period is demarcated by the highest energy cost, the algorithm avoids this region.

Referring to the switching function and the associated temperatures of the water inside each respective ESTWH, it may be observed that, with the higher hot water demands, compared to the first peak period in Fig. 4.37, the switching algorithm is able to avoid the peak period once more. Similarly, this peak period is a high-risk maximum demand penalty region and while no switching takes place, no power is drawn, and no risk of incurring penalties exist for this region.

4.4.2.2 e) Standard ToU period [19h00 to 22h00)

During this third, standard period, no switching on events for any of the ESTWH are required as the temperatures in the storage tanks remain within acceptable limits, despite the high frequency of hot water demands from the building.

4.4.2.2 f) Off-peak ToU period [22h00 to 24h00)

The last pricing region is an off-peak period and is described as the least costly region for energy usage. Therefore, with reference to the entire system, switching was delayed in previous periods, so that the cost of energy is reduced by using this period to switch *on*.

In this case, compared to the previous off-peak period, most intervals are available for switching to take place, without risking maximum demand charges.

4.4.2.3 Summer case

This Section presents the results of the optimal operation, during an average summer day. The organization of the illustrated results are analogous to the winter case. The variable data, as a result of applying optimal switching control, is shown in Figs. 4.39 to 4.42. In Fig. 4.43, the power draw of the entire system is indicated. In the subsequent section, the results are discussed for each ToU tariff region.

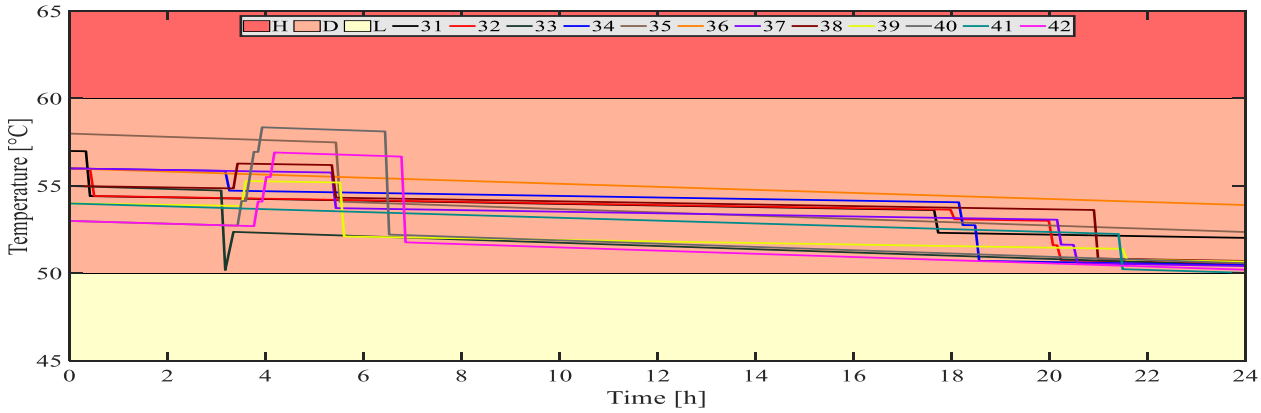

Fig. 4.39: Summer optimal control case - Level 5 ESTWH temperatures

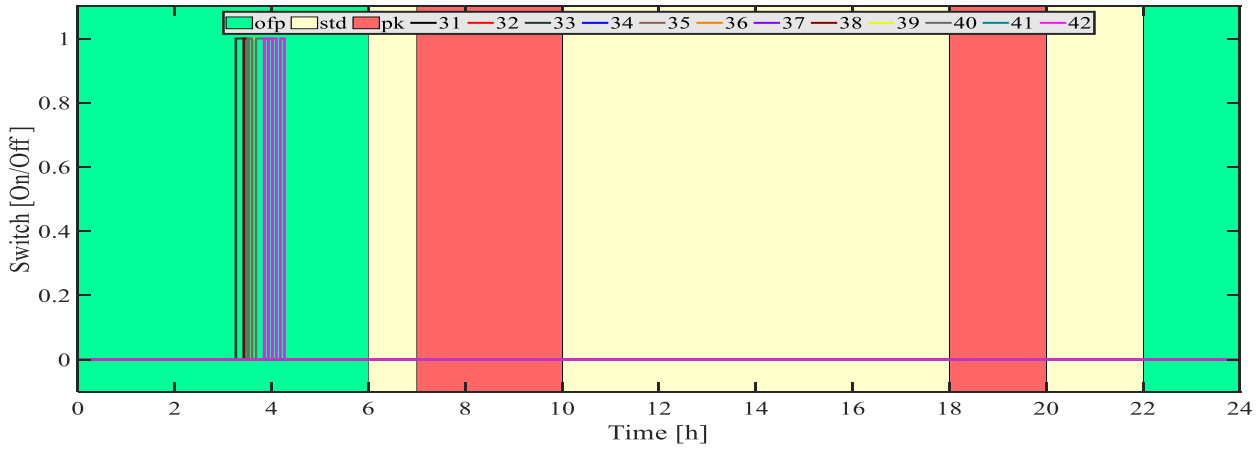

Fig. 4.40: Summer optimal control case - Level 5 ESTWH switching functions

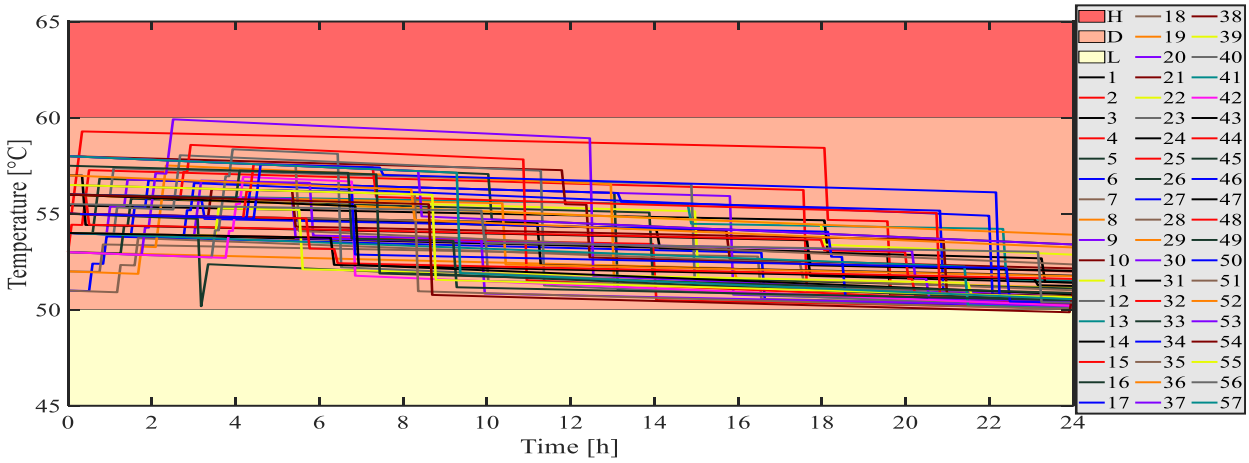

Fig. 4.41: Summer optimal control case - Aggregate ESTWH storage tank temperatures

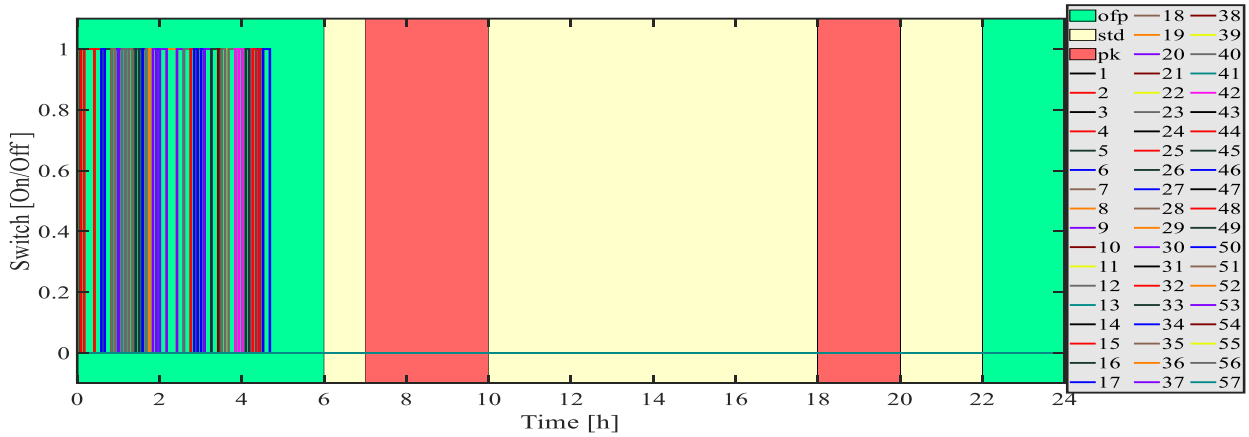

Fig. 4.42: Summer optimal control case - Aggregate ESTWH switching functions

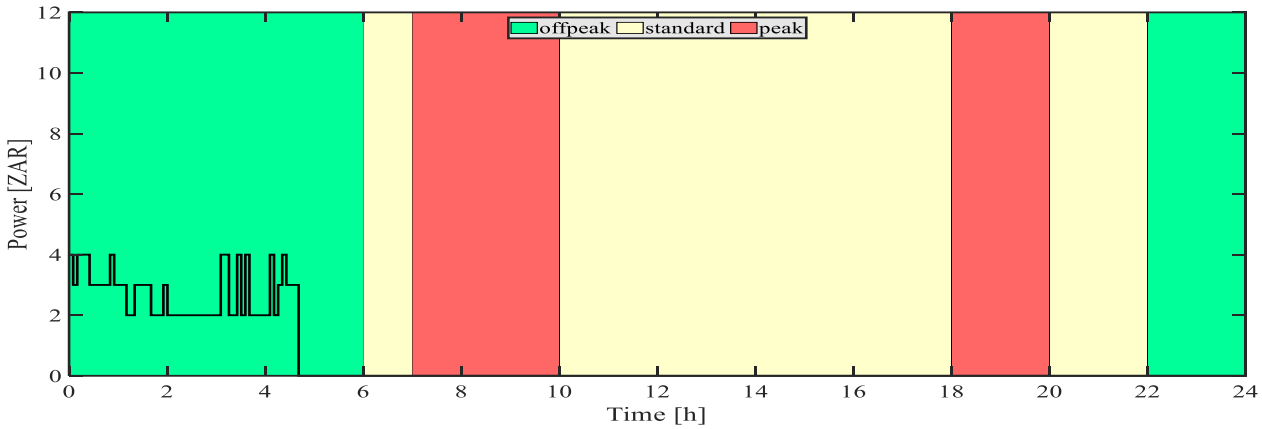

Fig. 4.43: Summer optimal control case - Total ESTWH power draw

4.4.2.4 Summer optimal control case discussion

4.4.2.4 a) Off-peak ToU period [00h00 to 06h00)

With reference to Figs. 4.39 and 4.40, the level 5 ESTWHs have five switching *on* events occurring during the off-peak period. Similar to the winter case, switching takes place in advance, so that the temperature levels do not fall below the lower temperature constraint, during the high-cost regions of the ToU tariff.

The switching function and the associated storage tank temperatures of the entire system is shown in Figs. 4.41 and 4.42, respectively. As with the winter case, the majority of switching takes place during this off-peak period, with most sampling intervals filled with ESTWHs that are switched *on*, while reducing the risk for maximum demand charges.

4.4.2.4 b) Standard ToU period [06h00 to 07h00)

Referring to the same figures, as in the off-peak period, the level 5 ESTWHs, have no switching events.

Assessing the entire systems' switching function and temperature profiles, reveals that none of the ESTWHs require additional energy to maintain the desired temperature.

4.4.2.4 c) Peak ToU period [07h00 to 10h00)

As with the winter case, neither the level 5 ESTWHs or any of the other ESTWHs on the other levels switched *on*. Subsequently, the risk of incurring maximum demand penalties have been reduced to zero and the use of energy during the costly peak region of the ToU tariff has been mitigated.

4.4.2.4 d) Standard ToU period [10h00 to 18h00)

During this second, standard period, no switching on events for any of the ESTWH are required as the temperatures in the storage tanks remain within acceptable limits, despite the high demand for hot water from the consumers/patients in the building.

4.4.2.4 e) Peak ToU period [18h00 to 20h00)

Similar to the previous peak period, not a single ESTWH switches *on* during this period, in order to avoid the high energy costs associated with this period. Therefore, the potential for maximum demand penalization has been eliminated.

4.4.2.4 f) Standard ToU period [19h00 to 22h00)

As with the previous period, none of the ESTWH are required to switch *on*, as temperatures are deemed adequate for the consumers in the building. The developed algorithm ensured that hot water was available at any interval where electricity prices are highest, without switching *on* during these intervals. This last comparatively high cost ToU tariff region and medium risk maximum demand region has no possibility for incurring any energy costs during this period.

4.4.2.4 g) Off-peak ToU period [22h00 to 24h00)

Analogous to the winter optimal control case, no switching events are required during this off-peak period, as temperatures are still within acceptable limits. This was ensured by both the algorithm and the multifunctional chiller as energy recovery device.

4.5 ECONOMIC ANALYSIS

4.5.1 Daily potential cost savings

Figs. 4.44 and 4.45 illustrate the cumulative cost comparison between the optimally controlled system and the two baselines for the winter and summer cases, respectively.

From Fig. 4.44, a gradual increase in cost is observed during the off-peak period for baseline system 1 and the optimal control case. During the peak period, the curve follows a comparatively sharp upward trend, due to the higher energy cost for this period. This is particularly apparent for the baseline system 1. The optimal control case does not switch *on* during the peak period so that no costs are incurred at this stage. The standard period is characterized by a slower (gradual) increase in cost, compared to the peak period for both baseline systems. The second peak period of the day results in another rapid increase in costs for all systems drawing grid energy. During the following standard and off-peak periods, the cumulative cost curve returns to the normal cumulative trend. The cumulative cost for baseline 1, 2 and optimal control case applied to the system with the multifunctional chiller, is at this point, 10.7 USD, 3.08 USD and 1.53 USD, respectively.

From the same figure, the optimal control approach dictates that switching *on* events should occur in advance, where ESTWHs should start switching *on,* as soon as the day begins. As with the baseline cases, the rate of change in cost increments at each interval depends on the pricing region of the ToU tariff.

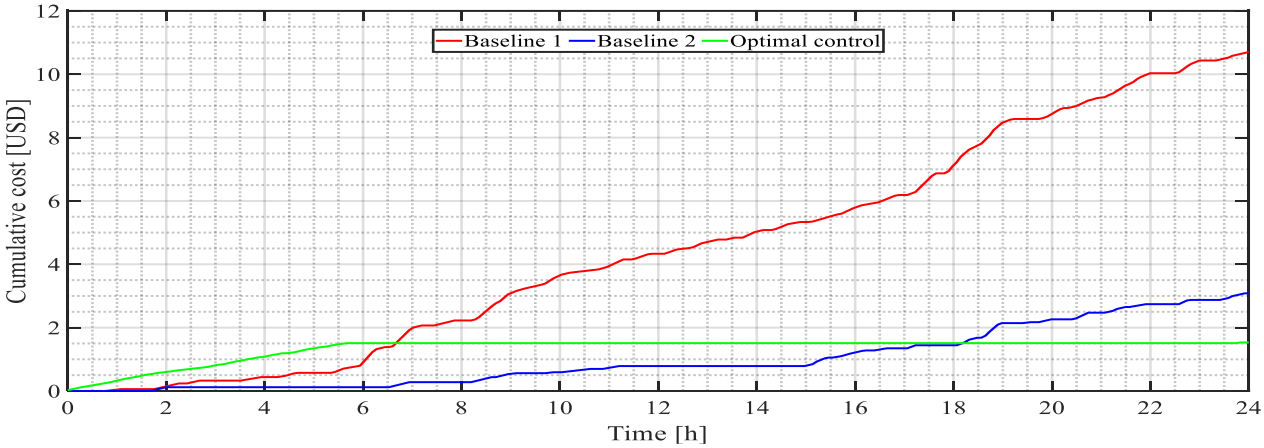

Fig. 4.44: Winter cumulative cost comparison

In Fig. 4.45, the cost curves for summer follow a dissimilar trend for the baseline 2 system. This case represents significantly lower overall energy costs. However, similar to the winter case, the system with optimal control, start switching *on* during the off-peak period, early in the morning and mitigates any further switching during the remainder of the day.

The total cost incurred at the end of the summer day, for the baseline system 1 and 2, is 3.40 USD and 1.43 USD, respectively. The optimal control case results in a potential cumulative cost of 0.73 USD.

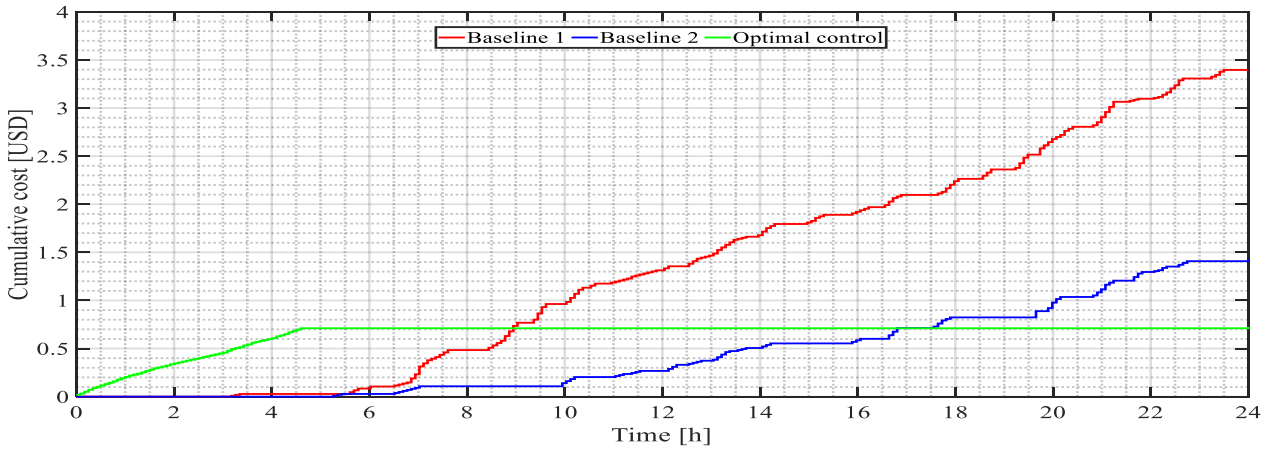

Fig. 4.45: Summer cumulative cost comparison

Table 4.3 indicates the winter daily energy savings between the baseline systems and optimal control approach. The winter savings, as a result of implementing the multifunctional

chiller, is 7.62 USD. This translates into a saving of 71,2.%. The application of optimal control to the multifarious system with energy recovery will yield a potential saving of 85.68%, compared to the baseline system 1 (without energy recovery).

The maximum demand charges decreased for the winter case, after the implementation of the multifunctional chiller, by 0.5 USD. Comparatively, the potential penalties incurred for the optimal control case, were reduced by 2.25 USD, translating into savings of 69% in maximum demand charges.

Table 4.3: Winter daily energy costs and savings

Cost	**Figure (USD)**
Baseline 1 (ToU)	10.70
Baseline 1 (Normalized Maximum demand (Md) @ $0.25/kVA)	3.25
Baseline 2 (ToU)	3.08
Baseline 2 (Normalized Maximum demand (Md) @ $0.25/kVA)	2.75
Proposed system - optimal control with MFC (ToU)	1.53
Proposed system - optimal control with MFC (Normalized Md @ $0.25/kVA)	1.00
Savings (Baseline 1 vs Baseline 2)	**7.62 (ToU)/0.5(Md)**
Savings (Baseline 2 vs Optimal control with MFC)	**1.55 (ToU)/1.75 (Md)**
Savings (Baseline 1 vs Optimal control with MFC)	**9.17 (ToU)/2.25 (Md)**

Table 4.4 illustrates the summer daily energy savings between the baseline systems and optimal control approach. The resultant summer savings after implementing the multifunctional chiller (baseline 2) is 1.97 USD. This translates into a saving of 57.94%. The multifarious water heating system with energy recovery and optimal control will achieve a potential saving of 78.53%, compared to the baseline system 1. Similar to the winter daily analysis, the maximum demand charges for summer decreased significantly for the baseline system 2 and optimal control case. The baseline system 2 showed a decrease of 1.25 USD, while the optimal control case revealed a further reduction in costs. A potential penalty reduction of 1.25 is possible with the application of the optimal control algorithm. This

translates into savings of 55.6% in maximum demand charges, when compared to the multifarious system with energy recovery.

Table 4.4: Summer daily energy costs and savings

System cost description	Cost (USD)
Baseline 1 (ToU)	3.40
Baseline 1 (Normalized Maximum demand (Md) @ $0.25/kVA)	2.75
Baseline 2 (ToU)	1.43
Baseline 2 (Normalized Maximum demand (Md) @ $0.25/kVA)	2.25
Proposed system - optimal control with MFC (ToU)	0.73
Proposed system - optimal control with MFC (Normalized Md @ $0.25/kVA)	1.00
Savings (Baseline 1 vs Baseline 2)	**1.97 (ToU)/0.5 (Md)**
Savings (Baseline 2 vs Optimal control with MFC)	**0.70 (ToU)/1.25 (Md)**
Savings (Baseline 1 vs Optimal control with MFC)	**2.67 (ToU)/1.75 (Md)**

4.5.2 Annual potential cost savings

In Table 4.5, the annual winter and summer energy savings are shown. The energy costs for the winter and summer cases were used to calculate the annual savings. The annual savings were calculated according to the number of days in the low (summer) and high demand (winter) seasons.

Table 4.5: Annual energy cost savings

System cost description	Savings (USD)
Winter (Baseline 1 vs Baseline 2)	700.89 (ToU)/46 (Md)
Winter (Baseline 2 vs Optimal control with MFC)	142.64 (ToU)/161 (Md)
Winter (Baseline 1 vs Optimal control with MFC)	843.54 (ToU)/207 (Md)
Summer (Baseline 1 vs Baseline 2)	537.69 (ToU) /136.5 (Md)
Summer (Baseline 2 vs Optimal control with MFC)	191.62 (ToU)/ 341.25 (Md)
Summer (Baseline 1 vs Optimal control with MFC)	729.30 (ToU)/477.75 (Md)

Total savings (Baseline 1 vs Baseline 2)	**1238.58 (ToU)/182.5 (Md)**
Total savings (Baseline 2 vs Optimal control with MFC)	**334.26 (ToU)/502.25(Md)**
Total savings (Baseline 1 vs Optimal control with MFC)	**1572.80 (ToU)/684.75 (Md)**

A total annual energy cost saving of 1421.08 USD or 48% may be achieved with the implementation of the multifunctional chiller as opposed to a cooling only unit. The potential cost savings for the optimally controlled multifarious water heating system with energy recovery may yield 2257.59 USD or 76.21% in energy cost savings. In retrospect, the application of the optimal control algorithm to the multifarious water heating system with energy recovery may demonstrate a maximum energy cost saving of 836.51 USD or 28.22%.

4.5.3 Life cycle cost analysis

In order to determine the feasibility of implementing the energy recovery system, a life cycle cost analysis was conducted. Eq. (3.18), used in the previous chapter is used in this section to determine the total life cycle cost of the energy recovery system. The energy recovery part of a suitably sized multifunctional chiller is considered as the initial implementation cost.

The cost of implementing the optimal control method is insignificant compared to the cost of the recovery system. The commissioning/replacement of a cooling-only chiller was necessary to supply HVAC processes of the hospital in this case study. Therefore, in this analysis, the cost of the cooling only chiller system may be neglected, as it does not contribute to the water heating processes. Rather, only the implementation cost of the energy recovery system is calculated. The energy recovery system cost was attained by subtracting the price of the cooling-only chiller system from the cost of the multifunctional chiller. The considered chillers have matching cooling capacities, with their respective costs and the cost difference shown in Table 4.6.

Table 4.6: Initial implementation cost (energy recovery system)

Unit type	Cost (USD)
Thermocold 4 Pipe Chiller	55 223.53
Thermocold Cooling only chiller	37 055.88
Cost difference	**18 167.65**

From the Table, a cost difference of 18 167.65 USD was noted and then used as the initial implementation cost in the life cycle cost analysis.

The life cycle cost analysis covers a 20 year project lifetime for both these cases, while a 10% annual increase in electricity is assumed for the years that follow after the implementation of the energy recovery system. Additionally, an annual operation and maintenance cost of 1%, subjected to an inflation rate of 5%, is considered for the analysis [149].

In Fig. 4.46, the life cycle cost for the system under the ToU tariff only, is presented. Fig. 4.47 illustrates the life cycle cost of the system, under both ToU and maximum demand charges, owing to the maximum possible savings, that may be of result. Each of these figures illustrates two break-even points. These points indicate when each system will break-even. The referred systems are; the baseline system 2 and then optimally controlled system with energy recovery. These two systems are compared to baseline system 1.

In both these figures, the starting point for baseline system 2 and the optimal control case is the implementation cost. The baseline system 1 does not have an initial implementation cost, due to the absence of the multifunctional chiller system.

From Fig. 4.46, the break-even point for the baseline system 2 was observed to be 8.27 years, at 31 060 USD. The implementation of the optimal control approach to the system, with a multifunctional chiller, reduced the break-even time by 2.8 years to 7.03 years, at a cost of 24 150 USD. At the end of the project lifetime, after 20 years following implementation, a potential cost saving of 102 737.28 USD may be observed for the baseline system 2, which translates to a project lifetime saving of 52.43 %. Comparing the baseline 1 system, with the optimal control case, indicated a saving of 136 922.70 USD in 20 years or 69.88 % at the end of the project life cycle.

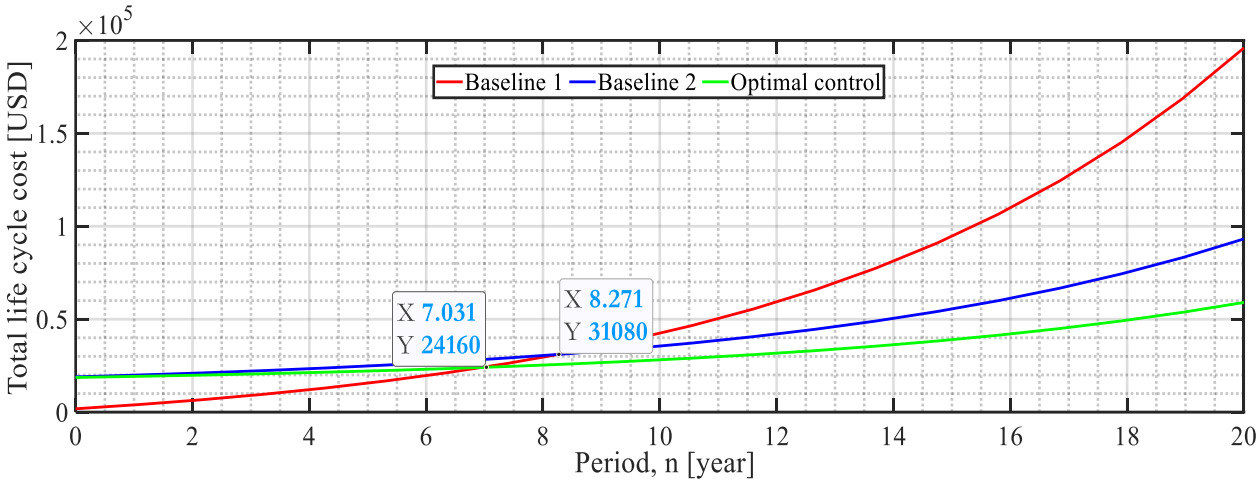

Fig. 4.46: Life cycle cost analysis (ToU)

In Fig. 4.47, the break-even point of the baseline system 2 and system with optimal control and energy recovery system is shown. It should be noted that in this case, where both the maximum demand and ToU tariff is considered, the maximum possible energy savings are shown. This means that the maximum demand evaluation could only be conducted by assuming that the load demands of other equipment in the building are constant throughout the day, except for the multifarious ESTWH systems.

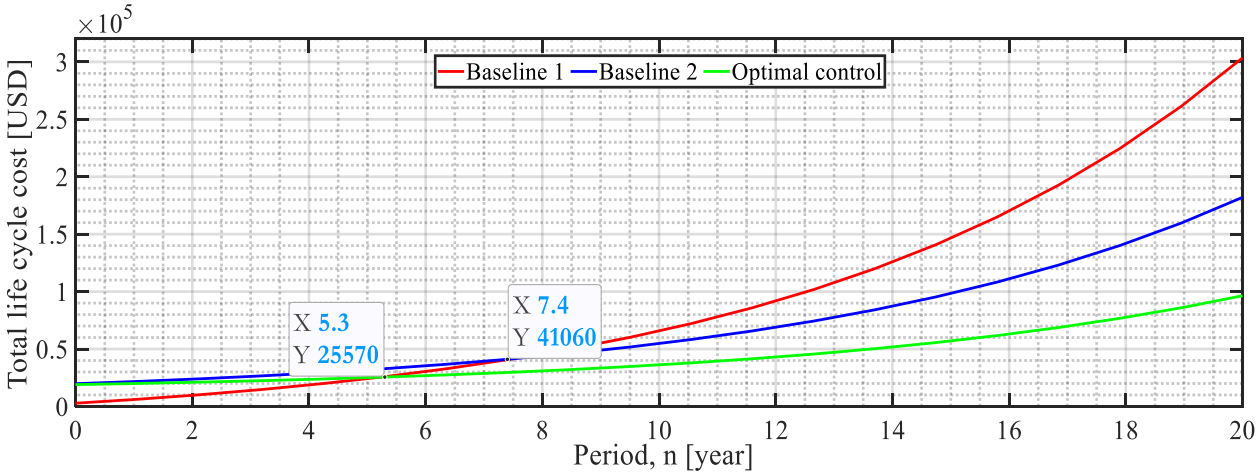

Fig. 4.47: Life cycle cost analysis (ToU tariff and maximum demand)

A practical example of this, entails the proposed system in Chapter III. The proposed system may be connected to the entire healthcare entity's loads, without the multifarious water heating system. In this case, where the load is capped at a certain threshold, any additional load, such as the water heating equipment, should be subjected to peak clipping methods of control, in addition to demand shifting strategies. This will minimize the costs incurred as a result of reducing the maximum demand across the entire control horizon, and by extension, each evaluated month.

The break-even point for the baseline system 2, was observed to be 7.4 years, at 41 410 USD. In hindsight, this point was further reduced by 2.152 years after the implementation of the optimal control technique, so that the proposed system would break even at 5.3 years, with a cost of 25 620 USD. At the end of the evaluated 20 year project, a potential cost saving of 121 433.23 USD may be observed for the baseline system 2, translating into 40% project lifetime cost savings. The optimal control approach, compared to the baseline 1 system, indicates a saving of 207 076.06 USD or 68.23 %. Therefore, the energy recovery system may be proposed or recommended to any commercial building with similar water heating and HVAC requirements.

4.6 ECONOMIC FEASIBILITY COMPARISON FOR PROPOSED SYSTEMS

An economic analysis was conducted, considering the energy costs incurred by each baseline and proposed system for each scenario. A life cycle cost analysis was carried out to ascertain the break-even point for the dual axis PV tracking system, with energy storage in Chapter III, while in this Chapter IV, a multifunctional chiller system was considered. The results from each life cycle cost analysis, are presented in Table 4.7, for comparison.

The annual cost savings, attained through implementation of the proposed system and existing energy recovery system, with and without optimal control strategies applied, are further shown in Table 4.7. The costs are separated to highlight the savings, with respect to the ToU tariff and maximum demand charges, respectively.

Table 4.7: System cost saving and break-even point comparison,

Economic indicator	Model 1			Model 2		
	BL 1 vs Prop.	Prop. vs OC	BL 1 vs OC	BL 1 vs BL 2	BL 2 vs OC	BL 1 vs OC
Annual cost savings (ToU)	35.1 %	6.4%	41.5%	64.8%	50.47%	82.2%
Annual cost savings (Maximum demand)	10.5%	27.5%	38.0%	17.38%	57.91%	65.2%
Break-even point	9.3 years	No intersect	7.5 years	8.27 /7.4 years	No intersect	7.03/5.3 years
Project Lifetime savings	24.5 %	No intersect	34.5%	52.43%/ 40%	No intersect	69.88 %/ 68.23 %

where:

BL 1 denotes the baseline system 1;

BL 2 represents the baseline system 2;

Prop. is an abbreviation for the proposed system;

OC is an abbreviation for optimal control case, and refers to the proposed system in Chapter III and the baseline system 2 in Chapter IV, where optimal control was applied.

From the table and referring to the annual cost savings of Model 1, it may be observed that the proposed system, without optimal control, reduces the ToU tariff costs substantially. In contrast, the maximum demand savings are significantly higher for the scenario with optimal control.

The annual cost savings for Model 2, follows a similar trend with the implementation of the energy recovery system (baseline 2), compared to the system without (baseline 1). In this comparison, the energy recovery system results in substantial savings, more so than for the first model. In contrast to Model 1, the baseline system 2, vs. the optimal control case, presents significantly higher resultant cost savings. This proves that with adequate operation control, the energy cost savings may be increased substantially. The baseline system 1, considering only

the ToU tariff, compared to the HVAC thermal energy recovery with optimal control applied, may yield the highest savings at 69.88 %.

The maximum demand savings for each model case, is where the optimal control algorithm demonstrates the largest impact on energy costs. The maximum demand cost savings, that could potentially be achieved by implementing the proposed system without optimal control, approximately 57.91 %. Introducing the optimal control technique with the proposed system, may yield substantial energy cost savings, while the highest savings are achieved when compared to the first baseline (existing system).

Assessing the life cycle cost analysis results, for each model case, reveals that the optimal control technique effectively reduced the break-even point for Model 1 by 1.8 years. A minimum reduction of 1.2 years may be achieved with optimal control for the Model 2 system, considering only the ToU tariff cost savings. The projected lifetime savings were further increased by 6.4% for the Model 1 case, while a higher cost saving of 50.47% was observed when comparing the systems in terms of the ToU tariff. The impact of the optimal control applied to model 2, on maximum demand savings, is challenging to evaluate, as this highly depends on the entire load profile. However, a maximum potential saving, when considering both the ToU tariff and maximum demand charges, may be calculated. This revealed that, in the best-case scenario, assuming the total load of the healthcare facility is entirely constant, the break-even point may be further reduced by to up to 2.3 years. These savings may be realized practically, if the proposed system in Chapter III were to be implemented, to supply all loads except for the water heating equipment in the facility. The optimal control algorithm in Chapter III will limit the grid power to a predetermined threshold, while the optimal control strategy in Chapter IV, may ensure that adequate peak clipping is achieved on the water heaters, for energy cost minimization.

In hindsight, the largest cost savings were noted when deep equipment retro fitment projects are considered in this study. This is true for the proposed system in Chapter III and the recommended existing energy recovery system in Chapter IV. The applied optimal control techniques does not necessarily need to serve the only purpose of improving the feasibility of deep equipment retro-fitment projects. In the Chapter III case, only an energy storage system

may be used and controlled, to dispatch power optimally and economically to the load. However, in Chapter IV, a multifarious water heating system, without the energy recovery scheme, may benefit immensely from an optimal control approach. This means that substantial cost savings may be of result, if the optimal control algorithm is applied, without the need for any additional equipment. This mainly stems from the fact that most water heating systems already have an energy storage vessel for effective demand side management to be applied. Furthermore, this is a low risk, high return scenario where healthcare and other commercial building energy managers, with similar setups, can improve energy efficiency relatively quickly and with ease.

4.7 CONCLUSION

In this Chapter, a model was developed to represent the operation and optimal control of a multifarious water heating system at a medical facility, located in the Bloemfontein region, in South Africa.

Baseline systems and the optimal control approach were simulated and compared, to ascertain the potential savings under the ToU tariff and maximum demand charges.

The simulation results revealed that the system with the optimal control approach, was able to minimize energy costs, compared to the baseline system.

A break-even point was established from a life cycle cost analysis to determine the feasibility of implementing the energy recovery system. The break-even point was determined between two baseline systems, one of which consists of the multifarious water heating systems, without the energy recovery system (baseline 1) and the other with the energy recovery (baseline 2). An additional break-even point was calculated for the multifarious energy recovery system, with the optimal control algorithm applied, compared to the system without optimal control applied. Results from the analysis, when considering only the ToU tariff, revealed that the system, with energy recovery and without optimal control, would break-even in 8.26 years. The system to which optimal control was applied, would potentially break-even in 7.02 years.

The case where the ToU and maximum demand charges were considered, illustrated the maximum possible energy savings. The break-even point, considering all tariffs and charges, when comparing baseline 1 with baseline 2, was noted to be 7.48 years, while the break-even point for the optimal control case compared to baseline 1, was noted to be 5.32 years.

The maximum potential energy cost savings over a project lifetime of 20 years, for the baseline 2 system, compared to baseline 1, was observed to be 40%. Furthermore, a maximum potential energy cost saving of 68.23 % was noted, when comparing baseline 1 with the system with energy recovery and optimal control, over the considered project lifetime. These economic indicators for the proposed system may be highly beneficial to building energy managers in the commercial sector.

CHAPTER V: GENERAL CONCLUSION

5.1 SUMMARY

This Chapter serves as a conclusion on the research carried out on the optimal operation control and simulation of hybrid systems, connected to HVAC and water heating loads in a healthcare institution.

The major concern identified in this research, was the substantial energy usage and the associated costs, of HVAC and water heating systems operation, in large scale medical facilities. This was discussed in Chapter 2, along with energy efficiency initiatives, to reduce the energy usage costs of equipment linked to these processes.

In this research, it was assumed that an optimal control strategy applied to proposed systems, connected to these energy intensive processes, may substantially reduce the energy costs, when compared to existing systems and control methods. The aim, therefore, was to develop models of these systems and apply optimal control strategies, to these models, in order to attain the potential energy cost savings that may be of result.

In this work, optimal control strategies were developed for two models, wherein the operation was simulated, using the available exogenous variable data. The optimal control strategies were used to minimize energy costs, based on the ToU tariff and maximum demand charges. In the first model, a dual axis tracking PV system was proposed and developed with optimal control in Chapter III, while the second model consisted of an optimally controlled multifarious water heating system, with energy recovery in Chapter IV. Baseline systems were established for both models, in order to determine the economic feasibility of implementing the proposed or recommended existing systems. One baseline system was established for the first model, while the proposed system served as a second baseline, to be compared to the optimal control case. Similarly, the multifarious water heating system was simulated, with two baseline systems. Baseline system 1 consisted of the multifarious water heating system, without an energy recovery system, while baseline system 2 included the energy recovery system. Consequently, for model 1, one baseline and one proposed case was considered, and for model

2, two baselines were considered. The reason for this was that the recommended energy recovery system already existed in the case study. Therefore, three scenarios for each model were considered in this work Chapter IV.

In Chapter III, the simulation results revealed that a potential annual energy cost saving of 35.1% would be of result, considering only the ToU tariff, with the proposed system implemented. An additional energy saving of 6.4 % were observed with the application of the optimal control algorithm. The savings attained from reducing the maximum demand, by limiting the power supplied by the grid, was observed to be 10.5 % for the proposed system, without optimal control, and 38 %, with optimal control. The resultant total potential annual energy cost savings amounted to 30.8% for the proposed hybrid energy system and 40.9 %, with the application of the optimal control algorithm to the proposed system. A life cycle cost analysis revealed that a break-even point would be achieved in 8.8 years, with the implementation of the proposed system, while the implementation of optimal control techniques, may reduce the break-even point by as much as 1.82 years. Additionally, the life cycle cost analysis projected savings of up to $11.87 Million USD, over the project lifetime of 20 years, translating into savings of 34.53% for the evaluated 2018 load profile. In this model case, 137 168,60 USD were saved, as a result of reducing the maximum demand and introducing a renewable energy system, with energy storage.

In Chapter IV, the simulation results indicated that the system with the optimal control approach, was able to reduce energy costs significantly, compared to the baseline system, without optimal control applied. The break-even point was determined between two baseline systems, one of which, consisted of the multifarious water heating systems without the energy recovery system (baseline 1) and the other, with the energy recovery system (baseline 2). Results from the analysis, when considering only the ToU tariff, revealed that the system, with energy recovery and without optimal control, would break-even in 8.27 years. The system, to which optimal control was applied, would potentially break-even in 7.03 years. The case where the ToU and maximum demand charges were considered, illustrated the maximum possible energy savings. The break-even point, considering all tariffs and charges, when comparing

baseline 1 with baseline 2, was noted to be 7.4 years, while the break-even point for the optimal control case compared to baseline 1, was noted to be 5.3 years.

The maximum potential energy cost savings, over a project lifetime of 20 years, for the baseline 2 system compared to baseline 1, was observed to be 40%. Furthermore, a maximum lifetime potential energy cost saving of 68.23 % were noted, when comparing baseline 1 with the system with energy recovery and optimal control applied.

Comparing the results of the life cycle cost analyses for each model case, reveals that the optimal control technique effectively reduced the break-even point for the proposed system in Model 1 by 1.8 years. A minimum reduction of 1.2 years may be achieved with optimal control for the system in Model 2, considering only the ToU tariff cost savings. The projected lifetime savings were further increased by 6.4% for the Model 1 case, while a higher cost saving of 50.47% was observed, when comparing the systems in terms of the ToU tariff. These savings may be realized practically, if the proposed system in Chapter III were to be implemented, to supply all loads, except the water heating equipment in the facility. The optimal control algorithm in Chapter III will limit the grid power to a predetermined threshold, while the optimal control strategy in Chapter IV, may ensure that adequate peak clipping is achieved on the water heaters for energy cost minimization.

In hindsight, the findings of the study present the potential energy and associated cost reductions and, in turn, the reduction of the carbon footprint of the healthcare facility under evaluation. The potential energy reduction achieved in this study, aligns with the post-2015 National Energy Efficiency Strategy (NEES). The NEES documentation indicates that an energy reduction target of 37% in specific energy usage should be reached by 2030. A revised 12L tax deduction, a tax incentive for deep energy efficiency retrofits and the application of optimal control algorithms, may ensure that the potential energy reduction of 37% is achieved within the allowed timeframe. As a result of this, a reduction in the total operating costs of the building may be realized. This, in turn, may avail funds for additional sustainable energy management initiatives to be implemented to further reduce energy usage and all associated costs. Ultimately, with the resultant additional funds available, medical equipment may be

replaced/upgraded, to enhance patient care, while mitigating the sharp rises in the already high medical costs to patients.

5.2 SUGGESTIONS FOR FURTHER RESEARCH

Further studies may include the simulation of renewable energy source systems or alternative energy efficient water heating technologies, coupled to the existing multifarious water heating setup. This will, by extension, require an in-depth economic analysis, to determine the feasibility of implementing such initiatives. Several smart control technologies may be applied to the evaluated systems, to achieve similar results as the optimal control techniques. Open-loop optimal energy management was considered at this stage of the research, to determine the preliminary economic impact and feasibility of implementing the approach to a healthcare institution. Closed-loop simulations may be considered as part of future research. This may include the application of the following control techniques: hybrid predictive, fuzzy logic, neural network, model predictive control, etc.

This thesis has been presented as part of an ongoing research project, at the Central University of Technology. The next step may include real-time closed-loop modelling and implementation of the system.

This is not the conclusion on optimal control of HVAC and water heating systems; several questions remain unanswered. In this study, a healthcare institution in Bloemfontein is considered. The methods in this research may be applied to various geographical locations, with different input parameters, which may in turn, alter the configuration of the proposed hybrid systems.

REFERENCES

[1] Van Staden, Adam Jacobus, Jiangfeng Zhang, and Xiaohua Xia. "A model predictive control strategy for load shifting in a water pumping scheme with maximum demand charges." Applied Energy 88, no. 12 (2011): 4785-4794.

[2] Koko, S. P., K. Kusakana, and H. J. Vermaak. "Grid-interactive micro-hydrokinetic with pumped-hydro storage: The case study of three South African demand sectors." In 2017 International Conference on the Domestic Use of Energy (DUE), pp. 83-88. IEEE, 2017.

[3] Jiang, Peng, Yee Van Fan, and Jiří Jaromír Klemeš. "Impacts of COVID-19 on energy demand and consumption: Challenges, lessons and emerging opportunities." Applied Energy (2021): 116441.

[4] Cunningham, A. Designing Energy Efficient Hospitals? First Let's Give You the Facts on Existing Performance; Western Cape Government Health Department: Sandton, South Africa, 2015.

[5] Chawla, Sagar, Shaheen Kurani, Sherry M. Wren, Barclay Stewart, Gilbert Burnham, Adam Kushner, and Thomas McIntyre. "Electricity and generator availability in LMIC hospitals: improving access to safe surgery." Journal of Surgical Research 223 (2018): 136-141.

[6] Hohne, Percy Andrew, Kanzumba Kusakana, and Bubele Papy Numbi. "Improving Energy Efficiency of Thermal Processes in Healthcare Institutions: A Review on the Latest Sustainable Energy Management Strategies." Energies 13, no. 3 (2020): 569.

[7] Karodia, Anis Mahomed. "The South African Government‟ s Proposed Implementation of the National Health Insurance Plan (NHI): A Disaster Waiting to Happen."

[8] Bargain, Olivier, and A. Ulugbek. "Poverty and Covid-19 in Developing Countries." Bordeaux University (2020).

[9] Gopalakrishnan, Bhaskaran, Kartik Ramamoorthy, Edward Crowe, Subodh Chaudhari, and Hasan Latif. "A structured approach for facilitating the implementation of ISO 50001 standard in the manufacturing sector." Sustainable Energy Technologies and Assessments 7 (2014): 154-165.

[10] García-Sanz-Calcedo, Justo, Awf Al-Kassir, and Talal Yusaf. "Economic and environmental impact of energy saving in healthcare buildings." Applied Sciences 8, no. 3 (2018): 440.

[11] Pérez-Lombard, L.; Ortiz, J.; Pout, C. A review on buildings energy consumption information. Energy Build. 2008, 40, 394–398.

[12] Allouhi, A.; El Fouih, Y.; Kousksou, T.; Jamil, A.; Zeraouli, Y.; Mourad, Y. Energy consumption and efficiency in buildings: Current status and future trends. J. Clean. Prod. 2015, 109, 118–130.

[13] Cunningham, A. Designing Energy Efficient Hospitals? First Let's Give You the Facts on Existing Performance; Western Cape Government Health Department, Sandton, South Africa, 2015.

[14] Eberhard, A.; Naude, R. The South African renewable energy independent power producer procurement programme: A review and lessons learned. J. Energy S. Afr. 2016, 27, 1–14.

[15] Amowine, N.; Ma, Z.; Li, M.; Zhou, Z.; Azembila Asunka, B.; Amowine, J. Energy Efficiency Improvement Assessment in Africa: An Integrated Dynamic DEA Approach. Energies 2019, 12, 3915.

[16] Aydin, Y.C.; Mirzaei, P.A.; Akhavannasab, S. On the relationship between building energy efficiency, aesthetic features and marketability: Toward a novel policy for energy demand reduction. Energy Policy 2019, 128, 593–606.

[17] Javied, T.; Rackow, T.; Franke, J. Implementing energy management system to increase energy efficiency in manufacturing companies. Procedia CIRP 2015, 26, 156–161.

[18] Prashar, A. Adopting PDCA (Plan-Do-Check-Act) cycle for energy optimization in energy-intensive SMEs. J. Clean. Prod. 2017, 145, 277–293.

[19] Van Heerden, M.; Mathews, M.J.; Marais, J.H. PRACTICAL IMPLEMENTATION OF THE ISO 50 001 STANDARD FOR LARGE INDUSTRIES. In Proceedings of the Institute for Industrial Engineering Conference (SAIIE),North West Province, South Africa, 27-29 October 2016; pp. 515-523.

[20] Asif, M.; Searcy, C. Towards a standardised management system for corporate sustainable development. TQM J. 2014, 26, 411–430.

[21] International Energy Agency. Energy Efficiency and the Environment; OECD/IEA: Paris, France, 1991.

[22] Xia, X.; Zhang, J. Energy efficiency and control systems–from a POET perspective. IFAC Proc. Vol. 2010, 43, 255–260.

[23] Hoexter, M.F. Achieving more with less: The state of energy conservation and energy efficiency. In Sustainable Communities Design Handbook; Butterworth-Heinemann, California, USA 2010; pp. 45–63.

[24] Xia, X.; Zhang, J.; Cass, W. Energy management of commercial buildings-a case study from a POET perspective of energy efficiency. J. Energy S. Afr. 2012, 23, 23–31.

[25] Xia, X.; Zhang, J. Energy audit-from a POET perspective. In Proceedings of the International Conference on Applied Energy (ICA2010), Singapore, 21-23 April 2010; pp. 1200–1209.

[26] Zhang, S.; Tang, Y. A POET Based Energy Audit Methodology for WWTPs. In Proceedings of the 2018 IEEE 37th Chinese Control Conference (CCC), Wuhan, China, 25–27 July 2018; pp. 7399–7404

[27] Zhang, H.; Xia, X.; Zhang, J. Optimal sizing and operation of pumping systems to achieve energy efficiency and load shifting. Electr. Power Syst. Res. 2012, 86, 41–50.

[28] Teich, S.T.; Faddoul, F.F. Faddoul. Lean management—The journey from Toyota to healthcare. Rambam Maimonides Med. J. 2013, 4, e0007.

[29] Xia, Xiaohua, and Lijun Zhang. Industrial energy systems in view of energy efficiency and operation control. Annual Reviews in Control. 2016 ,42, 299-308.

[30] May, G.; Barletta, I.; Stahl, B.; Taisch, M. Energy management in production: A novel method to develop key performance indicators for improving energy efficiency. Appl. Energy 2015, 149, 46–61.

[31] Vikhorev, K.; Greenough, R.; Brown, N. An advanced energy management framework to promote energy awareness. J. Clean. Prod. 2013, 43, 103–112.

[32] Brounen, D.; Kok, N.; Quigley, J.M. Quigley. Energy literacy, awareness, and conservation behavior of residential households. Energy Econ. 2013, 38, 42–50.

[33] Strezov, V.; Evans, A.; Evans, T.J. Assessment of the economic, social and environmental dimensions of the indicators for sustainable development. Sustain. Dev. 2017, 25, 242–253.

[34] Yong, J.Y.; Klemeš, J.J.; Varbanov, P.S.; Huisingh, D. Cleaner energy for cleaner production: Modelling, simulation, optimisation and waste management. J. Clean. Prod. 2016, 111, 1–16.

[35] Knoll, T.; Omar, M.I.; Maclennan, S.; Hernandez, V.; Canfield, S.; Yuan, Y.; Bruins, M.; Marconi, L.; Van Poppel, H.; N'Dow, J.; et al. Key steps in conducting systematic reviews for underpinning clinical practice guidelines: Methodology of the European Association of Urology. Eur. Urol. 2018, 73, 290–300.

[36] Wang, Z.; Norris, S.L.; Bero, L. The advantages and limitations of guideline adaptation frameworks. Implement. Sci. 2018, 13, 72.

[37] Zhang, S.; Tang, Y. Optimal schedule of grid-connected residential PV generation systems with battery storages under time-of-use and step tariffs. J. Energy Storage 2019, 23, 175–182.

[38] Hatch, M. J. Organization Theory: Modern, Symbolic, and Postmodern Perspectives; Oxford University Press: Oxford, UK, 2018.

[39] EE Publishers. Energy Usage and Efficiency at Medical Facilities—EE Publishers. Available online: https://www.ee.co.za/article/energy-usage-and-efficiency-in-hospitals-clinics-and-medical-facilities.html (accessed on 5 March 2019).

[40] Guide to Best Practice Maintenance and Operation of HVAC Systems for Energy Efficiency. pp. 36–37. Available online: http://ee.ret.gov.au/energy-efficiency/non-residential-buildings/heating-ventilation-and-air-conditioning-hvac (accessed on 24 January 2012).

[41] Eskom. Heating, Ventilation and Air Conditioning (HVAC) Systems: Energy-Efficient Usage and Technologies; Eskom Energy Management Information Pack: Brochure 5; Eskom Holdings SOC Ltd, Johannesburg, South Africa. 2015.

[42] Teke, A.; Timur, O. Assessing the energy efficiency improvement potentials of HVAC systems considering economic and environmental aspects at the hospitals. Renew. Sustain. Energy Rev. 2014, 33, 224–235.

[43] Hepbasli, A.; Kalinci, Y. A review of heat pump water heating systems. Renew. Sustain. Energy Rev. 2009, 13, 1211–1229.

[44] Hohne, P.A.; Kusakana, K.; Numbi, B.P. A review of water heating technologies: An application to the South African context. Energy Rep. 2019, 5, 1–19.

[45] Dettenkofer, M.; Scherrer, M.; Hoch, V.; Glaser, H.; Schwarzer, G.; Zentner, J.; Daschner, F.D. Shutting down operating theater ventilation when the theater is not in use: infection control and environmental aspects. Infect. Control Hosp. Epidemiol. 2003, 24, 596–600.

[46] Hoyt, T.; Arens, E.; Zhang, H. Extending air temperature setpoints: Simulated energy savings and design considerations for new and retrofit buildings. Build. Environ. 2015, 88, 89–96.

[47] Eskom Geyser Fact Sheet. 2015. Available online: http://www.pcb.org.za/wp-content/uploads/2015/04/EskomGeyserFactSheet.pdf (accessed on 15 March 2019).

[48] Serban, I., and C. Marinescu. Battery energy storage system for frequency support in microgrids and with enhanced control features for uninterruptible supply of local loads. International Journal of Electrical Power & Energy Systems 54 (2014): 432-441.

[49] Ford, B.E.; Fowler, K.M.; Anderson, C.J. Using Metered Data for Energy and Water Evaluations; No. PNNL-28036; Pacific Northwest National Lab.(PNNL): Richland, WA, USA, 2018.

[50] Fan, C.; Xiao, F.; Li, Z.; Wang, J. Unsupervised data analytics in mining big building operational data for energy efficiency enhancement: A review. Energy Build. 2018, 159, 296–308.

[51] Wang, J.; Wang, B.; Wu, R.; Zhang, H. On Unmanned Electric Power System and Its Development Strategy. In Proceedings of the 2018 Joint International Advanced Engineering and Technology Research Conference (JIAET 2018), Xi'an China, 26-27 May 2018; Atlantis Press, Paris, France: 2018.

[52] Kriel, C.J.R.; Joubert, H.P.R.; Marais, J.H. The influence of variable speed drives on electric motor operating temperatures. In Proceedings of the 2013 IEEE 10th Industrial and Commercial Use of Energy Conference, Cape Town, South Africa, 20–21 August, 2013; pp. 1–6.

[53] Reynolds, L. Energy Efficiency in Buildings–Evolution of a Standard Series; SANS: Pretoria, South Africa, 2010; Volume 204.

[54] Krarti, M.; Menyhart, K.; Shekar, V.; Park, B. Dynamic Insulation Systems. In Advanced Energy Efficient Building Envelope Systems; ASME Press, New York, USA: 2017.

[55] Harris, A.; Kilfoil, M.; Uken, E.A. Domestic Energy Savings with Geyser Blankets; Cape Peninsula University of Technology: Cape Peninsula, South Africa, 2007.

[56] Hohne, P.A.; Kusakana, K.; Numbi, B.P. Techno-economic Comparison of Timer and Optimal Switching Control applied to Hybrid Solar Electric Water Heaters. In Proceedings of the 2018 IEEE International Conference on the Industrial and Commercial Use of Energy (ICUE), Cape Town, South Africa, 13–15 August 2018; pp. 1–6.

[57] Dezfouli, M.M.S.; Moghimi, S.; Azizpour, F.; Mat, S.; Sopian, K. Feasibility of saving energy by using VSD in HVAC system, a case study of large-scale hospital in Malaysia. WSEAS Trans. Environ. Dev. 2014, 10, 15–25.

[58] Gavaldà; L; Garcia-Nuñez, M.; Quero, S.; Gutierrez-Milla, C.; Sabrià, M. Role of hot water temperature and water system use on Legionella control in a tertiary hospital: An 8-year longitudinal study. Water Res. 2019, 149, 460–466.

[59] Hohne, P.A.; Kusakana, K.; Numbi, B.P. Operation Cost Minimisation of Hybrid Solar/Electrical Water Heating Systems: Model Development. Adv. Sci. Lett. 2018, 24, 8076–8080.

[60] James, C.P. Remote Generator Fuel Monitoring System. U.S. Patent 7,072,801, 4 July 2006.

[61] Staphanos, S.; Keyes, M.; Cacciatore, G. Generator Monitoring, Control and Efficiency. U.S. Patent 6,912,889, 5 July 2005.

[62] Albeahdili, H.M.; Connecting Physical Infrastructure to the Cyber Space Using the Internet of Things (IOT) Devices. J. Eng. Appl. Sci. 2019, 14, 4631–4640.

[63] Hohne, P. A., K. Kusakana, and B. P. Numbi. "Scheduling and economic analysis of hybrid solar water heating system based on timer and optimal control." Journal of Energy Storage 20 (2018): 16-29.

[64] Kermani, Mostafa, Behin Adelmanesh, Erfan Shirdare, Catalina Alexandra Sima, Domenico Luca Carnì, and Luigi Martirano. "Intelligent energy management based on SCADA system in a real Microgrid for smart building applications." Renewable Energy 171 (2021): 1115-1127.

[65] Faschang, M.; Cejka, S.; Stefan, M.; Frischenschlager, A.; Einfalt, A.; Diwold, K.; Andrén, F.P.; Strasser, T.; Kupzog, F. Provisioning, deployment, and operation of smart grid applications on substation level. Comput. Sci.-Res. Dev. 2017, 32, 117–130.

[66] Barreto, L.; Amaral, A.; Pereira, T. Industry 4.0 implications in logistics: An overview. Procedia Manuf. 2017, 13, 1245–1252.

[67] Domat. 2018. Available online: https://domat-int.com/en/products/online-documentation/select-right-hmiscada-control-system (accessed on 15 March 2019).

[68] Türkay, B.E.; Telli, A.Y. Economic analysis of standalone and grid connected hybrid energy systems. Renew. Energy 2011, 36, 1931–1943.

[69] Ren, Z.; Grozev, G.; Higgins, A. Modelling impact of PV battery systems on energy consumption and bill savings of Australian houses under alternative tariff structures. Renew. Energy 2016, 89, 317–330.

[70] EE Publishers. Energy Management Systems Save Money—EE Publishers. 2017. Available online: http://www.ee.co.za/article/energy-management-systems-save-money.html (accessed on 29 March 2019).

[71] Odufuwa, O.Y.; Kusakana, K.; Numbi, B.P. Review of optimal energy management applied on Ice Thermal Energy Storage for an air conditioning system in commercial buildings. In Proceedings of the 2018 IEEE Open Innovations Conference (OI), Johannesburg, South Africa, 3–5 October 2018; pp. 286–293.

[72] Kumaresan, V.; Chandrasekaran, P.; Nanda, M.; Maini, A.K.; Velraj, R. Role of PCM based nanofluids for energy efficient cool thermal storage system. Int. J. Refrig. 2013, 36, 1641–1647.

[73] Khandelwal, A.; Talukdar, P.; Jain, S. Energy savings in a building using regenerative evaporative cooling. Energy Build. 2011, 43, 581–591.

[74] Mahlia, T.M.I.; Saktisahdan, T.J.; Jannifar, A.; Hasan, M.H.; Matseelar, H.S.C. A review of available methods and development on energy storage; technology update. Renewable and Sustainable. Energy Rev. 2014, 33, 532–545.

[75] Kastner, W.; Neugschwandtner, G.; Soucek, S.; Newman, H.M. Communication systems for building automation and control. Proc. IEEE 2005, 93, 1178–1203.

[76] Ramadan, M.; El Rab, M.G.; Khaled, M. Parametric analysis of air–water heat recovery concept applied to HVAC systems: Effect of mass flow rates. Case Stud. Therm. Eng. 2015, 6, 61–68.

[77] Zhai, X. Q., M. Qu, Yue Li, and R. Z. Wang. "A review for research and new design options of solar absorption cooling systems." Renewable and sustainable energy reviews 15, no. 9 (2011): 4416-4423.

[78] Hohne, P.A.; Kusakana, K.; Numbi, B.P. Operation cost and energy usage minimization of a hybrid solar/electrical water heating system. In Proceedings of the 2018 IEEE International Conference on the Domestic Use of Energy (DUE), Cape Town, South Africa, 3–5 April 2018; pp. 1–7.

[79] Leonzio, G. Solar systems integrated with absorption heat pumps and thermal energy storages: State of art. Renew. Sustain. Energy Rev. 2017, 70, 492–505.

[80] Seddegh, S.; Wang, X.; Henderson, A.D.; Xing, Z. Solar domestic hot water systems using latent heat energy storage medium: A review. Renew. Sustain. Energy Rev. 2015, 49, 517–533.

[81] Chaichana, C.; Charters, W.W.; Aye, L. An ice thermal storage computer model. Appl. Therm. Eng. 2001, 21, 1769–1778.

[82] Lees, M.J.; Taylor, J.; Chotai, A.; Young, P.C.; Chalabi, Z.S. Design and implementation of a proportional-integral-plus (PIP) control system for temperature, humidity and carbon dioxide in a glasshouse. In II IFAC/ISHS Workshop: Mathematical & Control Applications in Agriculture & Horticulture; ISHS Acta Horticulturae: Belguim 1994; Volume 406, pp. 115–124.

[83] Hohne, P.A. Optimal Energy Management of a Hybrid Solar Water Heating System with Grid Connection Under Time-Based Pricing. Ph.D. Thesis, Central University of Technology, Bloemfontein, Free State, South Africa, 2017.

[84] Nel, P.J.C.; Booysen, M.J.; Van der Merwe, B. Energy perceptions in South Africa: An analysis of behaviour and understanding of electric water heaters. Energy Sustain. Dev. 2016, 32, 62–70.

[85] Booysen, M.J.; Engelbrecht, J.A.A.; Ritchie, M.J.; Apperley, M.; Cloete, A.H. How much energy can optimal control of domestic water heating save? Energy Sustain. Dev. 2019, 51, 73–85.

[86] Booysen, M.J.; Engelbrecht, J.A.A.; Molinaro, A. Proof of concept: Large-scale monitor and control of household water heating in near real-time. Presented at the International Conference on Applied Energy ICAE 2013, Pretoria, South Africa, 1–4 July 2013.

[87] Energy.gov.za. Department of Energy. 2016. Available online: http://www.energy.gov.za/files/policies/Annex-B-Energy-Efficiency-Measures.pdf (accessed on 23 March 2019).

[88] Watermeyer, R. An overview of the current National Building Regulations and their impact on engineering practice. Civ. Eng. Siviele Ingenieurswese 2014, 22, 41–44.

[89] Energy.gov.za. Department of Energy. 2016. Available online: http://www.energy.gov.za/files/policies/Annex-D-Basis-for-Targets.pdf (accessed on 26 March 2019).

[90] Ras, Daniel Gerhardus. The Development and Assessment of the Mayoral Dashboard Performance Monitoring System in the City of Cape Town. Ph.D. Thesis, Stellenbosch University, Stellenbosch, South Africa, 2016.

[91] Department of Defense Washington, DC. Military Standard: Definitions of Term for Reliability and Maintainability; Technical report MIL-STD-721C; Department of Defense Washington DC: Washington, DC, USA, 1981.

[92] Fact Sheet: IBE Energy Savings from Maintenance|Building Efficiency Initiative|WRI Ross Center for Sustainable Cities. Available online: https://buildingefficiencyinitiative.org/resources/fact-sheet-ibe-energy-savings-maintenance (accessed on 20 December 2019).

[93] Frankel, M.; Heater, M.; Heller, J. Sensitivity Analysis: Relative Impact of Design, Commissioning Maintenance and Operational Variables on the Energy Performance of Office Buildings; New Buildings Institute, Portland, USA 2012.

[94] Giebeler, G.; Krause, H.; Fisch, R.; Musso, F.; Lenz, B.; Rudolphi, A. Refurbishment Manual: Maintenance, Conversions, Extensions; Walter de Gruyte, Basel, Switzerland 2012.

[95] Bourg, J. Water Conservation; Air Force Water Conservation Guidebook: Millennium Energy LLC, Burgettstown, USA 2004.

[96] Kusakana, K. Optimal Operation Control of Hybrid Renewable Energy Systems. Ph.D. Thesis, Central University of Technology, Bloemfontein, Free State, South Africa, 2015.

[97] Afram, A.; Janabi-Sharifi, F. Theory and applications of HVAC control systems–A review of model predictive control (MPC). Build. Environ. 2014, 72, 343–355.

[98] Aslam, S.; Hannan, S.; Sajjad, M.U.; Zafar, M.W. PLC based model predictive control for industrial process control. Int. J. Adv. Appl. Sci. 2017, 4, 63–71.

[99] Di Cairano, S. An industry perspective on MPC in large volumes applications: Potential Benefits and Open Challenges. IFAC Proc. Vol. 2012, 45, 52–59.

[100] Serale, G.; Fiorentini, M.; Capozzoli, A.; Bernardini, D.; Bemporad, A. Model predictive control (MPC) for enhancing building and HVAC system energy efficiency: Problem formulation, applications and opportunities. Energies 2018, 11, 631.

[101] Kepplinger, P.; Huber, G.; Petrasch, J. Autonomous optimal control for demand side management with resistive domestic hot water heaters using linear optimization. Energy Build. 2015, 100, 50–55.

[102] Hohne, P.A.; Kusakana, K.; Numbi, B.P. Scheduling and economic analysis of hybrid solar water heating system based on timer and optimal control. J. Energy Storage 2018, 20, 16–29.

[103] Rankin, R.; Rousseau, P.G.; van Eldik, M. Demand side management for commercial buildings using an inline heat pump water heating methodology. Energy Convers. Manag. 2004, 45, 1553–1563.

[104] Sichilalu, S.; Mathaba, T.; Xia, X. Optimal control of a wind–PV-hybrid powered heat pump water heater. Appl. Energy 2017, 185, 1173–1184.

[105] Sichilalu, S.; Tazvinga, H.; Xia, X. Optimal control of a fuel cell/wind/PV/grid hybrid system with thermal heat pump load. Sol. Energy 2016, 135, 59–69.

[106] Sichilalu, S.M.; Xia, X. Optimal energy control of grid tied PV–diesel–battery hybrid system powering heat pump water heater. Sol. Energy 2015, 115, 243–254.

[107] Sichilalu, S.M.; Xia, X. Optimal power dispatch of a grid tied-battery-photovoltaic system supplying heat pump water heaters. Energy Convers. Manag. 2015, 102, 81–91.

[108] Wanjiru, Evan M., Sam M. Sichilalu, and Xiaohua Xia. Optimal integrated diesel grid-renewable energy system for hot water devices. Energy Procedia 2016, 103, 117-122.

[109] Sichilalu, S.; Xia, X.; Zhang, J. Optimal scheduling strategy for a grid-connected photovoltaic system for heat pump water heaters. Energy Procedia 2014, 61, 1511–1514.

[110] Tahavori, M.; Leth, J.; Kallesøe, C.; Wisniewski, R. Optimal control of nonlinear hydraulic networks in the presence of disturbance. Nonlinear Dyn. 2014, 75, 539–548.

[111] Tahavori, M.; Jensen, T.N.; Kallesøe, C.; Leth, J.; Wisniewski, R. Toward model-based control of non-linear hydraulic networks. J. Vib. Control 2013, 19, 2145–2153.

[112] Sichilalu, S.M.; Xia, X. Optimal power control of grid tied PV-battery-diesel system powering heat pump water heaters. Energy Procedia 2015, 75, 1514–1521.

[113] Wanjiru, E.M.; Sichilalu, S.M.; Xia, X. Model predictive control of heat pump water heater-instantaneous shower powered with integrated renewable-grid energy systems. Appl. Energy 2017, 204, 1333–1346.

[114] Li, Z.; Sun, J. Disturbance compensating model predictive control with application to ship heading control. IEEE Trans. Control Syst. Technol. 2012, 20, 257–265.

[115] Davies, H.T.; Nutley, S.M. (Eds.) What Works? Evidence-Based Policy and Practice in Public Services; Policy Press, Bristol, UK: 2000.

[116] Bélanger, J.; Venne, P.; Paquin, J.N. The what, where and why of real-time simulation. Planet Rt 2010, 1, 25–29.

[117] Tang, Y.; Wang, Q.; Tai, W.; Chen, B.; Ni, M. Real-time simulation of cyber-physical power system based on OPAL-RT and OPNET. Autom. Electr. Power Syst. 2016, 40, 15–21.

[118] Saad, H.; Ould-Bachir, T.; Mahseredjian, J.; Dufour, C.; Dennetière, S.; Nguefeu, S. Real-time simulation of MMCs using CPU and FPGA. IEEE Trans. Power Electron. 2015, 30, 259–267.

[119] Faruque, M.O.; Strasser, T.; Lauss, G.; Jalili-Marandi, V.; Forsyth, P.; Dufour, C.; Dinavahi, V.; Monti; Kotsampopoulos P; Martinez JA; Strunz K.; Saeedifard M.; Wang X.; Shearer D.; Paolone M. Real-time simulation technologies for power systems design, testing, and analysis. IEEE Power Energy Technol. Syst. J. 2015, 2, 63–73.

[120] DOE. Energy Efficient Buildings: Sustainable Energy Africa; Department of energy (DOE): Pretoria, South Africa, 2017.

[121] Hohne, P. A., K. Kusakana, and B. P. Numbi. "Model validation and economic dispatch of a dual axis pv tracking system connected to energy storage with grid connection: A case of a healthcare institution in South Africa." Journal of Energy Storage 32 (2020): 101986.

[122] Rekioua, Djamila, and Ernest Matagne. Optimization of photovoltaic power systems: modelization, simulation and control. Springer Science & Business Media, 2012.Giglmayr, Sebastian, Alan C. Brent, Paul Gauché, and Hubert Fechner. "Utility-scale PV power and energy supply outlook for South Africa in 2015." Renewable Energy 83 (2015): 779-785.

[123] Srivastav, Amul Kumar, Abhishek Kumar Gupta, Rishabh Raj Jaiswal, and Sarvesh Kumar Gupta. "Modelling and Simulation of Photo voltaic System Using Matlab/Simulink." In Journal of Physics: Conference Series, vol. 1579, no. 1, p. 012024. IOP Publishing, 2020.

[124] Kumar, Raj, and S. K. Singh. "Solar photovoltaic modeling and simulation: As a renewable energy solution." Energy Reports 4 (2018): 701-712.

[125] Kusakana, Kanzumba. "Optimal scheduled power flow for distributed photovoltaic/wind/diesel generators with battery storage system." IET Renewable Power Generation 9, no. 8 (2015): 916-924.

[126] Hohne, P. A., K. Kusakana, and B. P. Numbi. "Optimal energy management and economic analysis of a grid-connected hybrid solar water heating system: A case of Bloemfontein, South Africa." Sustainable Energy Technologies and Assessments 31 (2019): 273-291.

[127] Kusakana, Kanzumba. "Operation cost minimization of photovoltaic–diesel–battery hybrid systems." Energy 85 (2015): 645-653.

[128] Cut.ac.za. 2020. CUT | CUT Solar Project: The Sun Is The Limit. [online] Available at: <https://www.cut.ac.za/news/cut-solar-project-the-sun-is-the-limit> [Accessed 6 April 2020].

[129] Bester, Jean Ernst, Ahmed El Hajjaji, and Augustin Mpanda Mabwe. "Modelling of Lithium-ion battery and SOC estimation using simple and extended discrete Kalman

Filters for Aircraft energy management." In IECON 2015-41st Annual Conference of the IEEE Industrial Electronics Society, pp. 002433-002438. IEEE, 2015.

[130] Chang, Wen-Yeau. "The state of charge estimating methods for battery: A review." ISRN Applied Mathematics 2013 (2013).

[131] Ng, Kong Soon, Chin-Sien Moo, Yi-Ping Chen, and Yao-Ching Hsieh. "Enhanced coulomb counting method for estimating state-of-charge and state-of-health of lithium-ion batteries." Applied energy 86, no. 9 (2009): 1506-1511.

[132] The Southern African Universities Radiometric Network (SAURAN):Available online at: https://sauran.ac.za/ [Accessed 24 Mar. 2020].

[133] Eldin, SA Sharaf, M. S. Abd-Elhady, and H. A. Kandil. "Feasibility of solar tracking systems for PV panels in hot and cold regions." Renewable Energy 85 (2016): 228-233.

[134] Singh, Shakti, Mukesh Singh, and S. C. Kaushik. "A review on optimization techniques for sizing of solar-wind hybrid energy systems." International Journal of Green Energy 13, no. 15 (2016): 1564-1578.

[135] Lan, Hai, Shuli Wen, Ying-Yi Hong, C. Yu David, and Lijun Zhang. "Optimal sizing of hybrid PV/diesel/battery in ship power system." Applied energy 158 (2015): 26-34.

[136] EE Publishers. (2017). Energy management systems save money – EE Publishers. [online] Available at: http://www.ee.co.za/article/energy-management-systemssave-money.html [Accessed 8 Dec. 2017].

[137] Hohne, P. A., Kusakana, K., & Numbi, B. P. (2019). Optimal energy management and economic analysis of a grid-connected hybrid solar water heating system: A case of Bloemfontein, South Africa. Sustainable Energy Technologies and Assessments, 31, 273-291.

[138] World inflation data. Historic inflation South Africa – CPI inflation. <http://www.inflation.eu/inflation-rates/south-africa/historic-inflation/cpi-inflationsouth-africa.aspx> [Last accessed: 24 March 2020].

[139] Gerber, Stefan, A. J. Rix, and M. J. Booysen. "Combining grid-tied PV and intelligent water heater control to reduce the energy costs at schools in South Africa." Energy for sustainable development 50 (2019): 117-125.

[140] Hohne, Percy Andrew. "Optimal energy management of a hybrid solar water heating system with grid connection under time-based pricing." PhD diss., Bloemfontein: Central University of Technology, Free State, 2017.

[141] Diao, Ruisheng, Shuai Lu, Marcelo Elizondo, Ebony Mayhorn, Yu Zhang, and Nader Samaan. "Electric water heater modeling and control strategies for demand response." In 2012 IEEE power and energy society general meeting, pp. 1-8. IEEE, 2012.

[142] Hohne, P. A., K. Kusakana, and B. P. Numbi. "Operation cost minimisation of hybrid solar/electrical water heating systems: Model development." Advanced Science Letters 24, no. 11 (2018): 8076-8080.

[143] Hohne, P. A., K. Kusakana, and B. P. Numbi. "Optimal energy management and economic analysis of a grid-connected hybrid solar water heating system: A case of Bloemfontein, South Africa." Sustainable Energy Technologies and Assessments 31 (2019): 273-291.

[144] Hohne, P. A., K. Kusakana, and B. P. Numbi. "Operation cost and energy usage minimization of a hybrid solar/electrical water heating system." In 2018 international conference on the domestic use of energy (DUE), pp. 1-7. IEEE, 2018.

[145] Sichilalu, Sam M. "Optimal control of renewable energy/grid hybrid systems with heat pump load." PhD diss., University of Pretoria, 2016.

[146] Sichilalu, Sam, Henerica Tazvinga, and Xiaohua Xia. "Optimal control of a fuel cell/wind/PV/grid hybrid system with thermal heat pump load." Solar energy 135 (2016): 59-69.

[147] Hohne, Percy A., Kanzumba Kusakana, and Bubele P. Numbi. "Optimal Energy Management and Economic analysis of a grid-connected Hybrid Solar Water Heating System in Bloemfontein." In 2018 IEEE PES/IAS PowerAfrica, pp. 515-520. IEEE, 2018.

APPENDIX A: PARTIAL ALGORITHM FORM FOR CHAPTER 3 MODEL

The proposed model and optimization model was solved using the OPTI toolbox SCIP algorithm in MATLAB with the following form in Eqs. (A.15) –(A.22):

and may be transformed to the general OPTI toolbox algorithm solver form in Eqs. (A.1) – (A.8):

$$\min_x f^T x, \tag{A.1}$$

$$\text{subject to: } Ax \le b, \tag{A.2}$$

$$A_{eq}x = b_{eq}, \tag{A.3}$$

$$l_b \le x \le u_b, \tag{A.4}$$

$$c(x) \le d \tag{A.5}$$

$$ceq(x) \le deq \tag{A.6}$$

$$x_i \in z \tag{A.7}$$

$$x_j \in \{0,1\} \tag{A.8}$$

where: *f* in Eq. (A.1) is the vector containing the objective function, which is subject to the constraints in Eqs. (A.2) - Eqs. (A.8). In Eq. (A.2) and Eq. (A.3), the linear inequality and equality sparse matrices are shown as *A* and *Aeq,* respectively, while *b* and *beq* are vectors. The decision variable in Eq. (A.4), *x*, is constrained by lower and upper bounds, l_b and u_b. Eq (A.5) shows *c* and is a vector of functions containing inequality constraints, while *d* is a vector. Similarly, in Eq. (A.6), *ceq* is a vector of functions for the nonlinear equality constraints with *deq* as a vector. The decision variable constraints in Eq. (A.21) and Eq. (A.22) are given by *xi* and *xj,* which must be integer and binary numbers, respectively.

The objective functions in Eq. (A.1) and Eq. (A.2) is transformed to the general solver form, as shown in Eq. (A.9).

For grid energy cost minimization f_1:

$$f^T x = [p_1 \dots p_N, p_1 \dots p_N] \begin{bmatrix} P_{1,0} \dots P_{1,N} \\ P_{5,0} \dots P_{1,N} \end{bmatrix}_{2N \times 1}. \tag{A.9}$$

For PV power output maximization f_2:

$$f^T x = [0 \dots 0_N] \begin{bmatrix} P_{2,0} \dots P_{2,N} \end{bmatrix}_{N \times 1}. \tag{A.10}$$

The same method is applied for the matrices and vectors in Eqs. (A.2) and (A.3), which refers to Eqs. (3.3), (3.7) and (3.13) for the equality constraint, while the inequality constraints refer to Eqs. (3.4-3.6) and (3.11).

The control variables are restricted between the lower bound (l_b) and upper bound (u_b), shown in Eq. (A.11) and Eq. (A.12).

$$l_b^T = [0 \dots 0_N, 0 \dots 0_N, 0 \dots 0_N, 0 \dots 0_N, 0 \dots 0_N], \tag{A.11}$$

$$u_b^T = [\infty_1 \dots \infty_N, P_{PV,1} \dots P_{PV,N}, P_{PV,1} \dots P_{PV,N}, \infty_1 \dots \infty_N, \infty_1 \dots \infty_N]. \tag{A.12}$$

APPENDIX B: EXTENDED CHAPTER 4 RESULTS

B.1 Winter baseline system 1:

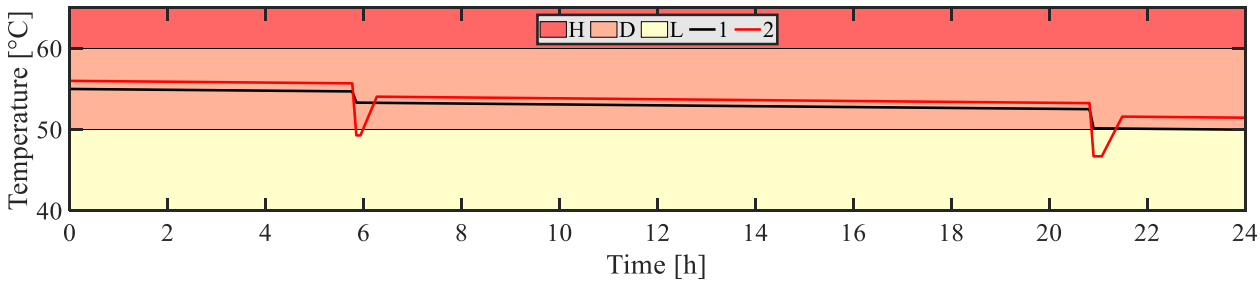

Fig. B.1.1: Basement ESTWH temperatures

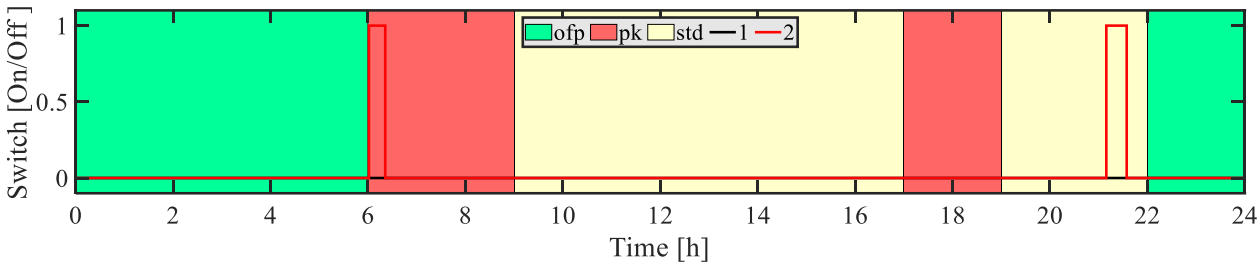

Fig. B.1.2: Basement ESTWH switching functions

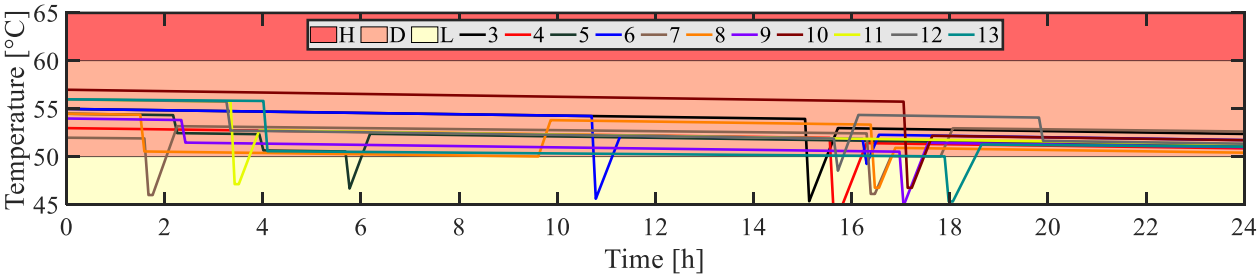

Fig. B.1.3: Level 2 ESTWH temperatures

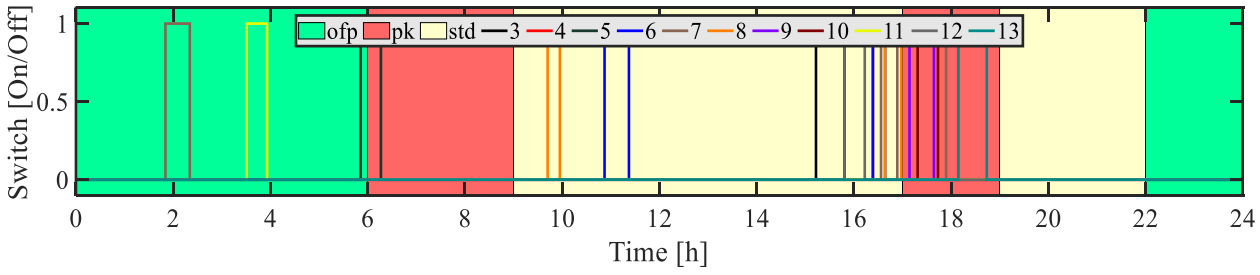

Fig. B.1.4: Level 2 ESTWH switching functions

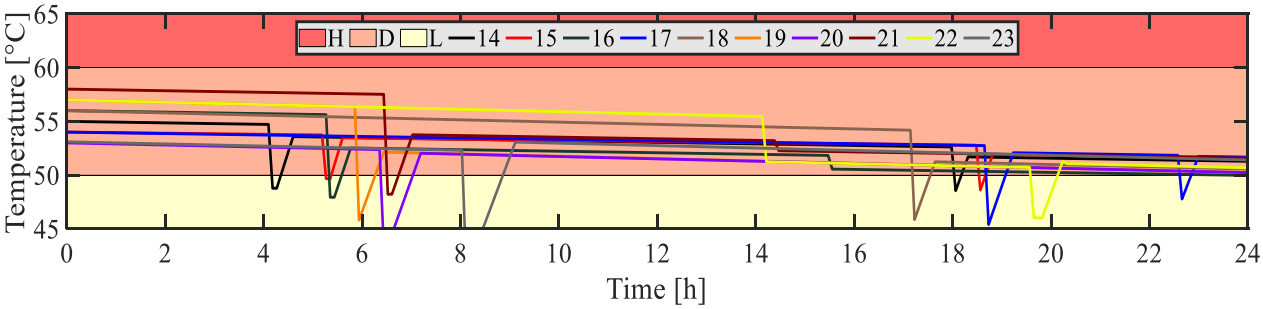

Fig. B.1.5: Level 3 ESTWH temperatures

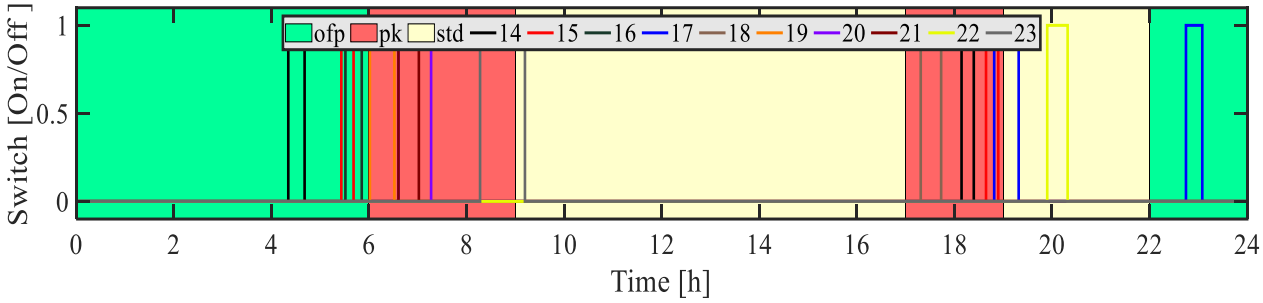

Fig. B.1.6: Level 3 ESTWH switching functions

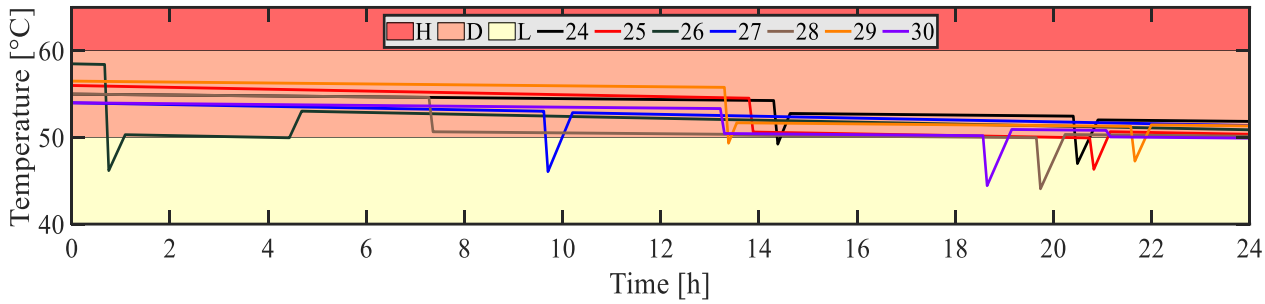

Fig. B.1.7: Level 4 ESTWH temperatures

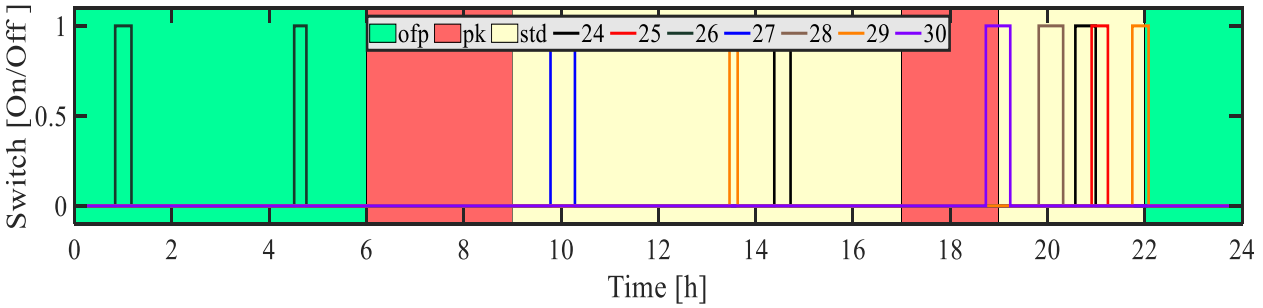

Fig. B.1.8: Level 4 ESTWH switching functions

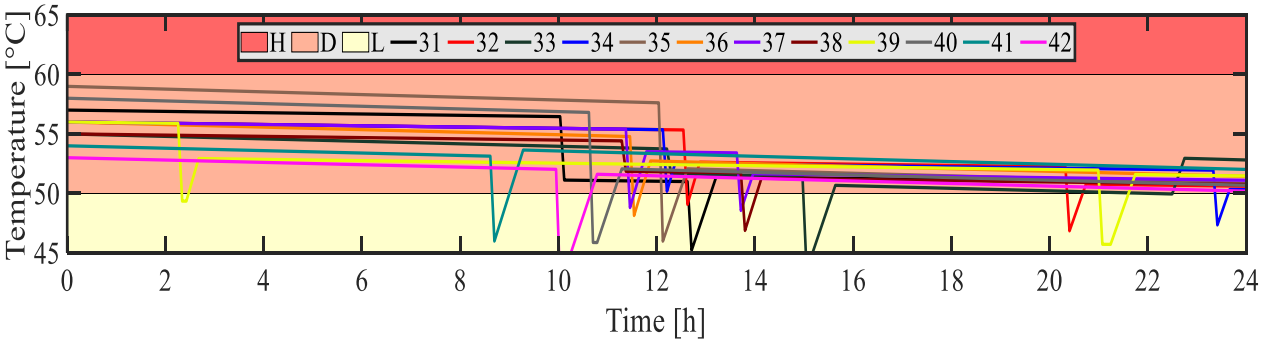

Fig. B.1.9: Level 5 ESTWH temperatures

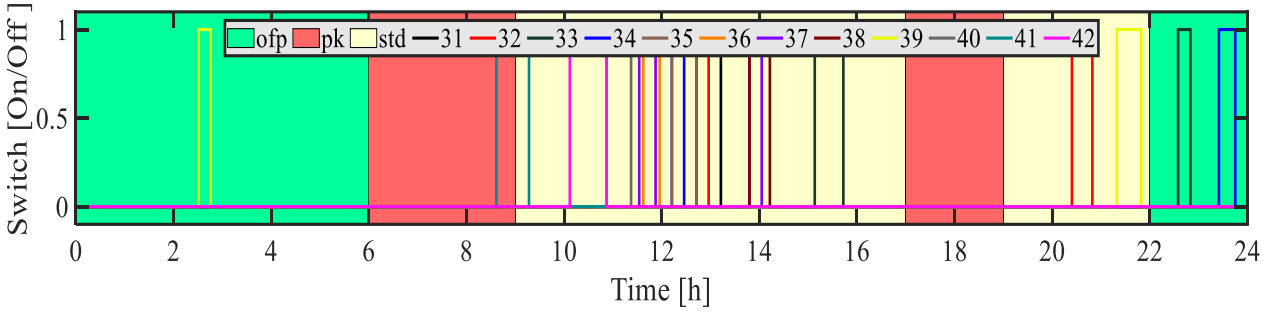

Fig. B.1.10: Level 5 ESTWH switching functions

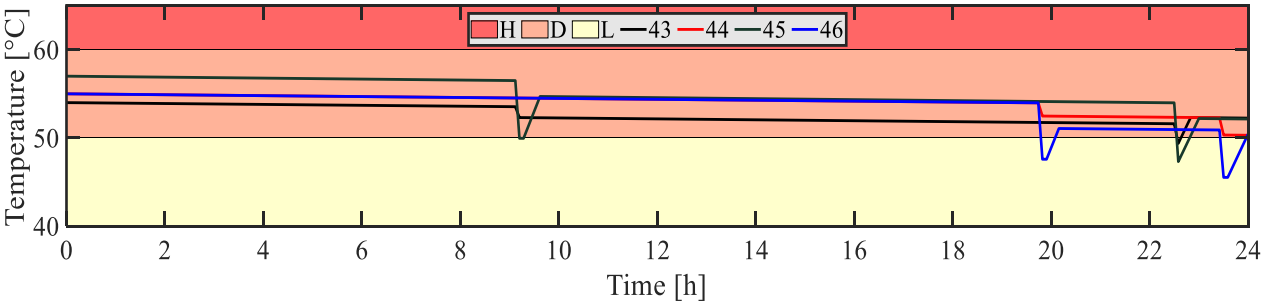

Fig. B.1.11: Level 6 ESTWH temperatures

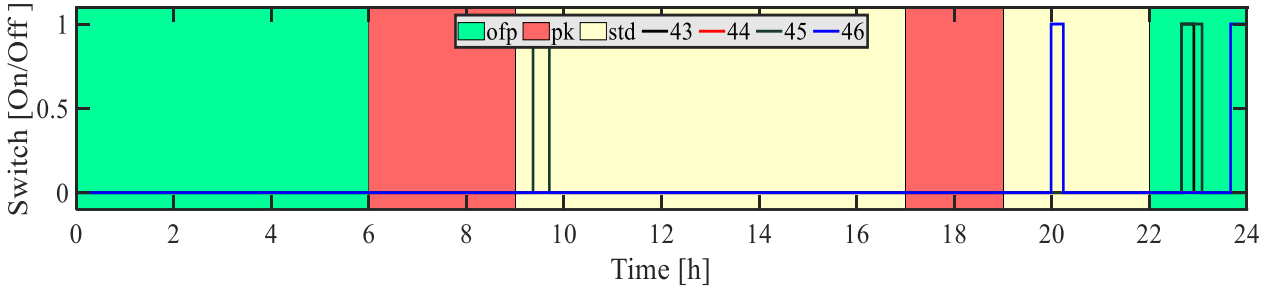

Fig. B.1.12: Level 6 ESTWH switching functions

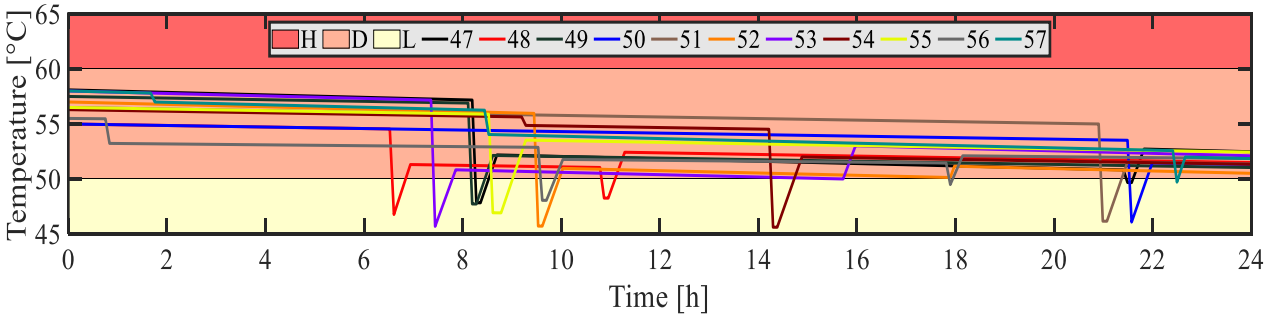

Fig. B.1.13: Level 7 ESTWH temperatures

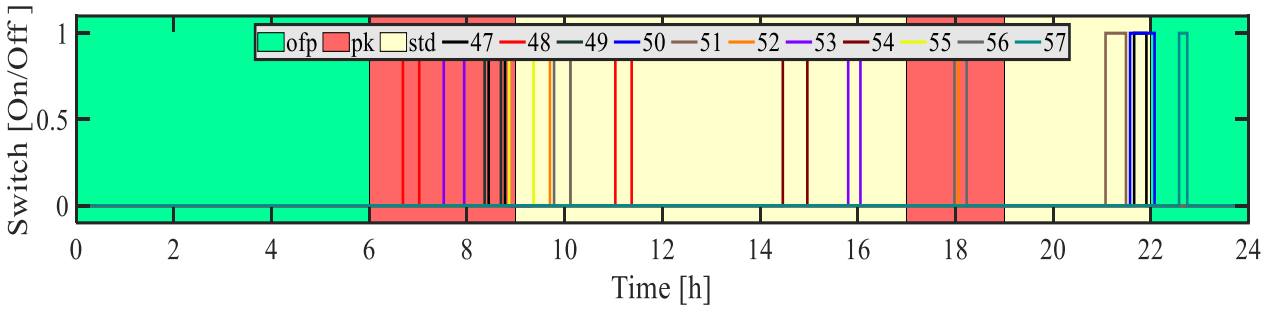

Fig. B.1.14: Level 7 ESTWH switching functions

B.2 Winter baseline system 2:

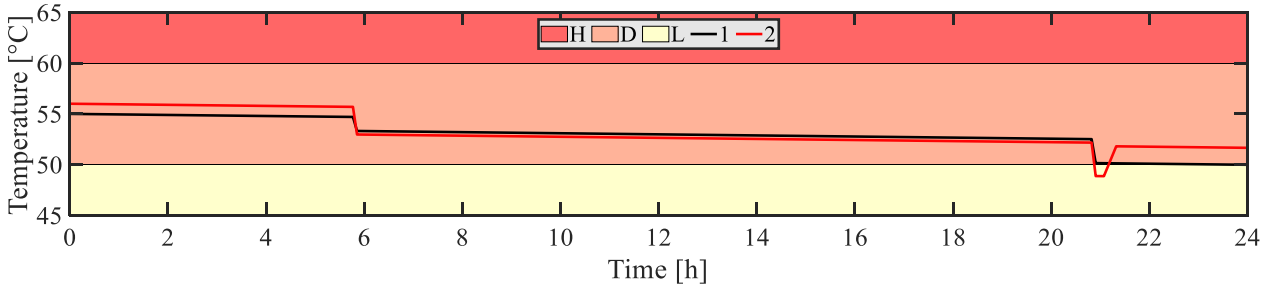

Fig. B.2.1: Basement ESTWH temperatures

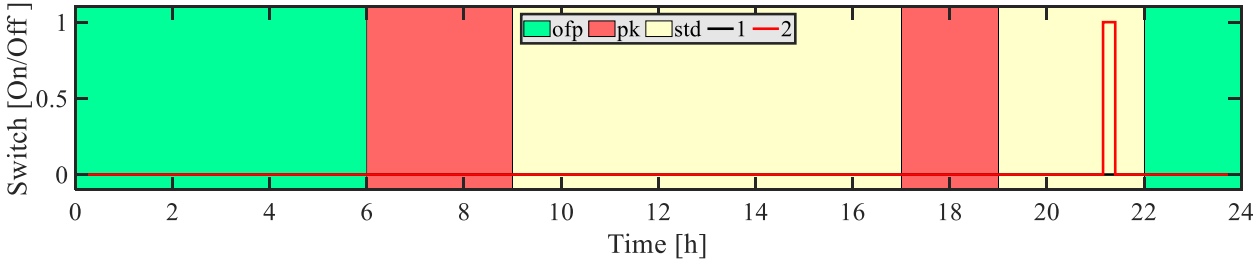

Fig. B.2.2: Basement ESTWH switching functions

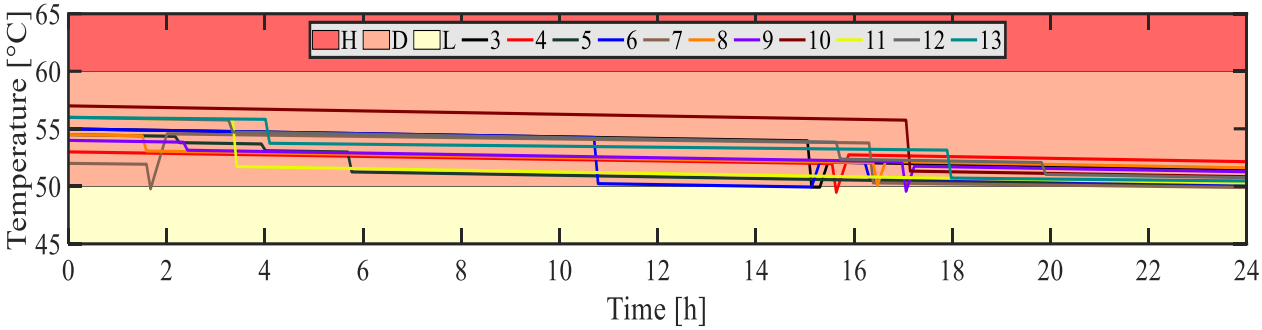

Fig. B.2.3: Level 2 ESTWH temperatures

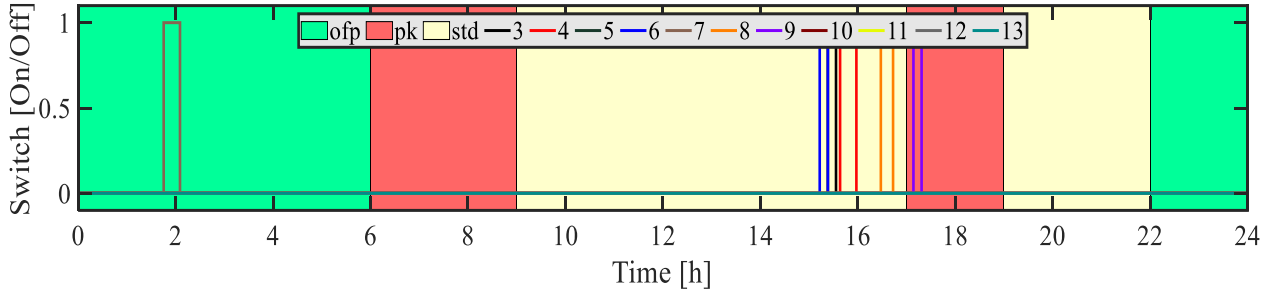

Fig. B.2.4: Level 2 ESTWH switching functions

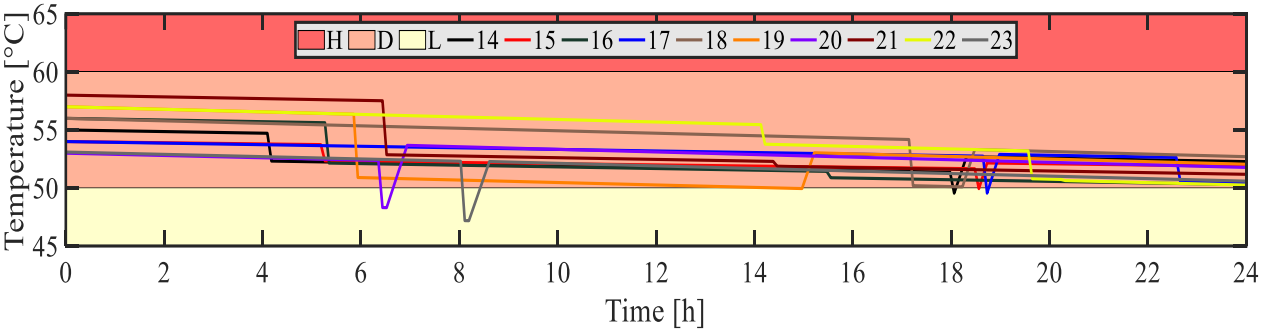

Fig. B.2.5: Level 3 ESTWH temperatures

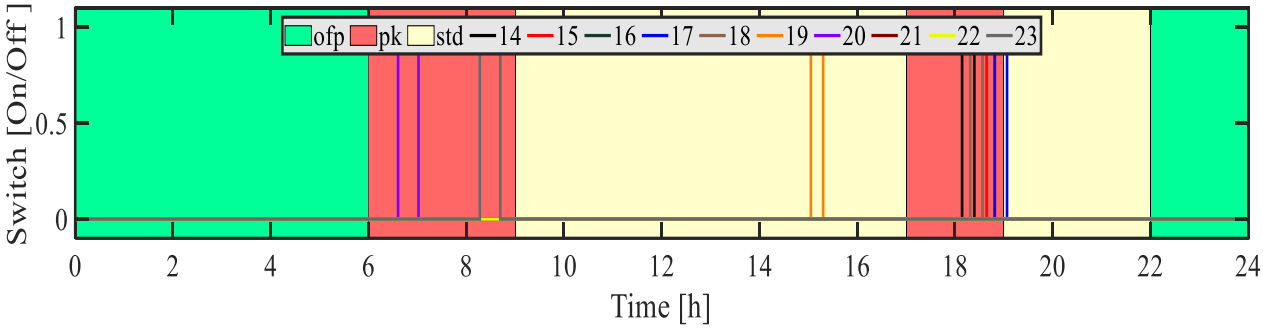

Fig. B.2.6: Level 3 ESTWH switching functions

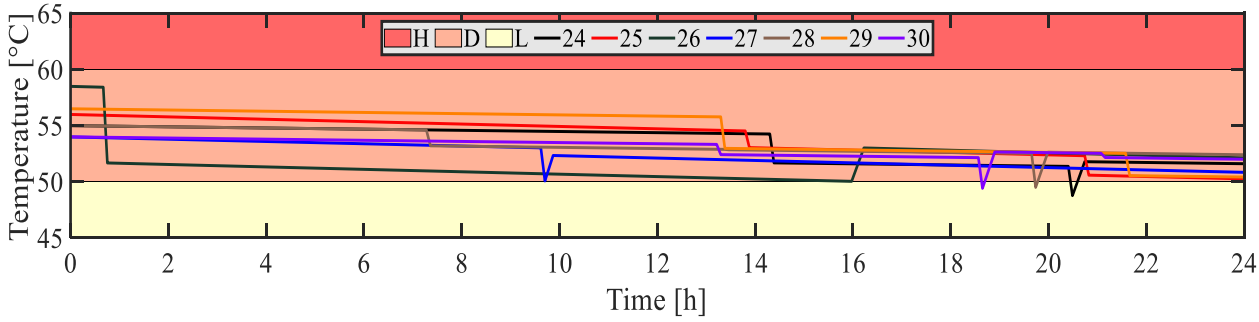

Fig. B.2.7: Level 4 ESTWH temperatures

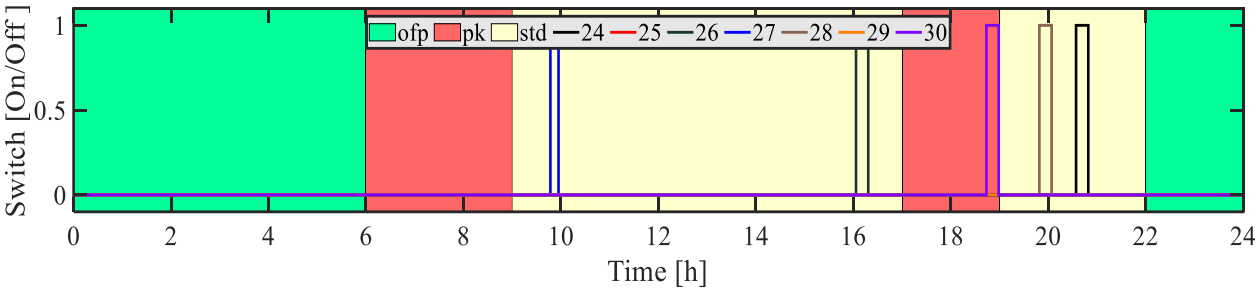

Fig. B.2.8: Level 4 ESTWH switching functions

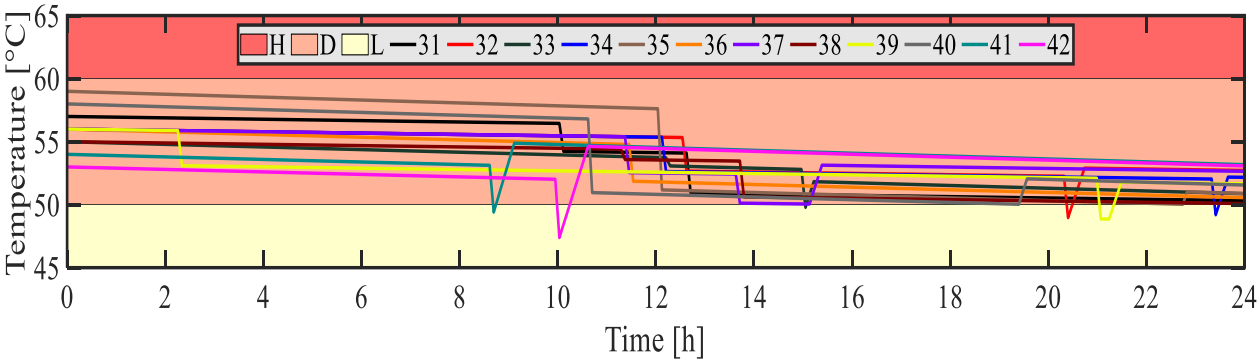

Fig. B.2.9: Level 5 ESTWH temperatures

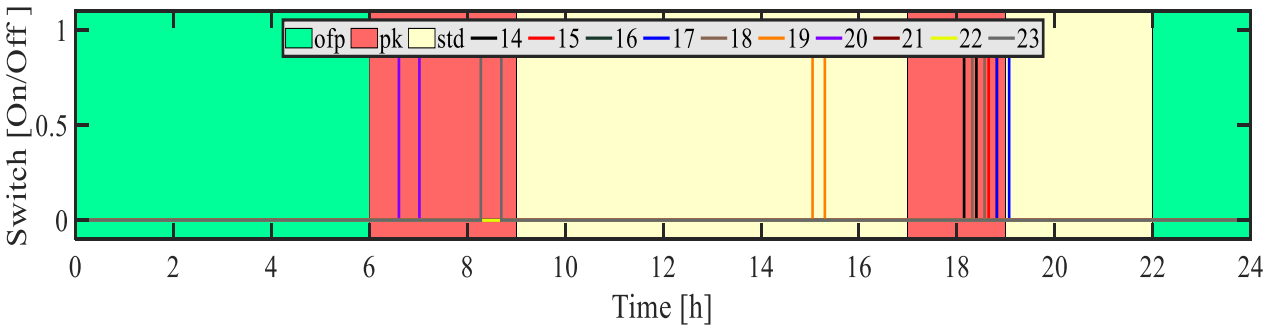

Fig. B.2.10: Level 5 ESTWH switching functions

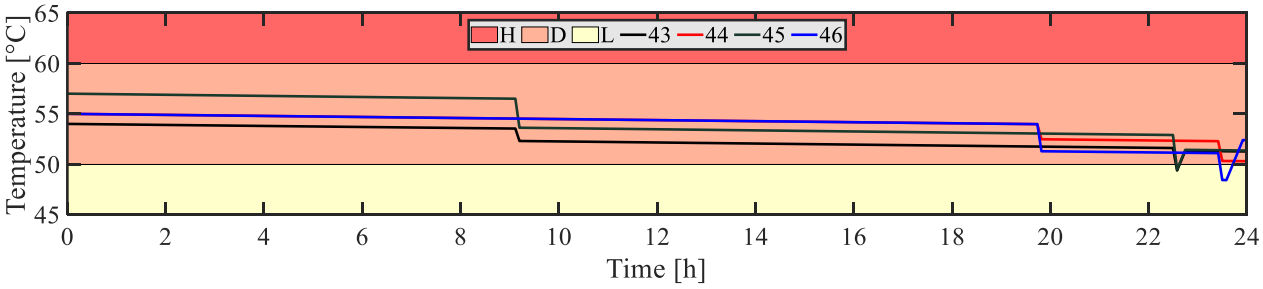

Fig. B.2.11: Level 6 ESTWH temperatures

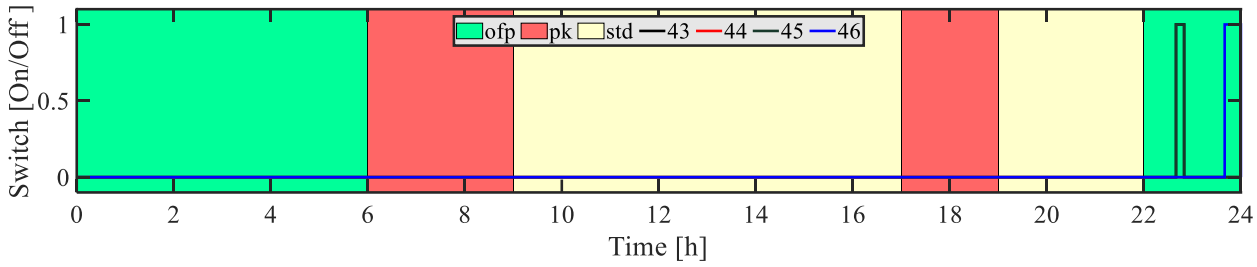

Fig. B.2.12: Level 6 ESTWH switching functions

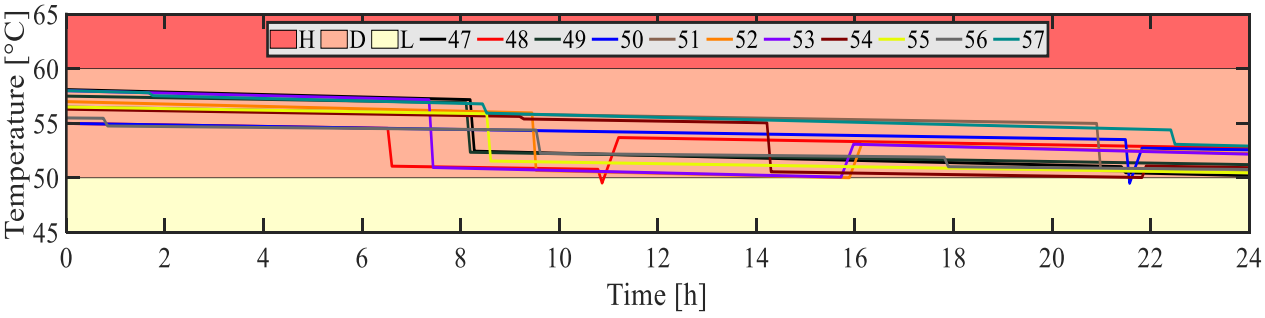

Fig. B.2.13: Level 7 ESTWH temperatures

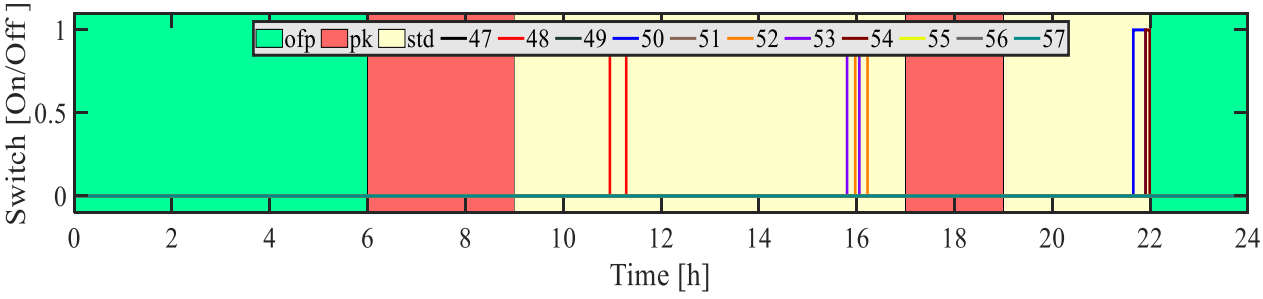

Fig. B.2.14: Level 7 ESTWH switching functions

B.3 Winter optimal control case:

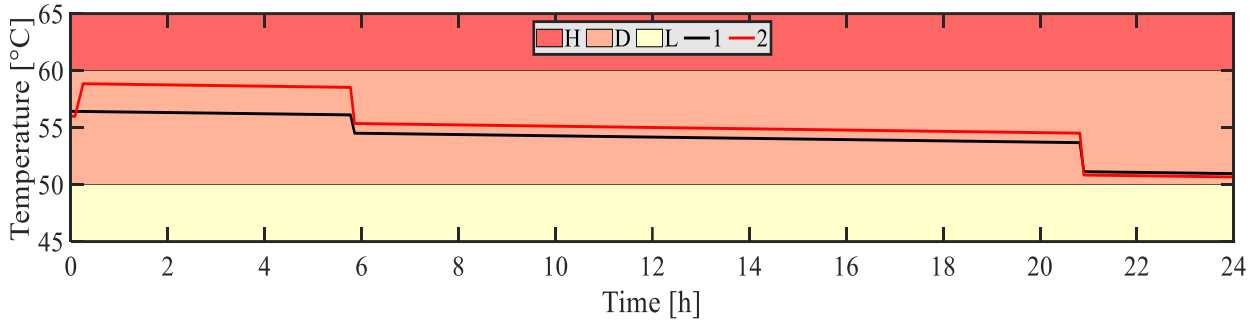

Fig. B.3.1: Basement ESTWH temperatures

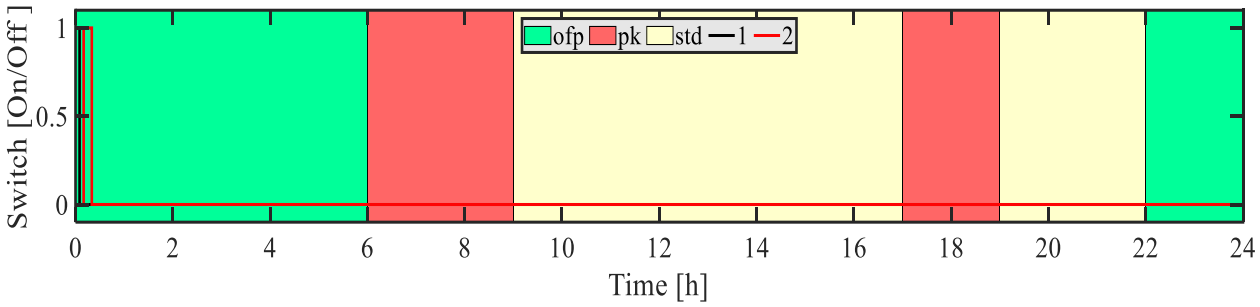

Fig. B.3.2: Basement ESTWH switching functions

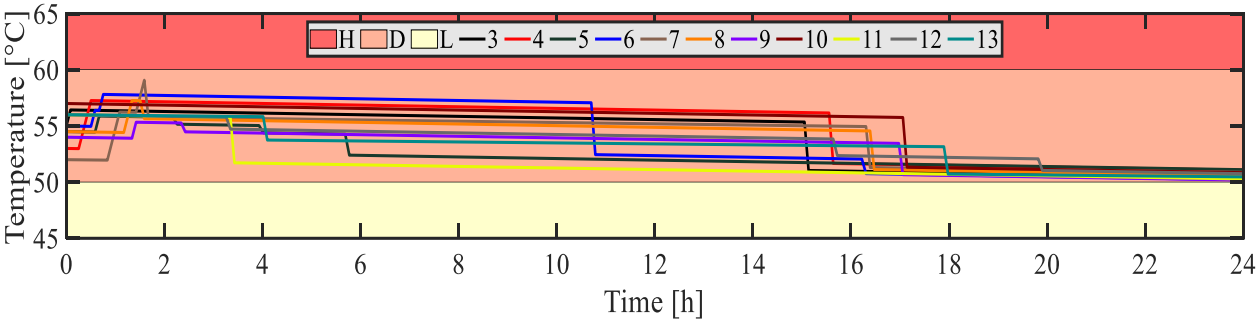

Fig. B.3.3: Level 2 ESTWH temperatures

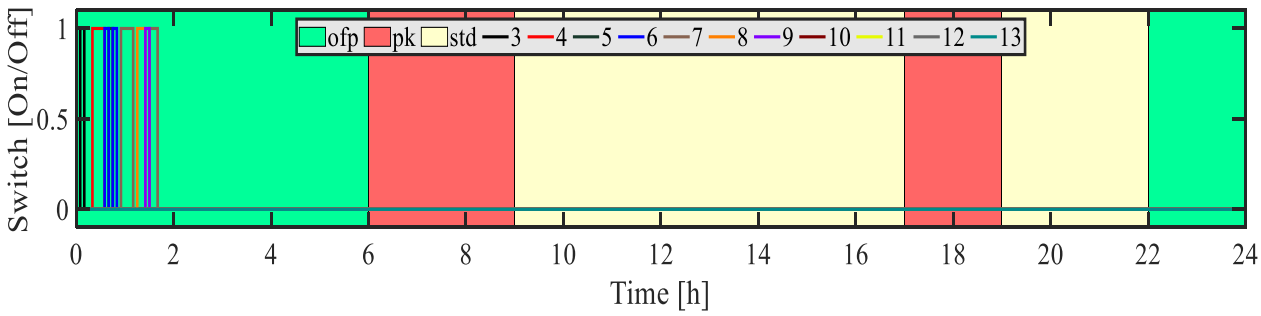

Fig. B.3.4: Level 2 ESTWH switching functions

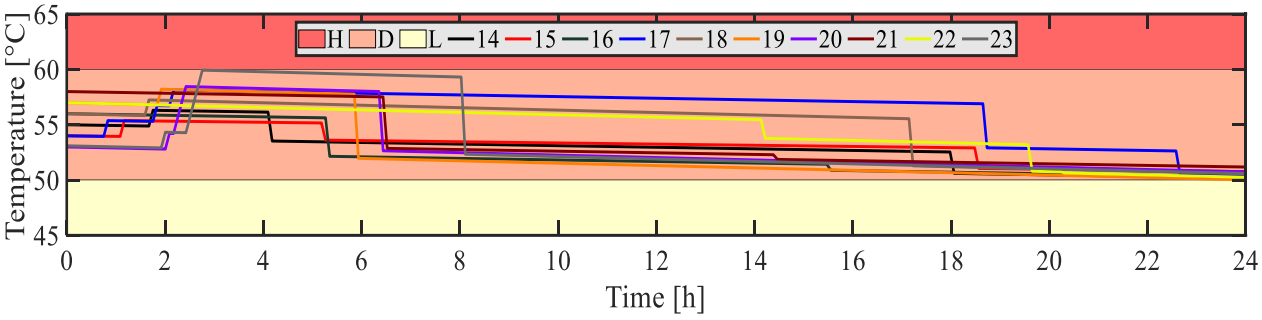

Fig. B.3.5: Level 3 ESTWH temperatures

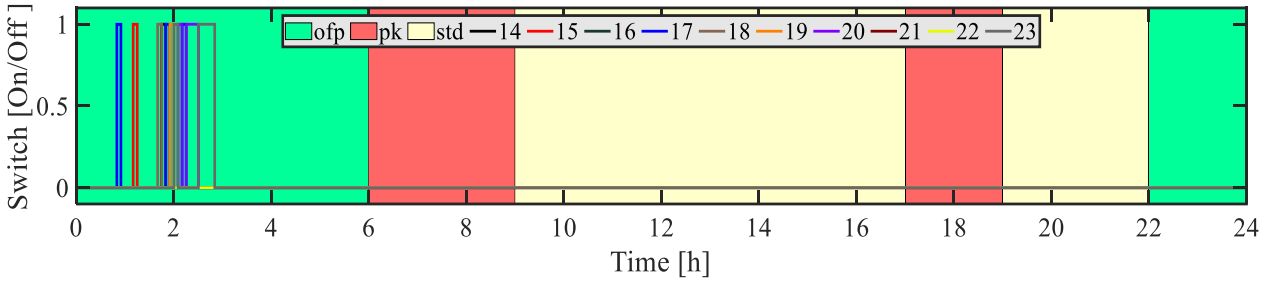

Fig. B.3.6: Level 3 ESTWH switching functions

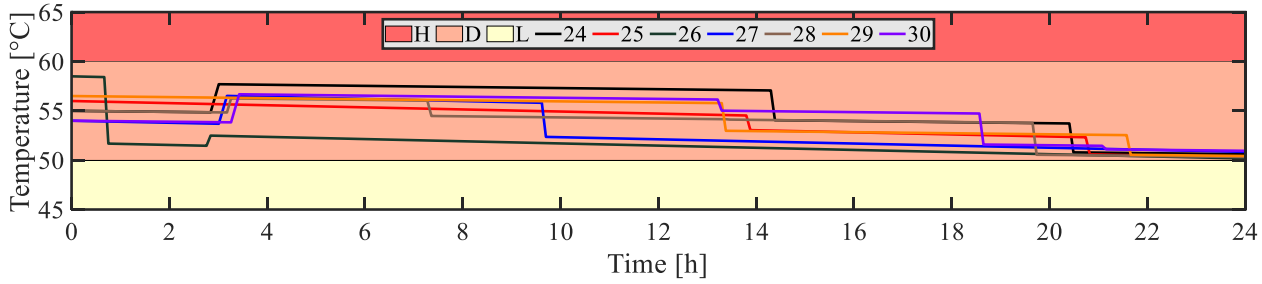

Fig. B.3.7: Level 4 ESTWH temperatures

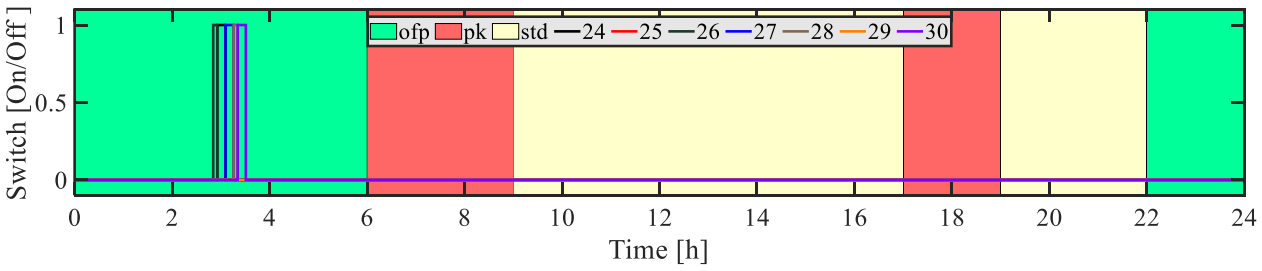

Fig. B.3.8: Level 4 ESTWH switching functions

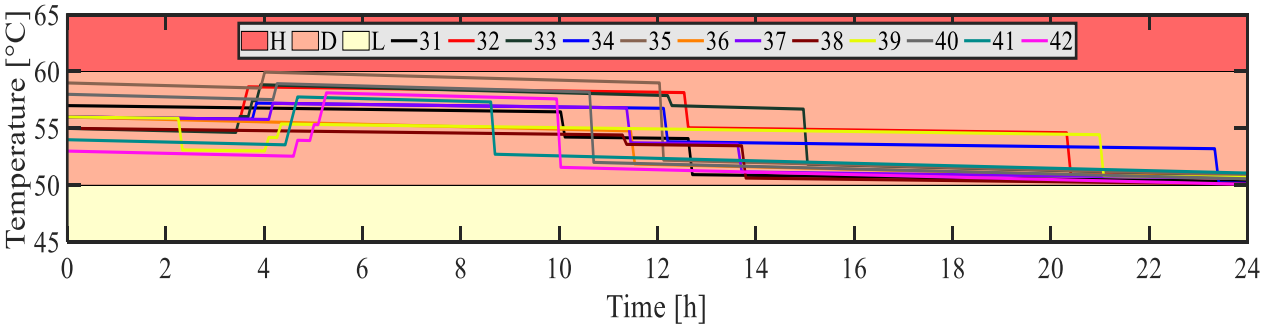

Fig. B.3.9: Level 5 ESTWH temperatures

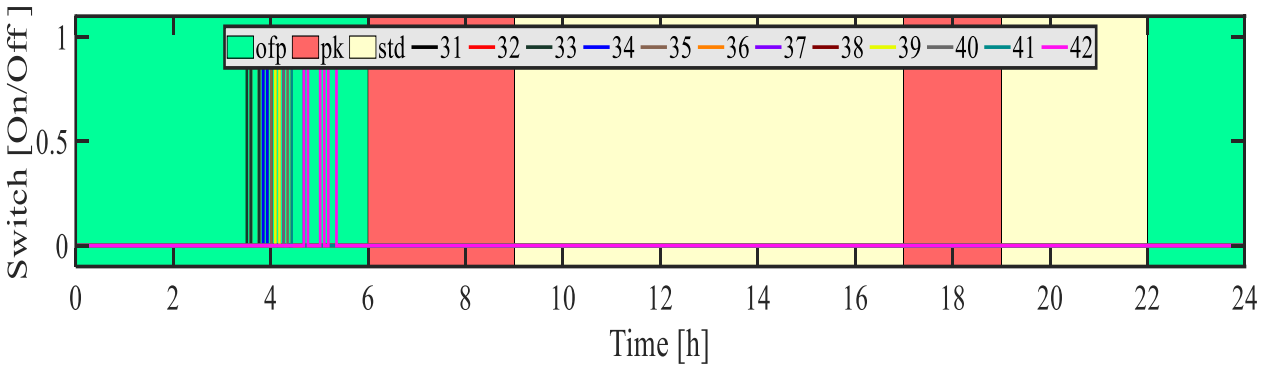

Fig. B.3.10: Level 5 ESTWH switching functions

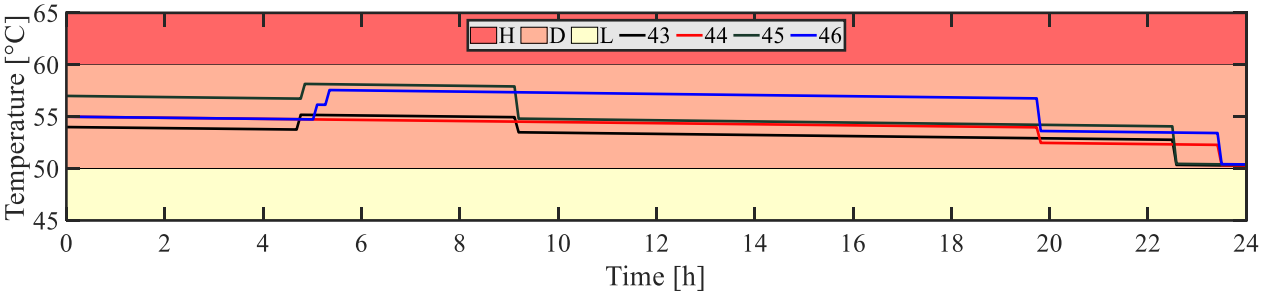

Fig. B.3.11: Level 6 ESTWH temperatures

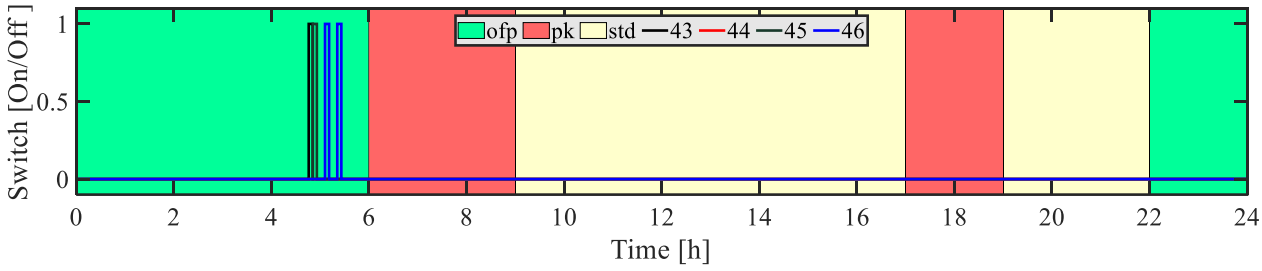

Fig. B.3.12: Level 6 ESTWH switching functions

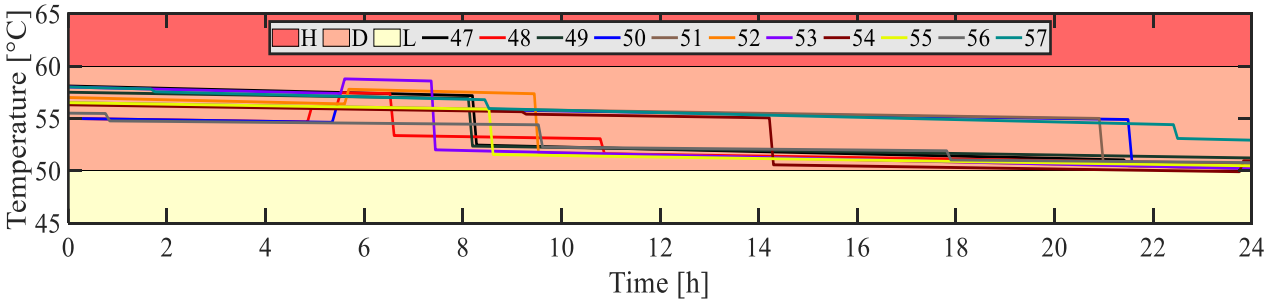

Fig. B.3.13: Level 7 ESTWH temperatures

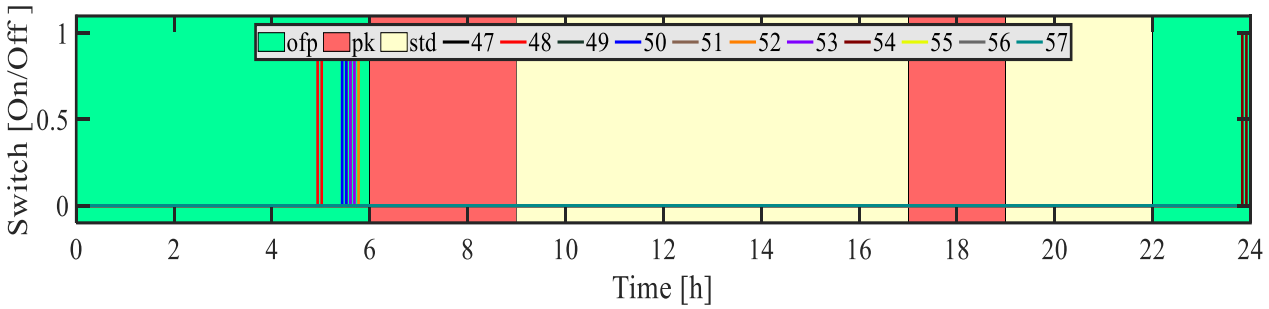

Fig. B.3.14: Level 7 ESTWH switching functions

B.4 Summer baseline system 1:

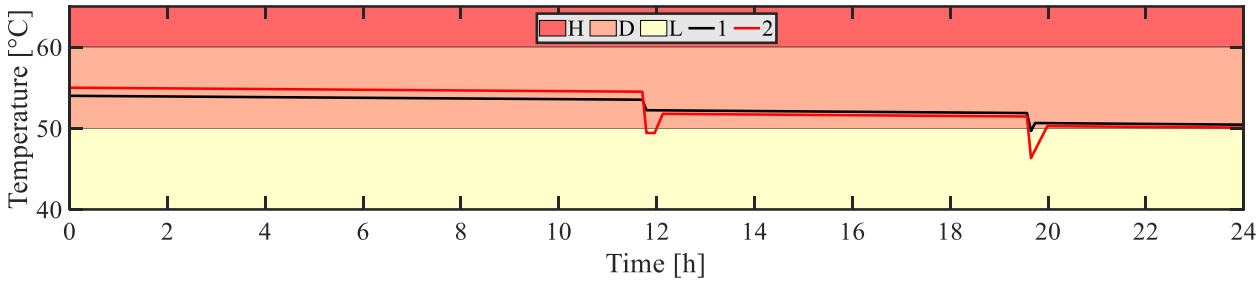

Fig. B.4.1: Basement ESTWH temperatures

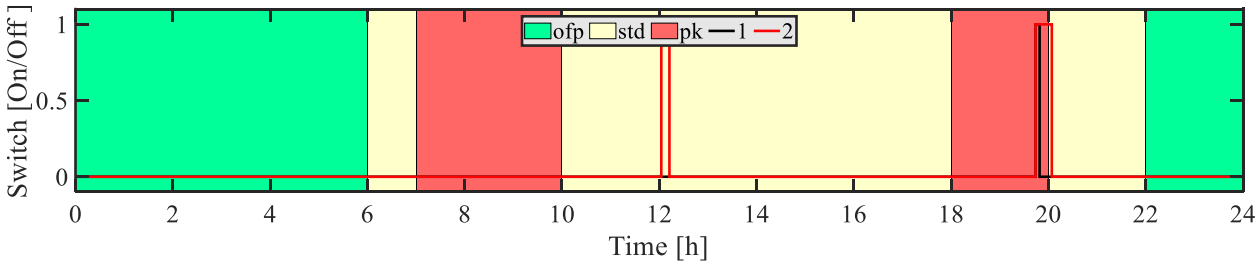

Fig. B.4.2: Basement ESTWH switching functions

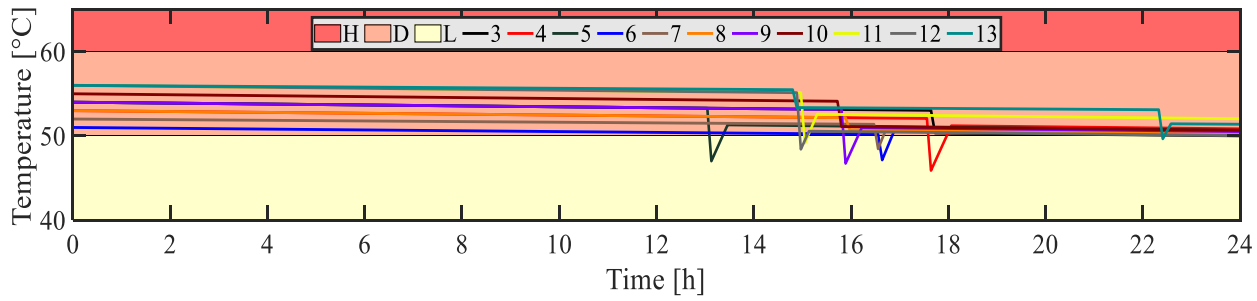

Fig. B.4.3: Level 2 ESTWH temperatures

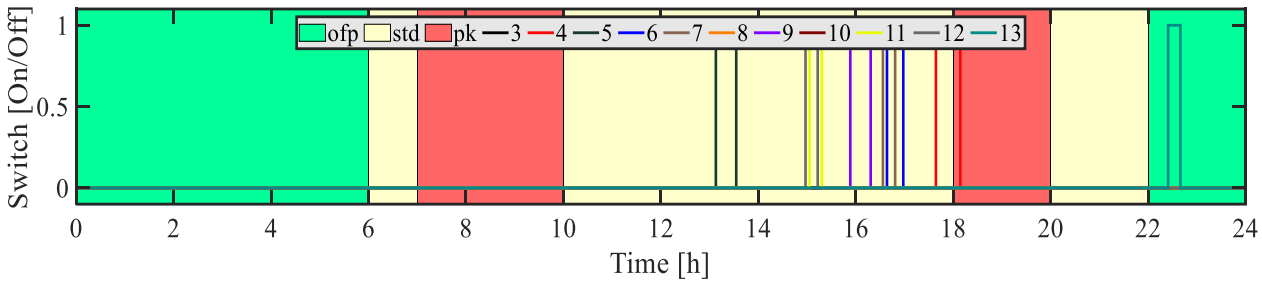

Fig. B.4.4: Level 2 ESTWH switching functions

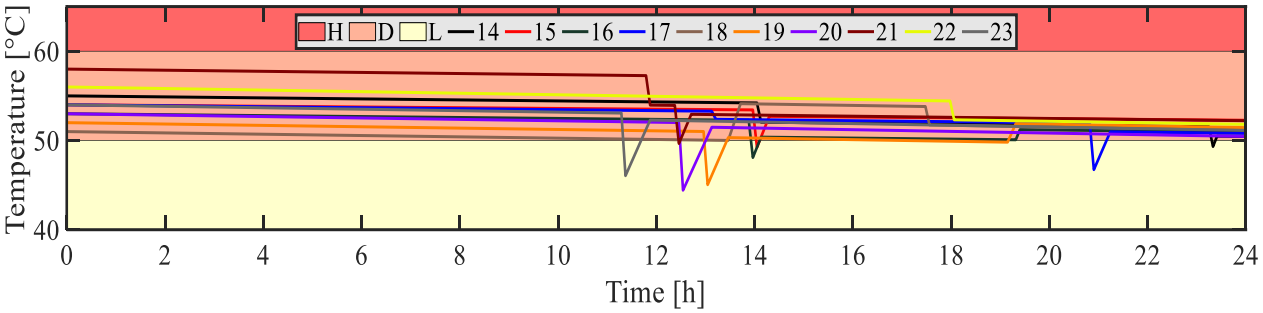

Fig. B.4.5: Level 3 ESTWH temperatures

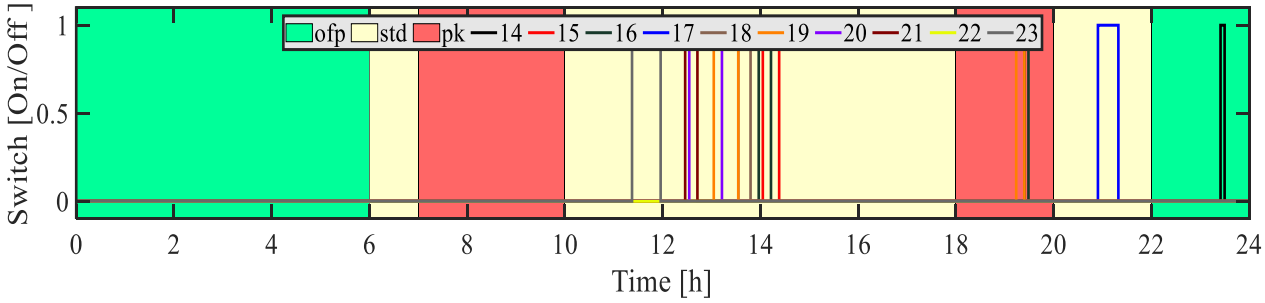

Fig. B.4.6: Level 3 ESTWH switching functions

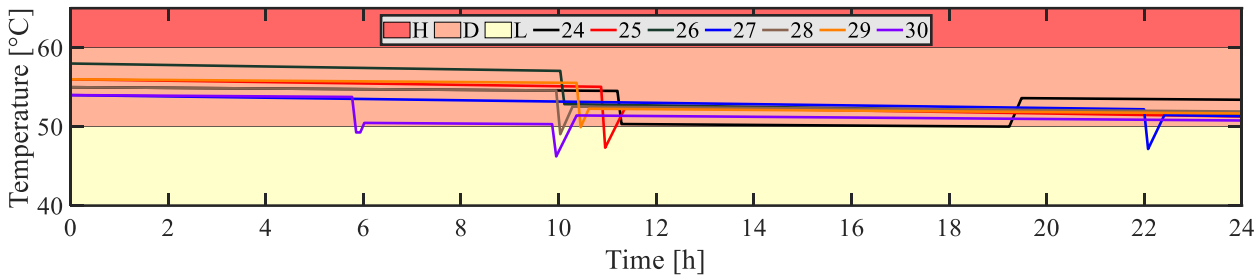

Fig. B.4.7: Level 4 ESTWH temperatures

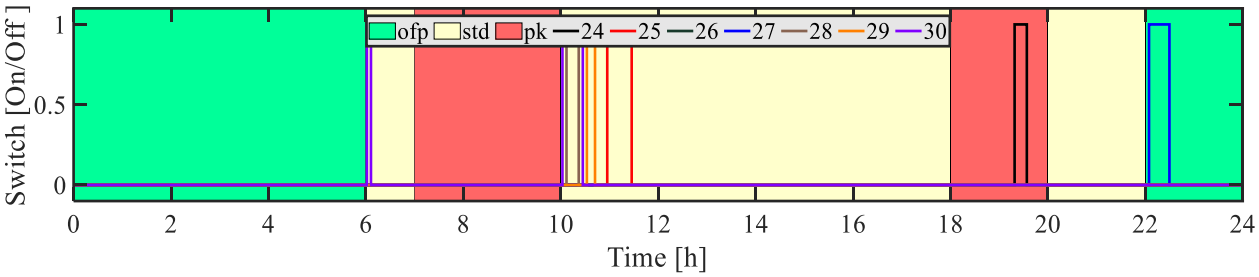

Fig. B.4.8: Level 4 ESTWH switching functions

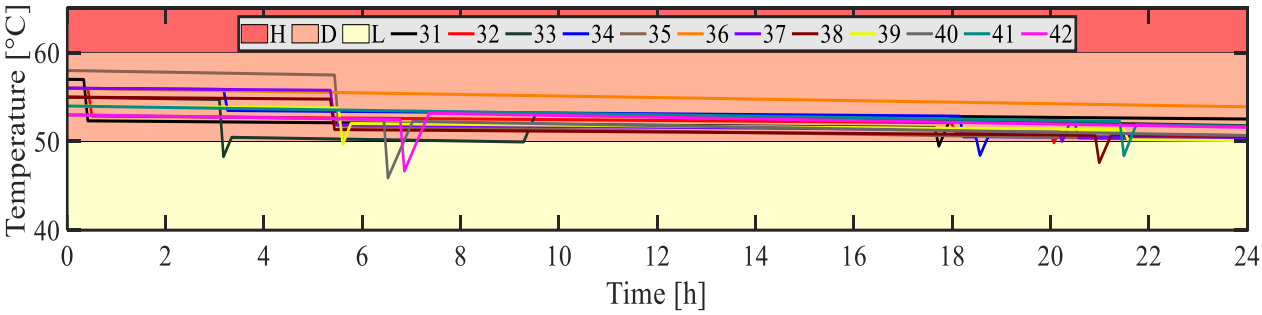

Fig. B.4.9: Level 5 ESTWH temperatures

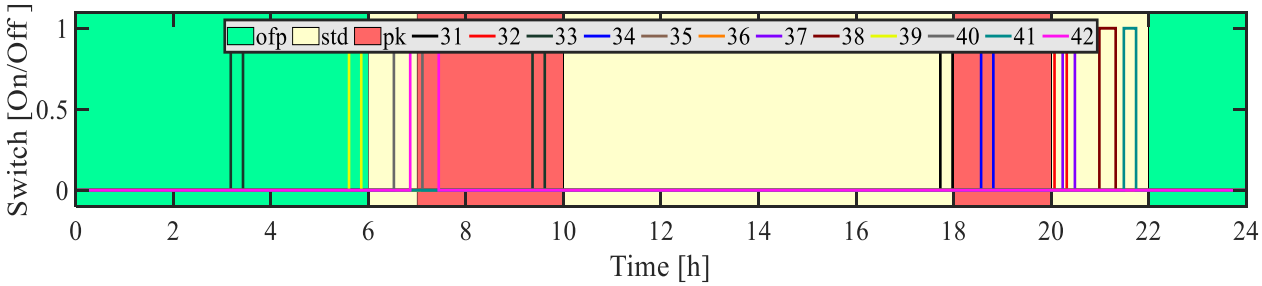

Fig. B.4.10: Level 5 ESTWH switching functions

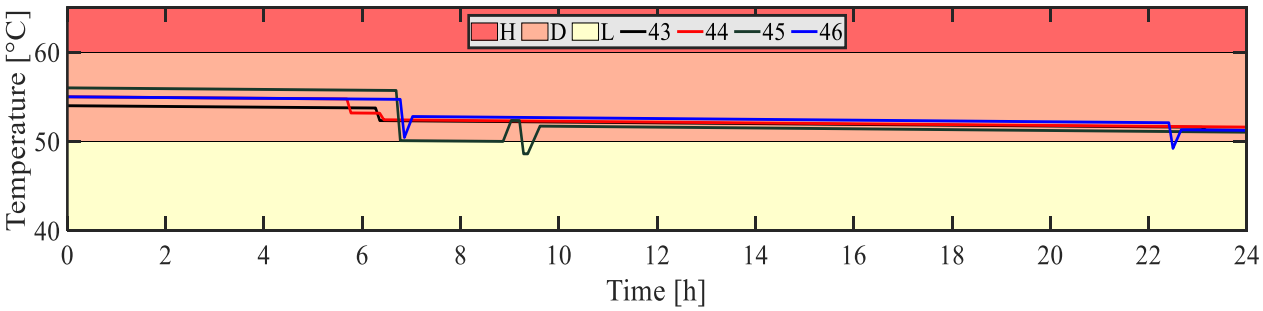

Fig. B.4.11: Level 6 ESTWH temperatures

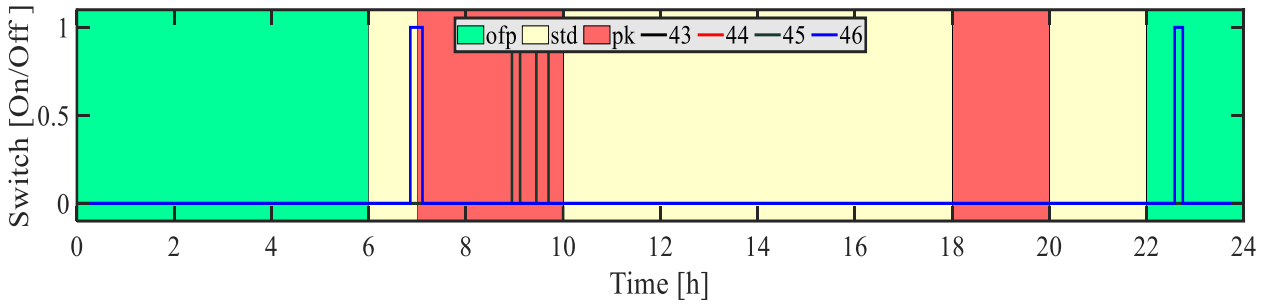

Fig. B.4.12: Level 6 ESTWH switching functions

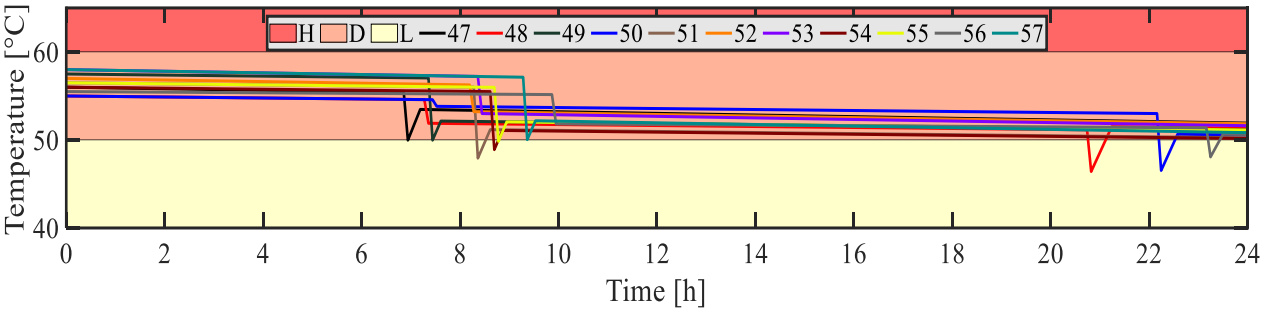

Fig. B.4.13: Level 7 ESTWH temperatures

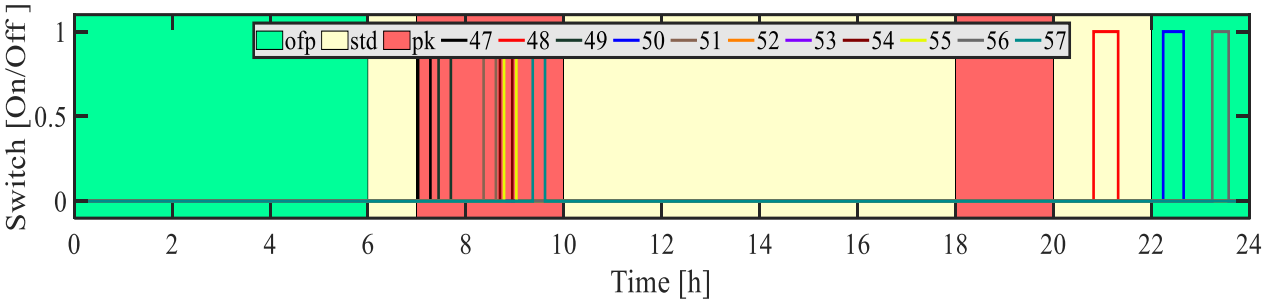

Fig. B.4.14: Level 7 ESTWH switching functions

B.5 Summer baseline system 2:

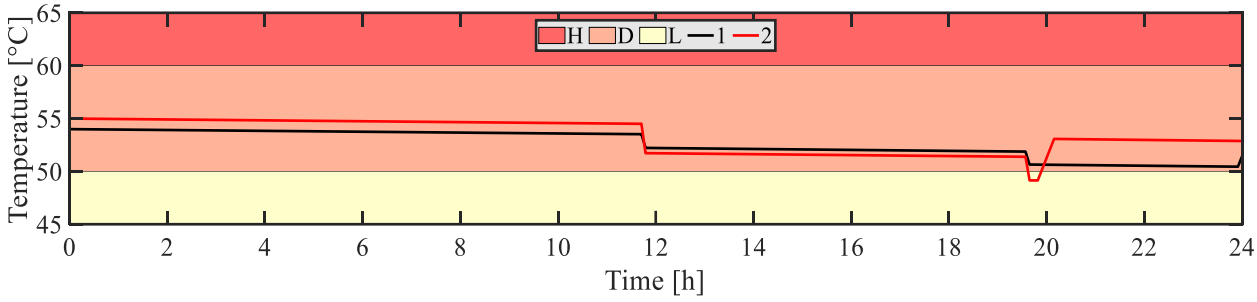

Fig. B.5.1: Basement ESTWH temperatures

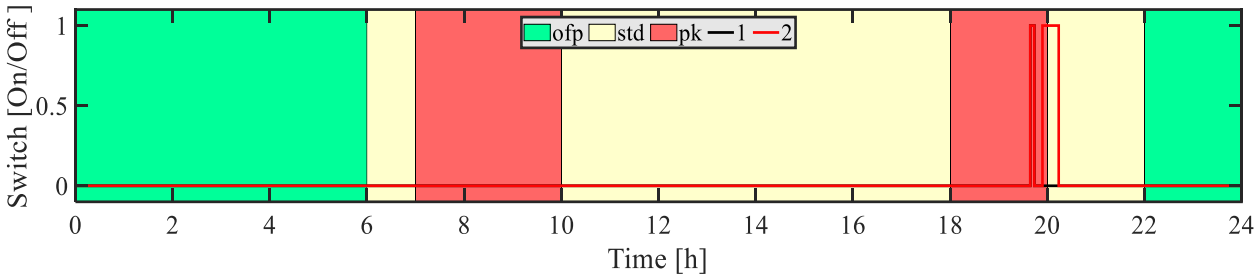

Fig. B.5.2: Basement ESTWH switching functions

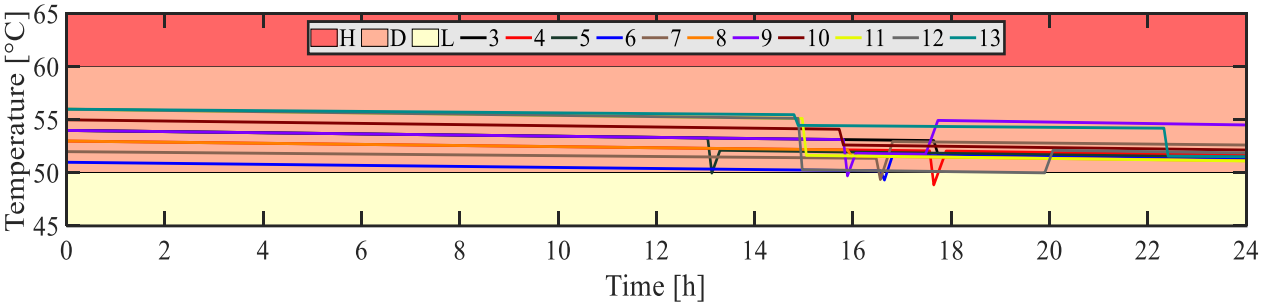

Fig. B.5.3: Level 2 ESTWH temperatures

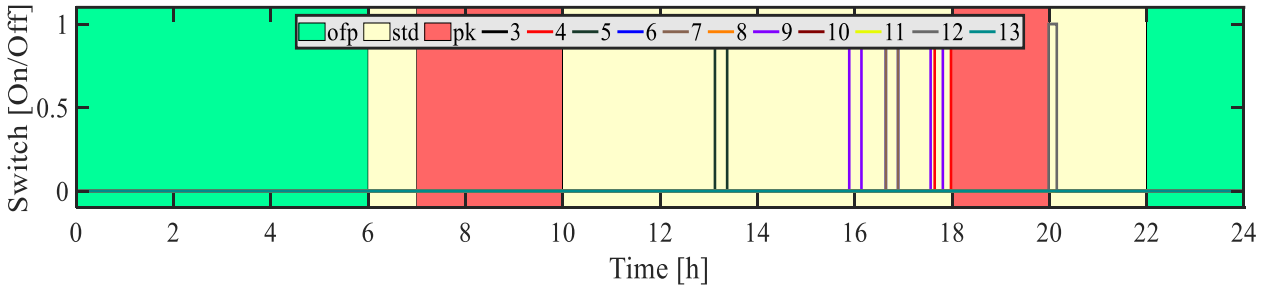

Fig. B.5.4: Level 2 ESTWH switching functions

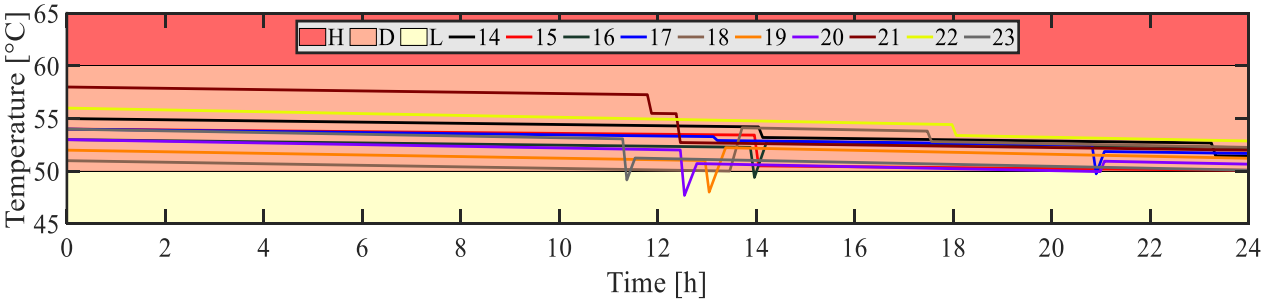

Fig. B.5.5: Level 3 ESTWH temperatures

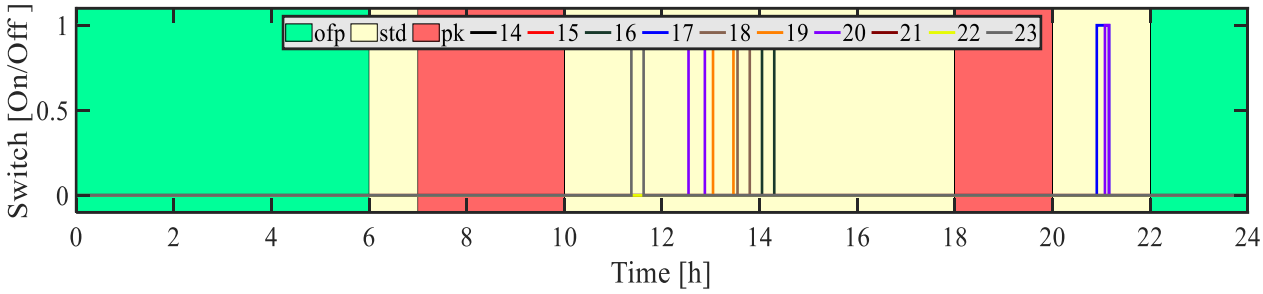

Fig. B.5.6: Level 3 ESTWH switching functions

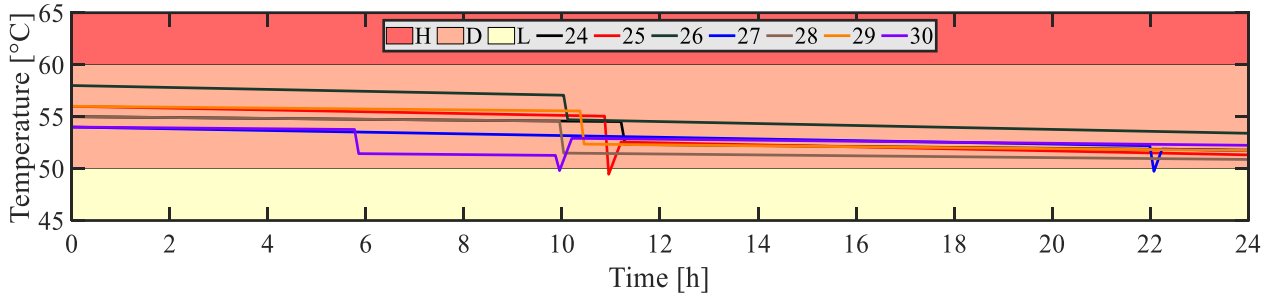

Fig. B.5.7: Level 4 ESTWH temperatures

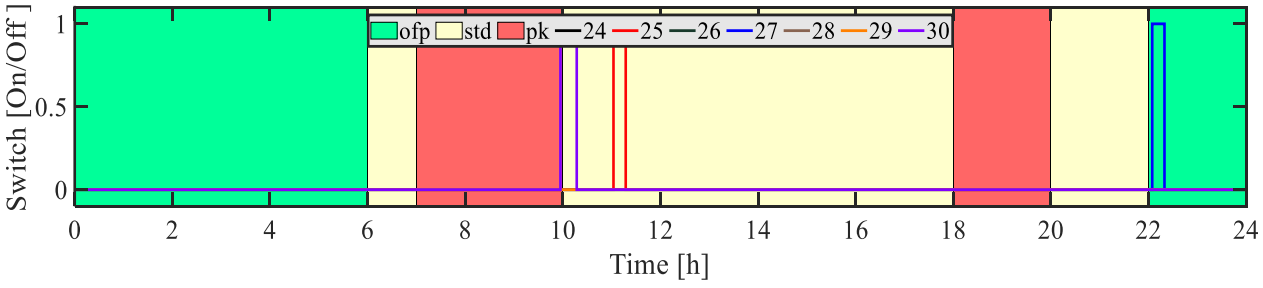

Fig. B.5.8: Level 4 ESTWH switching functions

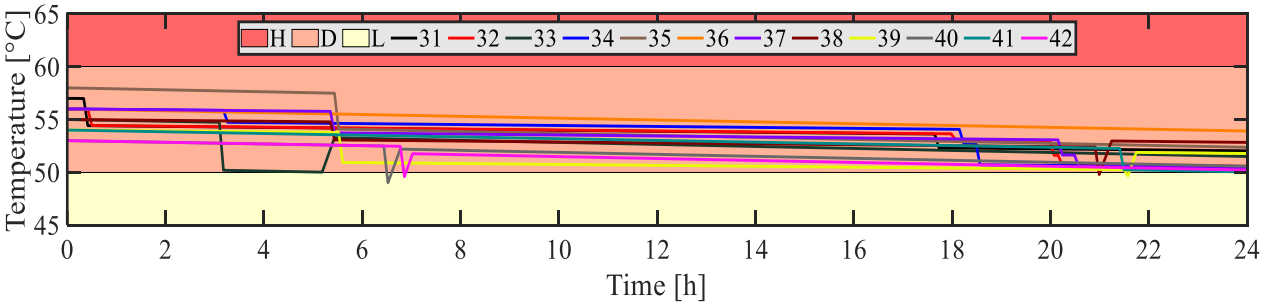

Fig. B.5.9: Level 5 ESTWH temperatures

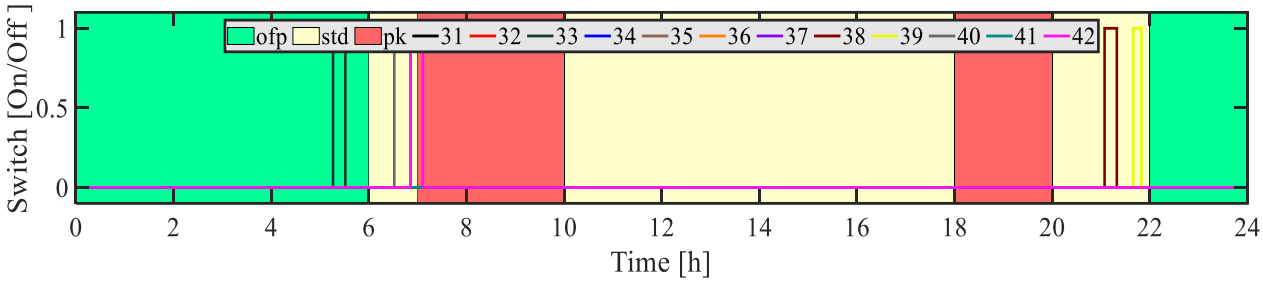

Fig. B.5.10: Level 5 ESTWH switching functions

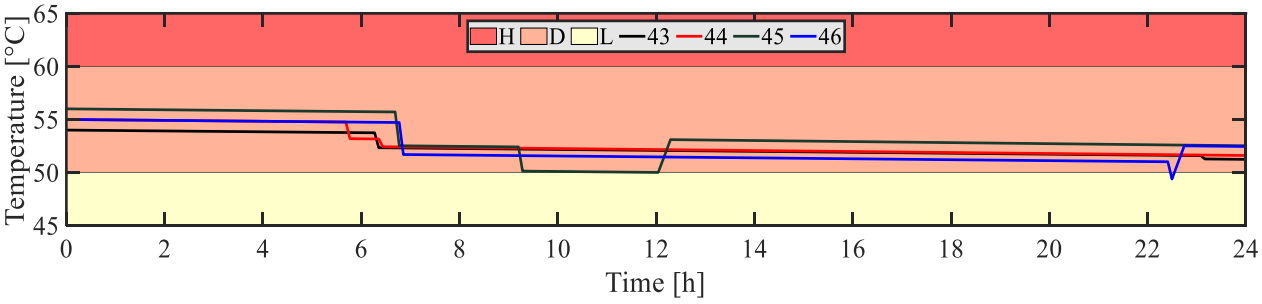

Fig. B.5.11: Level 6 ESTWH temperatures

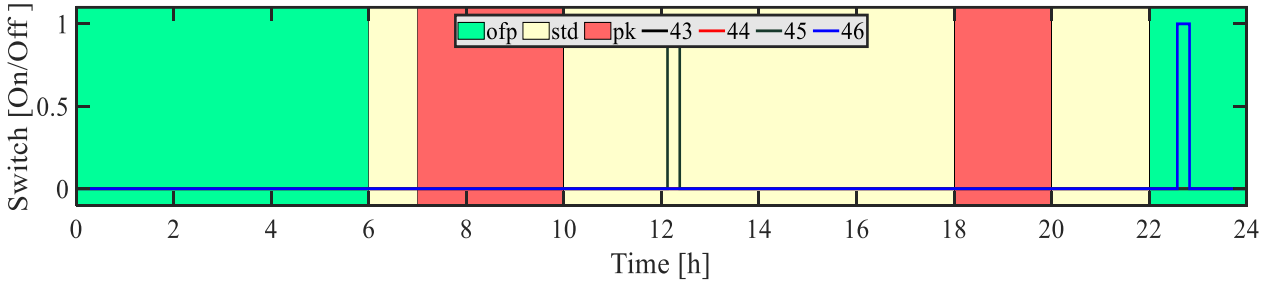

Fig. B.5.12: Level 6 ESTWH switching functions

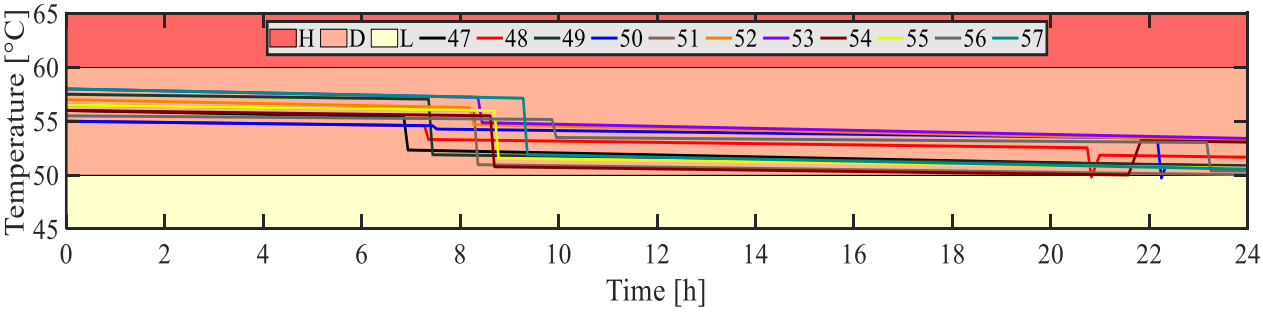

Fig. B.5.13: Level 7 ESTWH temperatures

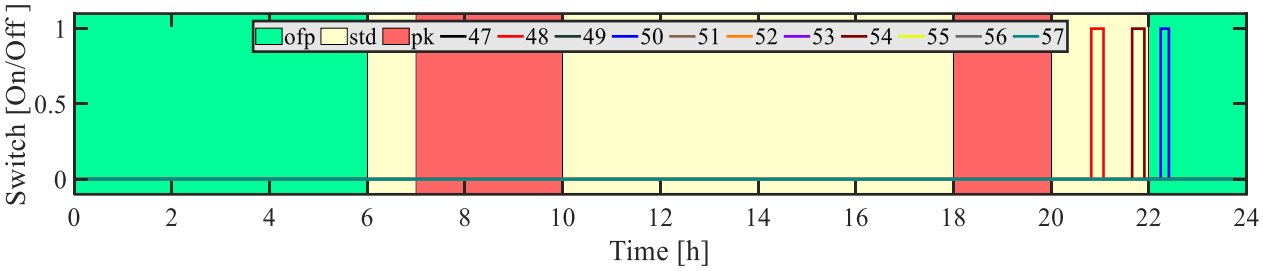

Fig. B.5.14: Level 7 ESTWH switching functions

B.6 Summer optimal control case:

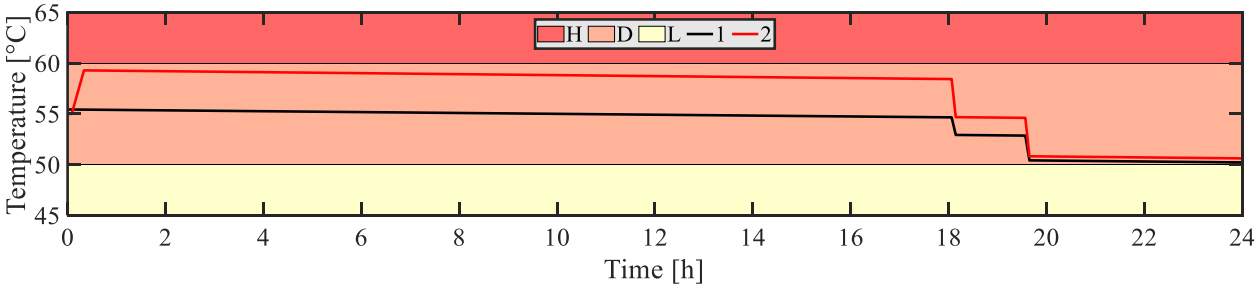

Fig. B.6.1: Basement ESTWH temperatures

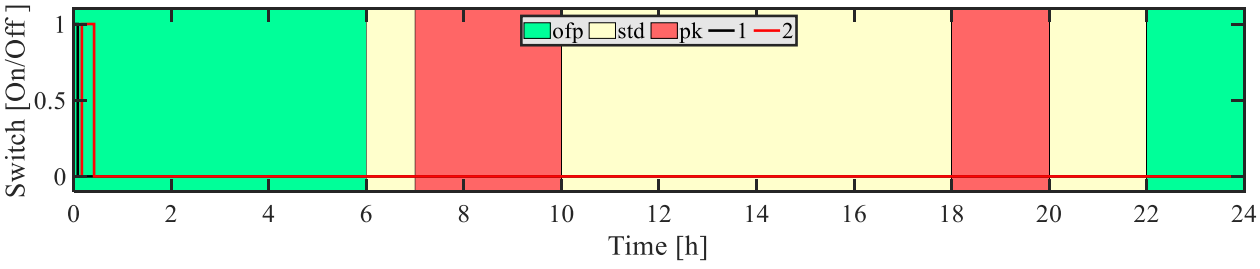

Fig. B.6.2: Basement ESTWH switching functions

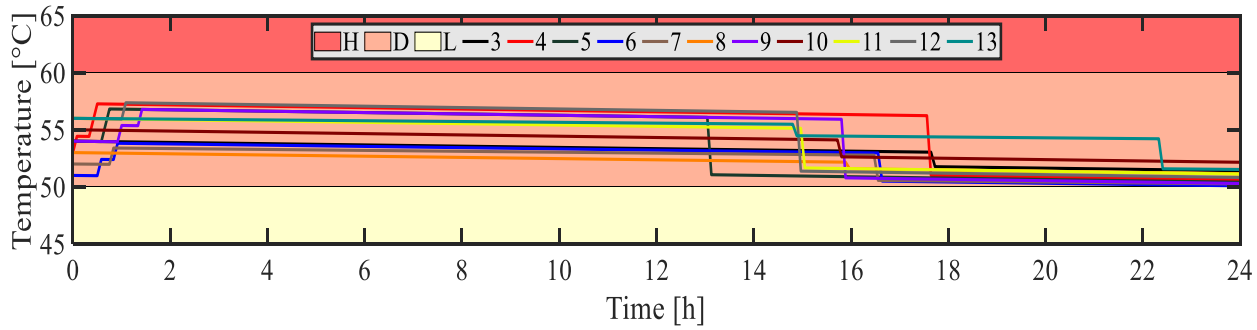

Fig. B.6.3: Level 2 ESTWH temperatures

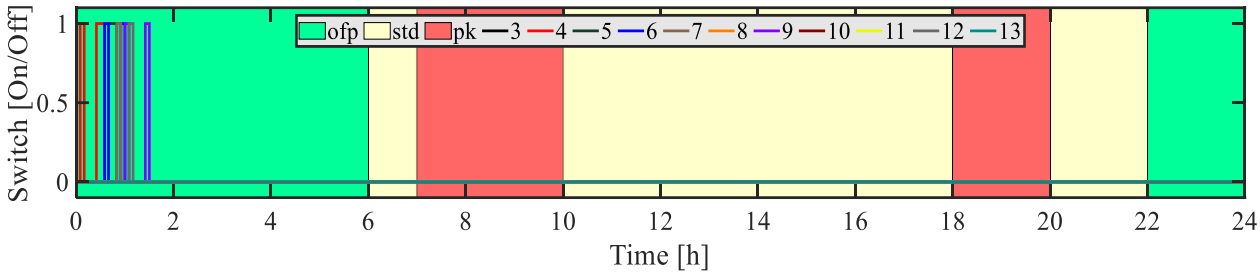

Fig. B.6.4: Level 2 ESTWH switching functions

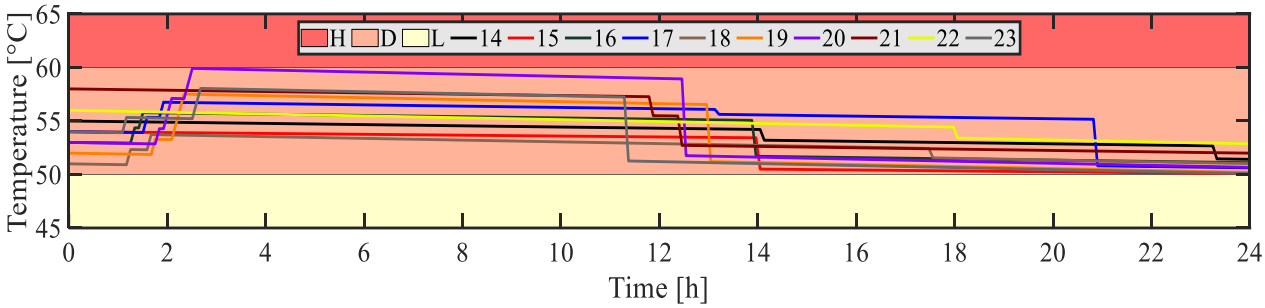

Fig. B.6.5: Level 3 ESTWH temperatures

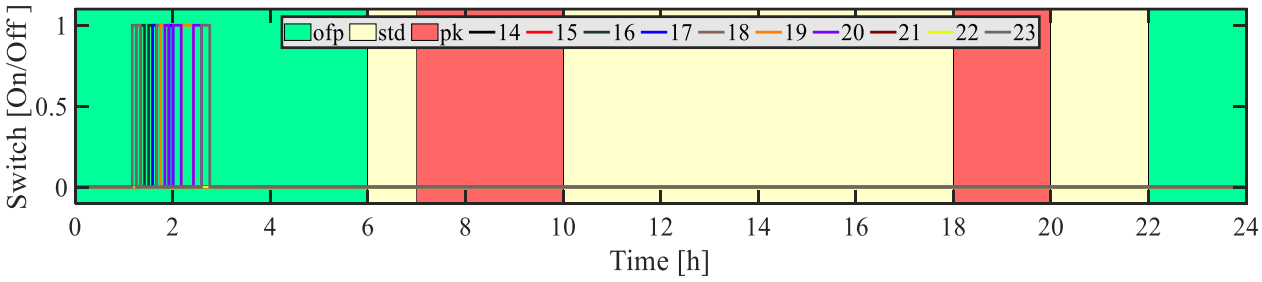

Fig. B.6.6: Level 3 ESTWH switching functions

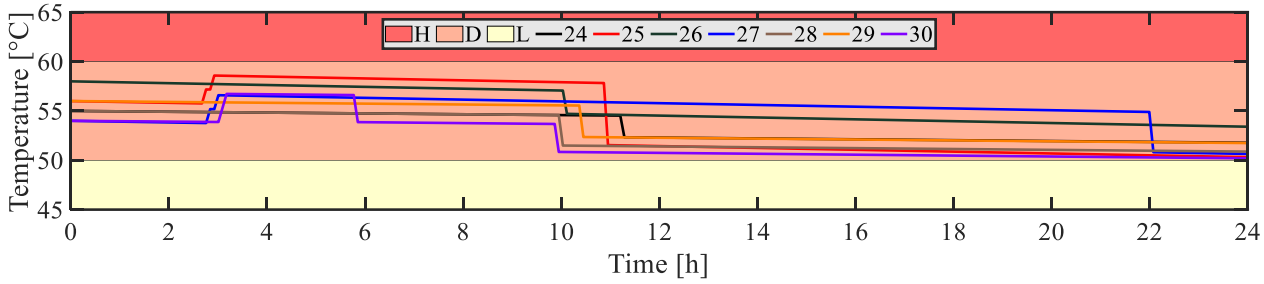

Fig. B.6.7: Level 4 ESTWH temperatures

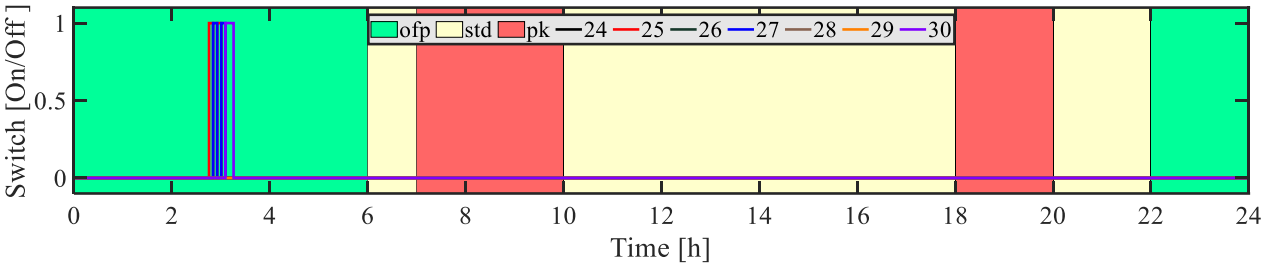

Fig. B.6.8: Level 4 ESTWH switching functions

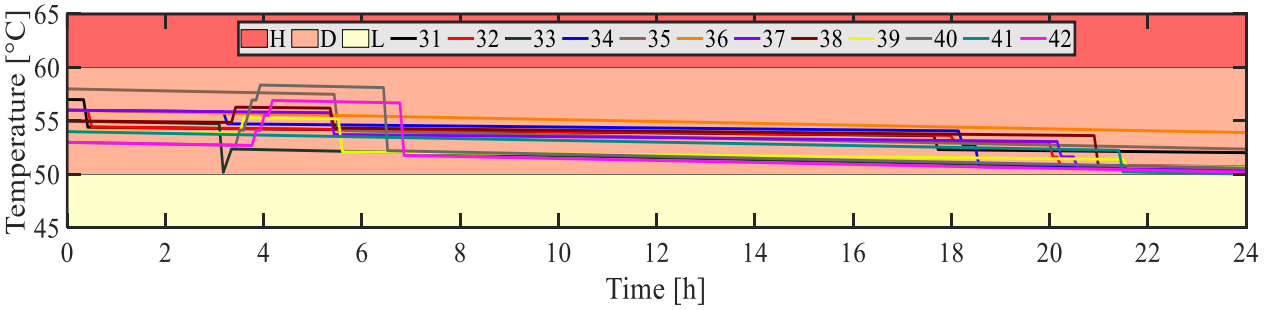

Fig. B.6.9: Level 5 ESTWH temperatures

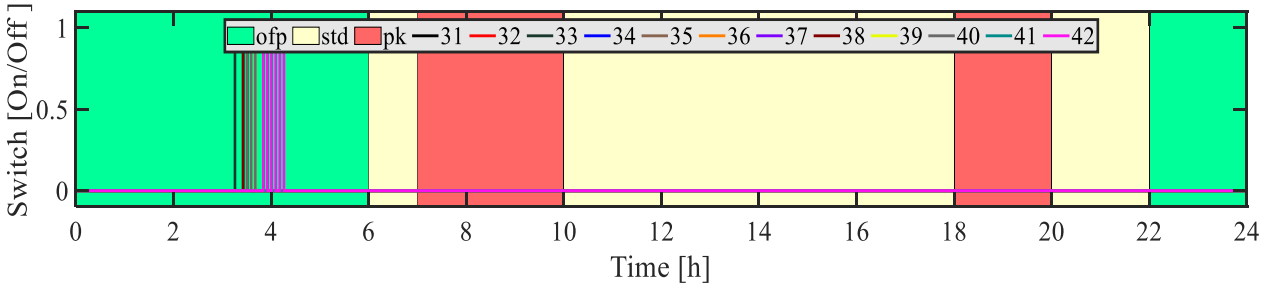

Fig. B.6.10: Level 5 ESTWH switching functions

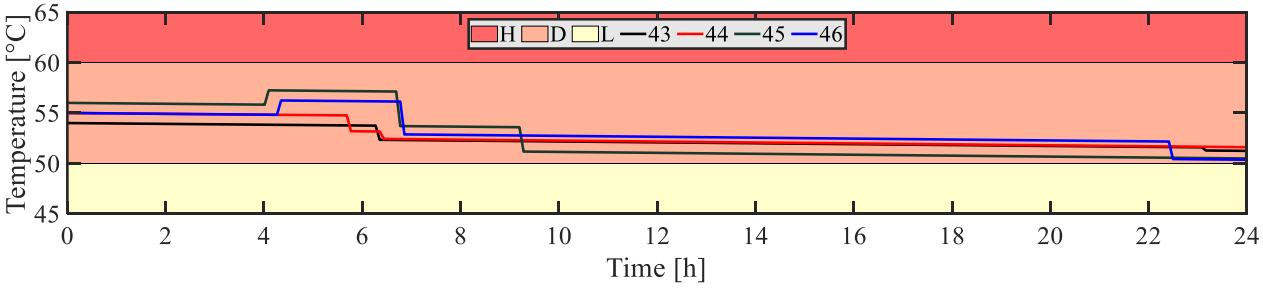

Fig. B.6.11: Level 6 ESTWH temperatures

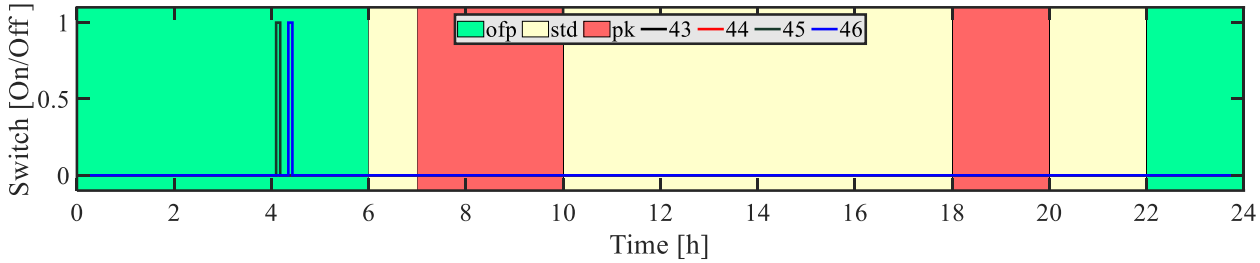

Fig. B.6.12: Level 6 ESTWH switching functions

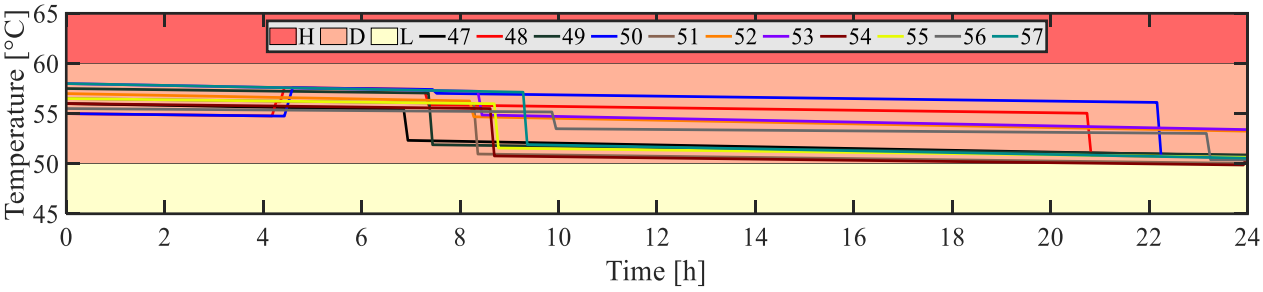

Fig. B.6.13: Level 7 ESTWH temperatures

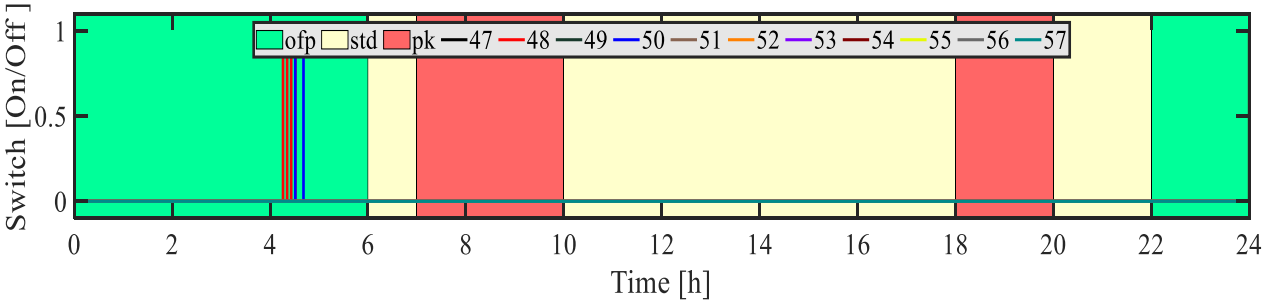

Fig. B.6.14: Level 7 ESTWH switching functions

APPENDIX C: LIFE CYCLE COST ANALYSIS OF POST IMPLEMENTATION OF PROPOSED SYSTEM IN CHAPTER III

Year	Energy costs*			Maintenance*		Cumulative cash flows*		
	BL1	Prop	OC	Prop	OC	BL1	Prop	OC
0						0	1640000	1640000
1	335557	232124	198370	16400	16400	335557	1888524	1854770
2	385890	266943	228125	33620	33620	721446	2172687	2100115
3	443773	306984	262344	51701	51701	1165220	2497752	2380540
4	510339	353032	301696	70686	70686	1675559	2869768	2701221
5	586890	405986	346950	90620	90620	2262450	3295689	3068106
6	674924	466884	398993	111551	111551	2937374	3783504	3488030
7	776163	536917	458842	133529	133529	3713536	4342399	3968849
8	892587	617454	527668	156605	156605	4606123	4982930	4519593
9	1026475	710073	606818	180836	180836	5632598	5717232	5150641
10	1180446	816584	697841	206277	206277	6813045	6559258	5873924
11	1357513	939071	802517	232991	232991	8170558	7525043	6703155
12	1561140	1079932	922894	261041	261041	9731698	8633024	7654099
13	1795311	1241921	1061329	290493	290493	11527009	9904397	8744879
14	2064608	1428210	1220528	321418	321418	13591617	11363532	9996332
15	2374299	1642441	1403607	353888	353888	15965916	13038444	11432410
16	2730444	1888807	1614148	387983	387983	18696360	14961345	13080652
17	3140011	2172128	1856270	423782	423782	21836371	17169273	14972722
18	3611012	2497948	2134711	461371	461371	25447383	19704810	17145022
19	4152664	2872640	2454917	500840	500840	29600047	22616918	19639408
20	4775563	3303536	2823155	542282	542282	34375610	25961896	22504005

*Expressed in USD

APPENDIX D: LIFE CYCLE COST ANALYSIS OF POST IMPLEMENTATION OF PROPOSED SYSTEM IN CHAPTER IV

Year	Energy costs*			Maintenance*		Cumulative cash flows*		
	BL1	BL2	OC	BL2	OC	BL1	BL2	OC
0						0	18168	18168
1	2962	1541	705	182	705	2962	19890	19054
2	3407	1772	811	191	811	6369	21853	20056
3	3918	2038	932	200	932	10287	24092	21188
4	4505	2344	1072	210	1072	14792	26645	22471
5	5181	2695	1233	221	1233	19973	29562	23925
6	5958	3100	1418	232	1418	25932	32893	25575
7	6852	3564	1631	243	1631	32784	36701	27449
8	7880	4099	1875	256	1875	40664	41056	29580
9	9062	4714	2157	268	2157	49726	46038	32005
10	10421	5421	2480	282	2480	60147	51741	34767
11	11984	6234	2852	296	2852	72131	58271	37915
12	13782	7169	3280	311	3280	85913	65751	41506
13	15849	8245	3772	326	3772	101762	74322	45604
14	18227	9481	4338	343	4338	119989	84146	50284
15	20961	10904	4988	360	4988	140950	95409	55632
16	24105	12539	5737	378	5737	165055	108326	61746
17	27721	14420	6597	397	6597	192775	123143	68740
18	31879	16583	7587	416	7587	224654	140142	76743
19	36660	19071	8725	437	8725	261314	159650	85905
20	42159	21931	10033	459	10033	303474	182041	96398

*Expressed in USD